THE STRUCTURAL and METAMORPHIC GEOLOGY of the TONALE PASS AREA, NORTHERN ITALY.

by

JOHN RICHARD MENDUM.

Ph.D. UNIVERSITY OF EDINBURGH 1976

Looking south from the Passo di Contrabandieri down the Valbiolo to the Tonale Pass and the northern margin of the Adamello Massif. The tonalite of the Adamello Massif weathers to form high, rugged peaks such as La Presanella (left) and Cima Busazza (right).

ABSTRACT

An area of 28 sq.km. has been mapped in detail around the Tonale Pass in Northern Italy. The area is divided into two regional geological units, the Central Alps and Southern Alps, by the Tonale Line. This major east-west trending lineament is marked by a 40 m. to 70 m. wide sub-vertical band of cataclasite and brecciated pseudotachylite, representing a narrow zone of repeated movement in both the Hercynian and Alpine orogenies.

South of the Tonale Line, the Southern Alps consist of Greenschist facies, pelitic and semi-pelitic schist, quartzite and minor amphibolite. The metasediments, collectively termed the Edolo Schists, have been folded by two major fold sets; f_1 - tight to isoclinal, minor folds with an axial plane cleavage sub-parallel to the bedding and axes gently plunging W to SW; f_3 - southward facing, asymmetrical, open to tight major and minor folds with axes plunging gently west to southwest. Minor f_5 folds with similar axial directions are also present. Later small shear zones and joints are compatible with uplift in a N - S directed stress field.

These features also affect the Adamello massif, - a body of tonalite, biotite-quartz-diorite and minor diorite which intruded the metasediments in the Lower Oligocene. Along the northern margins of the massif, the tonalite and biotite-quartz-diorite are foliated, the intensity of foliation decreasing away from the contact. Deformed xenolith measurements give maximum strain ratios of X : Y : Z = 8.8 : 6.2 : 1 (k = 0.08), implying shortening of 73.6%. Textural and mineralogical observations suggest that this deformation occurred during the cooling of the intrusion. Taking the intrusive body to be approximately spherical, and using the time-temperature curves of Lovering (1935), a compressive strain rate of 5.8×10^{-14}/sec. is obtained.

Cordierite, garnet and sillimanite are developed in the metasediments adjacent to the intrusive contact, and biotite and andalusite are widespread in the inner 0.3 km.

of the 0.8 km. wide aureole. The mineralogy implies intrusion at around 900°C with metamorphic assemblages formed at P total = P fluid ≈ 3 kb.

North of the Tonale Line is a 0.7 to 1 km. wide zone of foliated quartz-feldspar-phengite gneiss. The gneiss is strongly lineated near its northern margin and measurements on fragmented feldspar show that the rock unit has undergone strong flattening strain and that the lineation corresponds to the axis of maximum strain (X) with minimum $\sqrt{\lambda}$ values of about 2 : 1. Quartz preferred orientation studies suggest that the X axis was sub-vertical further south where 1 to 4 cm. diameter feldspar augen are well developed. The observed assemblages are consistent with phengite formation by the reaction

$$5\ \text{K feldspar} + 3\ \text{Andesine} + \text{Biotite} + 5H_2O \rightleftharpoons 6\ \text{Phengite} + 9\ \text{Quartz} + 3Na^{+} + 1.5Ca^{++} + 3O^{--}$$

The presence of fragmented feldspars, and phengite concentration along specific microscopic zones in the gneiss, suggest that P H_2O/P total ratios were close to 1. Factors determining phengite composition are complex and include pressure, temperature, bulk rock composition, associated mineral phases, molar concentration and activity of various ions and ionic complexes in the fluid, and f O_2. As shown by data from the Stavel Gneiss, and from other workers, phengite d spacing is strongly controlled by Si - Al substitution.

The Stavel Gneiss contains rare, southward verging, small scale, open to close, asymmetrical f_5 folds. Kink bands (f_6) are also present. Biotite retrogression to chlorite occurs in gneisses of the Central Alps adjacent to the Stavel Gneiss.

The Central Alps, north of the Stavel Gneiss, comprise several thrust sheets of paragneiss, schist and quartzite. In the area mapped paragneiss is absent north of the Peio Line, a major mylonite zone across which large scale differential movement occurred in the late Alpine event (f_5). The paragneisses consist of pelitic and semi-pelitic gneiss, marble, amphibolite and minor quartzite. In the

initial Caledonian Upper Amphibolite grade metamorphism (m_1), sillimanite, garnet, biotite, andesine, staurolite(?) and muscovite have formed in pelitic assemblages; grossularite, diopside, K feldspar, forsterite and vesuvianite in impure marbles; and hornblende and labradorite, and in parts garnet, in amphibolite. No record of this event was found north of the Peio Line. The later Hercynian event (m_2) (Upper Greenschist - Lower Amphibolite grade) has resulted in partial retrogression and oligoclase/andesine, chloritoid, clinozoisite, garnet, biotite, chondrodite and tremolite are all well-developed. The Early Alpine Upper Greenschist - Lower Amphibolite grade event (m_3) and the Late Alpine, Lower to Upper Greenschist grade event (m_4) are restricted to mylonites and zones of strong f_3 or f_5 deformation. Pegmatites and quartz veins were intruded into the gneisses during the Hercynian event. A small ultrabasic intrusion and numerous andesite dykes were emplaced between the m_3 and m_4 events.

Six distinct fold sets are recognised in the paragneiss sequence. Interference patterns caused by three superimposed fold sets are common in banded marbles. The dominant gneissic banding pre-dates all fold phases, except north of the Peio Line.

f_1 - tight to isoclinal, minor folds with gentle E to W plunging axes and the gneissic banding axial planar to the folds. Post dates the m_1 metamorphism.

f_2 - small to medium scale open to tight folds and cuspate structures (at marble/gneiss contacts) with SE plunging axes - Restricted to marble bands and adjacent gneiss.

f_3 - open to tight, asymmetrical folds on all scales with a N vergence (except in most marbles where S vergence) and gentle E - W plunging axes.

f_4 - "crenulation" and chevron type minor folds generally with a N vergence. Axes plunge to 070° - 250°. Restricted in occurrence - particularly well-developed in phlogopitic marble.

f_5 - small to medium scale open to close "parallel" folds generally verging upwards or southwards.

f_6 - minor conjugate kink band sets and large scale open folds with axes plunging steeply S or N.

The f_1 and f_3 fold events also strongly affected the metasediments of the Southern Alps. The correlation is based on the similarity of style, axial direction and geological age. A simplification in the tectonic history of the area results if such a correlation is accepted. The f_2, f_3 and f_4 events constitute the Early Alpine deformation event.

Mylonite zones are associated with f_3 and f_5 folds. They range from a few mm. to 50 m. wide, and using garnet "trails", minor fold geometry and measurable small-scale shear zones, values of shear strain (γ) between 10 and 20 have been calculated. The mylonitic gneiss adjacent to these zones has been shown by folded vein measurements, boudinage features and deformed sillimanite porphyroblasts and feldspar crystals, to be affected by a strong flattening strain. The texture, mineralogy and strain associated with mylonites is consistent with ductile deformation under moderate water pressure, within narrow zones of strong differential movement.

Quartz c-axis orientation measurements on 7 specimens can be explained in terms of a pseudo two-girdle pattern related to tectonic stress field, although local inhomogeneity occurs in coarse grained rocks.

ACKNOWLEDGEMENTS.

This work was carried out at the Grant Institute of Geology, University of Edinburgh, while the author was in receipt of a 2 year N.E.R.C.Research Studentship. I wish to thank Dr. M.R.W. Johnson very much for his helpful advice and interested supervision of this project, and Professor G.Y. Craig for his permission to use departmental facilities.

I have benefited from discussions with Drs.R.F.Cheeney, B.Harte (University of Edinburgh), G.J.Wilson (Monash University), R.H.Sibson (Imperial College) and other research students at the University of Edinburgh, notably R.T.C.Frost, G.A. Yarwood and T.H.E. Heaton. The technical staff under the direction of C.Chaplin, and the librarians Mrs.J.Nicholas and Mrs.T.Grieve have also assisted the author on many occasions. I am grateful to Drs.P.Hill and B.Jeffries for their patient instruction on the use of the electron microprobe and processing of the data.

Whilst in the field the people of Vermiglio, particularly Pietro Zanoni and family, were most helpful to the author and his family; their assistance is gratefully acknowledged.

Without the assistance and encouragement of my wife, whose help has been invaluable in the field and in the preparation of this thesis, this project would not have been completed. I must thank her for drafting almost all the diagrams in this thesis. My mother has efficiently carried out both the rough and final typing with great patience and her help is greatly appreciated.

CONTENTS

1.00 INTRODUCTION

The basic aim of this thesis is to describe and interpret the structure and metamorphism of the Tonale Pass area in Northern Italy. The area lies astride the Tonale Line, a regionally important lineament which marks the southern limit of the Austro-Alpine Nappes. An attempt is made to assess the role that this structure has played in the geological history of the region. In the thesis particular attention has been given to determining the nature of the strain and changes in texture and mineralogy in the mylonites, and the association of mylonites with the northward thrusting of the Austro-Alpine Nappes. The area is subdivided into five major tectonic and lithological units; from south to north, the Adamello massif, the Southern Alps, the Tonale Line, the Stavel Gneiss and the Central Alps. Within the Central Alps thick mylonites separate tectonic sub-units. The structural, metamorphic and igneous events are placed in their chronological order and a model for their genesis is proposed.

1.10 GEOGRAPHY

The area mapped is approximately triangular in shape and totals about 28 sq. km. It is centred around the Tonale Pass, a grassy wide saddle lying between the Val di Sole in the east, and the Val Camonica in the west. A small ski resort has been developed at the summit of the pass. Figure 1 (inset) shows the location of the area in relation to other geographical features. A major road, S.S.42, connecting Bolzano and Edolo, traverses the area and minor roads (commonly loose surface) provide good access to other parts of the area. The Italy - Austro-Hungary border followed the watershed between the Val di Sole and Val Camonica, and the Tonale Pass area was the scene of bitter fighting in the 1914-18 war.

The area has a maximum relief of about 1800 m. and ranges in absolute height from 1200 m. in the Val di Sole to 2970 m. at Vetta d'Albiolo. The topography of the area is shown in Figure 1 and is due to the effects of the Pleistocene glaciations. Glacial striae trending about

Figure 1. - Map showing the relief features of the Tonale Pass area with a location map (inset).

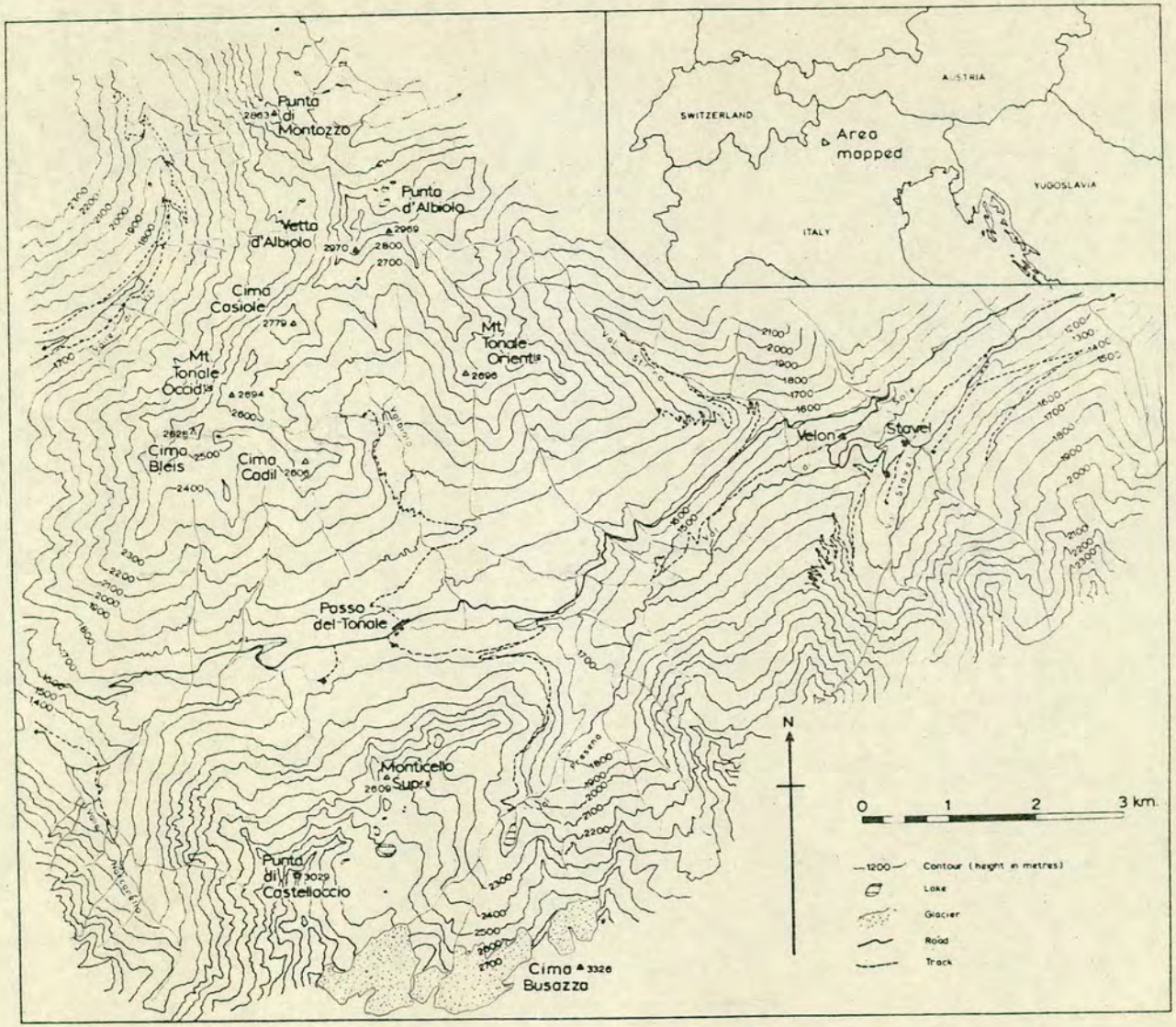
AUSTRIA
SWITZERLAND
Area mapped
YUGOSLAVIA
ITALY
Punta di Montozzo
2863
Punta d'Albiolo
Vetta d'Albiolo
2970
2959
Cima Casiole
2779
Mt. Tonale Occid.le
2694
Mt. Tonale Orient.le
2696
Cima Bleis
2625
Cima Cadil
2608
Passo del Tonale
Monticello Sup.re
2609
Punta di Castelloccio
3029
Cima Busazza
3326
Velon
Stavel
N
0 1 2 3 km.
1200 Contour (height in metres)
Lake
Glacier
Road
Track

N-S show that there was a major southerly movement of ice at least in the area north of the Tonale Pass. Minor striae trending 070° to 090° show that smaller valley glaciers were present subsequent to the main ice retreat. The higher parts of the area (+ 2000 m.) consist of sharp ridges and large amounts of marginal scree. The north facing slopes are generally steep and are partially covered by very loose scree, whereas those facing south have long ridges, large expanses of fresh rock and more gentle slopes, as shown in Plate 1. On the ridges wartime trenches commonly provide good outcrop. Moraines are common in the valley bottoms. The area was deforested before the 1914-18 war and only small alder trees have since grown in some parts. Between about 1800 m. and 2000 m. gently sloping, grassy alps are underlain by boulder clay at least 30 m. thick in parts. Exposure in these areas is very poor except in stream sections. Between 1200 m. to 1400 m. and 1800 m. steep coniferous wooded hillsides are present. Outcrop is patchy but some good stream sections do occur. In the Val di Sole thick alluvial deposits are found in parts. There are also several rock barriers through which the river has cut deep gorges.

Snow covers the land above 1800 m. for about 7 months of the year (late October to late May generally). In summer maximum temperatures in this upper region are between 8°C and 18°C. Snow is not uncommon even in mid-summer. The annual rainfall is about 125 cm. with spring and late autumn the times of maximum precipitation.

1.20 METHODS OF STUDY

The project has been carried out largely using traditional methods. Almost all rock outcrops within the mapped area were visited. Where large areas of rock are exposed, traverses along the ridges (Central Alps) or selected traverses at intervals (Adamello massif) were made. Detailed structural observations were made where possible, and measurements obtained from any features which could be used as strain markers (e.g. folded pegmatite veins, deformed xenoliths, sillimanite porphyroblasts). About 150 thin sections

Plate 1 - Rocky ridge between Vetta d'Albiolo (left) and Mt. Tonale Orientale (right) showing the typical mode of outcrop in the Central Alps on south facing slopes. The section shows moderate to steeply dipping pelitic gneiss marble and amphibolite. A small dunite intrusion is seen in the central part of the ridge. Mylonites are present at several points in the gneiss sequence.

were made on representative rock types from the area. Mineralogical and textural studies were carried out and further measurements were made for strain determination (quartz aggregates). Quartz c-axis orientation measurements were made on seven orientated thin sections from various parts of the area, using a universal stage. Routine mineral identifications and phengite unit cell spacings were determined using the X-ray Diffroactometer (Cu K α radiation). Phengite and feldspar compositions from specimens of Stavel Gneiss were obtained using the Cambridge Electron Microprobe.

1.30 REGIONAL GEOLOGY

The area studied lies across the Tonale Line, a major lineament dividing the Southern Alps to the south, and the Austro-Alpine Nappes to the north. Figure 2 shows the regional setting of the area. Oxburgh (1968) has defined the southern limit of the Eastern Alps as the Tonale Line and its easterly continuation the Judicaria, Pusteria and Gailtal Lines. Palaeozoic and Mesozoic sediments generally have differing depositional and tectonic histories across this lineament (Van Hilten, 1960, Oxburgh, 1968 p.100).

The Southern Alps, a series of schists and gneisses termed the Edolo Schists in the area mapped, decrease in metamorphic grade from west to east. Mesozoic sediments and volcanics showing only minor Alpine folding lie above these metamorphics. Hercynian and Alpine tonalite and granodiorite intrusions are common, particularly adjacent to the Tonale Line. The Alpine folds have a southerly vergence. The Southern Alps are regarded as part of the Dinarids (Kober, 1955).

The Austro-Alpine Nappes, which extend up to 180 km. (more generally 100 - 120 km.) north of the Tonale - Judicaria - Pusteria - Gailtal Line in parts of Austria, consist of a series of allochthonous sheets of high grade Caledonian para and orthogneiss, Palaeozoic and Mesozoic sediments, volcanics and Hercynian intrusions. The detailed geometry of parts of the Austro-Alpine Nappes is still incompletely known but the general sequence is:- a) autochthonous

Figure 2 - Regional Geology of the Central - Eastern Alps showing the geological setting of the Tonale Pass area.

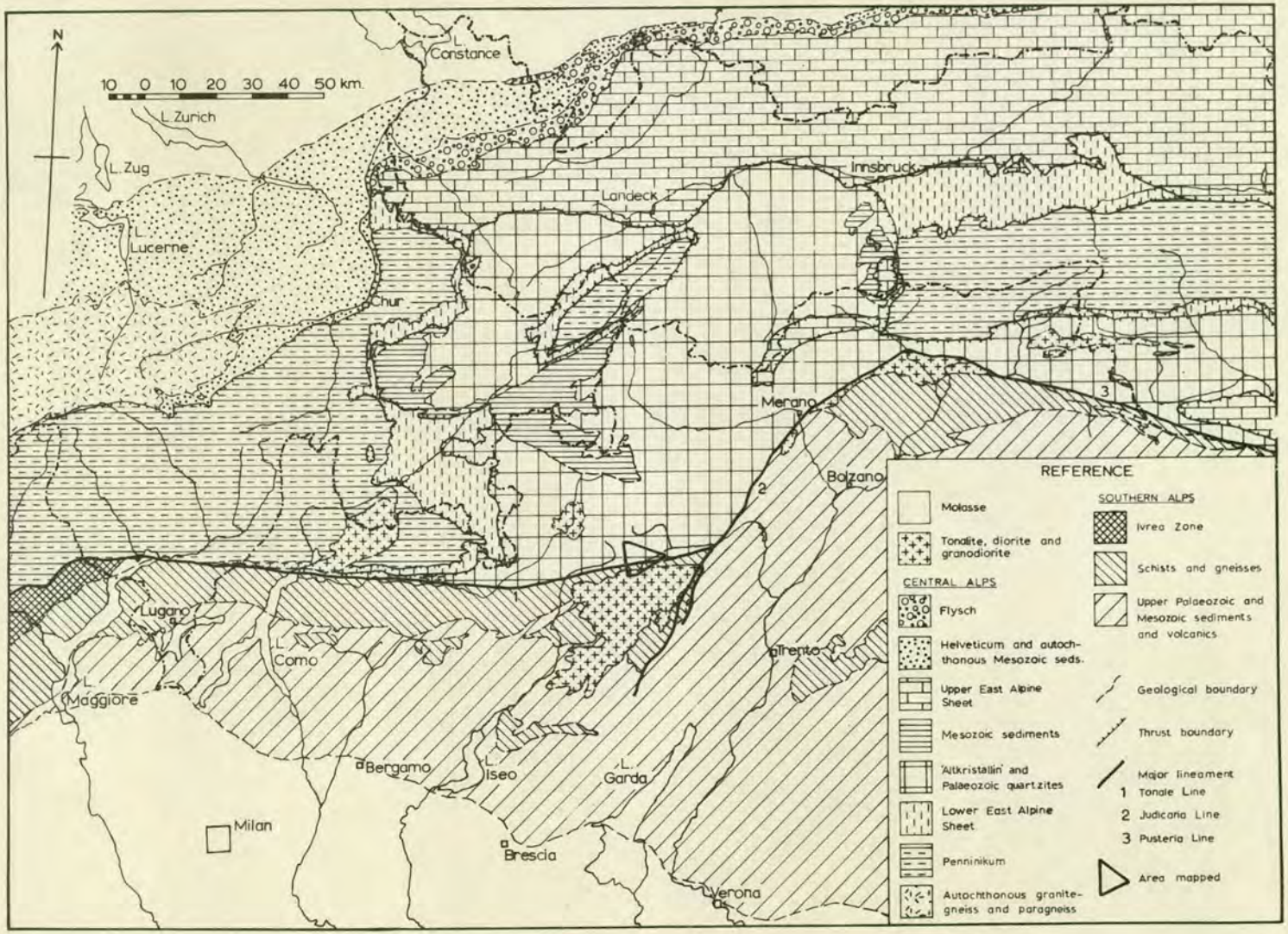
N
10 0 10 20 30 40 50 km.
L. Constance
L. Zurich
L. Zug
Lucerne
Chur
Landeck
Innsbruck
Merano
Bolzano
Trento
Lugano
L. Como
L. Maggiore
Bergamo
Iseo
L. Garda
Milan
Brescia
Verona
1
2
3
REFERENCE
Molasse
Tonalite, diorite and granodiorite
CENTRAL ALPS
Flysch
Helveticum and autochthonous Mesozoic seds.
Upper East Alpine Sheet
Mesozoic sediments
'Altkristallin' and Palaeozoic quartzites
Lower East Alpine Sheet
Penninikum
Autochthonous granite-gneiss and paragneiss
SOUTHERN ALPS
Ivrea Zone
Schists and gneisses
Upper Palaeozoic and Mesozoic sediments and volcanics
Geological boundary
Thrust boundary
Major lineament
1 Tonale Line
2 Judicaria Line
3 Pusteria Line
Area mapped

basement para- and orthogneiss. b) strongly deformed Palaeozoic and Mesozoic sedimentary cover and c) relatively undeformed Mesozoic and Tertiary sediments (mainly limestones).

Alpine metamorphism and extensive northward thrusting resulted in complex interleaving of the sequence stated above. Subsequent uplift along an east-west axis has exposed all the units in the Hohe Tauern Range. A similar sequence is exposed at the western margin of the Austro-Alpine Nappes in the Bernina Range (SE Switzerland), although the presence of the Late Alpine Bergell intrusion complicates the tectonic relationships. Late Alpine tonalites and granodiorites in the Austro-Alpine Nappes are restricted to the area lying between the Tauern Window and the Pusteria Line.

1.40 Local Geology

The area mapped can be conveniently sub-divided into four geological units. From south to north these are a) the Adamello massif and its contact aureole, b) the Southern Alps, c) the Stavel Gneiss, d) the Central Alps. Map A shows the distribution of the detailed lithologies in the Tonale Pass area. The following section is a brief outline of the geology of the Tonale Pass area. Some of the main conclusions from the present work are also presented.

The Adamello massif and Southern Alps are separated from the Stavel Gneiss and Central Alps by the Tonale Line, a major east-west trending lineament. The Line is marked by a 40 to 70 m. wide sub-vertical zone of brecciated pseudotachylite.

(a) The Adamello massif is a composite intrusive body consisting, in the area mapped, of tonalite and biotite-quartz-diorite with minor associated diorite plutons. K-Ar and Rb-Sr cooling dates on biotites range from 30 to 45 m.y. (Borsi et al, 1966). Adjacent to the northern margin of the massif the tonalite and biotite-quartz-diorite are foliated, the intensity of foliation decreasing away from the contact. Maximum finite strain values

calculated from deformed xenoliths are X : Y : Z = 8.8:6.2:1. Strain values may be directly correlated with the degree of foliation development. All strain values lie very close to the line K = 0.08 (Flinn,1962) indicating strong flattening. Large new biotite flakes have grown in the tonalite, but deformation, recovery and partial recrystallization only, have occurred in the biotite-quartz-diorite. Later kink bands and joints are developed in the massif.

The aureole of the Adamello massif is 0.7 km. wide and contact metamorphic effects range from minor phengitic mica growth in the outer parts to extensive sillimanite and cordierite and minor garnet growth in the inner parts. Experimental data have been used to show that contact temperatures of about 700°C were attained (see 2.83).

(b) The Southern Alps consist of Greenschist facies, pelitic and semi-pelitic schist, quartzite and minor amphibolite. Evidence of two major fold events and several localised minor events is observed in these rocks. The earlier major event has formed tight to isoclinal small-scale folds with an axial plane foliation generally sub-parallel to the bedding. The later south facing asymmetrical open to tight folds are superimposed on these earlier structures. Both early and later fold axes plunge gently west to southwest. Textural evidence from the aureole shows that the later folds pre-date the intrusion of the Adamello massif. A later f_5 deformation event, probably responsible for foliation development in the Adamello massif, has "tightened up" many of the earlier folds particularly adjacent to the intrusion margin.

(c) The Stavel Gneiss is a foliated quartz-feldspar-phengite gneiss which crops out in a narrow belt trending approximately east-west. Because of the lack of structural and metamorphic continuity between the Stavel Gneiss and adjacent units, it is here considered as a separate geological unit. The gneiss commonly shows a strong gentle westerly plunging lineation caused by quartz, phengite and more rarely feldspar, growth along the intersection of crude banding and the phengitic foliation. Thin section

observations show that the lineation corresponds to the extension direction, with minimum strain values, calculated from fragmented plagioclase feldspar, of 1.87:1. Some extension has also occurred in the direction perpendicular to the lineation in the foliation plane, showing that the strain lies in the flattening field. The present mineralogy of the gneiss is a product of metasomatic reactions. The original mineralogy was probably quartz-orthoclase-andesine-biotite, possibly with muscovite and sillimanite.

(d) The Central Alps lie north of the Stavel Gneiss and consist of pelitic gneiss, marble and amphibolite which are well exposed in the area north and west of the Tonale Pass. The unit is part of the Altkristallin sheet, a large allochthonous basement gneiss sheet, and forms the southernmost exposures of the Austro-Alpine Nappes. Abundant sillimanite, garnet (almandine), andesine and muscovite are developed in the pelitic gneiss and grossular, diopside, microcline, idocrase and norbergite (clinohumite group) in the impure marbles. These original parageneses lie in the Upper Amphibolite facies grade and have been modified in parts by lower grade Hercynian, and Early and Late Alpine metamorphic events. The Alpine metamorphism was largely confined to narrow zones in the paragneiss sequence.

Pegmatites and quartz veins intruded the gneisses during the Hercynian event. Andesite and quartz monzonite dykes and small ultramafic pods were emplaced subsequent to the main Early Alpine movements but prior to the later f_5 uplift event. The ultramafic intrusions have resulted in the growth of large diopside and zoisite crystals in adjacent impure marbles.

1.41 Structure

The regional structure in the Central Alps consists of a large monoclinal fold with a gentle southerly dipping limb to the north and a steeply dipping limb adjacent to the Stavel Gneiss. This latter limb commonly dips north, forming a "backfold" structure similar to that defined by Argand (1916) in the Western Alps. The Stavel Gneiss and Southern Alps consist essentially of steep to sub-vertically

dipping sequences.

A complex sequence of minor structures is developed in the Tonale Pass area and these have been termed f_o - f_6. Late fault and joint patterns have been omitted from this sequence. Figure 3 shows the geometry and orientation of the structures which have developed in the four geological units. Figure 4 shows the relationships of structure and sequence derived from field observations and known isotopic age determinations. The Stavel Gneiss phengite foliation formation pre-dates the f_6 structures and may pre-date f_5 structures. It may be associated with either the f_3 or f_5 event. The complete range of structures is not developed in any one area; the marbles of the Central Alps commonly show evidence of six separate structural events (f_o - f_5) with up to four sets of folds (f_1 - f_4) in any one outcrop.

The f_1 event in the Central Alps consists of tight to isoclinal minor folds with an axial planar gneissic foliation. This foliation is sub-parallel to the gneissic compositional banding but rarely a small angular discordance can be observed between the two structures. f_1 fold axes plunge gently east or west, although later fold and strain events have considerably modified this initial orientation in many areas. In the Southern Alps, f_1 tight to isoclinal minor folds with a well developed axial plane cleavage are commonly seen. Fold axes plunge gently to moderately southwest and northeast. In both units the f_1 folds face S. to SE., and no large scale f_1 structures were observed.

The f_3 folds have similar axial orientations in the Central and Southern Alps, although those in the Southern Alps show a greater spread in orientation. They also have a more chevron-type profile than those in the Central Alps which are approximately "similar" in style. Both sets of folds show corresponding degrees of asymmetry, but f_3 folds in the Central Alps are generally tighter and show a consistent sense of overturning to the north, whereas in the Southern Alps, the folds are more open and less abundant, and there is a constant sense of overturning to the south.

Figure 3 - The geometry and orientation of structures recorded in the Tonale Pass area. The f_0 folds in the Central Alps are poorly defined and were formed coeval with the gneissic foliation which then became the dominant planar structure in this area. The f_3 folds show differing vergence north and south of the Tonale Line - the significance is discussed in the text.

	ADAMELLO	SOUTHERN ALPS	STAVEL GNEISS	CENTRAL ALPS
f_o				Formation of gneissic banding parallel to bedding. Poorly defined isoclinal folding with axes plunging SW to W.
f_1		Dominant foliation sub-parallel to bedding. Small-scale, close to isoclinal folds. Axes W to SW.		Biotite foliation sub-parallel to banding. Small-scale tight to isoclinal folds, commonly of quartz veins. Axes plunge E - W and folds verge to S. L_1 lineation common.
f_2				Large to small-scale, open to tight folds restricted to marble bands. No related foliation. Axes plunge moderately SE. Cuspate structures. L_2 lineation in marble.
f_3		Large to small-scale, open to tight asymmetrical folds with a S vergence. Axes plunge gently SW. Locally developed foliation.	Penetrative phengite foliation striking approx. E-W. Strong L_3 sub-horizontal lineation in parts.	Strong foliation in mylonitic zones - associated intersection lineation L_3. Regional to small-scale open to very tight asymmetrical folds generally with a northerly vergence. E - W plunging axes - more rarely plunge to S. Associated thrusts.
f_4				Large to small-scale, open to close chevron folds. Axes plunge to 070° or 250°. Crenulation lineation. Folds locally developed. Weak crenulation cleavage.
f_5	Penetrative biotite foliation striking ENE. Only found near N margin.	Weak biotite foliation in inner hornfels. Small-scale, open to close, S verging folds. Axes plunge gently W to SW.	Medium to small-scale, open asymmetrical folds with a S vergence. Axes plunge gently SW.	Medium to small-scale, open to tight, neutral to southward verging parallel folds. Axes plunge gently E or W. Only locally developed.
f_6	Sub-vertical shear zones(sinistral) trending NE. Late joints.	Kink bands with sub-vertical to steeply SW plunging axes.	Medium-scale, open folds with steep S plunging axes. Kink bands and tension gash arrays.	Small-scale conjugate kink bands locally developed. Regional open folds with steeply plunging axes to the S.

Figure 4 - Relationships between structure and sequence in the Tonale Pass area. The geological history of the area is related to known age dates in other parts of the Alps (see 8.20) and the sequence of structural and metamorphic events is sub-divided into four main periods, Caledonian, Hercynian, Early and Late Alpine.

AGE	CENTRAL ALPS	TONALE LINE	SOUTHERN ALPS
Cambrian or earlier.	Deposition of pelitic sequence with calcareous bands (marls, siltstones, shales, limestones)		
500 m.y. (Cambro-Ordovician)	'Caledonian' deformation and metamorphism to Upper Amphibolite facies (sillimanite grade). Gneissic banding formed. f_0 folding. Quartz veins.		
Upper Palaeozoic	Deposition of fine-grained sandstone, siltstone and minor marble and shale. Serpentine. (N. of Peio Line)		Deposition of siltstone, quartz sandstone and shale. Minor basic dyke intrusion.
295 m.y. (Upper Carboniferous)	'Hercynian' deformation and metamorphism to Lower Amphibolite facies. f_1 folding. Abundant pegmatites (250 m.y.) and minor granitic intrusions.	Probable fault movements. (pseudotachylite formed)	'Hercynian' deformation and metamorphism to Greenschist facies. f_1 folding.
Middle to Upper Cretaceous.	'Early Alpine' deformation and Upper Greenschist to Lower Amphibolite facies metamorphism. f_2 and f_3 folding. Mylonite generation and northward thrusting. Subsequent f_4 folding.	Differential movements. (cataclasite formed) Formation of Stavel Gneiss. (phengite, feldspar)	Greenschist facies metamorphism. f_3 southward facing folds formed.
Eocene-Oligocene.	Hornblende porphyry (andesite) dyke intrusion. Dunite intrusion.		Intrusion of the Adamello Massif at 30-40 m.y.
Middle Oligocene.	'Late Alpine' local deformation and Lower Greenschist facies metamorphism. f_5 folding. Minor mylonites. Uplift.	Fault movements. Minor south verging f_5 folding in Stavel Gneiss.	Deformation of the margins of the Adamello Massif and its aureole.
	Formation of f_6 kink bands and large scale open folds.	Minor lateral movements. f_6 kinks in Stavel Gneiss.	f_6 kink bands formed. Uplift. Joint pattern formed in the Adamello Massif.

In both units, folds are developed on major and minor scales, and the structures are developed prior to calc-alkaline (Southern Alps) and trachytic and ultramafic (Central Alps) intrusives. It is important to note that the directions of tectonic transport differed across the Tonale Line during the f_3 event. The Stavel Gneiss appears to lack f_3 structures. Correlation of f_1 and f_3 structures across the Tonale Line is discussed in section 8.11.

The f_2 and f_4 structures are absent from the Southern Alps. It is possible that the f_5 event in the Southern Alps resulted in the development of the marginal foliation in the Adamello massif and tightening of the pre-existing f_1 and f_3 folds in the contact aureole. The major f_5 uplift and "backfolding" was largely restricted to the Central Alps and Stavel Gneiss units.

f_6 kink bands can be mapped over the whole of the Tonale Pass area, although their axial orientation varies with that of the layering in which they are developed.

1.50 TERMINOLOGY

This section is intended to explain the many abbreviations used in the text and to clarify the specific meaning implied by the author of certain geological terms.

X, Y, Z - the maximum, intermediate and minimum strain ratios respectively, of the strain ellipsoid.

$\sqrt{\lambda}_1, \sqrt{\lambda}_2, \sqrt{\lambda}_3$ - the maximum, intermediate and minimum finite principal strain values respectively.

$\sqrt{\lambda}$ - the amount of strain in any direction.

γ - shear strain, defined as $\tan\psi$ where ψ is the angle of unit shear.

$\sigma_1, \sigma_2, \sigma_3$ - the maximum, intermediate and minimum principal stresses respectively, of any given stress state.

τ - shear stress

e - strain

$\dot{e}$ - strain rate

T - temperature

P - pressure. In the context of metamorphic reactions P is generally taken as P fluid,

which is assumed to equal P total.

P total - total pressure, generally equal to ρ. g.z. where ρ = rock density, g = acceleration due to gravity, and z = depth below the earth's surface.

P fluid - total fluid pressure

P H_2O - partial pressure of water

P CO_2 - partial pressure of carbon dioxide (generally P H_2O + P CO_2 = P fluid)

X H_2O - proportion of water in the fluid.

X - proportion of carbon dioxide in the fluid.

f O_2 - oxygen fugacity. In experimental work this is generally defined by buffer reactions.

F.M.Q. - Fayalite + O_2 Magnetite + Quartz

H.M. - Hematite Magnetite + O_2

N.N.O. - Nickel + O_2 Nickel oxide

f S_2 - sulphur fugacity

planar orientations (e.g. bedding, foliation, joint cleavage) are expressed as, for example, 070/58°SW where 070 is the strike, 58° the dip and SW is the direction of dip of the planar feature.

linear orientations (e.g. lineations, fold axes, slickensides) are expressed as a plunge towards a direction; for example 12° to 174°:

mylonite - the term is used to describe a fine-grained, generally finely-banded rock, in which mineralogical and textural changes are widespread. Mylonite forms from a coarser-grained parent rock in narrow planar zones of high strain. The work in this thesis shows that these zones are site of differential movement. The textural changes result largely from a reduction in grain size and the effects of high rotational strain. Recrystallization and recovery of quartz are the most important processes involved in quartz rich rocks. Feldspar and garnet are fractured and comminuted, although some new growth of both minerals (particularly albite and oligoclase/andesine in the case of feldspar) has occurred in the mylonites described here.

phyllonite - a mylonite of slaty or phyllitic appearance with an average matrix grain size less than 0.05 mm. No mineralogical or metamorphic connotation is implied.

mylonitic gneiss - this refers to a pre-existing pelitic or semi-pelitic gneiss which has a visible superimposed foliation, due to the later f_3 deformation.

recrystallization - the term is used in the sense described by Spry (1969) and Wilson (1973), in that it refers to new grain development as a result of the migration of high angle boundaries.

recovery - in a textural sense, recovery is the result of the movement of dislocations to form sub-grains and ultimately polygonization (Spry, 1969; Wilson 1973).

Metamorphic minerals are designated by symbols for brevity in parts of the text and on several diagrams. The following abbreviations are used:-

Ab	- Albite	Ilm	- Ilmenite
Act	- Actinolite	Kf(Kfsp)	- K feldspar
Alm	- Almandine	Ky	- Kyanite
An	- Anorthite	Lim	- Limonite
And	- Andalusite	Liq	- Liquidus
Anth	- Anthophyllite	Mag	- Magnetite
Ap	- Apatite	Mg.Chl	- Magnesian chlorite
Bi	- Biotite	Mg.Co	- Magnesian cordierite
Br	- Brucite	Micro	- Microline
Ca	- Calcite	Monz	- Monzonite
Chl	- Chlorite	Mu	- Muscovite
Chond	- Chondrodite	Norb	- Norbergite
Clin	- Clinozoisite	Phl	- Phlogopite
Clinochl	- Clinochlore	Ph.Mu	- Phengitic Muscovite
Co	- Cordierite	Pl	- Plagioclase
Ctd	- Chloritoid	Py	- Pyrophyllite
Di	- Diopside	Qz(Q)	- Quartz
Dol	- Dolomite	Ser	- Sericite
Ep	- Epidote	Sill	- Sillimanite
Fe.Co	- Iron cordierite	Sph	- Sphene
Fo	- Forsterite	St	- Staurolite

Ga	- Garnet(Alm.rich)	Ta	- Talc
Gehl	- Gehlerite	Tourm	- Tourmaline
Geoth	- Geothite	Trem	- Tremolite
Grand	- Grandite	Vap	- Vapour
Gross	- Grossularite	Ves	- Vesuvianite
Hb	- Hornblende	Wo	- Wollastonite
Hem	- Hematite	Zir	- Zircon

2.00 ADAMELLO MASSIF

2.10 INTRODUCTION

The Adamello massif is a composite intrusive body composed of tonalite, quartz diorite, granodiorite and minor leucocratic members. The massif is approximately 36 km. wide at its northern margin of outcrop, tapering to 12 km. towards the south west. Part of the northern margin of the massif lies within the area studied. The distributions of rock types in the massif and the surrounding rocks are shown in Figure 5.

Trener in 1904 recognised the basic subdivisions of the Adamello massif and more recent work (Bianchi and Dal Piaz, 1940; Bianchi et al, 1970) have amplified the number of subdivisions and described their petrology in great detail.

The general surface outcrop form of each recognizable unit in the northern half of the massif is ovoid. As these intrusions are separate bodies, it is apparent that the youngest body is the biotite-quartz-diorite east of Cima Presanella. The tonalite surrounding this body in turn post-dates the larger mass of biotite-quartz-diorite to the south. The granodiorites, leucotonalites, granites etc. in the southern part of the Adamello massif probably post-date the tonalite and biotite-quartz-diorite.

In outcrop the tonalite and biotite-quartz-diorite are massive, widely-jointed and weather to form the higher more rugged topography in the area mapped. The tonalite crops out in the south eastern part of the area mapped, and forms the summits of Cima Busazza (3326m.), and Cima Presanella (3558m.), which both lie a few kms. south of the area. The biotite-quartz-diorite which crops out in a tongue-shaped area south and east of the Tonale Pass, generally forms less angular topography than the tonalite although it forms the summit of Punta di Castellaccio (3029 m).

2.11 Contact Relationships.

The Adamello massif is intrusive into pelitic

Figure 5 - Map of the differing rock types which comprise the Adamello Massif. The foliation shows a greater degree of development in the later plutons in the northern part of the Massif. The interference pattern shown, suggests that later individual plutons have risen in approximately the same position as earlier ones.

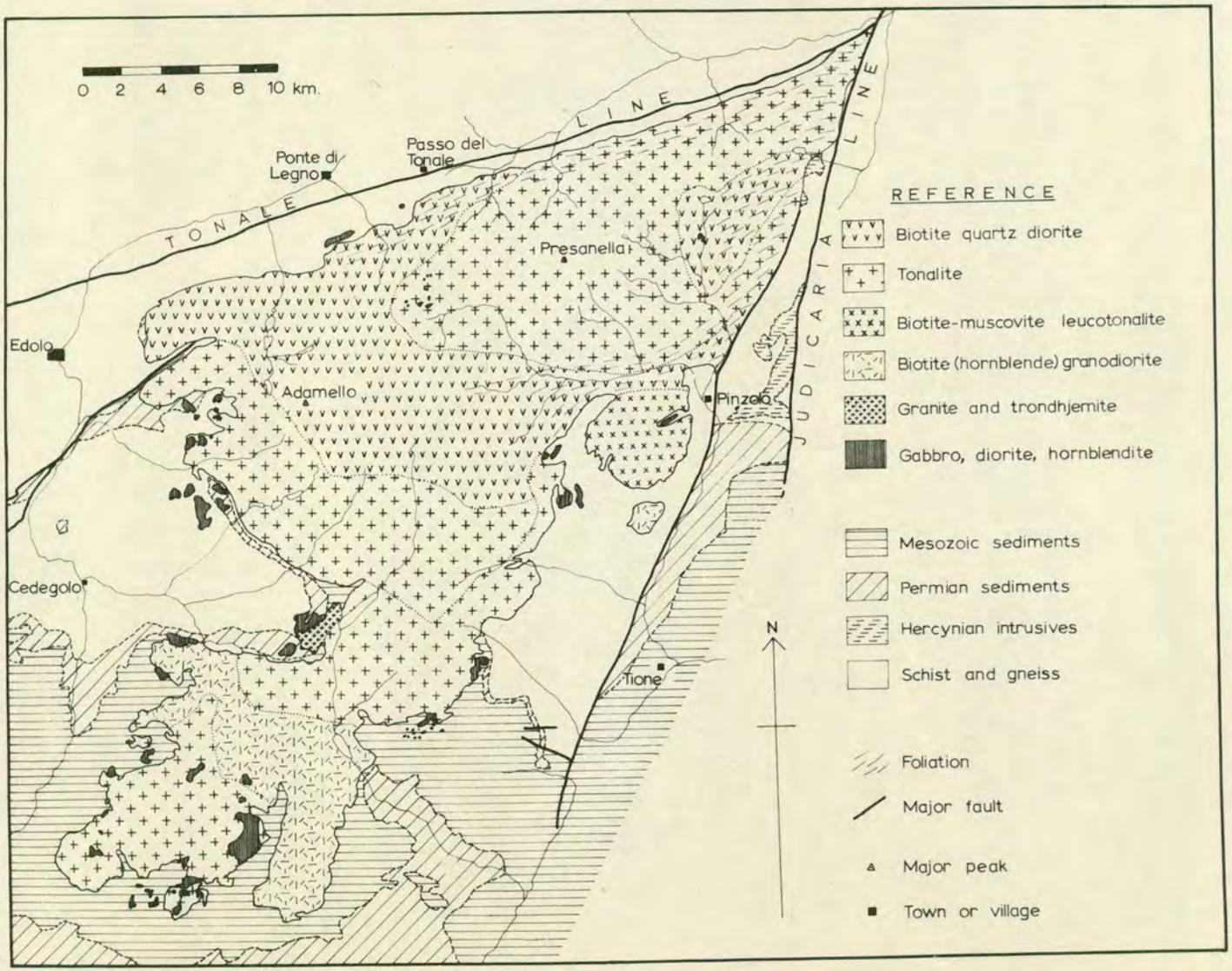
0 2 4 6 8 10 km.
TONALE LINE
Ponte di Legno
Passo del Tonale
Presanella
Edolo
Adamello
Pinzolo
JUDICARIA LINE
Cedegolo
Tione
N
REFERENCE
Biotite quartz diorite
Tonalite
Biotite-muscovite leucotonalite
Biotite (hornblende) granodiorite
Granite and trondhjemite
Gabbro, diorite, hornblendite
Mesozoic sediments
Permian sediments
Hercynian intrusives
Schist and gneiss
Foliation
Major fault
Major peak
Town or village

schists and psammites of the Edolo Schists in its northern part, and into Permian and Mesozoic sediments in its southern part. In the area mapped, only contacts with the Edolo Schists were observed. The Linea della Gallinera, a prominent northeast trending lineament in the Edolo Schists and Permo-Mesozoic sediments, is truncated by the Adamello massif at its north-eastern intrusive margin. In contrast, the Tonale Line and Judicaria Line appear to control the tectonic position of the Adamello massif. 1.5 km. southwest of the Tonale Pass, the biotite-quartz-diorite/Edolo schists contact dips 60° to 70° north over a vertical distance of 150 m., although local variations are present. Although the intrusion locally truncates the quartzites and semi-pelites of the Edolo Schists sequence, its northern contact trends sub-parallel to the regional strike of the Edolo Schists.

The contact between the tonalite and biotite-quartz-diorite is well-exposed at M459 in the Val Presena. The contact locally dips 65° to 75° E. with fine grained tonalite, containing 2 to 5 mm. biotite plates but only small hornblendes, forming the marginal phase of the tonalite. Neither rock type shows any visible tectonic or flow foliation. The later tonalite intrusion has caused no apparent effects in the biotite-quartz-diorite. There is a distinctive change in xenolith compositions across the tonalite / biotite-quartz-diorite contact. Uniformly fine-grained, mesocratic biotite-feldspar-quartz-hornblende xenoliths are restricted to the tonalite, whereas those in the biotite-quartz-diorite show more compositional variation with fine-grained leucocratic biotite-quartz-feldspar, quartzite, and quartz-biotite - andalusite (sillimanite) xenoliths common.

2.12. Relationship with 'Peri-Adriatic' Suite.

The Adamello intrusion shows chemical, textural and mineralogical similarities with the 'Peri-Adriatic' Suite (Karl, 1959), a series of tonalite and granodiorite intrusions. These bodies lie near the Tonale-Judicaria-

Pusteria-Gailtal Lineament which has acted as a major structural control on their intrusion. The exceptions to this statement are the Rieseferner and Wollanerköpf instrusions near the Austro-Italian border (near Brunico), which lie north of the Pusteria Line. The intrusives, with the exception of the Adamello, Reiseferner and Wollanerköpf bodies, have been shown to be Permo-Carboniferous (Hercynian). Borsi et al (1972) obtained Rb-Sr whole rock isochron ages of 275±4 m.y. for the Mt. Croce massif, 281±6 m.y. for the Bressanone massif and 291±2 m.y. for the Ivigna massif. A similar age of 274±9 m.y. (Rb-Sr whole rock) was obtained for the Mt. Sabion granodiorite (Borsi et al, 1966) which lies almost adjacent to the Adamello massif. These intrusions are associated with the extensive Early Permian volcanism which in the Bolzano area of N.Italy is represented by a sheet of ash flow tuffs, and minor agglomerates and lavas, 65 km. by 60 km. and 1 km. thick (Rutten, 1969, p. 333; Maucher, 1960).

Biotites from tonalite and granodiorite in the Hercynian Mt. Sabion and Bressanone massifs give Rb-Sr ages of 31±10 m.y. and K-Ar ages of 41 m.y. (Borsi et al, 1972) where a strong Alpine foliation is developed. Rb-Sr and K-Ar ages from biotites in various parts of the Adamello massif (Mt.Adamello, Mt.Sostino, Corno Alto) range from 45±2 m.y. to 31±3 m.y. (Borsi et al, 1966). Chessex (1962) obtained a zircon alpha particle activity age of 39 m.y. These tonalites and granodiorite specimens showed no internal deformation. These ages agree with those obtained by Gulson (1973) from U-Pb ratios in sphene, monazite, allanite and zircon, from the Bergell granodiorite. Zircons contain an old Pb component and their original age may be interpreted as 90 to 150 m.y. No overgrowths are seen on the zircons and the true age of intrusion is 30 m.y. (Gulson, 1973). The nearby Novate Granite gives a poor Rb-Sr isochron age of 25 m.y. (Gulson, 1973). Wenk (1973) has questioned the validity of the Late Alpine age of the Bergell granodiorite and has shown that the body contains a

varied sequence of structures and "cataclastic" features. It is possible that these structures are equivalent to those of the f_5 event in the Tonale Pass area, and hence the Bergell and Adamello intrusions would then be of similar age. The f_5 event is represented in the Tonale area by upward facing open to tight folds, development of mylonites (e.g. Peio Line) and development of the foliation in the marginal parts of the Adamello massif. Biotite and zircon alpha particle activity ages for the Bergell granodiorite are consistently lower than sphene, monazite etc. U-Pb ages, suggesting that they record a subsequent uplift event at about 24 m.y. (Chessex, 1962; Armstrong et al, 1966). The only other documented Alpine intrusions outcrop near Biella, west of Lake Maggiore, where diorite and monzonite give consistent Rb-Sr and K-Ar biotite ages of 29 - 33 m.y. (Carraro and Ferrara, 1968). These intrusions are partly fault controlled and lie a few kms. south of the Insubric Line in a similar tectonic position to the Adamello massif. Andesitic volcanism is locally developed in the Western Alps and this has also been dated at around 30 m.y.

2.20 TONALITE

2.21 Introduction

The tonalite is well-exposed in the Val Presena, approximately 1.25 km. south of the intrusion margin. It is a massive, medium-grained black and white mesocratic rock with a colour index of 27 (% of biotite + hornblende + accessories). Large tabular hornblende prisms up to 1 cm. long (average 5mm.) lie in a matrix of biotite plates 2 to 4 mm. in diameter, plagioclase, quartz, and minor orthoclase and accessories. The hornblendes show a crude alignment which defines a weak flow foliation trending 075° to 085°; approximately parallel to the tonalite/biotite-quartz-diorite contact.

2.22 Xenoliths

Uniformly fine-grained mesocratic biotite-quartz-feldspar xenoliths, commonly with small hornblende laths,

and more rarely with andalusite or sillimanite are common in the tonalite. These latter two minerals are only found in xenoliths near the tonalite/Edolo schists contact in the area 2 km. south west of Stavel. The xenoliths range from 1.5 to 25 cm. in diameter and constitute about 3% of the tonalite (2% to 10%) with more xenoliths found near the intrusion margin. They generally contain more biotite than the enclosing tonalite, presumably reflecting the initial xenolith composition and its progress towards equilibrium with the saturated components of the magma (biotite and hornblende at high temperatures) (Bowen, 1928). The constant composition and lack of internal structure suggests that these xenoliths may represent absorbed biotite-quartz-diorite into which the tonalite has been intruded. In the upper Val Presena, 1 to 2 m. wide, angular, coarse grained xenoliths which consist of about 45% euhedral hornblende (average 1 cm. long), about 35% plagioclase, subsidiary biotite, minor quartz and accessories are present in the tonalite. These probably represent residual dioritic fractions of the tonalitic magma.

The biotite-quartz-feldspar (hornblende) xenoliths have a variable rounded to sub-rounded shape and in many places the flow foliation diverges around the xenoliths. Strongly elongate xenoliths generally lie within a few degrees of the foliation plane. Irregularly orientated hornblende crystals occur in a zone leading from the ends of many xenoliths, in a manner similar to flow line patterns resulting from slow laminar flow around a fixed object. Average foliation shape is 1.2 : 1.05 : 1 (A : B : C) taking A as the line of maximum dip of the flow foliation and A and B as lying in the plane of the foliation. The xenoliths become progressively more deformed towards the northern margin of the tonalite intrusion, accompanied by the development of a tectonic foliation.

In the more central parts of the tonalite intrusion around Cima Presanella, the tonalite is coarse-grained with tabular hornblende prisms up to 2 cm. long (average

1 cm.) and 1 cm. wide (average 0.5 cm) in a matrix of quartz, plagioclase, biotite, orthoclase and accessories. Xenoliths are less abundant but larger in size (up to 3 m. in diameter) and are commonly near spherical in shape. Small hornblende laths are ubiquitous in these xenoliths. In some parts a weak flow foliation is present.

2.23 Mineralogy.

In thin section, euhedral to anhedral green hornblendes with small biotite and plagioclase inclusions lie in a matrix of euhedral andesine, partially corroded zoned plagioclase, large biotite flakes, euhedral quartz and minor orthoclase with accessory apatite, monazite, zircon and magnetite.

The hornblendes show rare simple and lamellar twinning (parallel to 100) and are pleochroic, α very pale brown, β mid-olive green, γ dark green. They are biaxial negative with a high 2V. The presence of biotite, andesine and monazite inclusions show that hornblende growth occurred when small andesine, biotite and monazites were already present in the magma. Typical hornblendes from calc-alkaline rocks have Mg/Fe^{2+} of about 1 and a moderate content of Al($\sim$1.5Al) (Deer et al, 1966). The observed optical properties are consistent with a hornblende of this composition. In some specimens high relief, brown (γ) to dark green (β and α) pleochroic anhedral hornblendes (biaxial negative, moderate 2V) are present. These more Fe^{2+} rich hornblendes are later than the euhedral hornblendes, biotite and some plagioclase. Rarely hornblende shows a simple two phase zoning with the marginal zone enriched in Fe^{2+}. The presence of two hornblendes of differing composition is readily explained by considering the cooling history of tonalitic magma. Hornblendes in gabbroic rocks show a typical Mg/Fe^{2+} ratio of 3 whereas those in granites typically show a ratio of $\sim$0.05 (Deer et al, 1966). There is a systematic increase in Fe^{2+} content in hornblendes as the magma becomes more acid and crystallises at lower temperatures. Since

tonalitic magma becomes progressively more sodic and acidic as magma temperature falls, we would expect a change in hornblende composition towards Fe^{2+} enrichment. The presence of two separate phases cannot be simply explained and kinetic and miscibility factors may be important.

Zoned plagioclases, 0.2 to 2 mm. long, are abundant in the tonalite. In many of the Hercynian 'Peri-Adriatic' intrusions zoning is preserved by gefüllte plagioclase (Karl, 1959; Cliff et al, 1971). Small clinozoisite and white mica microlites partially replace the original plagioclase and yet still preserve a zoning pattern. This alteration seems to be typical of Permo-Carboniferous tonalitic intrusions which have been subjected to Alpine Greenschist facies metamorphism.

The zoning observed in the tonalite of the Adamello Massif is oscillatory normal (Vance, 1962). The inner core compositions range from bytownite to labradorite, as shown by extinction angle, relief and nature of the interference figure. Bianchi et al (1970) have recorded core compositions up to An_{85} (high bytownite). In the area studied, the majority of cores have a relatively constant composition of about An_{65}. Since the Val Presena outcrops lie near the tonalite intrusion margin, these compositions are probably atypical of the whole body. A specimen taken adjacent to the contact (M390) shows fragmented and corroded zoned plagioclase with rims of about An_{32} and cores of about An_{60}. The more sodic rims generally have a composition of An_{39-43}. Oscillatory zoning between An_{40} and An_{50-55} is very common in the outer parts of these phenocrysts although the marginal zones show gradational normal zoning. Zoned plagioclase crystals have commonly been partially corroded by matrix andesine, quartz and orthoclase. In many cases, the crystal cores also show patchy zoning (see Vance, 1965). Variable amounts of the labradorite core have been replaced by optically continuous more sodic plagioclase, whose composition is identical to that of the innermost oscillatory zone. Poikilitic inclusions of quartz are

found in these sodic patches. A brief review of the origin of normal, oscillatory and patchy zoning is given in appendix 1. These features are in accord with the slow uprise of a low H_2O content magma.

The matrix feldspar laths in the tonalite range in composition from An_{37} to An_{48} (Michel-Levy method), averaging An_{41}. Albite twinning is very abundant in these laths. Compositions up to An_{55} are reported from the central part of the intrusion (Bianchi et al, 1970) and rarely small labradorite laths up to An_{61} are present in tonalites from the Val Presena. Minor sericitic alteration has occurred in some specimens.

Biotites form approximately equidimensional plates 0.01 to 5 mm. in diameter (generally 1.6 to 2 mm.) They are foxy-brown, suggesting a high Ti/Fe^{3+} ratio (Deer et al, 1966), strongly pleochroic (very pale to dark brown) and apparently typical of intermediate igneous biotites. Abundant apatite and minor zircon and monazite inclusions are present, the latter two minerals commonly with associated pleochroic halos. Kinking and "recrystallization" are common in biotites where the later tectonic foliation is present. Some minor open kinks are present even in the apparently undeformed tonalite. Minor chloritic alteration is common. Later, angular green biotite (high Fe^{3+} content) flakes, up to 0.2 mm. across, have grown adjacent to the brown biotites in most tonalite specimens.

Quartz forms large anhedral grains 0.5 to 5 mm (average 3 mm.) across, in which faint strain shadows are present. Rarely, sub-grain mosaics can be seen even in the apparently undeformed tonalite.

Potash feldspar forms small irregular anhedral grains generally associated with quartz aggregates. No sericitic alteration is seen. Potash feldspar and quartz commonly corrode hornblende and calcic plagioclase.

Epidote is developed both as a replacement mineral of the calcic cores of zoned plagioclase (grains 0.02 to 0.1 mm. across), and as late stage larger anhedral grains up to 1 mm. across. These latter grains are invariably developed adjacent to hornblende, biotite or chlorite,

and plagioclase, suggesting that epidote grows as a result of localised diffusion of iron from the ferromagnesium minerals and Ca and Al from calcic plagioclase. Apatite rarely occurs in the tonalite matrix. Accessory magnetite and rare calcite are also generally present.

2.30 BIOTITE-QUARTZ-DIORITE.

2.31 Introduction

The biotite-quartz-diorite is exposed in the Punta di Castellacio - Monticello range south of the Tonale Pass. It is a massive, black and white mesocratic to leucocratic rock with a colour index of 20 (% of biotite + accessories). Biotite plates up to 5 mm. across (more generally 2 mm.) define a weak foliation and lie in a matrix of plagioclase, quartz, minor orthoclase and accessories. Within 1.1 to 1.5 km. of the biotite-quartz-diorite intrusive margin, a tectonic foliation is developed, which becomes progressively more intense as the margin is approached. 620 m. northwest of the summit of Punta di Castellacio, this foliation discordantly cuts the locally irregular biotite-quartz-diorite/quartzite contact. Hence it cannot be a flow foliation. As the foliation is superimposed on the marginal parts of both the biotite-quartz-diorite and tonalite intrusions, irrespective of their relative contact orientations, it must postdate both intrusions. The marginal 100 m. of the biotite-quartz-diorite is more leucocratic and significantly more quartz-rich than the central part of the intrusion.

2.32 Xenoliths

Xenoliths are very abundant in the biotite-quartz-diorite and show large size and compositional variations. In the marginal 50m. of the intrusion, large angular xenoliths of hornfelsed quartzite and more rarely pelitic rocks up to 100m. long (average 6m.) are present (M159, T96). These xenoliths may retain their original structures in their central parts and show only partial assimilation into the magma. At T96, abundant pyrite was seen in a large pelitic xenolith.

More commonly, smaller more rounded xenoliths, 1 to 30 cm. in diameter (rarely up to 2 m. long) are present. These are generally mottled black and pale grey, fine grained, and consist of quartz-feldspar-biotite with subsidiary andalusite and sillimanite common. More rarely, elongate to angular grey quartzitic xenoliths are seen. Tight folds are preserved in some xenoliths with quartz-rich bands outlining the fold profile. The xenoliths in the tectonically undeformed parts of the biotite-quartz-diorite disrupt the very weak foliation, showing that some effects are due to flow foliation. Rounded fine-grained xenoliths rarely show biotite depleted zones around them. For example, at M458 B, a 2cm. wide zone of biotite depletion surrounds a 10.5 cm. diameter rounded fine-grained biotite-rich quartz-feldspar-biotite xenolith. This implies that the biotite has grown preferentially in the xenolith, owing to favourable chemical and physical factors (e.g.f O_2,P H_2O, kinetic factors, temperature). The fact that biotite has not been replenished in this outer margin shows that virtually no mixing has occurred since the time of biotite formation at $\sim 860^{\circ}C$ (Piwinski and Wyllie, 1968). Diffusion rates in the cooling magma must also be too small to eliminate the depletion zone, and fluid movement cannot be important in the magma.

Plate 2 shows a large deformed biotite-rich xenolith in the foliated marginal zone of the biotite-quartz-diorite. When the foliation is very weak, the elongate xenoliths generally still lie within the foliation plane. This suggests that there may be a weak flow foliation which has caused some preferred orientation prior to the later tectonic effects.

2.33 Mineralogy.

In thin section, the biotite-quartz-diorite consists of euhedral, partly corroded, zoned plagioclase and biotite flakes in a matrix of euhedral andesine, anhedral quartz, minor potash feldspar and accessory epidote, chlorite, ilmenite, magnetite and apatite.

Plate 2 - Large deformed biotite rich xenolith in the foliated marginal zone of the biotite - quartz - diorite (M193). The xenoliths generally show an oblate ellipsoidal shape when deformed and the plane of flattening is coincident with the biotite foliation. Xenoliths in biotite - quartz- diorite show relict metasedimentary features, unlike many of those in the tonalite.

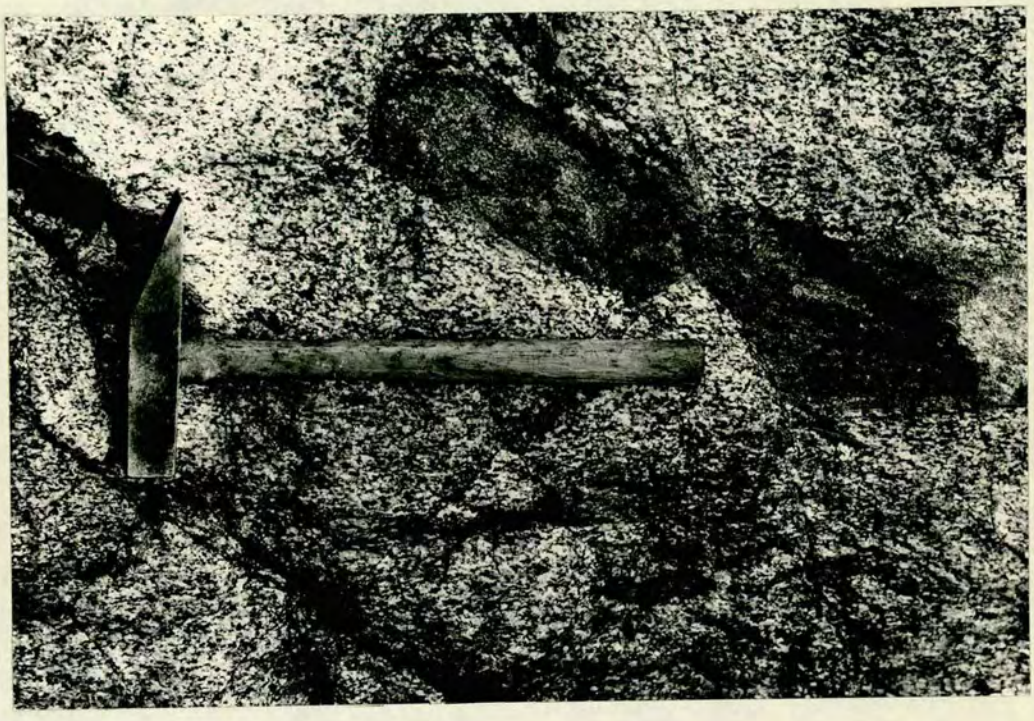

The zoned plagioclase crystals vary in width from 0.2 to 1.5 mm., and resemble those found in the tonalite. Calcic cores up to high labradorite (An_{65}) are almost always surrounded by oscillatory-normal zoned rims (An_{55-45} generally). The marginal normally zoned outer rims have a composition An_{45-40}. Many zoned plagioclases show patchy zoning. The more sodic plagioclase is ~An 45 whereas the unreplaced parts of the cores are ~An_{60-65}. (estimates based on relief, biaxial interference figures, 2V and extinction). Small quartz and sericite (? altered potash feldspar) poikilitic inclusions occur in the more sodic patches. These features are explained in the preceding section on the tonalite.

Approximately rectangular, commonly albite and more rarely pericline twinned andesine and labradorite laths make up the largest single component of the biotite-quartz-diorite. Although their composition ranges from An_{40} to An_{45}(average An_{42}) as determined by optical methods (Michel-Levy) this may be only typical of the marginal parts of the intrusion. Bianchi et al (1970) record consistently higher values for the anorthite content. In some thin sections of the biotite-quartz-diorite, small labradorite grains (An_{61} approx.) are present and more rarely small corroded bytownites (An_{75}, μ>labradorite, biaxial -ve, 2V~85°) grains are found.

2.40 CHEMICAL AND MINERALOGICAL COMPOSITION.

The chemical and mineralogical composition of the tonalites and biotite-quartz-diorites is fairly typical for calc-alkaline intrusive igneous rocks (Figure 6). The silica content is somewhat lower than is normally found (see Krauskopf 1967). The compositions given in Figure 6 are taken from Bianchi et al (1970).

2.50 GENESIS OF THE TONALITE AND BIOTITE-QUARTZ-DIORITE.

2.51 Summary of proposed mechanisms

The origin of tonalite and granodiorite (calc-alkaline to granitic) magmas has been the subject of much controversy. Such magmatic bodies are typical of

Figure 6 - Chemical and mineralogical composition of the intrusive rocks of the Adamello Massif, within or adjacent to the area mapped. The values are taken from Bianchi et al, (1970).

Mineralogical and chemical composition of intrusive rocks of the Adamello Massif (Bianchi et al, 1970).

Mineralogical Composition.

	Plagioclase (with % An)		Quartz	K feldspar	Biotite	Hornblende	Accessories
Tonalite (53 specs)	48.7	(49)	21.5	2.7	15.2	10.5	1.4
Biotite quartz diorite (25 specs)	47.7	(48)	28.9	3.1	17.9	1.2	1.2
Leucotonalite (12 specs)	53.2	(46)	25.6	4.5	10.5	5.4	0.8

Chemical Composition.

Oxide	PR 24 to'	PR 16 to'	PR 4 to'	AC 14 qd'	AC 13 qd'
SiO_2	59.95	61.90	58.68	63.38	64.41
Al_2O_3	17.28	16.66	17.53	17.18	17.54
Fe_2O_3	0.78	1.39	1.22	0.46	0.30
FeO	5.44	4.22	4.92	4.33	4.33
MnO	0.14	0.13	0.13	0.10	tr.
MgO	2.98	2.53	3.35	2.12	2.18
CaO	6.31	6.22	6.91	4.83	4.58
Na_2O	2.55	2.65	2.67	2.91	2.64
K_2O	2.04	2.48	1.66	2.58	2.24
TiO_2	0.85	0.62	0.73	0.61	0.62
P_2O_5	0.18	0.03	0.12	0.10	0.04
H_2O^+	1.45	0.85	1.67	1.02	1.06
H_2O^-	0.11	0.36	0.21	0.10	0.02
total	100.06	100.04	99.80	99.72	99.96
	Foliated tonalite Lago Barco	Tonalite Rif Segantini Val d'Amola	Tonalite Val Presena	Foliated biotite-quartz-diorite Laghi di Monticello, Passo Paradiso, Tonale.	Biotite-quartz-diorite N.W. face of Punta Intelvi, U. Val Seria.

continental margin orogenic belts, and a gradation from dioritic or tonalitic magmas near the coast to more K_2O rich granitic magmas inland is seen in western North America (Bateman and Dodge, 1970; Moore et al, 1963) and the Andes (James, 1971). A similar pattern is seen in andesites in Island Arcs (Kuno, 1960; 1968; Miyashiro, 1972) with K_2O increasing away from the trench. Hatherton and Dickinson (1969) and Jakes and White (1970) found that K_2O content was directly proportional to the depth of the underlying Benioff zone. Hence it is tempting to relate calc-alkaline magma generation to plate subduction. The major theories for the origin of calc-alkaline magmas are:-

1) Contamination of basic magmas by assimilation of crustal material or mixing with acidic magmas (Larsen,1938; Piwinski, 1968).

2) Partial melting of sialic crustal material (Fyfe,1973; Brown, 1973; Turner and Verhoogen, 1960).

3) Fractional crystallization of basaltic magmas (Bowen, 1928; Osborn 1962).

4) Partial melting of wet peridotitic mantle (Kushiro, 1973; Osborn, 1962; Yoder, 1969; O'Hara, 1965; Lambert and Wyllie, 1970).

5) Partial melting of crustal or mantle materials (lithospheric plate) in subduction zones (T.H.Green and Ringwood, 1968; Dickinson, 1960).

Recent summaries (Wyllie, 1973; Boettcher, 1973) have favoured the connection of plate tectonics and magma generation but differ as to the effects of water and depth of generation. Jakes and White (1970) and Boettcher (1973) favour the progressive dehydration of amphiboles to $\sim$90 k.m. and phlogopite to $\sim$175 km. to account for the trace element distribution data and K_2O and TiO_2 enrichment inland. The water released may melt the subducted plate or more probably cause partial melting of the overlying mantle material. The possible influence of frictional heating at the subducted plate - mantle contact is discussed quantitatively by Turcotte and Schubert (1973).

2.52 Formation and mode of emplacement of Calc-alkaline magma

The pressure, temperature and P H_2O conditions prevailing at the time of calc-alkaline magma generation have been experimentally determined by several workers (T.H.Green and Ringwood, 1968; Piwinski, 1968; Piwinski and Wyllie, 1968; Harris et al, 1970). These are given in Figure 7(a). Cann (1970), Brown (1971), and Fyfe (1973) have all presented cogent theoretical arguments to show that such a magma cannot be water saturated at least during its rise in the crust. The initial water content of calc-alkaline magmas is reasonably well-known. Boyd (1961) has shown that intermediate ignimbrites generally contain $\sim 4\%$ H_2O and Eggler (1972) has deduced that andesitic lava from Paracutin, Mexico, contained $2.2 \pm 0.5\%$ water at its time of eruption. Brown (1973) found from field and experimental studies that 10% to 12% H_2O is needed to saturate granite melts whereas only 2% H_2O is a reasonable approximation for initial tonalitic melts. Roedder and Coombs (1967) have shown that two immiscible fluids may be found in sodic granite, a sillicate rich fluid with minor CO_2 and fluorite, and a H_2O-CO_2-NaCl fluid. Hence a considerable proportion of the magmatic fluid may be CO_2. If partial melting occurs, then Tuttle and Bowen (1958) showed that the amount of partial melting is related to availability of water and P,T. conditions. Thus if a tonalite melt forms, large quantities will be obtained in comparison with granite melts since only 2% to 4% H_2O is needed for saturation.

Fyfe (1971, 1973) has shown that if partial melting occurs, then small melt fractions will rapidly rise and coalesce until the zone of solid crustal or mantle material is attained. The asthenosphere, which is generally thought to be a zone of partial melting, has a viscosity of about 5×10^9 poise(Nur, 1974) based on earthquake relaxation spectra phenomena and post-glacial rebound. The melt will accumulate until a cooler zone is reached, where the high viscosity ($\sim 10^{21}$ poise) will prohibit the rise of melt fractions at any feasible

Figure 7(a) - Mineral stabilities with reference to pressure (P H_2O) and temperature (T) during melting of tonalite.~~component~~. The percentage melt for given pressures (P H_2O) is also graphically plotted against temperature. The hypothetical curve for the Adamello tonalite is extrapolated from published data (Piwinski 1968; Harris et al, 1970)

Figure 7(b) - Pressure (P H_2O) and temperature (T) relations for tonalite melts (solidus and liquidus) with various water contents. The Adamello tonalite is thought to have risen through the upper crust with decreasing water pressure.

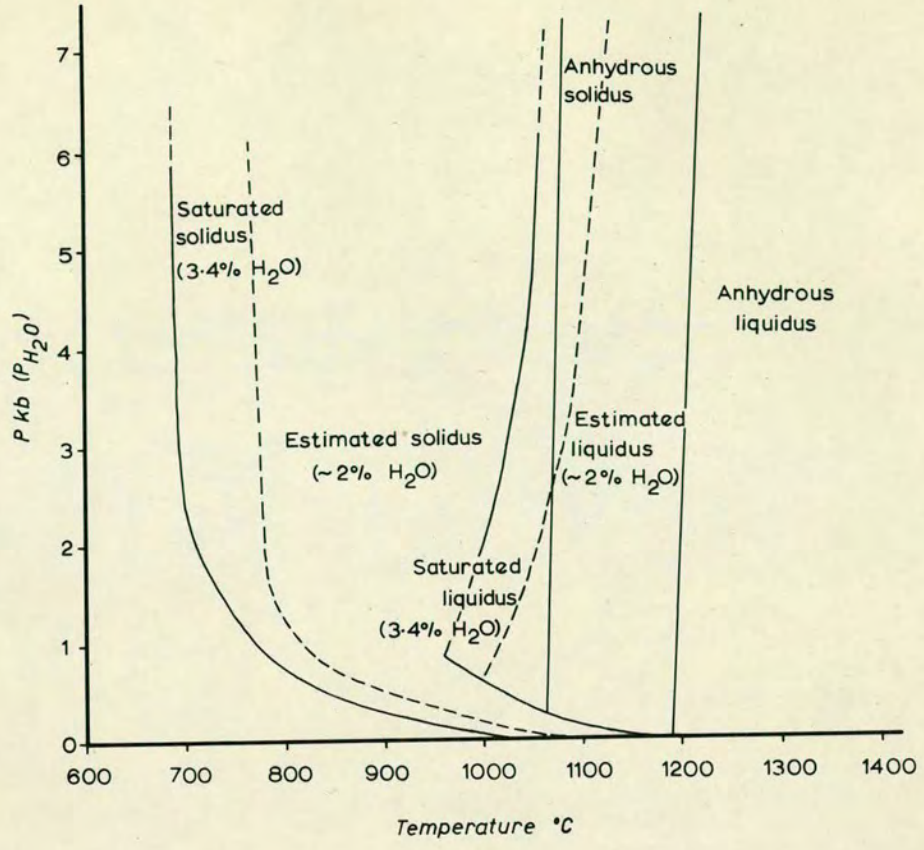
Anhydrous solidus
Saturated solidus (3·4% H_2O)
Anhydrous liquidus
Estimated solidus (~2% H_2O)
Estimated liquidus (~2% H_2O)
Saturated liquidus (3·4% H_2O)
P kb (P_{H_2O})
Temperature °C

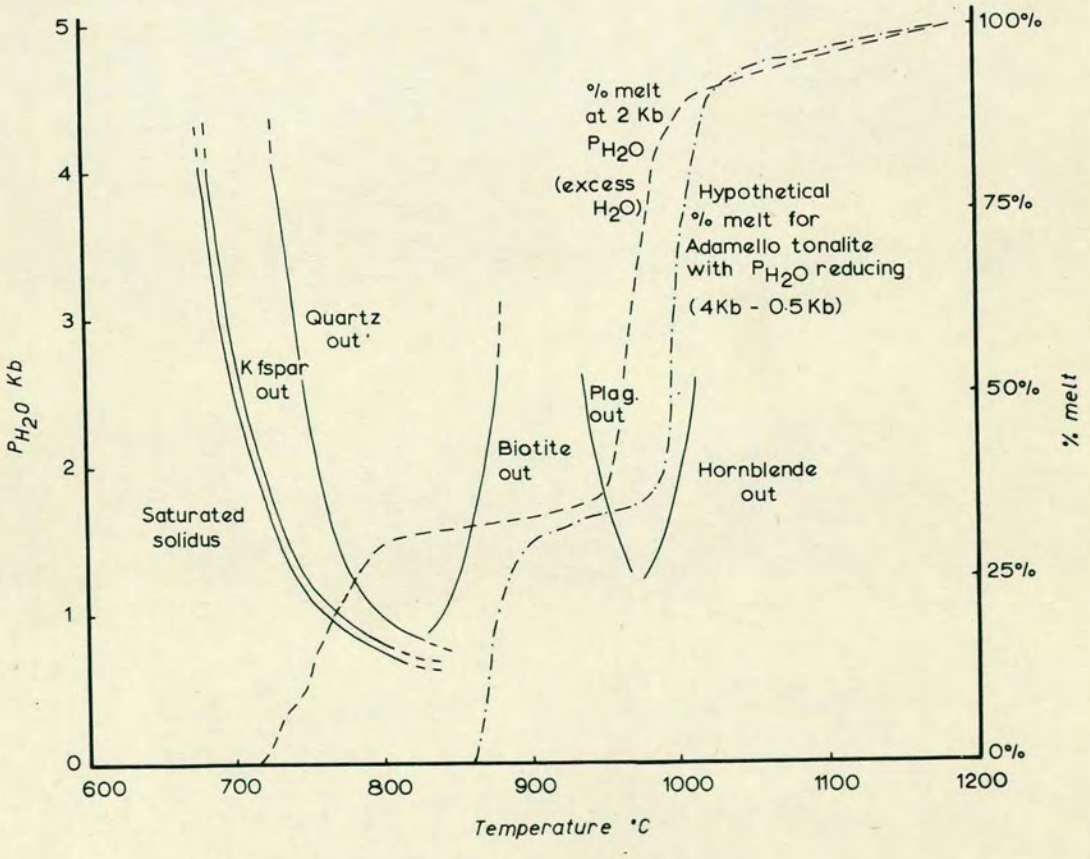
% melt at 2 Kb P_{H_2O} (excess H_2O)
Hypothetical % melt for Adamello tonalite with P_{H_2O} reducing (4Kb - 0·5Kb)
Quartz out
K fspar out
Plag. out
Biotite out
Hornblende out
Saturated solidus
P_{H_2O} Kb
% melt
Temperature °C

geological rate. When the melt accumulation becomes large enough, a density instability is set up (Ramberg, 1967) and a pluton forms in a manner analgous to a salt dome. Observations from Peru show that the rate of pluton rise through the crust is about 1 - 2 cm/year (Fyfe, 1971). Although these calculations are based on very crude approximations of movement (Stokes Law, Taylor instability theory), they nevertheless give some quantitative idea of the stages involved in pluton formation.

Problems arise with a multiple intrusion if it may be approximated to a number of separate "bubbles". The bubbles must absorb or displace each other unless they lie at basically different crustal levels. If the intrusion takes place by a series of separate emplacements, we may expect the first pluton to be relatively large, to have initiated a large enough instability for diapiric uprise, and to penetrate only to moderately high crustal levels due to contact and assimilation effects. Later intrusions may be smaller, because by using the same channel, they would rise through pre-heated material (hence more ductile) and penetrate the original pluton. They would rise until cooling and pressure reduction together with assimilation and high country rock viscosity caused crystallization. Smaller plutons may thus lie within larger bodies. The extra volume due to intrusion must be taken up by displacement and strain in the surrounding rocks. Geological evidence from the Sierra Nevada Batholith (Hyndman, 1972, p.143) suggests that plutons generally rise by a buoyancy mechanism with only minor assimilation.

Several workers (Smith, 1960; Geze, 1962; Tabor and Crowder, 1969) have recorded instances of "granitic" plutons breaking the surface to form volcanic materials. Pressure decrease may cause dehydration to occur and any appreciable CO_2, HCl, S, etc. gas content in the magma will also result in H_2O undersaturation. Low water or undersaturated melts in the crust may be expected to form ignimbrites or ash flow tuffs in particular circumstances. Maucher (1960) has shown

that the Permian Bolzano porphyries consist of quartz latite to trachyandesite ignimbrites with agglomerates and lavas. Assuming that about 70% of the porphyries are ignimbrites or ash flow tuffs, then a sphere of radius 8.7 km. would be needed to supply the amount of material required. This value is of the same order as the average pluton size in the Sierra Nevada (8 km.), Saudi Arabia (10 km.) and Adamello Massif (8.5 km.). The composition of the 'porphyry' sequence is consistent with a bulk tonalite composition.

2.53 Conditions of emplacement.

In order to obtain quantitative values for the contact temperatures and aureole time - temperature relations, it is necessary to estimate intrusion and solidification temperatures. The crystallization of plagioclase is the critical factor regarding the melt-crystal fraction. The presence of corroded and oscillatory zoned plagioclase show that pressure and temperature were lowered by pluton rise during their growth. The growth of matrix plagioclase of composition An_{41} suggests temperature of around 1000°C at intrusion (Tuttle and Bowen, 1958), assuming a low water content of about 3% and hence a water pressure at crystallization of 0.5 to 1.5 kb. (Harris et al, 1970). Tonalite melting relations determined with excess water by Piwinski (1968) show that plagioclase An_{41} goes out at temperatures of 950°C at P H_2O of 1.5 kb. The proportion of melt changes rapidly around this temperature from about 85 % melt to about 30% melt (P H_2O = 1 kb) dependent on plagioclase composition and the exact modal composition of the tonalite or biotite-quartz-diorite. Figure 7(b) shows the estimate of % melt for the Adamello Tonalite. The graphs given by Piwinski (1968) suggest that at 0.5 kb P H_2O, temperatures of the order of 960°C to 1000°C are reasonable for the commencement of plagioclase crystallization; and hence virtual cessation of magma rise. This value is about 100°C above the saturated solidus at 0.5 kb (Piwinski and Wyllie, 1968; Harris et al,1970).

Hence 960°C to 860°C is a reasonable estimation of the temperature range for tonalite and biotite-quartz-diorite crystallization, assuming a decrease in P H_2O as magma rise occurs. Detailed work on major and trace elements from biotites in tonalites (Alberquerque, 1973) showed that they crystallized at temperatures around 800°C with a buffered oxygen fugacity (f O_2) of 10^{-14} to 10^{-15}, close to the F.M.Q. buffer. Rutherford (1973) has shown that Al-Fe biotites will be stable in undersaturated rocks up to 860°C if P H_2O>2Kb and f O_2 lies on the F.M.Q. buffer. Although these data cannot be applied to the silica saturated tonalite-quartz-diorite systems, it is interesting that the conclusions Rutherford obtained are compatible with the other data available. Hence crystallization down to about 860°C is approximately compatible with biotite experimental data if P H_2O/P total ratio is close to unity. Czamanske and Wones (1973) deduce from amphibole and biotite compositions from Finnmark that monzonite crystallization occurs coincident with H_2O loss at P H_2O = P total (1 kb in this instance) and associated increase in f O_2. In such a case, crystallization and saturation with silica occurs and Al-rich amphiboles and biotites become unstable with corrosion occurring, as seen in the Adamello tonalites and quartz-diorites. Crystallization is complete before assimilation occurs. This observation and explanation can also be used to explain the development of epidote adjacent to ferromagnesian minerals. The epidote would form at temperatures below 600°C (Liou 1973) at f O_2 of 10^{-14} (close to H.M. buffer) and P H_2O of 0.5 to 1 kb. It is thus a late stage mineral.

Very few dykes extend radially from the Adamello massif and quartz and pegmatite veins are rare within or associated with the massif in its northern part. These facts suggest that only small quantities of magmatic fluid were present at the time of crystallization. Shieh and Taylor (1969) have shown that isotopic exchange (O^{18}/O^{16}, D/H) between plutonic and meteoric water is

limited to a maximum distance of 1 m. either side of the intrusion in several plutons of the Sierra Nevada Batholith; and that the effects of outward magmatic fluid migration are negligible for these calc-alkaline and granodiorite intrusions. Meteoric water is drawn in by the convection system set up by the intrusion of a hot body, and then moves upwards.

Heat effects, which cause the metamorphic aureole to develop, generally extend up to half the width of the pluton (d) into the country rock (e.g. Hietanen, 1974; Turner, 1968; Shieh and Taylor, 1969), although notable effects only occur to about $\frac{1}{4}$d. Local factors cause distinct variations in the width of aureole associated with individual intrusions, and the above statements must only be taken as broad generalizations.

2.60 STRUCTURE AND STRAIN ESTIMATES

2.61 Foliation development

The most widespread and prominent structure in the biotite-quartz-diorite and tonalite is a penetrative foliation. The foliation is defined by biotite flakes which show a very strong preferred orientation, particularly in the marginal parts of the tonalite and biotite-quartz-diorite. Here the foliation planes are 2mm. apart and provide a crude splitting surface when the rock is broken. More generally the rock will not break preferentially parallel to the foliation since the biotite content is only 15% - 18%. In the biotite-quartz-diorite no new macroscopic crystal growth is seen. In contrast, new ovoid biotite platy aggregates up to 1.8 cm. in diameter, have grown in the foliation plane of the tonalite. The long axis is coincident with the maximum dip direction of the foliation. The hornblende laths show a tendency to lie within the foliation plane but no notable preferred orientation within this plane was seen.

The foliation is restricted to the marginal 1 to 1.5 km. of the tonalite and biotite-quartz-diorite and the adjacent 0.6 km. of the contact aureole in the area

mapped. The distribution and trend of the foliation in the whole Adamello Massif is shown in Figure 5. The preferential foliation development in the small body of biotite-quartz-diorite, 1 km. east of Cima Presanella (Bianchi et al, 1970) is in accordance with the idea that this body is the latest intrusion in the northern part of the massif. The foliation in the northern part of the Adamello massif has a strike sub-parallel to that of the intrusion margin and this boundary has controlled the foliation development. Away from the intrusion margin, for example in the Punta di Castellaccio-Monticello area, the foliation orientation changes to about 060°/vertical. Hence the Z axis of the strain ellipsoid associated with the foliation plunges about 0° to 150° (c.f. joint pattern). Foliation orientation is shown in Figure 8(a). The orientation is locally more variable in the southern more weakly foliated part of the tonalite and biotite-quartz-diorite.

The foliation intensity shows a regional gradual decline southwards in the biotite-quartz-diorite, the marginal 500 m. being a zone of similar foliation intensity. Only slight local variations are seen. In the tonalite, the decline is more irregular with more strongly foliated zones commonly occurring between zones of weaker development. It is these zones from which high strain values were obtained.

In thin section, major textural and minor mineralogical changes are seen in the tonalite and biotite-quartz-diorite.

In the tonalite, the hornblende shows only minor fracturing and the biotite inclusions show only minor kinking. The plagioclase is generally fractured and movement has occurred along these fractures. In thin sections normal to the foliation plane, the fractures lie at 30° to 70° (average 50°) to the foliation trace. In some grains two conjugate shear fractures about 70° apart are seen. The sense of shear across the fractures

Figure 8(a) - Stereogram of the foliation orientation in the intrusive rocks of the Adamello Massif within the Tonale Pass area. No significant difference was noted between measurements in the tonalite and biotite - quartz - diorite. The range of orientation reflects that of the margin of the massif as the strike of the foliation is generally parallel to that of the intrusion margin.

Figure 8(b) - Strain values derived from measurements on deformed xenoliths shown on a Flinn plot ($^{X}/_{Y}$ versus $^{Y}/_{Z}$). The values are geometrical means at separate localities (see Appendix 2(a), Figures 52(a), (b)). The values all lie very close to the line K = 0.08.

Final maximum aspect ratio is 10.53 : 6.5 : 1

Mean initial shape is 1.2 : 1.05 : 1

Assuming coincidence of the initial and final maximum, intermediate and minimum axes the mean finite strain ratio is 8.78 : 6.19 : 1.

% shortening assuming no volume loss = 73.6% k = 0.0805

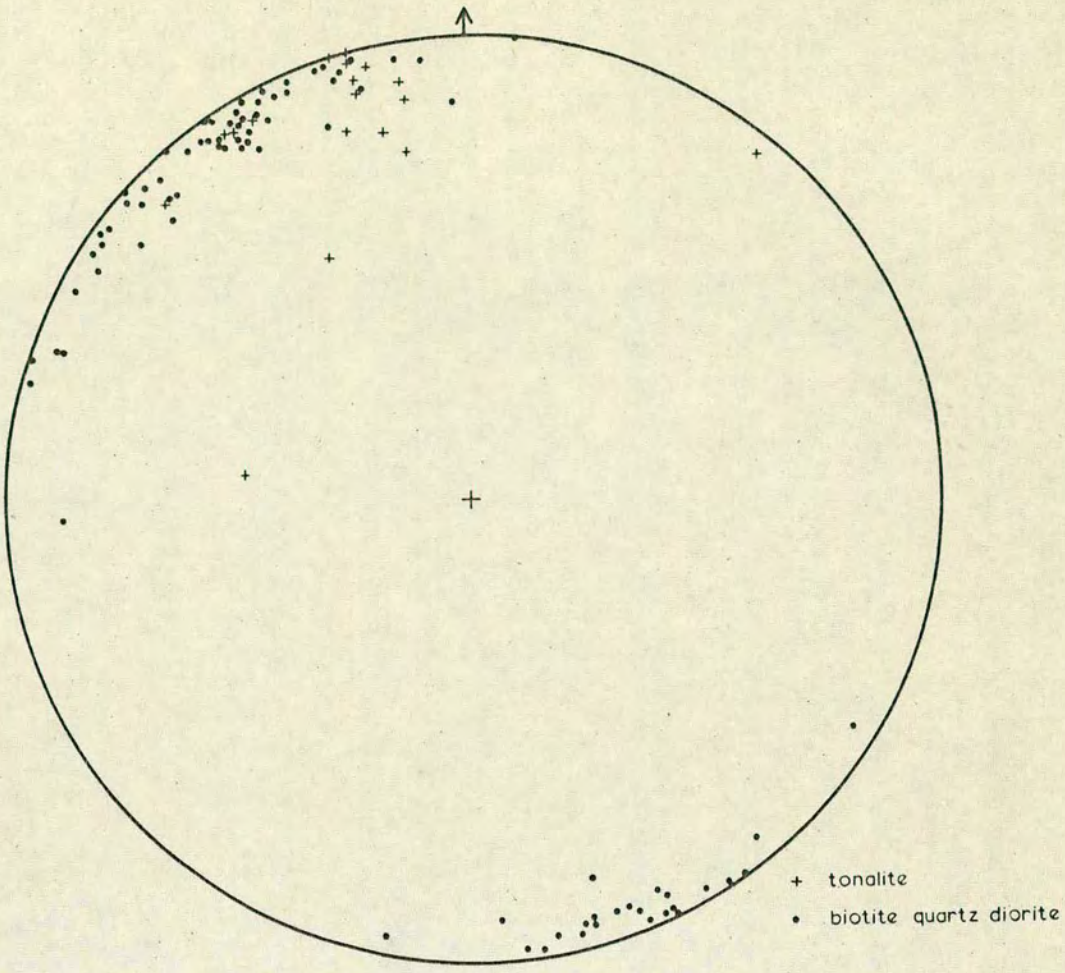
+ tonalite
• biotite quartz diorite

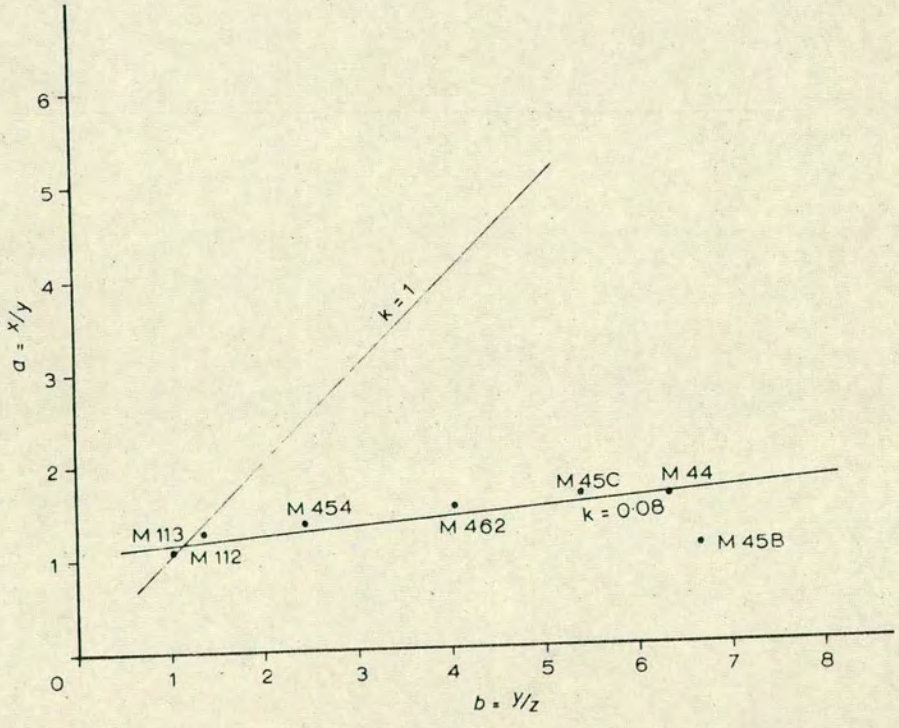
a = x/y
b = y/z
k = 1
k = 0·08
M 113
M 112
M 454
M 462
M 45C
M 44
M 45B
0
1
2
3
4
5
6
7
8

shows that compression normal to the foliation has occurred. The fractures may be infilled with biotites when dilation has occurred. The biotite in the tonalite has grown in small angular to skeletal plates which relate to the new foliation, and these plates form the larger ovoid platy aggregates seen in hand specimen. Kinking is very abundant in the biotites with kink axes up to 20° from the foliation trace. This implies that mica slip occurs at a low angle to its basal cleavage. In the larger biotite plates (2 to 4 mm. across) the optical orientation changes across the kink band axes which lie at <10° to the foliation trace; recovery has apparently occurred across these slip planes. Within these newly formed crystallographic zones the biotite is again kinked with axes at about 20° to the foliation trace. Kink axes are thus progressively rotated towards the foliation plane by increasing strain and metamorphic conditions are suitable for recovery to occur such that biotite "sub-grains" are formed with misorientation across the kink axes. Further kinking has then occurred at higher strains at the initial angle within the new crystallographic orientation. The result is that an original large biotite plate is changed on deformation to a series of "ribbons" whose long dimension lies parallel to the foliation trace.

Strong linear strain shadows are common in some of the quartz, lying within 10° of the foliation trace. No deformation lamellae are seen however (c.f. Southern Alps). Quartz veins and associated epidote commonly infill small fractures in the rock. Recrystallization of large quartz grains has occurred in some specimens and dentate boundaries are common in these aggregates. Spry (1969, p.24) has shown that dentate grain boundaries have a high surface energy and are typical of recrystallization under stress. Lines of minute inclusions are common in the recrystallized quartz. Minor undeformed green biotites have grown associated with or subsequent to this deformation. Minor marginal chloritization of biotite and sericitization of potash feldspar are also found in the foliated tonalite.

In the biotite-quartz-diorite similar features are seen. Plagioclase crystals are fractured and albite twin lamellae show up small kink zones. Large and skeletal biotites are strongly deformed and show a texture identical to the one described above. Plate 3 illustrates the stages of deformation in biotites in the biotite-quartz-diorite. Misorientation across the kink boundaries is more marked in some of these sections than in those in the tonalite. Minor undeformed green biotites and limonite are commonly associated with the deformed foxy brown biotites. These features show that oxygen fugacity (f O_2) was high during or subsequent to the deformation. Chlorite and magnetite, and more rarely white mica laths (muscovite or paragonite), replace parts of the biotite. Quartz deformation varies from anhedral sub-grain development in the less deformed biotite-quartz-diorite to highly elongate grains with finely dentate boundaries in the more deformed parts. These latter grains are seen bent around feldspar in response to local stress trajectories developed around the more resistant grains. Biotite and quartz show stronger deformation features in the quartz-rich zones in thin section than in the plagioclase-rich parts. These features show that strain on the microscopic scale is very heterogeneous.

These deformation features and mineralogical changes show that the foliation formed under P.T. conditions within the stability field of biotite, probably with high f O_2. The quartz recrystallization features are consistent with at least Upper Greenschist conditions. The growth of epidote, sericite, chlorite and green biotite show that a fluid phase was present.

2.62 Strain values from deformed zenoliths

The abundance of deformed xenoliths of constant composition in the marginal parts of the tonalite has been used to determine strain values which relate to the intensity of foliation. Tectonically undeformed xenoliths were measured at two localities (M112 and M113) in the Val Presena, in three perpendicular planes related

Plate 3.

(a) Large partly skeletal biotite crystals in weakly foliated biotite - quartz - diorite (M160).

(b) Large strongly kinked biotite crystal in moderately strongly foliated biotite - quartz - diorite (M142). Note the change in optical orientation across the kink axes.

(c) Elongate aggregate of ribbon-like crystals formed by progressive re-orientation by kinking and subsequent recovery. Minor small green biotites are also present. Strongly foliated biotite - quartz - diorite (M189).

Note that the degree of deformation and recovery is greatest adjacent to the later tonalite and decreases westward. (see Map 2).

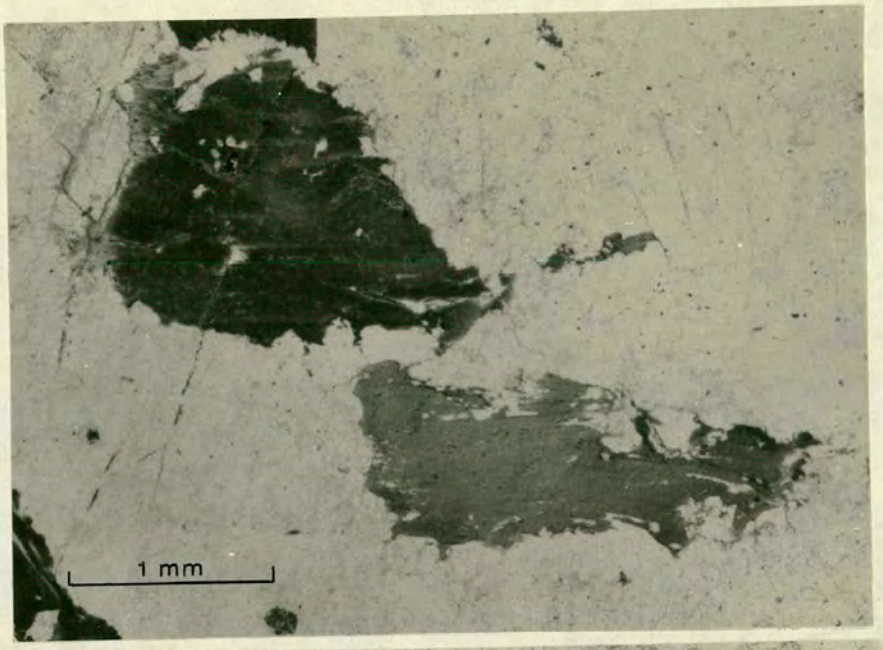
1 mm

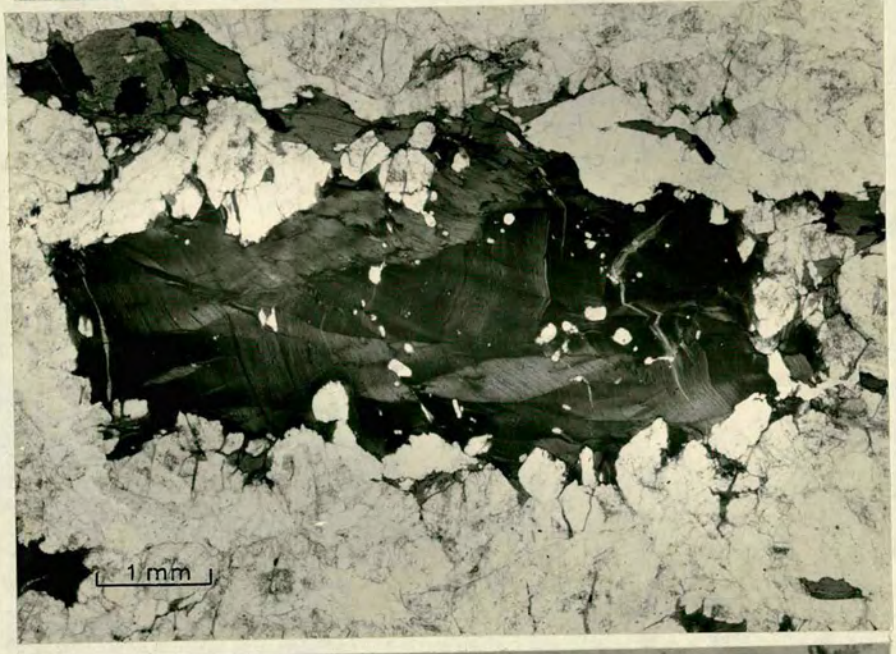
1 mm

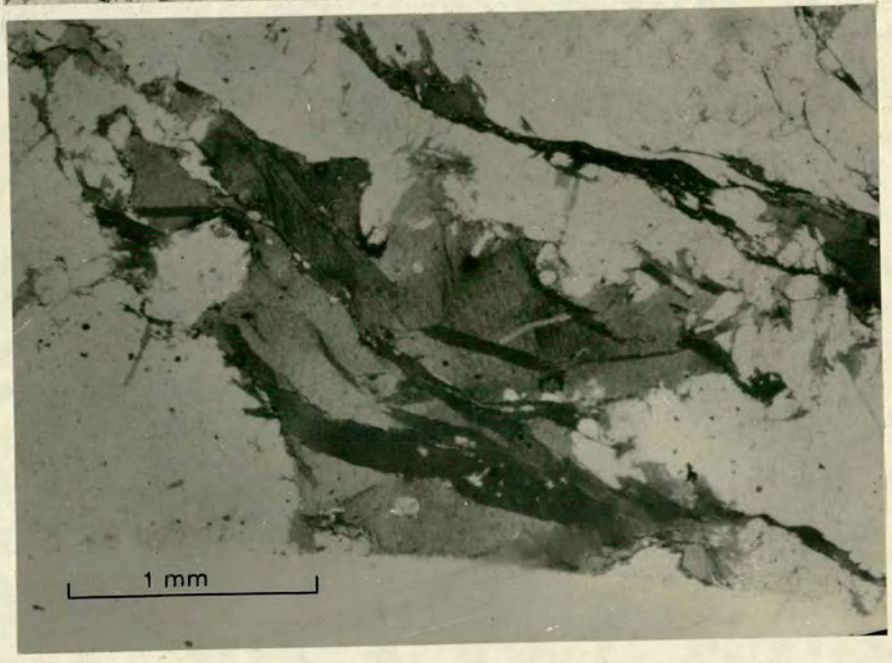
1 mm

orthogonally to the flow foliation. Since the flow foliation has a similar orientation to the tectonic foliation, the initial shape ratios in these planes may be compared to those measured relative to the tectonic foliation in the more marginal parts of the massif. All shapes were approximated to ellipses in the measured planes. Where ever possible, at least 30 measurements were taken in three perpendicular planes, since Hossack (1968) has shown that this number of measurements is generally sufficient to give a valid strain ratio. In the outcrops containing deformed xenoliths this condition was rarely fulfilled. The measurements of deformed xenoliths were orthogonally related to the foliation (XY plane), with the X direction taken as the maximum dip direction in this plane. Measurements in the XY and YZ planes were generally more difficult to obtain than those in the XZ plane, owing to a lack of suitably orientated joint surfaces. A total of 132 measurements were made on the deformed xenoliths, and 130 on undeformed xenoliths. The measurements and related graphical plots are given in Appendix 2(a). The ratios were graphically drawn such that $X/Y.Y/Z = X/Z$ compatible with the best fit lines. In the undeformed tonalite there is a considerable spread of initial ratios. Figure 8(b) shows the strain at all the localities on a deformation plot (Flinn 1962). With the exception of M45B, the points all lie on a line $k = 0.08$, implying strong flattening. Maximum strain values, allowing for the initial shape factor, are $X : Y : Z = 8.78 : 6.19 : 1$. This gives a maximum value of shortening of 73.6%. The values for M45B appear to be somewhat spurious. The small number of xenoliths measured, together with the possible variable initial shape, preclude any geological interpretation of this result. Although it is tempting to postulate that these values suggest a linear strain path it is thought that they merely represent differing strain rates in the tonalite with a maximum at the intrusion margin.

A section was traversed within the foliated biotite-quartz-diorite south of Tonale Pass. Within the unfoliated rock to the south, some almost perfectly spherical fine-grained quartz-feldspar-biotite xenoliths were noted. As these are traced north they are deformed into near perfect ellipsoids. Cursory measurements (see Appendix 2(b) on these xenoliths have been used to construct the X/Z strain variation diagram shown in Figure 9. Although the measurements are not as numerous or accurate as those for the tonalite, the section quantitatively illustrates the gradual strain changes in the biotite-quartz-diorite. Maximum shortening values of about 65% have been calculated using their average k value (0.08) and the measured values closest to the intrusion margin.

The identical k values for the two lithologies is corroborative evidence for a tectonic, and not igneous, event. The formation of the foliation, and strain recorded by deformed xenoliths are related, since the foliation intensity reflects strain values and no subsequent deformation has occurred. It is suggested that the deformation occurred at least partly when the igneous bodies were undergoing cooling and minor uplift. Since the tonalite apparently post-dates the biotite-quartz diorite, it would probably be in a more ductile state during deformation. This may account for the variation in foliation intensity and growth of large new biotite aggregates in the tonalite, compared to the more homogeneous nature of the strain and lack of large new biotite aggregates in the biotite-quartz-diorite. The strain and related foliation development are attributed to the f_5 event, since f_6 kink bands with similar orientations to those found in the other structural units, postdate foliation formation. The age relations derived from field observations show that the foliation formation post-dates the emplacement of the Adamello Massif (hence post f_3), and f_4 is only locally developed in marbles and certain gneiss zones of the Central Alps. The deformation of the aureole and marginal parts of the

Figure 9 - Section across the margin of the biotite - quartz - diorite intrusion south of Tonale Pass. The section shows the field relations and variation in strain in relation to foliation intensity. The strain ellipsoids are derived from cursory measurements of initially spherical xenoliths. The section also shows the structural setting of the dykes found adjacent to the margin of the biotite - quartz - diorite (see section 2.72).

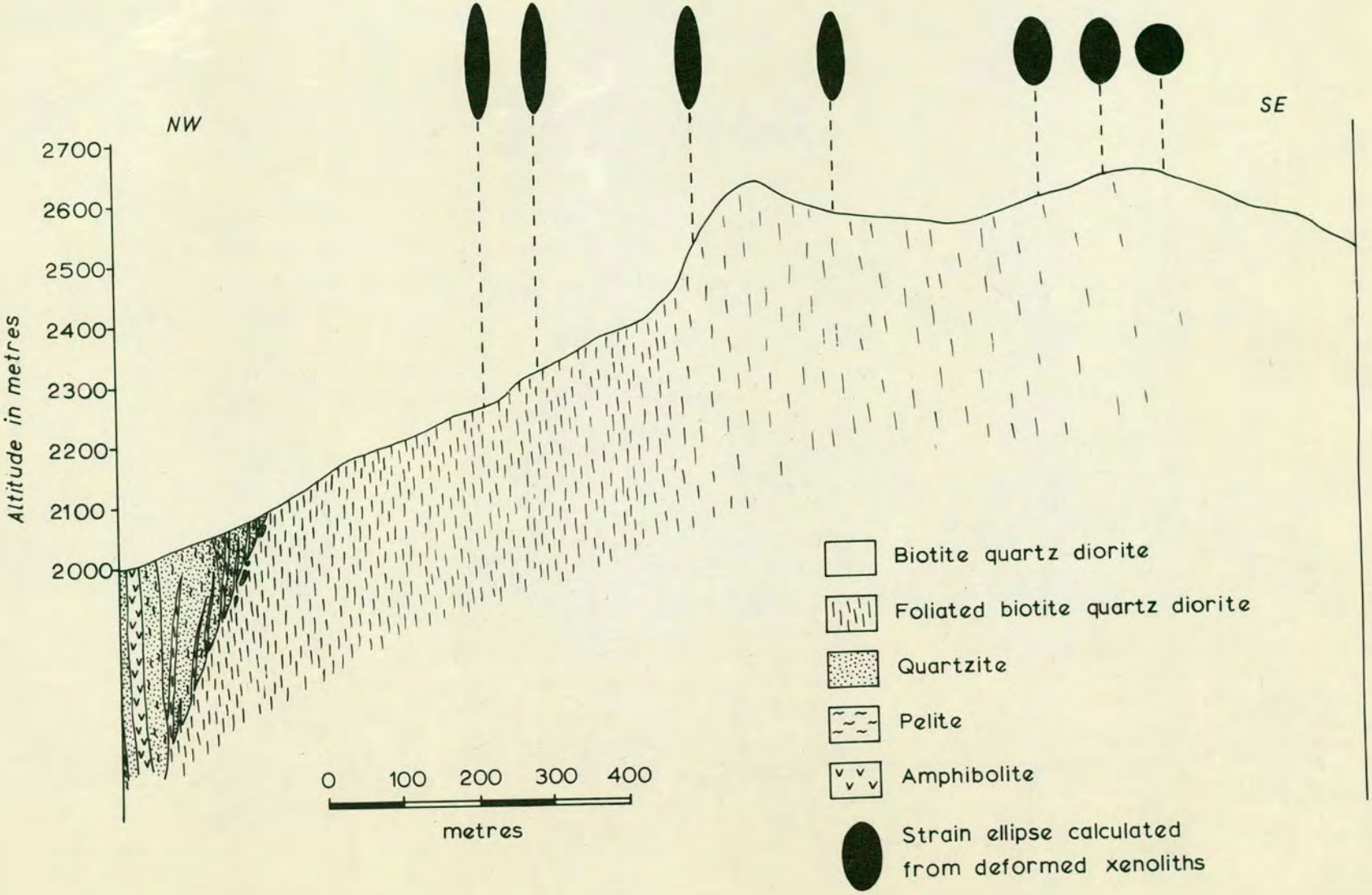
NW
SE
Altitude in metres
2700
2600
2500
2400
2300
2200
2100
2000
0
100
200
300
400
metres
Biotite quartz diorite
Foliated biotite quartz diorite
Quartzite
Pelite
Amphibolite
Strain ellipse calculated from deformed xenoliths

Adamello massif may be related to the uplift of the Stavel Gneiss.

2.63 Shear Zones

Shear zones occur locally in the highly foliated part of the tonalite and biotite-quartz-diorite. As shown in Figures 10(a) and (b), zones vary in strike between 020° and 055° and in dip between 85° N.W. and 83° S.E. The zones postdate the foliation and all show a sinistral sense of movement. Shear zones, aligned sub-parallel to the intrusion/country rock contact, are abundant in the hornfels and tonalite adjacent to the contact. Quartz and chlorite slickensides (fibre growths in part) are abundant on minor fault planes in the contact zone. These lineations are variable in dip and direction but generally plunge about 10° either side of the horizontal, indicating that relative lateral movement has occurred. The shear zones are attributed to local heterogeneous simple shear across sub-vertical zones.

At M322, two conjugate shear zones are present in foliated biotite-quartz-diorite. The geometry of these zones is shown in Figure 11(a). The angle between the zones is only 44°, although maximum shortening occurs along a line bisecting this angle. Ramsay (1967, p.454) has shown that the intersection of two conjugate kink bands is generally coincident with the σ_2 (intermediate stress) axis and that the σ_1 (maximum principal stress) axis generally bisects the larger angle between the two bands. This depends on the assumption that the initial layering (in this case the foliation) contains two of the principal stress axes. In this outcrop the zones show maximum shortening (and hence σ_1 direction) along a line plunging 8° to 330°. The intersection of the two shear zones which coincides approximately with the σ_2 axis, plunges 6° to 239°. Hence σ_3 plunges 80° to 113°. These stress orientations are broadly similar to those implied by the foliation orientation (c.f. joints), suggesting that the two events are closely related in time.

Figure 10(a) - Stereogram showing structural features within the Tonalite Intrusion. The sub-horizontal NE trending chlorite lineation shows that sinistral lateral movement has occurred along the NE trending sub-vertical joints. Shear zones commonly have a similar orientation.

Figure 10(b) - Stereogram showing structural features within the biotite - quartz - diorite, excluding joints (see Figure 11(b)). Chlorite slickensides (fibre growth) have a similar orientation to those in the tonalite. Some quartz - feldspar veins infill dextral shear joints. Joint orientations in the small diorite intrusion are also shown.

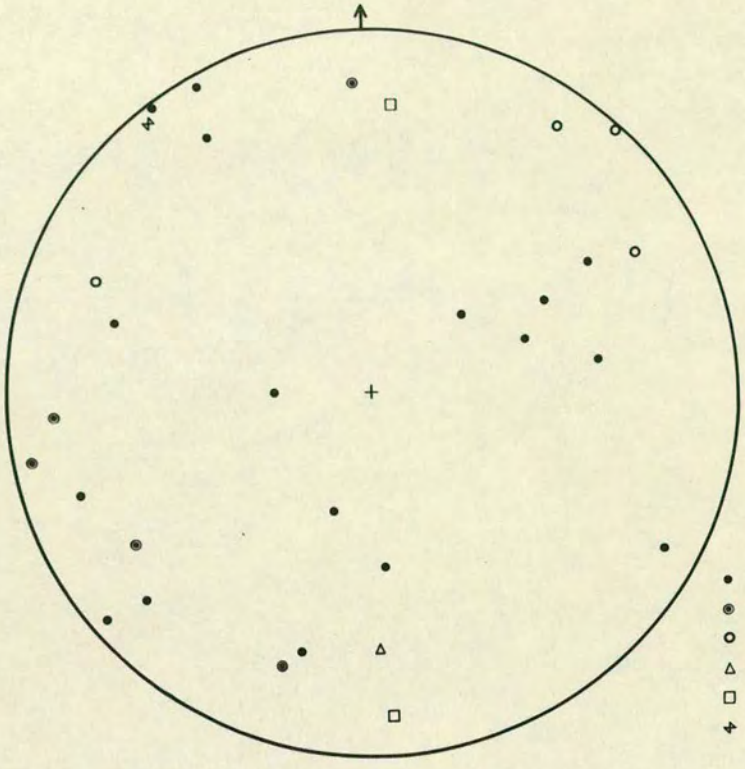

- Pole to joint
- Joint with chlorite
- Chlorite lineation
- Chlorite - pseudotachylite vein
- Pole to vein
- Pole to shear zone

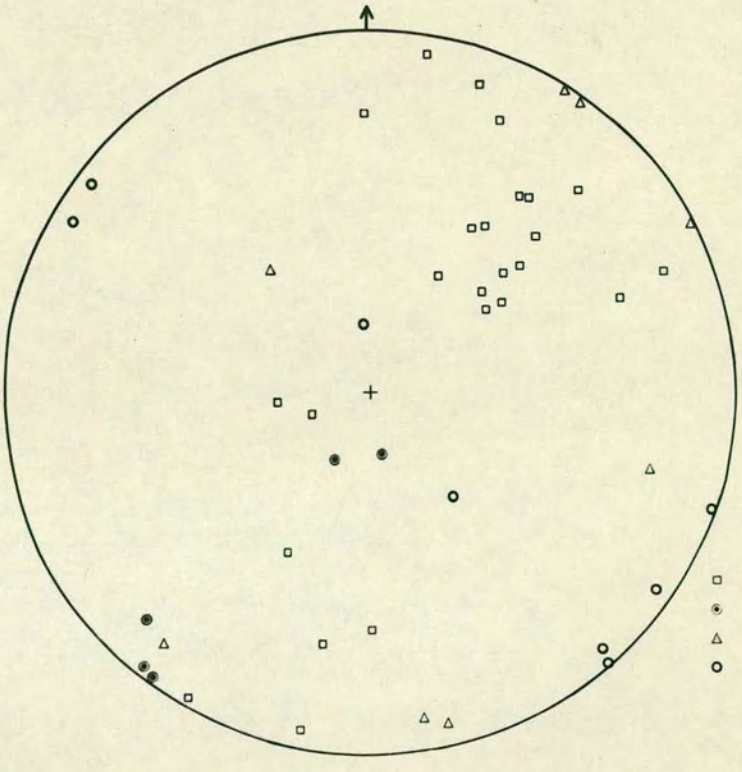

- Pole to quartz feldspar vein
- Pole to joint in diorite
- Chlorite slickensides (fibre growths)
- Pole to shear zone

Figure 11(a) - Stereogram showing the geometry of conjugate shear zones in foliated biotite - quartz - diorite. The principal stress directions are derived from this geometry.

Figure 11(b) - Stereogram of the joint orientations in the biotite - quartz - diorite. Four diffuse maxima are distinguished; Joints trending 030° - 040° ; Joints trending 135° - 140° ; Joints dipping around 20°E ; Joints trending about 060°. The 060° joints have formed preferentially along the foliation in the marginal parts of the intrusion. The 030° - 040° and 135° - 140° joints areconjugate shear joints and imply a principal maximum stress directed horizontally at 173° - 353°. Chlorite is well-developed on the 030°- 040° joints.

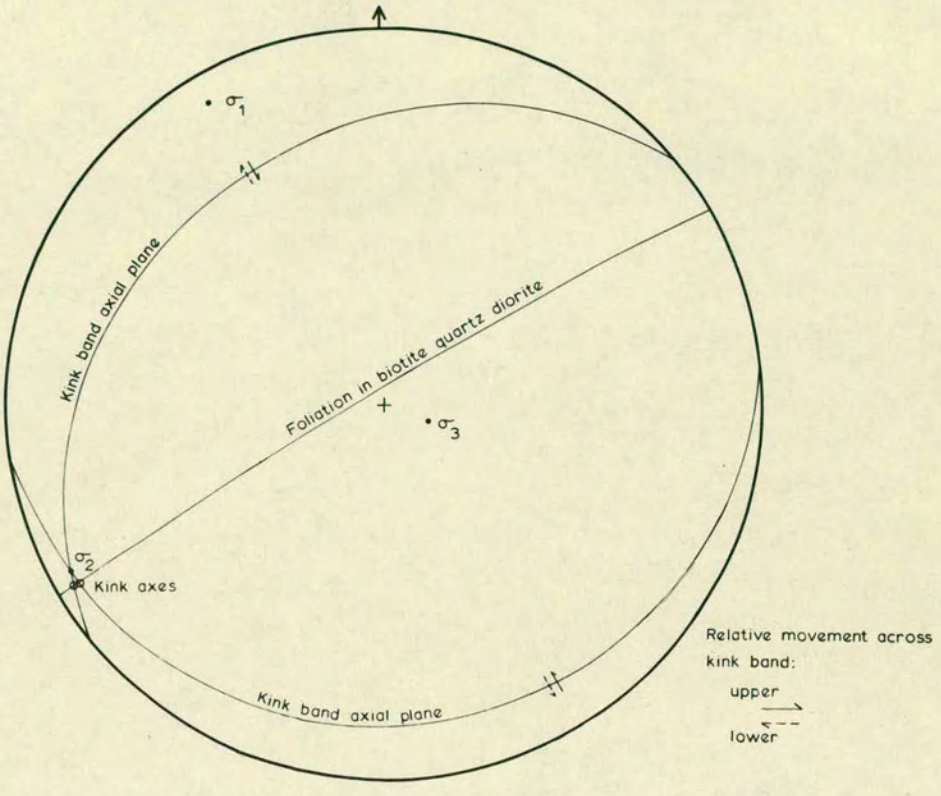
σ_1
Kink band axial plane
Foliation in biotite quartz diorite
σ_3
σ_2
Kink axes
Kink band axial plane
Relative movement across kink band:
upper
lower

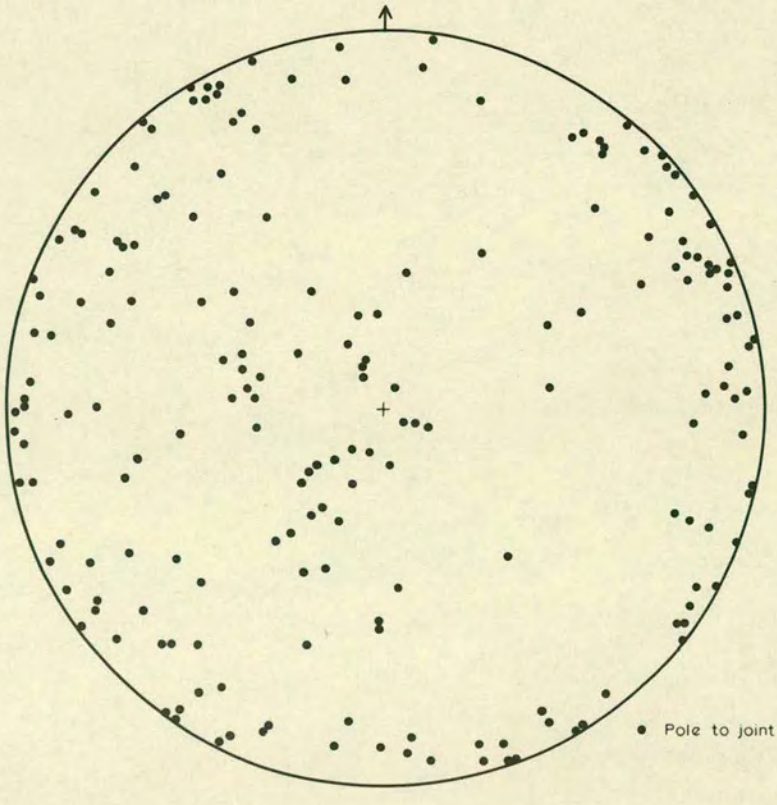
Pole to joint

2.64 Joints

Widely-spaced joints are abundantly developed in both the tonalite and biotite-quartz-diorite.

Joint orientations and a synthesis of the regional pattern in the biotite-quartz-diorite are shown in Figure 11(b). Four diffuse maxima may be distinguished, and the average value for each maximum is given in Figure 12(a). The S joints commonly contain chlorite infillings and 030° - 040° joints may show slickensides (fibre growths ?) plunging gently north-east or south-west. Gently plunging slickensides only rarely occur on the 135° joints. Where the biotite-quartz-diorite is strongly foliated, the S joint orientations reflect the influence of this plane of weakness and trend about 060° instead of 030° - 040°. Gently dipping joints, which range generally from 10° to 30° either northeast or southeast, are common in the biotite-quartz-diorite. Chlorite infills of these joints are rare.

The consistent evidence of dominantly lateral movement on the S joints shows that these are shear joints. Sinistral displacement of veins is rarely seen along the 045° joints. According to Anderson (1951) and Price (1966), the maximum principal stress axis (σ_1) bisects the lesser angle between conjugate shear joints. This is consistent with movement sense in this area and hence the σ_1 axis trends 173° - 353° in the biotite-quartz-diorite. The σ_2 axis dips approximately vertically and the σ_3 axis trends 083° - 263°. The presence of quartz-feldspar-biotite veins in the plane normal to σ_3 suggests that this stress may be tensional. These axes appear to be orthogonally related to the present land surface. The results should be compared to those derived from shear zone orientations, which show a similar value for the σ_1 axis but an interchange of σ_2 and σ_3 orientations. The joints are related to uplift, cooling, and contraction of the Adamello massif in a south southeast - north northwest directed stress field. Price (1966, p.136) has predicted that such stress changes will occur on uplift, assuming residual stress in

Figure 12(a) - Synthesis of the joint pattern in the biotite-quartz-diorite. The shear joints are marked S and commonly show sub-horizontal chlorite slickensides and/or fibre growths. The quartz - feldspar vein orientations suggest that the minimum principal stress may be tensional.

Figure 12(b) - Stereogram showing the geometry of the planar and linear structures in the diorite aureole. The features are thought to result from intrusion of the diorite body. The curved fold hinges and common disharmonic profiles of the minor folds reflect the rapid strain rates and heterogeneous nature of the strain.

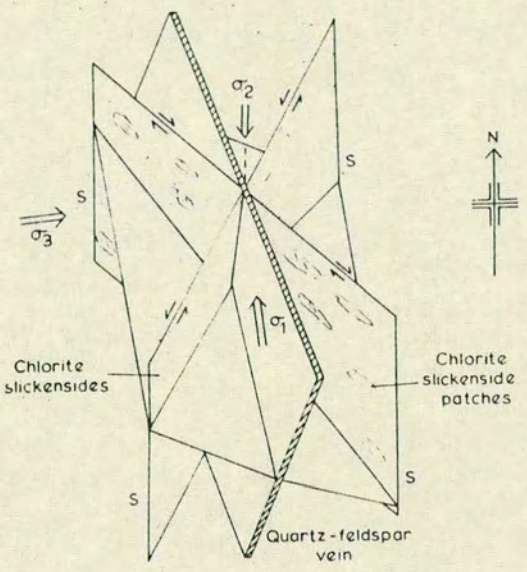
σ2
S
S
σ3
σ1
N
Chlorite slickensides
Chlorite slickenside patches
S
S
Quartz-feldspar vein

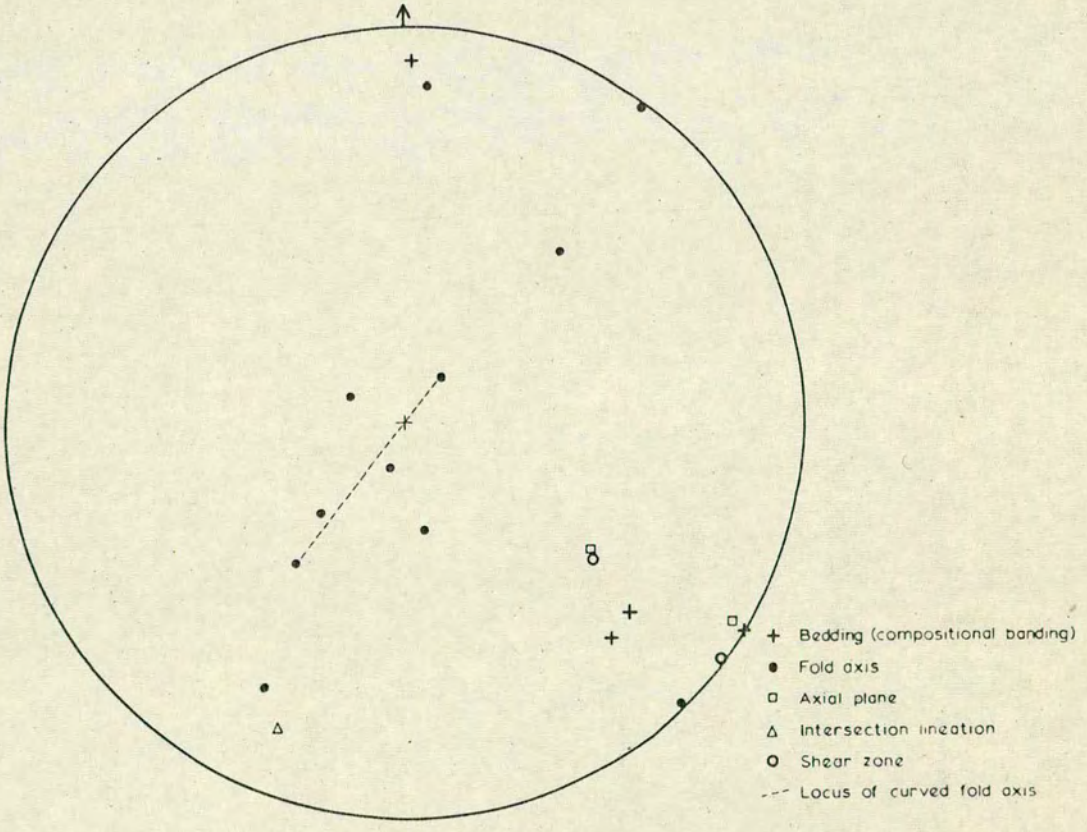
+ Bedding (compositional banding)
• Fold axis
□ Axial plane
△ Intersection lineation
O Shear zone
--- Locus of curved fold axis

the rock. The joint system is similar to that described by Van Hilten (1960) from the Val di Non area of the Southern Alps. He deduced that σ_1 acted in the direction 160° - 340°.

Only a small number of measurements of joint orientation were made in the tonalite and these are similar to those obtained from the biotite-quartz-diorite. Figure 10(a) shows that data for joints, veins, and chlorite lineations in the tonalite.

2.65 Veins

Veins are relatively sparse in the northern part of Adamello massif, compared to the frequency normally found in granitic intrusives. This is suggestive of low fluid content of the tonalite and biotite-quartz-diorite magma at the time of solidification. Rarely quartz-feldspar-biotite veins merge faintly into the tonalite (e.g. M.347), but more generally the veins clearly cross-cut the foliated biotite-quartz-diorite or tonalite. The veins post-date the shear zones and in at least some areas they post-date joint formation. 1 to 22 cm. wide quartz-feldspar-biotite veins with orientations clustering around 135/45°SW., are locally abundant in the biotite-quartz-diorite (figure 10(b). Some veins are flanked by chlorite, showing that they were injected subsequent to joint formation.

At M349, 0.75 km. north of Punta di Castellaccio, two phases of vein intrusion may be distinguished. The earlier 5 to 10 cm. wide medium-grained quartz-feldspar-biotite veins have a range in orientation from 160/62°W to 158/75° W, and the vein biotite is aligned parallel to the foliation in the surrounding biotite-quartz-diorite. Later 1 to 2 cm. wide veins, with similar orientations and compositions, are unfoliated and cross-cut earlier veins. At M322, two thin quartz-feldspar-hornblende-muscovite veins trending 146/36° S.W. cross-cut kink folded and foliated biotite-quartz-diorite. The apparent displacement across the vein was measured as 10 cm., the upper part having moved relatively towards 145°. It is possible here that the vein caused the shear zone to form

in the manner observed and that no appreciable displacement has occurred. Hence, assuming that both sets of veins are related to late stage igneous effects, the period necessary for foliation, shear zone and even joint formation must not be very long after the emplacement of the massif.

In the tonalite the veins lie approximately in the plane containing σ_2 and σ_3(as defined by joint synthesis) and are not related to the shear joint orientations as in the biotite-quartz-diorite. Sparse quartz-feldspar veins, 1 to 15 cm.wide, cross-cut undeformed xenoliths in the more central parts of the tonalite. Quartz-epidote, epidote and more rarely epidote-chlorite veins are common in the joint planes of the tonalite. Thin epidote-quartz veins may form a finely anastomosing network in the tonalite. At M393, 15m. southeast of the tonalite/biotite-quartz-diorite contact in the central Val Presena, an irregular 1 to 2 cm. vein of pseudotachylite and chlorite, trending 090/60°N. lies in massive unfoliated tonalite. Philpotts (1964) has shown that pseudotachylite results from frictional heating due to fault movement under very low water pressures. He cited an example where pseudotachylite is formed in a monzonite intrusion with temperatures above 400°C at the time of formation. Mackenzie and Brune(1972) calculated the amounts of movement necessary for pseudotachylite development, and placed restrictions on the boundary conditions. Assuming that very localised slip occurred along the pre-existing chlorite-filled joint, and taking frictional shearing stress values of about 200 bars and a shearing stress (total shearing stress minus frictional shearing stress) of about 50 bars (minimum values) the displacement is approximately 20 cm. The presence of pseudotachylite is due to the presence of the chlorite, which created a low friction zone.

2.70 MINOR RELATED INTRUSIVE ROCKS

2.71 Diorite intrusion and associated structures

2.25 km. west southwest of the Tonale Pass, a small

approximately circular section hornblende diorite intrusion crops out poorly over an area about 250 m. in diameter. It consists of unfoliated, massive fine-grained hornblende diorite with hornblende laths up to 5 mm. long (average 3 mm.) in a fine-grained feldspar, biotite and minor quartz matrix. 3 cm. diameter rounded fine-grained quartz-feldspar-biotite xenoliths and minor hornblende pods are seen in parts. The intrusion has a regular joint pattern and joint orientations are shown in Figure 10(b). The two dominant sets are similar in orientation to those developed in the nearby biotite-quartz-diorite.

Related to the intrusion is an approximately 30 m. wide hornfels zone. No structural or mineralogical changes were noted beyond this zone. This aureole differs markedly in structure and texture from that associated with the large tonalite and biotite-quartz-diorite intrusions. South and east of the diorite outcrop, hornfelsed semi-pelite and quartzite, the latter flaggy in parts, are tightly folded, sheared, faulted and partly brecciated. Quartz pods and small veins are very abundant, particularly in the faults and shear zones. The geometry of the planar and linear structures in the aureole is given in Figure 12(b). The fold axes lie in a vertical plane trending NE - SW, which is coincident with the shear zone, bedding and fold axial plane orientations. The strike of the bedding may be traced around the intrusion although the dip is variable.

The folds are disharmonic, open to isoclinal in style, commonly with rounded hinges. They range from 1 to 2 mm. in width up to 10 cm. Shear zones truncate the fold limbs and the two features show apparent continuity. The folds generally face south-east and are markedly asymmetrical in some parts. The sense of shear across the folds and abundant shear fractures is relatively downwards to the southeast. These structural features are unique in style and orientation in the area mapped and are hence related to the small diorite intrusion. Almost all the data shown in Figure 12(b) was obtained

from the hornfels on the southeast side of the intrusion, where the sense of shear is related to the relative upward movement of the diorite intrusion to the northwest. It is suggested that the level of exposure is such that we are seeing the hornfels above the southeast part of the intrusion. Upward fluid movement has resulted in the dominant hornfels texture and local development of quartz pods and limonite. The deformation features are due to the strain imposed by intrusion. It is suggested that the disharmonic folds reflect the locally high strain rates (hence the rounded hinges) and resultant heterogeneous strain. Differential shear must be invoked to explain the formation of many of the folds. Roberts (1970) has shown that maximum shear stress trajectories develop at a considerably higher angle of dip than that of the intrusion boundary in the upper part of the intrusion. This agrees well with the orientation of the observed shear zones and small faults.

2.72 Dykes

Dykes are common in the biotite-quartz-diorite aureole up to 300 m. from the intrusion contact. In contrast, only rarely are dykes found up to 50 m. from the tonalite intrusive margin. The difference is attributed to the different depths of intrusion (see 2.84).

The dykes related to the biotite-quartz-diorite range from 30 m. to 15 cm. in width (generally 1 to 2 m. wide) and are well exposed on the ridge northwest of Punta di Castellaccio. 11 major dykes were noted in a 300 m. wide hornfels zone. North of the biotite-quartz-diorite/Edolo Schist contact in the Tonale Pass area, 5 or 6 dykes are generally seen with one dyke at least 20 m. thick. The dykes are composed of fine to medium-grained quartz-rich biotite-leuco-quartz-diorite and are generally injected parallel to the bedding at lithological boundaries such as quartzite/pelite contacts. At M213, 600 m. northwest of Punta di Castellaccio, a flat lying aplite dyke 1 m. wide cuts the biotite-quartz-diorite dyke and adjacent hornfels. This dyke presumably infills a tensional joint

in the aureole. Biotite invariably shows an alignment parallel to the sides of the dyke. Rarely minor muscovite is present. At T273, 1.5 kms. southwest of Tonale Pass, a 25 cm. dyke lies in a small shear zone. The dyke trends 045/vertical but 1.5 m. higher up it bends to 044/65°N.W., and the dyke and shear zone "pinch" out. The level of exposure of the biotite-quartz-diorite (upper part of pluton) suggests that these dykes represent less viscous, more acidic parts of the magma which are injected along shear zones. Roberts (1970) has shown that shear zones would be expected to have a near vertical trend at this level of intrusion (marginal dip approximately 70° north). Hence we would expect dykes to extend to a maximum distance of 375 m. from the intrusion margin for a 4 km. diameter pluton. This value is in good agreement with the observed distribution of dykes.

The dykes associated with the tonalite are very irregular in form and consist of leucocratic quartz-feldspar-biotite. They are associated with quartz-feldspar veins and pods. Since we are looking at a lower level of intrusion here, the magma would not tend to form shear or dilation zones and the observed dykes and veins are attributed to minor anatexis of semi-pelite.

2.80 CONTACT AUREOLE

2.81 Introduction

Within the pelitic to quartzitic sequence of the Southern Alps (Edolo Schists), a metamorphic aureole is developed. No mineralogical differences were observed between the assemblages relating to the tonalite and biotite-quartz-diorite. Since experimental data (Piwinski and Wyllie 1968) show that similar intrusion temperatures may be expected we may consider the two aureoles together as due to a single event. It will be shown later that the two events are separated by a geologically short period of time.

At the eastern margin of the Adamello massif (Val Rendena) garnet-staurolite and garnet-cordierite-

sillimanite-corundum assemblages have been described (Justin-Visentin and Zanettin, 1968) from iron rich pelites. At the southern margin of the massif wollastonite occurs in mesozoic limestone (Schiavinato 1946) suggesting a high temperature of intrusion or low X CO_2 values in the aureole.

2.82 Mineralogy and textures

Near the Tonale Line, particularly in the areas of the Tonale Pass (near Funivia station) and 2.5 k.m. south west of Velon, there is little apparent change in the pre-existing Greenschist facies mineralogy of the Edolo Schists. Minor sericite (white mica) is developed.

Between 150 m. and 700 m. from the intrusion margin, muscovite is developed as new crystals 0.1 to 0.7 mm. long. In the outer parts of the aureole, the muscovite shows slight green pleochroism suggesting that it is phengitic. These grains have grown in pre-existing sericite (white mica) or chlorite-biotite aggregate and appear to be the major metamorphic effect in the outer part of the aureole. Some skeletal chlorite (penninite) has formed and minor recrystallization of biotite is seen in thin section. 550 m. from the intrusive contact, at T.211, quartz pods are common in the pelitic schist. New elongate quartz grains are formed, with axial ratios averaging 6/1 in the plane normal to the foliation containing the lineation. Older relict grains are common, and these contain abundant deformation bands sub-parallel to the foliation trace. Deformation lamellae (Böhm lamellae) commonly lie at 80° to 90° to the deformation bands. In some parts recrystallized quartz ribbons are bent around the margins of relict quartz grains. These quartz features may pre-date the biotite-quartz-diorite intrusion but their development is more consistent with events associated with and subsequent to intrusion.

About 250 m. from the intrusion margin, at T95B, fine-grained semi-pelite with a well-developed cleavage crops out. In thin section the cleavage is defined by phengitic muscovite laths (average 0.4 mm. long) and very

small biotite flakes growing in blue birefringent chlorite (penninite). The quartz is unstrained in parts but more generally shows weak strain shadows. The grains are partially to wholly recrystallized and show sub-grain mosaics and irregular grain boundaries. The grains are elongate along the trace of the foliation. These features suggest that quartz crystallization has occurred due to the effects of the Adamello intrusion. Temperatures of 350° to 400°C are suggested, since biotite has partly replaced chlorite. A quartzite close to this semi-pelite, at M95A, 270m. from the intrusion margin, consists of quartz with finely dentate grain boundaries and a lack of equilibrium angles. These features suggest that growth has occurred in a stress field (Spry, 1969, P.24; Bell and Etheridge 1973). Strain shadows are abundant but generally lie at 35° to the direction of grain elongation and are taken to reflect a later deformation event (c.f. shear zones in biotite-quartz-diorite, Stavel gneiss). Minor small biotites and sericitized orthoclase are also present. A macroscopic hornfels texture is observed in quartzitic rocks at distances <300 m. from the intrusive contact.

At about 300 m. from the intrusion margin, biotite is developed in the pelitic and semi-pelitic lithologies. About 200 - 300 m. from this margin, biotite plates (0.2 to 2 mm. long) become very abundant in the pelitic lithologies.

At M218, 250 m. from the biotite-quartz-diorite contact, a small band of amphibolite is exposed. Under the microscope this consists of laths of green hornblende (pleochroism; α pale green, β green, γ dark green; biaxial -ve, very high 2V - Mg rich hornblende) up to 1.5 mm.long, anhedral plagioclase(An_{26}-An_{40}) and zones of biotite. The andesine shows relief >lakeside, biaxial negative figures with a high to very high 2V, and Michel-Levy angles on albite twins of 10° to 23°. Large corroded rhombic section sphene crystals, anhedral apatites and "ragged" magnetite and possibly ilmenite grains are common.

The formation of biotite occurs where feldspar has altered to white mica, and the reaction involved is probably complex involving a bulk change in hornblende composition. The presence of a fluid phase is inferred for the necessary addition of K^+ and H_2O. These components were probably derived from the thick pelitic sequence to the north. A possible reaction is :-

$$\text{Hornblende} + \text{Plagioclase} + K^+ + H_2O \rightleftharpoons \overset{\text{Fe,Si poor}}{\underset{\text{Al rich}}{\text{Hblde}}} + \text{Biotite} + \text{White mica} + Na^+ + Ca^{++}$$

The presence of andesine cannot be used to infer metamorphic grade since it probably reflects the initial calcic nature of the plagioclase. Albite is present in the Edolo schists generally. Minor late stage thin prochlorite - sphene veins are present in the amphibolite.

230 m. from the tonalite intrusive margin, at T21, a highly pelitic dark grey schist consists in thin section of andalusite porphyroblasts up to 2 mm. long with poikiloblastic inclusions of quartz and biotite, in a matrix of quartz, biotite, muscovite (phengitic) and minor potash feldspar and chlorite. As shown in Plate 4, the biotite shows a strong preferred orientation, defining a strong foliation which wraps around the pre-existing andalusite porphyroblasts. Linear inclusion trails in many of the andalusites show a variable orientation in different porphyroblasts, indicating that rotation has occurred subsequent to andalusite formation.

120 m. from the tonalite intrusion contact (T20A), thin sections of semi-pelitic rocks from the hornfels show that subhedral andalusites (average 2 mm. wide) and aggregates of fibrous sillimanite (average 4 mm. long and 1 mm. wide) lie in a matrix of large anhedral cordierite (altered to sericite or pinite) grains, quartz, biotite, magnetite and rare chlorite and plagioclase. The cordierite rarely shows simple twinning. The plagioclase is oligoclase (Biaxial - ve, relief ≈ lakeside) and exhibits abundant strained and fractured albite twinning. Late stage muscovite laths up to 1 mm. long crosscut all the other minerals. Two biotite foliations 30° apart

Plate 4 - Photomicrograph showing rounded andalusite porphyroblasts with weakly orientated inclusions of quartz and biotite. The biotite in the matrix shows a strong preferred orientation and wraps around the andalusites. Pelitic schist (T21).

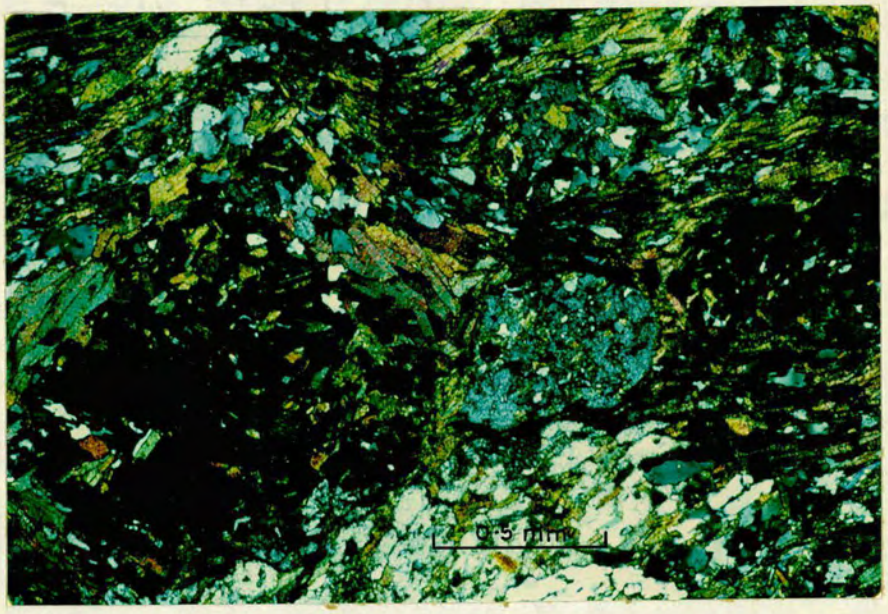
0·5 mm

may be seen; the earlier foliation is axial planar to small f_3 quartz vein folds; the later foliation is defined by biotite and sillimanite. The quartz shows strain shadows and rare deformation lamellae. Andalusite commonly contains quartz and biotite inclusions. Chlorite-biotite zones are common in the outcrop, showing that not enough time has elapsed for complete reaction.

At T17, a quartzite 100 m. from the tonalite contact, recrystallized quartz with undulose extinction and dentate boundaries makes up the bulk of the rock. A vein of quartz, muscovite and cassiterite occurs in the rock. Deformation lamellae are again seen in some quartz grains. Biotite and intergrown white mica post-date earlier vein muscovites and cross-cut the folded quartz veins seen in thin section.

At T274B, about 50 m. from the biotite-quartz-diorite contact, f_3 close to tight, concentric quartz vein folds lie in a hornfelsed semi-pelite. In thin section, the rock consists of poikiloblastic andalusites (average 2.5mm) and cordierite in a matrix of quartz, plagioclase (high oligoclase to high andesine), biotite, magnetite and minor orthoclose and fibrous sillimanite. At the margins of the andalusite very fine grained mosaics of potash feldspar (cordierite ?) and andalusite are present. The andalusites commonly contain "stubby" biotite flakes parallel to the f_3 foliation and hence post date this structure. Cordierites are commonly dusted with magnetite and contain quartz and biotite inclusions. Rarely very small sillimanite needles have grown in the cordierite. In all the hornfels thin sections, cordierite shows very pale yellow pleochroism and some alteration to pinite. The quartz occurs in approximately equidimensional grains 0.08 mm. in diameter with grain boundaries commonly pegged by small biotite and late stage white mica laths. Larger grains are present in the quartz veins. These veins show deformation bands parallel to a late f_5 foliation, defined in the rock by a strong alignment of biotite and white mica laths. This f_5 foliation commonly cross-cuts andal-

-usites and shows refraction through the more pelitic bands.

At T19A, about 10 m. from the tonalite contact, a mottled dark grey-white-black hornfelsed semi-pelite lies in a zone containing quartz-feldspar veins and pods and dykes of fine-grained leucocratic granitic material (quartz-feldspar-biotite-muscovite). The latter features are attributed to local anatexis. Small red garnets are present in some parts of the hornfels, which shows a weak foliation ranging from 115/80°S to 085/95°S in orientation. A similar development of garnet occurs in the 10 cm. adjacent to a fine-grained leuco-quartz-diorite dyke at M273, close to the biotite-quartz-diorite contact. Under the microscope, linear zones of sillimanite crystals lie in a matrix of irregular quartz grains with serriate grain boundaries, cordierite, orthoclase, biotite and minor oligoclase-andesine and accessory embayed pyrite.

The lack of muscovite, and growth of sillimanite in the inner 130 m. of the aureole, shows that we are in the Pyroxene Hornfels facies. Andalusite persists in to about 30 m. from the contact.

2.83 Discussion and Interpretation of the mineral assemblages

The range of contact metamorphic minerals in the aureole is shown in Figure 13. The mineral parageneses are dependent primarily on initial bulk composition and hence three divisions are made ; Pelite and semi-pelite; Quartzite; Amphibolite. The presence of only one band of amphibolite limits the assemblages which can be defined. Figure 14 shows experimental data relating to the various mineral assemblages in the aureole to P H_2O - T conditions.

Turner (1968) and Brown (1967) have both shown that biotite first appears in pelitic rocks due to reactions between low grade muscovites (commonly phengitic) and chlorites, commonly giving biotite - Mg chlorite - muscovite- quartz assemblages. The first appearance of biotite under P H_2O of a few kb is probably between 300° and 400°C. Phlogopite + quartz are stable up to temperatures of about 815°C (Luth, 1967) but Wones (1963) has shown that

Figure 13 - Range of observed assemblages in differing rock types in the contact metamorphic aureole of the Adamello Massif. The graph shows the distance from the intrusion margin that the various index minerals were first noted and probable temperature range over which these minerals formed (see text). The temperature profile in the aureole is hence derived.

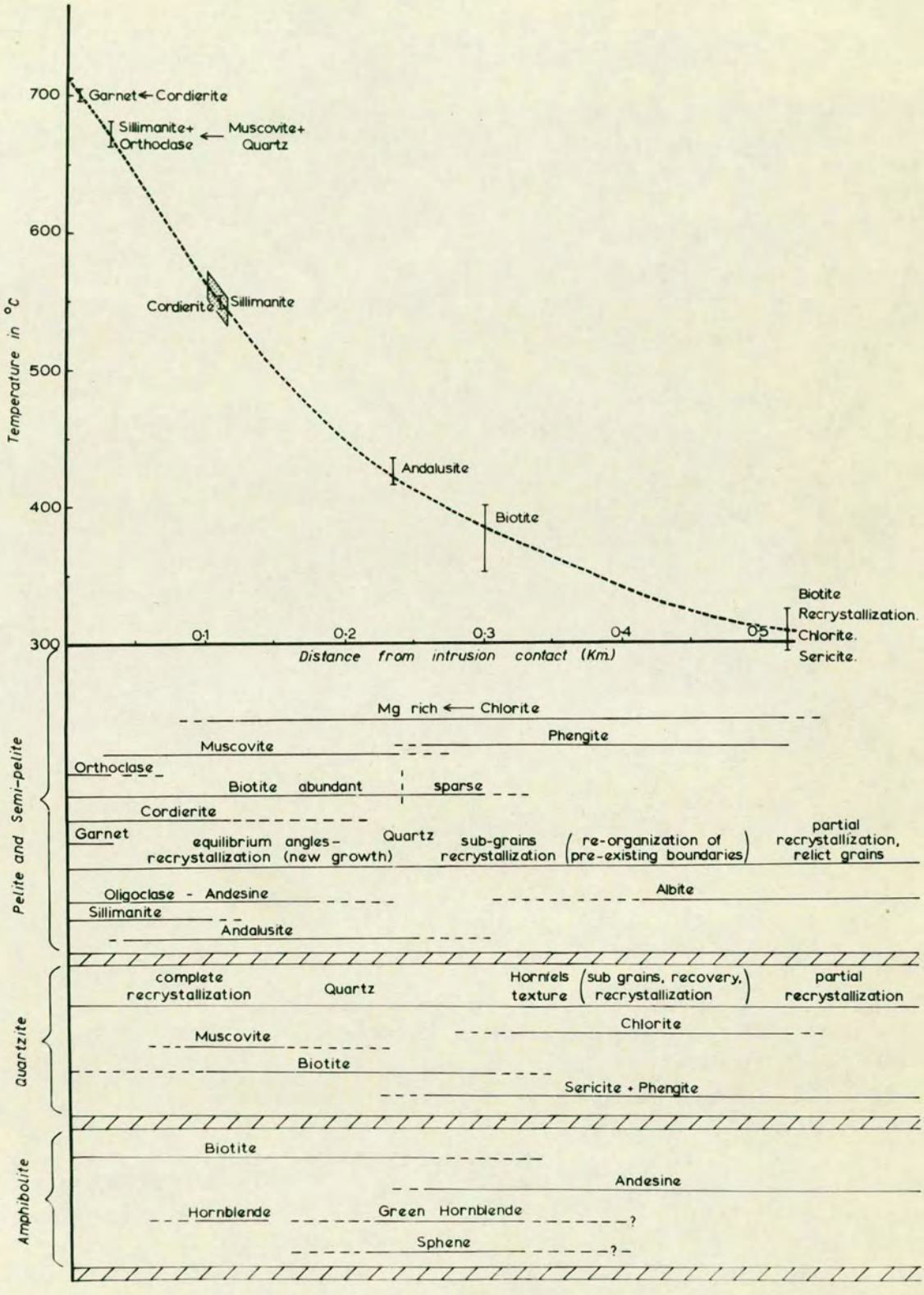
700
600
500
400
300
Temperature in °C
Garnet ← Cordierite
Sillimanite+ Orthoclase
← Muscovite+ Quartz
Cordierite
Sillimanite
Andalusite
Biotite
Biotite Recrystallization.
Chlorite.
Sericite.
0·1
0·2
0·3
0·4
0·5
Distance from intrusion contact (Km.)
Pelite and Semi-pelite
Mg rich ← Chlorite
Phengite
Muscovite
Orthoclase
Biotite abundant
sparse
Cordierite
Garnet
Quartz
equilibrium recrystallization
angles – (new growth)
sub-grains recrystallization
re-organization of pre-existing boundaries
partial recrystallization, relict grains
Oligoclase - Andesine
Albite
Sillimanite
Andalusite
Quartzite
complete recrystallization
Quartz
Hornfels texture
sub grains, recovery, recrystallization
partial recrystallization
Chlorite
Muscovite
Biotite
Sericite + Phengite
Amphibolite
Biotite
Andesine
Hornblende
Green Hornblende
?
Sphene
?

Figure 14. - Experimental data relating to assemblages found in the contact metamorphic aureole of the Adamello Massif. The thick arrow shows the probable pressure (3kb) and temperature range (715° to 300°C) which may be inferred from the various mineral assemblages in the aureole. For a key to the various minerals see 1.50.

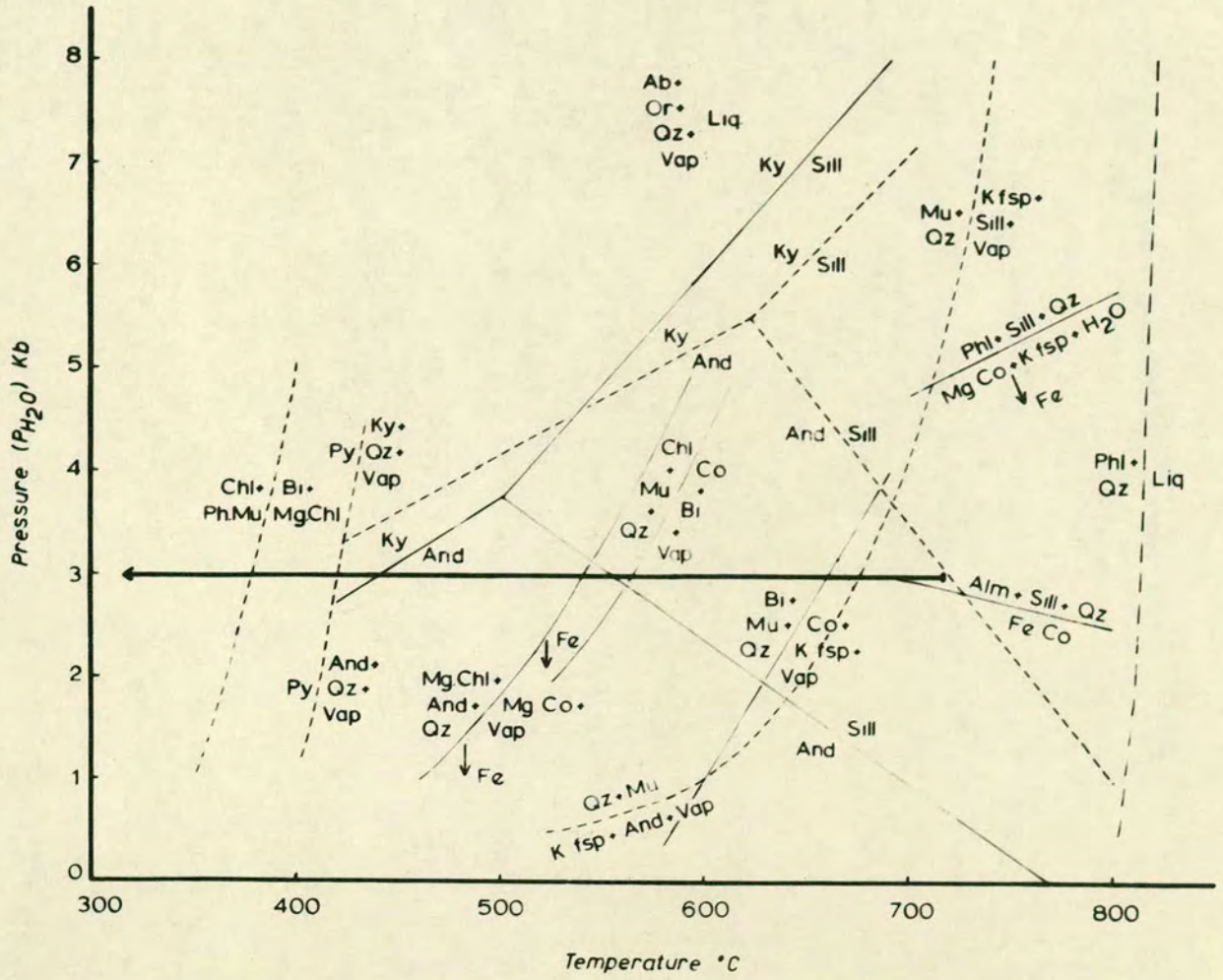
Pressure (P_{H_2O}) Kb
Temperature °C
0
1
2
3
4
5
6
7
8
300
400
500
600
700
800
Ab • Or • Qz • Vap
Liq
Ky
Sill
Ky
Sill
Mu • Qz
K fsp • Sill • Vap
Ky
And
Phl • Sill • Qz
Mg Co • K fsp • H_2O
Fe
Ky • Py • Qz • Vap
Chl • Bi • Ph.Mu, Mg.Chl
Ky
And
And
Sill
Chl
Co
Mu
Bi
Qz
Vap
Phl • Qz
Liq
Alm • Sill • Qz
Fe Co
Bi • Mu • Co • Qz • K fsp • Vap
Fe
And • Py • Qz • Vap
Mg.Chl • And • Qz
Mg Co • Vap
Fe
Sill
And
Qz • Mu
K fsp • And • Vap

appreciable Fe content reduced this temperature to nearer 700°C. It is well-known that slight variations in f O_2 affect the stability range greatly.

Muscovite is present in the outermost parts of the aureole, where sericite and phengite are common. Although it is present in all but the final 30 m. of the aureole it is generally a late stage mineral. Later recrystallization of the earlier muscovite has probably occurred. Muscovite + quartz break down to aluminosilicate + potash feldspar (Evans, 1965; Hess, 1969; Day, 1973; Althaus et al, 1970) at a temperature of about 675°C at P H_2O 3kb. The reaction is :-

$$KAl_2(Si_3Al)O_{10}(OH)_2 + SiO_2 \rightleftharpoons KAlSi_3O_8 + Al_2SiO_5 + H_2O$$

Muscovite Quartz K feldspar Sillimanite

Quartz fabrics and textures are related to temperature although the presence of deformation lamellae, even in sillimanite bearing hornfels, shows that other factors are also important (e.g. strain rate), since the lamellae are not seen in the high grade metamorphics north of the Tonale Line. The presence of dentate quartz grain boundaries in rocks from the aureole of the tonalite, even in the Pyroxene Hornfels facies, suggests that this aureole development occurred under a differential stress field (Spry, 1969) and was later than that of the biotite-quartz-diorite. The absence of markedly serriate boundaries in the inner parts of the biotite-quartz-diorite aureole suggests that near hydrostatic stress conditions existed. The later deformation event seen in the tonalite and its aureole is reflected in the inner part of the biotite-quartz-diorite aureole by the development of a biotite foliation which cross-cuts the hornfels minerals. In the tonalite aureole, biotite and sillimanite define this new foliation however. Biotite has grown in the biotite-quartz-diorite aureole, and recovery and recrystallization has occurred in the marginal parts of the biotite-quartz-diorite, showing that temperatures of over 300°C were prevailing at the time of deformation. A minimum time lag of 360,000 years may thus be obtained

(neglecting latent heat and fluid effects) between the two intrusions, from theoretical time - temperature studies (Lovering, 1935), assuming that the marginal parts of the biotite-quartz-diorite were at 300°C when the tonalite was intruded.

It is possible that the effects seen in the biotite-quartz-diorite and its aureole may be due to the later tonalite intrusion. However parts of the aureole showing a strong f_5 biotite foliation (e.g. T274B) lie 1.75 km. from the tonalite intrusion margin, and the evidence from the tonalite and biotite-quartz-diorite aureoles show that temperatures of 300°C are reached at distances of 400 - 600 m. from the intrusion margin. The time lag in intrusion appears to explain some of the textural, structural and mineralogical differences between the tonalite and biotite-quartz-diorite and their respective aureoles.

The presence of cordierite in the pelitic and semi-pelitic rocks of the aureole less than 150 m. from the intrusion margin may be taken to imply temperatures above 490°C at 3kb. P H_2O. Deer et al (1966) show that at pressures up to 5kb. P H_2O the reaction

$$\underset{\text{Mg Chlorite}}{Mg_4Al_4Si_2O_{10}(OH)_8} + \underset{\text{Pyrophyllite}}{2Al_2Si_4O_{10}(OH)_2} \rightleftharpoons \underset{\text{Mg Cordierite}}{2Mg_2Al_4Si_5O_{18}} + 6H_2O$$

occurs at temperatures of 450 - 525°C. Kerrick (1968) has shown that pyrophyllite reacts to form aluminosilicate + quartz + vapour at about 420° at 3 kb P H_2O. The reaction

chlorite + andalusite + quartz $\rightleftharpoons$ cordierite + H_2O

then defines the lower limit of cordierite. This occurs at about 540°C at 3kb (Seifert and Schreyer, 1970). The presence of Fe^{2+} will reduce this reaction temperature and pressure (P H_2O) to slightly lower values. We may take 540°- 560°C as an estimate of the temperature of first appearance of cordierite at P H_2O = 3kb, since the reaction

$$\underset{\text{Chlorite}}{(MgFe)_5Al_2(Si_3O_{10})(OH)_8} + \underset{\text{Muscovite}}{KAl_2(Si_3Al)O_{10}(OH)_2} + \underset{\text{Quartz}}{2SiO_2} \rightleftharpoons$$

$$\underset{\text{Cordierite}}{(MgFe)_2Al_4Si_5O_{18}} + \underset{\text{Biotite}}{K(MgFe)_3(Si_3Al)O_{10}(OH)_2} + 4H_2O$$

occurs at about 560° at P H_2O = 3kb (Seifert, 1970) and this may be more important than the preceding reaction. Winkler (1967) has shown that cordierite + potash feldspar + water may form from biotite + muscovite + quartz at temperatures of around 675°C at 3 kb P H_2O. These reactions are in agreement with P.T. data from other minerals and may account for the large amounts of cordierite observed in the inner parts of the aureole.

Richardson (1968) has shown that Fe cordierite changes to almandine + sillimanite + quartz at temperatures of 700° to 800°C and pressures greater than 2.5 to 3 kb P H_2O respectively. The garnet is an almandine-pyrope mixture dependent on the composition of the cordierite. The small red garnets observed adjacent to the biotite-quartz-diorite and granitic dykes, very close to the major intrusive contacts, probably result from this reaction. Mg content will raise reaction temperatures and pressures. These imply that temperatures over 700°C were attained at a minimum P H_2O of 3kb. Schreyer and Siefert (1969) show that Mg cordierite + alkali feldspar are unstable above 5.5 kb in the range 700° to 815°C. Hence a maximum pressure limit of 4.5 to 5 kb. is fixed by the presence of MgFe cordierite in the inner parts of the hornfels.

The occurrence of these garnets may be due to localised magnetic fluid migration such as has been noted by Turner (1968, p.223) and Shieh and Taylor (1969). The emanation of magmatic fluids along joints has been shown to give rise to wollastonite at temperatures of 675°C, P total 3kb and X CO_2 = 0.4 (Turner, 1968; Hyndman, 1972; Sapountzis, 1973). Similar contact temperatures were obtained by Shieh and Taylor (1969) from isotope studies on several mineral pairs from the Flynn grandiorite in Nevada. These temperatures are in agreement with the observed local anatexis adjacent to the tonalite.

The presence of aluminosilicate polymorphs, andalusite and sillimanite in the aureole can be used to determine temperature - pressure relations. Andalusite first appears by the dehydration of pyrophyllite.

$$Al_2Si_4O_{10}(OH)_2 \rightleftharpoons Al_2SiO_5 + 3SiO_2 + H_2O$$

Pyrophyllite Andalusite Quartz

This occurs at about 430°C at P H_2O 3kb. (Holm and Kleppa 1966).

Many sets of data are available for the aluminosilicate phase diagram but those given by Richardson et al (1969) and Holdaway (1971) are generally taken to be the most reliable to date. Holdaway discussed the discrepancies between the results of various workers. He showed that:- the presence of fibrolite in sillimanite may affect phase equilibria (Andalusite ⇌ Sillimanite) by about 200°C; intense grinding may cause strain in the components prior to reaction; Al - Si disorder occurs in experimentally formed sillimanite but is never found in natural specimens. The diagram given by Holdaway is consistent with thermochemical data and the observed assemblages in the Tonale Pass area. The values given by Richardson et al (1969) give improbably high pressure or temperature values to be consistent with the other data and theoretical curves.

Andalusite is present between about 250 m. and about 30 m. from the intrusion margin, whereas sillimanite occurs up to about 120 m. from the margin. Holdaway (1971) suggests that overstepping of 50°C or more between two phases may be expected since reaction entropies are very small. Hence a temperature of about 555°C may be inferred at P H_2O of 3 kb about 120 m. from the contact.

The temperature gradient inferred using the above experimental data is shown in Figure 13. The curve shows an exponential decrease away from the intrusion margin. It is important to realise that the maximum temperature in various parts of the aureole is not attained at the same time, the outer parts reaching maximum temperatures considerably later than the inner parts (Spry, 1969,p.126). Taking the cordierite data we may fix approximate pressure limits between 3 and 5 kb P H_2O. If P H_2O is almost equal to P total, a reasonable assumption if water migrates towards the intrusion in any quantity, and considering the metamorphic grade of the country rock prior to

intrusion, then the present depth of exposure would lie at 8.25 km. depth for 3 kb (taking rock density 2.8) and 14 km. depth for 5 kb. Assuming a geothermal gradient of 25°C/km. (Clark,1966) this would give country rock temperatures at the time of intrusion of 210°C (8.25 km.) and 350°C (14 km.) The former value is more compatible with observed data.

Buddington (1959) has classified plutons according to their depth of cover at intrusion. On the criteria given, the presently exposed levels of the Adamello massif in the Tonale Pass area are compatible with a depth of intrusion of about 8.25 km. below the surface. Using the orientation of the tonalite contact where it is undeformed (dips about 70°E in the Val Presena), simple trigonometry shows us that for a sphere of radius 4 km. the outcrops lie 5.4 km. below the top surface of the intrusion. Hence a cover thickness of only about 2.85 km. was present above the tonalite intrusion, whereas one of about 7.8 km. was present above the biotite-quartz-diorite using dips from near Tonale Pass. These values are in agreement with the features of the intrusions and their aureoles.

2.84 Structure and Strain Estimates.

The aureole shows a moderate to strong foliation whose orientation is generally approximately coincident with the intrusion margin and the f_1 and f_3 foliations. It is best seen in rocks with hornfels texture where it is defined by new biotite growth. The foliation is visible in outcrop in the tonalite aureole but not in the biotite-quartz-diorite aureole where the rock has a compact hornfels texture in hand specimen. In thin sections from this latter aureole, a strong alignment of biotite and minor white mica (muscovite ?) laths is seen. An intersection lineation plunging gently west to southwest is present in the tonalite aureole.

In the tonalite aureole, f_3 southward facing folds in the vicinity of the Tonale Line show open to close profile with interlimb angles of 100° to 60° and amplitude

/ wavelength ratios of about 1/2. As we approach the hornfels, these become progressively tighter and in the inner 200 m. of the aureole the interlimb angles decrease to 20° - 25° with amplitude/wavelength values of 2/1. These angular changes imply a shortening of about 63% in the inner part of the aureole, assuming pure flattening strain. Since this deformation is related to the foliation development in the tonalite and biotite-quartz-diorite (f_5 event) it approximates very closely to pure flattening. The shortening values are similar to those obtained from xenolith measurements in the tonalite and biotite-quartz-diorite and show that the f_5 deformation was localised around the intrusive margin, resulting in the increased strain seen in this area. It has been suggested by Buddington (1959) that foliation development around an intrusive contact is typical of many intermediate to shallow depth intrusions. The orientation of the foliation with reference to the separate pluton margins, and thin section studies in the biotite-quartz-diorite aureole preclude this possibility in the Tonale Pass area.

The folds in the biotite-quartz-diorite aureole show less tightening, and shortening values are lower than those stated above. The presence of quartz textures, showing recrystallization under stress in the outer parts of the aureole suggest that the deformation (f_5) occurred when the heat flux had migrated to those areas.

Taking the theoretical time-temperature relations given by Lovering (1935), we obtain a time of about 400,000 years for the cooling of the tonalite body to about 150°C above the country rock temperature. The effects of uplift during cooling may be assessed by considering uplift rates typical of orogenic areas, 0.2 to 0.4 mm/yr (Mueller, 1973; Clark and Jäger,1969). A temperature reduction of the order of 2° to 4° occurs assuming a geothermal gradient of 25°C/km., and a pressure reduction of 20 to 50 bars. Even if the geothermal gradient is 40°C/km. (unlikely from metamorphic assemblages in the Southern Alps) it is assumed the

temperature + pressure change may be ignored during the cooling of the intrusive body. The problem is thus a static one. If the foliation formation in the tonalite occurred during cooling, a conclusion suggested by the mineralogical and structural data, then shortening of 73.6% (e = -0.736) occurred in about 400,000 years. Such figures give us a compressive strain rate

$$-\dot{e} = \frac{0.736}{4.10^5 \cdot 3.15 \cdot 10^7} = 5.8 \cdot 10^{-14}/\text{sec.}$$

This value is of the same order as that obtained from the San Andreas fault ($3 \cdot 10^{-14}$/sec.). Although the value obtained here is subject to several uncertainties (particularly in the time factor) it nevertheless shows that tectonic strain rate was of the order of 10^{-14}/sec.

3.00 SOUTHERN ALPS

3.10 INTRODUCTION

The unit, which lies to the south of the Tonale Line, consists of metasediments in the area mapped. The rocks are collectively known as the Edolo Schists, although to the west the metamorphic grade increases and at Lake Como sillimanite bearing Hercynian gneiss is found. The intrusion of the Adamello massif has resulted in the development of contact metamorphic assemblages up to 800 m. from the intrusive contact. The metasediments weather to form the low ground on the south side of the Val di Sole, and in the Valle di Narcanello. Good outcrops are present along some stream sections but generally the outcrop is discontinuous.

3.20 LITHOLOGY

The unit consists of a series of sub-vertical bedded pelitic and semi-pelitic schist, quartzite and minor amphibolite. The lithological sequence is traceable across the width of the area and its regional strike lies at a low angle to the Adamello massif/Edolo Schist contact. The well-developed cleavage is commonly coincident with the bedding.

At M320 quartzite contains distinct non-inverted cross-bedding with the maximum angle between foresets and bedding modified by deformation to about 20°. Hence the Edolo Schist sequence becomes younger northwards.

A small fine-grained dolerite dyke cross-cuts pelitic gneisses at T215, but the m_1 metamorphism has converted the original basalt into a rock consisting of albite-biotite-sericite-chloritoid-hornblende with rare quartz.

Within the sequence is a finely banded amphibolite (T218, M163) 3 to 4 m. thick. This may be a thin basalt flow or a marl horizon. Without detailed geochemical studies it is not possible to distinguish between the two possibilities (see Leake ~~and Evans~~, 1964). No marble horizons crop out in this area and the amphibolite may be a basalt flow or sill. Some alteration of amphibolite has occurred due to contact metamorphism.

3.30 METAMORPHISM

The rocks of the Southern Alps have undergone two Greenschist grade regional metamorphic events, m_1 and m_2, although the intrusive Adamello massif has resulted in subsequent local development of high grade contact metamorphic assemblages (see 2.82, 2.83). The following assemblages were recorded in the metasediments and basaltic dyke:-

1) Qz - Ab - Ser - Bi - Kf	Pyrite - Mag - Tourm
2) Qz - Ab - Ser - Chl - Kf	Mag
3) Ab - Bi - Ctd - Ser - Hbl	Qz

These assemblages show only slight contact metamorphism. It is difficult to distinguish between original biotite and mimetic biotite after chlorite, grown during the contact metamorphic event, particularly in the area adjacent to the summit of the Tonale Pass. In thin section biotite is developed in some specimens axial planar to f_1 folds and also defining a foliation sub-parallel to the compositional banding. If this biotite is primary we are probably in the Upper Greenschist facies. The presence of chloritoid and blue-green hornblende in the basaltic dyke supports this conclusion.

More generally in the eastern part of the area, biotite is absent and assemblage 3) is developed in pelitic and semi-pelitic schist. Quartz pods, sweated out during the m_3 metamorphism, are locally abundant. These pods were folded by the f_3 event. It is probable that the m_1 metamorphism was of Hercynian age and locally reached biotite grade (P = 2.5kb to 4kb) whereas the subsequent m_2 metamorphism was only of chlorite grade (P = 3kb to 4 kb). In the eastern part of the area some retrogression from earlier biotite grade schist may have occurred during this later Early Alpine event.

3.40 STRUCTURE

The structure of the area is controlled by the effects of the f_1 and f_3 fold events and the intrusion of the Adamello massif. The f_2 and f_4 events are absent in the

Southern Alps.

3.41 f_1 event

During the m_1 metamorphism, close to isoclinal f_1 minor folds were formed. The folds affect thin-bedded sediments and pre-existing quartz veins. Figure 15(a) shows typical fold profiles which have a geometry close to similar. Wave-lengths vary from 1 cm. to 10 cm. and amplitudes from 0.5 cm. to 15 cm. Map 2 shows the axial orientations in the two major areas of outcrop, which vary from W to WSW in the east, to SW in the west. This reflects the regional swing of bedding and cleavage, the latter being axial planar to f_1 folds and defined by biotite and sericite. The folds show a general vergence to the N and NW but are locally variable. Although bedding/cleavage angle varies, particularly in the area immediately south of Tonale Pass (near Funivia station), no evidence of large scale f_1 folds was seen and it is probable that bedding was not orthogonally related to the principal stresses.

3.42 f_3 event

Open to tight, small to large scale folds affect most of the metasediments of the Southern Alps. The folds are generally asymmetrical and have a southerly vergence. At the head of the Val di Sole (M320) a large scale f_3 asymmetrical open fold has formed around a thick quartzite band in pelitic schist. The middle limb is nearly horizontal. Tight, f_3 minor folds are best developed in semi-pelitic rocks and the profiles commonly show a finely crenulate form (Figure 15(a)). Fold style varies with lithology and bed thickness. Wavelengths vary from 5 cm. to 200 m. and amplitudes from 5 cm. to 25 m. f_3 fold orientations are locally variable but commonly plunge southwest (Map 2). Axial planes strike northeast-southwest and dip steeply southeast, except where the bedding dips north at moderate angles. As seen in Figure 15(a), f_3 refolding of f_1 folds occurs. The f_3 folds do not become tight in such instances.

Figure 15(a) - Fold profiles in metasediments of the Southern Alps. All profiles are drawn looking down the fold axes. The f_1 folds have a penetrative axial planar fabric and generally verge N or NW. In contrast, the asymmetrical f_3 folds ~~in contrast~~ invariably verge to the S. In pelitic and semi-pelitic lithologies a weak axial planar f_3 cleavage is developed.

Figure 15(b) - Stereogram showing the orientation of the f_5 fold axes and f_6 kink band axes and axial planes. The f_5 fold axes generally plunge gently to the southwest. The f_6 kinks have sub-vertical axes and imply horizontal compression from a SE - NW direction.

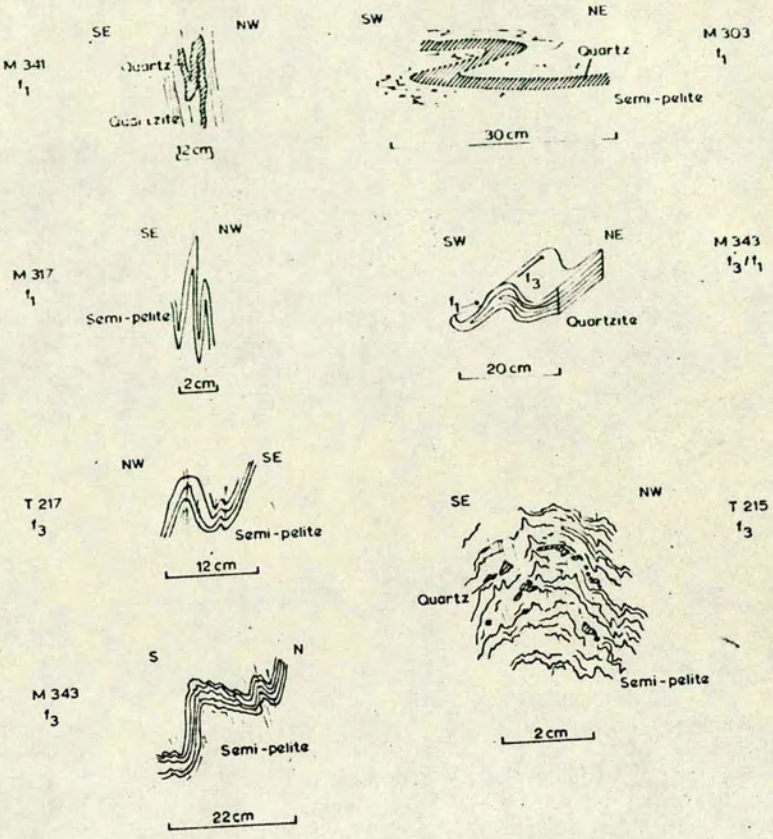
SE
NW
M 341
f_1
Quartz
Quartzite
12cm
SW
NE
M 303
f_1
Quartz
Semi-pelite
30cm
SE
NW
M 317
f_1
Semi-pelite
2cm
SW
NE
M 343
f_3/f_1
f_3
f_1
Quartzite
20cm
NW
SE
T 217
f_3
Semi-pelite
12cm
SE
NW
T 215
f_3
Quartz
Semi-pelite
2cm
S
N
M 343
f_3
Semi-pelite
22cm

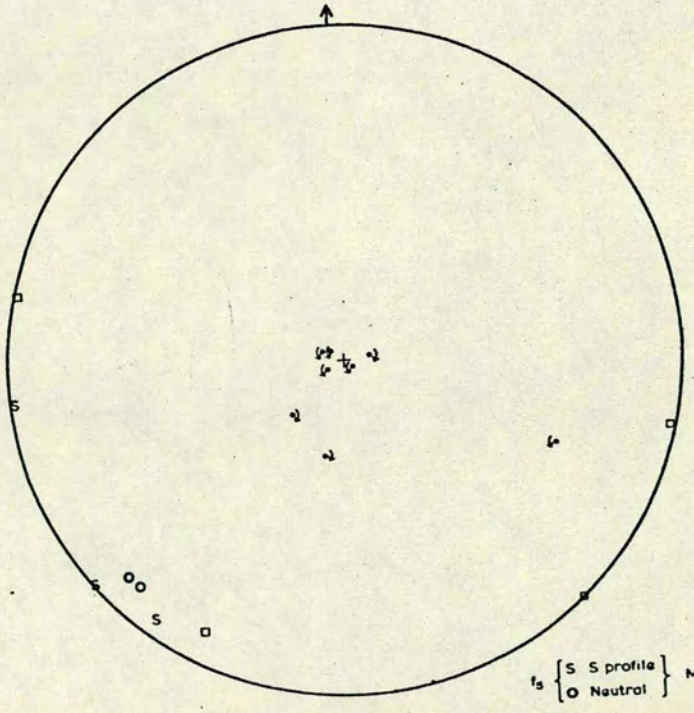
S
S
S
f_5 { S S profile, O Neutral } Minor folds
f_6 { Kink band axis with sense of rotation when viewed down axis; Pole to axial plane }

3.43 Effects of the intrusion of the Adamello massif

The Adamello intrusion has modified the regional strike of the metasediments of the Southern Alps. This causes a swing from around 085° in the Val di Sole to around 045° in the Punta di Castellacio area to the west. f_3 minor folds have a superimposed "annealed" hornfels texture in the 100 m. adjacent to the intrusive contact, showing that intrusion post-dated the f_3 event. Numerous sub-vertical dykes have also been injected into the metasediments close to the intrusion.

During the cooling of the intrusion, deformation occurred in the aureole with the amount of strain decreasing away from the contact. This flattening strain has resulted in the tightening of the pre-existing f_1 and f_3 folds and the formation of a new biotite foliation in the inner part of the aureole.

The mineral changes which have resulted in the metasediments due to intrusion, extend up to 800 m. from the contact. Biotite is only developed in the inner 300 m. Chlorite and phengitic muscovite are common in the outer parts. Quartz recovery and partial recrystallization has also occurred in this zone. A more comprehensive description of these changes is given in section 2.82.

3.44 f_5 and f_6 events.

The f_5 event has resulted in the formation of minor open to close, southward verging folds with west to southwest gently plunging axes. A weak lineation is associated with these folds. In the inner parts of the aureole, particularly adjacent to the tonalite, a strong gently westerly plunging lineation is developed in the quartzites in places. In some fissile beds a fine crenulation or strain slip cleavage has developed. The folds have wavelengths of 5cm. to 25 cm. and amplitudes of 2 cm. to 12 cm. Fold formation is probably closely related to the foliation development in the margin of the Adamello massif and the inner part of the contact aureole. f_5 fold axis orientations are shown in Figure 15(b).

The f_6 event has resulted in the development of minor dextral and sinistral kink bands. These kinks have axes plunging sub-vertically or steeply south to southeast as shown in Figure 15(b). The kink bands are only developed in fissile pelitic bands and rarely in finely-bedded semi-pelitic schists, and quartzites. The bands are consistent with shortening along the plane of the banding (E-W to NE-SW) or at a low angle to it. The predominance of dextral kinks with the steeply plunging axes to the southwest, suggests that the principal stress acted in a sub-horizontal plane in a SE-NW direction.

4.10 REGIONAL SIGNIFICANCE OF THE TONALE-INSUBRIC LINE.

The Tonale Line and its western extension, the Insubric Line, form a major tectonic boundary in the Alps. The location of this lineament is shown in Figure 2. Summaries of the important geological changes which take place across the Line are given by Gansser (1968) and Johnson (1973). In the author's opinion, it forms the southern limit of the Pennine and Austro-Alpine Nappes. The presence of a "Wurzel" or root zone north of the Tonale Line is included in almost all syntheses of the Eastern Alpine area. Figure 16 shows the tectonic relationships north of the Tonale Line in the western part of the Eastern Alps (Gwinner, 1971). The Tonale-Insubric Line and its eastern continuations, the Judicaria and Pusteria-Gailtal Lines, also act as regional metamorphic palaeomagnetic and geochronological boundaries. North of this lineament, Alpine metamorphism varies in grade from Upper Amphibolite (Ticino Dome) to Greenschist facies (E.Alps) whereas to the south of the lineament no Alpine metamorphism has been recorded. This metamorphism has been dated at 28 - 38 m.y. (Jäger et al, 1967; Hunziker, 1970; Jager, 1970) in the Ticino area. Field relations across the Gailtal Line in the Eastern Alps are poorly known at present; it has been suggested (Oxburgh, 1972) that the basement of the Southern Alps is continuous with the "Altkristallin" sheet of the Austro-Alpine Nappes. Similar ideas, expressed by Carraro et al (1970) relating the Valpelline Series and the gneisses in the Ivrea Zone (south of the Insubric Line) in the western Alps may be invalid since glaucophanitic paragenesés of early Alpine age have been found in the Valpelline Series by Dal Piaz et al (1971). However, it is possible that these two tectonic units may be correlated for events preceding the major Early Alpine movements. It is particularly significant that the lineament represents the southern margin of the Early

Figure 16 - Diagrammatic representation of regional structural relationships within the Eastern Austro-Alpine Nappes north of the Insubric Line. (from Gwinner, 1971). Solid arrows represent well-documented thrust movements of the various sheets. Dashed arrows show possible movements.

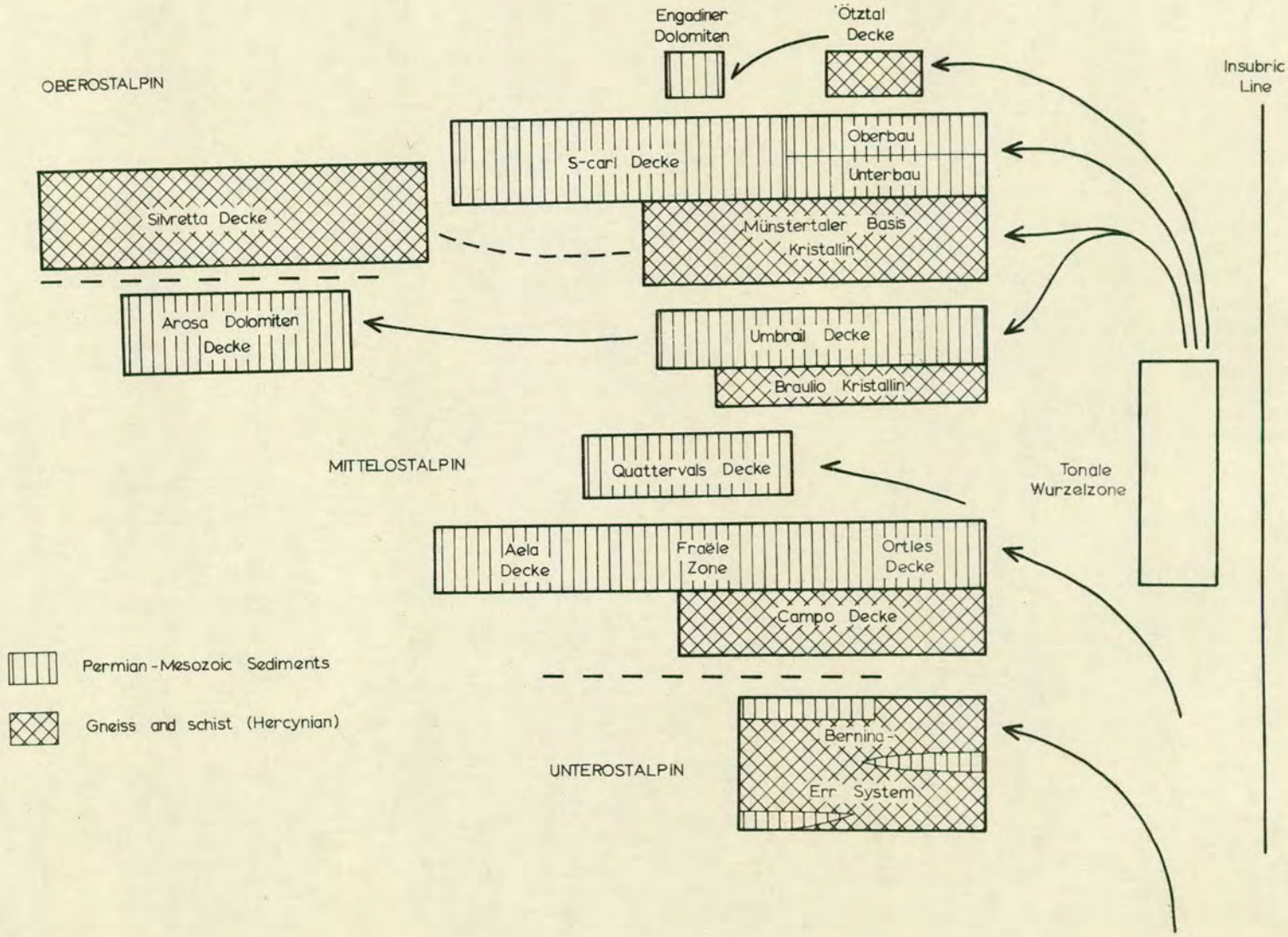
Engadiner Dolomiten
Ötztal Decke
OBEROSTALPIN
Insubric Line
Oberbau
S-charl Decke
Unterbau
Silvretta Decke
Münstertaler Basis Kristallin
Arosa Dolomiten Decke
Umbrail Decke
Braulio Kristallin
MITTELOSTALPIN
Quattervals Decke
Tonale Wurzelzone
Aela Decke
Fraële Zone
Ortles Decke
Campo Decke
Permian - Mesozoic Sediments
Gneiss and schist (Hercynian)
UNTEROSTALPIN
Bernina
Err System

Alpine (80 m.y.) high pressure - low temperature metamorphism in the Western Alps (Dal Piaz et al, 1972; Ernst, 1971; Chatterjee,1971). A similar earlier event may be postulated in the Eastern Alps from the evidence of Oberhauser (1968), who showed that the Walserberg Sandstone (Cenomanian - about 100 m.y.) of the Salzburg area contains widespread detrital glaucophane.

4.20. AGE AND GEOLOGICAL NATURE.

The Tonale-Insubric Line has acted as a tectonic boundary from at least Carboniferous times. The Ivrea Zone, a sequence of deep level basic and ultrabasic rocks and granulite facies gneisses, shows a strong thermal event at 290 - 300 m.y.(Köppel,1974; Graeser and Hunziker, 1968). Taken in context with geophysical evidence which suggests that the Ivrea body represents a transition between lower crust and upper mantle (Geise, 1968) Köppel (1974) has suggested that these Hercynian ages reflect the major uplift of the Ivrea Zone. A consistent reduction in ages from 315 m.y. to 185 m.y. from the Ceneri to the Ivrea Zone for K - Ar and Rb - Sr mineral ages, 450 m.y. to 275 m.y. for U - Pb monazite ages and 450 m.y. to 300 m.y. for U-Pb zircon ages, show that uplift occurred preferentially adjacent to the Insubric Line. The Canavese Zone, a linear belt of Carboniferous to Jurassic sediments, represent a unique facies associated with the Insubric Line (Reinhardt, 1966). Kahler and Prey (1963) have shown that the Upper Palaeozoic-Mesozoic sequence is complete south of the Gailtal Line whereas a Permo-Carboniferous unconformity is present north of the Line. Downfaulted wedges of Mesozoic (post Triassic) and Eocene sediments related to the South Alpine facies, lie adjacent to the Judicaria Line and the eastern part of the Tonale Line (Van Hilten,1960; Vecchia, 1957). Eocene conglomerates are locally developed along the Judicaria Line and these show an apparent northward provenance (Van Hilten, 1960; 1964). There is a notable difference in morphological aspect

of the Tonale - Insubric Line west and east of Locarno. East of Locarno several exposures show that it is a steep late Alpine fault across which uplift of the Central Alps has occurred (Argand, 1911; Gansser, 1968). The western extension of this fault, the Simplon - Centovalli Line has been shown by age dating (Hunziker, 1970) to be the site of late Alpine vertical differential movements of the order of 5 to 8 km. Sassi et al (1974) have reported the presence of lawsonite in Oligocene granitic intrusives adjacent to the Pusteria Line. Nitsch (1968) has shown that pressures over 3 kb. are necessary for lawsonite-quartz stability implying uplift of about 10 km.

The aseismic nature of the Tonale - Insubric Line is rather surprising considering that it appears to have been the site of large scale relative movements over a long period of time. No large scale gravity, seismic or magnetic anomalies occur beneath the Eastern Alps. Those in the Western Alps may be related to visible geological features which have Hercynian ages (i.e. Ivrea Zone), suggesting that we may be seeing the final stages of the Alpine orogeny. In more seismically active orogenic areas such as the Himalayas, Andes, Hellenides etc., large scale seismic gravity and magnetic anomalies are generally present.

4.30. NATURE OF THE TONALE LINE IN THE AREA MAPPED.

In the Tonale Pass area, the Tonale Line separates the Stavel Gneiss (Quartz-feldspar-phengite-muscovite gneiss) to the north, from the contact metamorphosed quartz - feldspar-sericite-chlorite schist and quartzite to the south. It also apparently exerts tectonic control on the intrusion of the Adamello massif. The line itself is marked by 40 to 70m. of dark to light grey, massive to sheared, cohesive breccia which is well exposed at two outcrops in the area mapped.

In thin sections (T11, T238) angular fragments of brown glass (pseudotachylite) up to 2 cm. (average 3 m.m.) and fragmented and partially altered potash feldspar and albite, lie in a very fine-grained to glassy matrix of

quartz, sericite-clinozoisite (?) - feldspar. Minor biotite, calcite and pyrite are present and magnetite and/or limonite are disseminated throughout the rock. Dark grey ultra fine-grained, thin, mylonite zones are present in the rock and small scale displacement has occurred across these zones. All the components of the rock are fractured or fragmented and may be elongated (e.g. pyrite). The rock may be termed a fine-grained microbreccia or cataclasite (Sibson, Tectonic Studies Conf. Dec. 1973; Higgins, 1971; Spry, 1969).

Sibson (1973) considered the theoretical constraints of faulting with relation to pressure, temperature and pore fluid pressure. He found that the production of cataclasite is consistent with large scale fault movements across a fault Zone only if pore fluid pressure is significantly large ($>0{\cdot}2$ lithostatic pressure). If large amounts of dilation occur or the rocks are relatively dry, pseudotachylite readily forms by frictional melting (Philpotts, 1964; Masch, 1973). This conclusion is in agreement with the observation of widespread sericitization of feldspar and presence of calcite in the cataclasite. The angular fragments of pseudotachylite then represent earlier fault movements at deep levels, at which melting more easily occurred. Mackenzie and Brune (1972) showed that the amount of melting which could occur on a single plane was limited to about 1 cm. in thickness. Once the melt has formed it acts as a lubricant for the release of almost all the elastic strain energy in the region of the shock. Philpotts (1964) has shown that pseudotachylite is enriched in the low melting fraction of granite composition and contained abundant H_2O and CO_2 gas. This gas content played an important part in the pseudotachylite mobility. We may conclude that the widespread abundance of pseudotachylite fragments in the cataclasite at the Tonale Line, shows that deep level differential movements have occurred across a 40 to 70 m. zone. The abundance of pseudotachylite veins in the gabbros of the Ivrea Zone, a

region known to have been at deep crustal or upper mantle levels, shows that it readily develops in a low water pressure environment.

In outcrops where the cataclasite is sheared, the schistosity has a variable orientation ranging from 090/75°S. to 070/75°N. The overall orientation of the Tonale Line is vertical in this area, although Van Hilten (1960) reported that it dips steeply north further east.

Van Hilten (1960) has shown that the Judicaria Line is a mylonite zone dipping steeply W.N.W. and Johnson (1973) reports that about 1 km. of mylonite characterises the Insubric Line in the Valle d'Ossola, N.W. Italy. The presence of Late Alpine faulting and the uplift of the Stavel Gneiss in the Tonale Pass area masks any earlier effects. North of the Stavel Gneiss zone lie a series of thrust sheets, the Central Alps, which form part of the "Altkristallin" Sheet (Oxburgh, 1968) of the Austro-Alpine Nappes. These sheets are separated by 10 to 50 m. mylonite zones.

4.40 CONCLUSIONS.

The Tonale Line is considered on the basis of the facts stated above to be a deep seated zone of repeated movement, at least since the Carboniferous. Large scale northward directed thrusting occurred north of the Line in Middle Cretaceous to Eocene times. Biotite ages of 78 to 88 m.y. and muscovite ages of about 86 m.y. in the southern parts of the Ötztal massif and the area surrounding the Tauern Window ("Altkristallin" sheet), show that an Early Alpine metamorphic event has occurred in the Eastern Alps. These ages are related to the major thrusting of the Austro-Alpine Nappes (Schmidt et al,1967; Harre et al, 1968; Cliff et al, 1971; Miller et al,1967; Lambert 1970). Oberhauser (1968) has shown that stratigraphic evidence from the Flysch, Helveticum and Molasse deposits strongly suggests that thrusting continued as late as 55 m.y. The heavy mineral contents of these units reflect the tectonic changes which occurred to the south (Woletz, 1967). In the Gosau beds (Dach-

stein area, near Salzburg) there was an abrupt change of heavy mineral content from chromite, zircon and subsidiary rutile and tourmaline to garnet in the Campanian (Upper Cretaceous). Similar changes are present in the Flysch where garnets occur in Cretaceous sediments, and in the Molasse where garnets are restricted to the Late Eocene to Middle Oligocene period.

Late Alpine movements have resulted in the uplift of the Stavel Gneiss and, by analogy with geochronological data across the Insubric Line to the west, uplift of the Central Alps. The Tonale Line has acted as a fault during this event. In the Val Morobbia (E. of Locarno, N.Italy) for example, ages change from 26 m.y. immediately north of the Insubric Line to 326 m.y. only 100 m. south of it (McDowell, 1968). Scheuring et al (1974) have shown from detailed age dating of the Biella tonalite-andesite suite, adjacent to the Ivrea Zone, that a vertical uplift of at least 3.5 km. (north side relatively up) has occurred across the Insubric Line in the Western Alps since the Oligocene.

5.00 STAVEL GNEISS

5.10 INTRODUCTION

This unit consists of massive, medium to coarse-grained, uniform quartz-feldspar-phengite-muscovite gneiss. It crops out within a narrow linear belt 0.7 to 1 km. wide, trending in an approximately 075° - 255° direction across the area mapped. The gneiss unit is bounded to the south by the Tonale Line and to the north by the paragneisses of the Altkristallin Sheet (Central Alps). The northern contact is a narrow mylonite zone and chloritisation of biotite in the adjacent paragneiss has occurred for up to 50m. Previous mapping my Bianchi, Dal Piaz et al (1940) restricted the outcrop of the Stavel Gneiss to a small area east of the Tonale Pass. However the present mapping has shown that the unit extends to the west of the Tonale Pass although outcrops are sparse. A similar lithology has been described from the Monte San Vigilio area (5km. south-west of Merano) adjacent to the Judicaria Line by Lorenzoni and Zanettin-Lorenzoni (1969). Although they term the rock a conglomerate gneiss, a photomicrograph and accompanying description show that the gneiss can be matched with the Stavel Gneiss.

5.20 LITHOLOGY AND TECTONIC RELATIONSHIPS

The Stavel Gneiss is mottled white, pink and grey-green, and has a well-defined but wavy foliation defined by the phengite. Prominent muscovites cross-cut the phengite foliation and the apparent rodding lineation of quartz, feldspar and phengite, which pitches gently west southwest to west in the gneiss. The lineation and foliation are very strong near the northern margin of the gneiss belt and in narrow zones within the gneiss; this gives the rock the appearance of an L tectonite (Turner and Weiss, 1963). In an approximately 100m. wide linear zone passing through Stavel, the weakly foliated gneiss contains abundant feldspar augen up to 2.5cm. in width (average 0.5cm. wide).

The age relationships between the gneiss and adjacent

geological units are difficult to ascertain as both contacts are tectonic. The presence of abundant phengite indicates that high water pressure was present during its growth, a fact compatible with the local retrogressive effects in the adjacent paragneiss. Similar foliated albite-quartz-phengite-epidote augen gneiss crops out in the Sesia Zone (Valle di Gressoney, N.W. Italy) near Gaby; K-Ar and Rb-Sr phengite ages of 61 m.y. and 71 m.y. respectively were obtained by Dal Piaz et al(1973). A zone of quartz-feldspar-muscovite gneiss 32km. long and 0.5 to 1km. wide has been described in the Southern Zillertaler Alps (N.Italy) by Borsi et al (1973). The gneiss contains augen of microcline, perthite and in parts albite, up to 10cm. across. Rb-Sr muscovite ages of 65 and 51 m.y. and Rb-Sr biotite ages of 16 to 23 m.y. were obtained from this gneiss which gave a whole rock isochron of 395 m.y. Assuming that slight modification of these latter muscovite ages has resulted from later thermal effects, there was localised development of phengite in widely separated parts of the Alps during the Early Alpine event (80 - 65m.y.)

5.21.
Mineralogy and Texture

In thin section the gneiss comprises orthoclase, microcline, perthite and albite and rarely oligoclase porphyroclasts in a matrix of recrystallized quartz, phengite, muscovite, subhedral albite and minor euhedral pyrite (limonite, hematite) and anhedral apatite and rarely calcite. Siderite is abundant in one section (T330B).

The albite and potash feldspar porphyroclasts, 1 to 5mm. in diameter, are sub-rounded to angular, commonly fractured and fragmented, and show bent twinning and strain shadows. Plate 5 shows a large fragmented low albite porphyroclast (specimen T344) with the spaces infilled with elongate recrystallized quartz and minor anhedral orthoclase. Grain elongation is approximately 2 : 1 with the long axis parallel to the separation vector. From measurement of fragment separation in a thin section perpendicular to the foliation and containing the lineation, a minimum strain value ($\sqrt{\lambda}$) of 1.87 parallel to the

Plate 5

(a) Fragmented and rotated low albite porphyroclast with elongate quartz grains and subsidiary feldspar in the resulting gaps. A phengite rich zone can be seen adjacent to the porphyroclast. Lineated Stavel Gneiss (T344) in which the direction of the lineation is coincident with the line of maximum separation of porphyroclast fragments.

(b) New smaller microcline and orthoclase grains formed adjacent to a large fractured microcline - microperthite porphyroclast. The rock is particularly phengite rich in this area. Feldspar rich phengite gneiss (T8). Some feldspar augen are composed entirely of these small unfractured irregular feldspar grains.

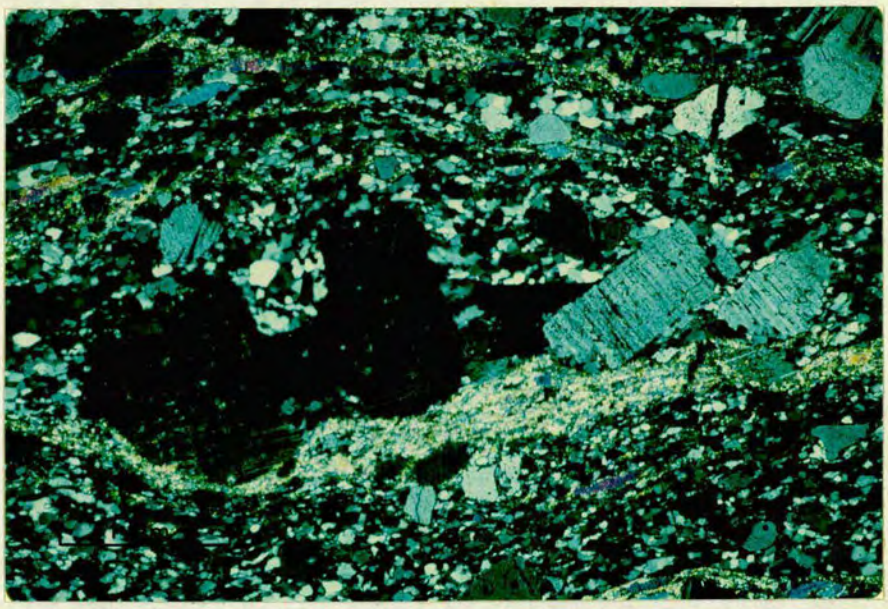

lineation, which pitches 5° to 257°, was obtained. The fragments show minor sinistral rotation but this is only a local effect due to interference of nearby grains. In other thin sections, strain values of 1.5 to 2 have been obtained by measurement of the fragment separation of feldspars parallel to the lineation. Extension has also occurred in the plane of the foliation perpendicular to the lineation and values of $\sqrt{\lambda}$ of up to 1.5 have been measured. In many porphyroclasts marginal corrosion has occurred and the dislocated crystals can no longer be exactly matched. Quartz is generally the corrosive mineral, or the product of the corrosive reaction.

Also within the gneiss are minor rounded anhedral feldspar grains and grain aggregates up to 5mm. in diameter. These porphyroblasts become abundant and reach 2.5cm. in the augen gneiss zone. The grains may show small amounts of fracturing, and consist of albite, microcline, orthoclase and perthite commonly with abundant small albite and quartz inclusions. The microcline grains, which generally consist of several separate crystals, have cross-hatched twin patterns of variable orientation within them. The phengite foliation abuts against these porphyroblasts in some specimens although it is partially deflected around them in others. Mutually intergrown microcline, albite and perthite constitute part of the large feldspar augen although some remnant K feldspar also occurs. Plate 5(b) shows new feldspar growth (microcline + orthoclase) around a large remnant microcline - microperthite porphyroclast. The presence of these feldspars is confined to the Stavel Gneiss unit in the area mapped.

Phengite is the dominant mica in the Stavel Gneiss and shows notable pale green pleochroism, particularly in the more southern exposures of the gneiss. It forms long aggregates of small grains 0.01 to 0.2mm. long, which show identical optical orientation. In some thin sections the phengite is localised in planar zones 0.2 to 2mm. wide, which appear to be related to small shear or fracture zones within the rock. 1 to 2 mm. wide phengite zones

commonly form sheaths around large orthoclase grains or aggregates (c.f. Cliff et al, 1971). Less pleochroic phengites up to 1 mm. long have formed in the larger phengite aggregates.

Muscovites up to 2 mm. in diameter post-date the phengite foliation and feldspar porphyroblast growth. In the central parts of the gneiss they have grown across the foliation trace at right angles. More generally they are developed at random angles within the phengite rich zones. Where muscovite grows across the foliation, the quartz grains locally show a dimensional elongation parallel to the new direction of growth. Some muscovites show kinking and strain shadows which may be correlated with either the f_5 minor folds or the f_6 kink bands present in many parts of the Stavel Gneiss.

Euhedral pyrite, up to 3 mm. in diameter, occurs in the southern part of the Stavel Gneiss. Pyrite (FeS_2) has a large stability field even at an S concentration as low as 10^{-6} M (Krauskopf, 1967, p.265; Ohmoto, 1972). Barnes and Czamanske (1967) show that pyrite is stable up to f O_2 values of 10^{-32} bars at a pH of about 4.5 and a temperature of 250°C. A decrease in sulphur-bearing ion concentration from $\Sigma S=0.1$ to $\Sigma S=0.01$ results in displacement of the pyrite field to higher f O_2 values. Pyrite stability in the Stavel Gneiss is governed by the reaction:-

$$3FeS_2 + 1.5\,O_2 \rightleftharpoons Fe_2O_3 + 2S_2$$

Mica-feldspar reactions raise f O_2 to high values; i.e. 10^{-11} to 10^{-20} bars at temperatures of 400°- 500°C (Turner 1968, p.124). Taking an estimate of $Log_{10}Kw = 11$ at 500°C (Barnes and Kullerud, 1961) and f $S_2 = 10^{-4}$ bars (Barton and Skinner, 1967) where

$$Kw = \frac{(a\ Fe_2O_3)(f\ S_2)^2}{(a\ FeS_2)^3\ (f\ O_2)^{3/2}}$$

then assuming that total pressure and P H_2O are constant and that the activity of the solids is unity, then $10^{11} = 10^{-8}/(f\ O_2)^{3/2}$ and hence f $O_2 = 10^{-12.17}$ bars at equilibrium. At 400°C, $Kw = 10^{19}$ and f $O_2 = 10^{-18}$ bars at

equilibrium. Even taking f S_2 as 10^{-2} bars, an unreasonably high estimate in view of the amount of pyrite in the gneiss, then at 500°C f O_2 = 10^{-10} bars at euilibrium. Provided that temperatures lie between 400° and 500°C, pyrite is stable in a moderately high oxidising system ($10^{-18} < f\ O_2 < 10^{-12}$).

To the north, limonite pseudomorphs after pyrite are common, particularly associated with phengite zones. Limonite also infills fractures near the northern margin of the gneiss. Limonite development is attributed to late stage, low temperature alteration when pyrite would be unstable at high f O_2 values.

It is tempting to correlate the muscovite growth with that seen in the mylonite zones, although there is no confirmatory evidence for this. Such a correlation would suggest that phengite development was related to the Early Alpine f_3 event.

5.30 STRUCTURE

The Stavel Gneiss has a poorly defined, coarse planar anisotropy defined by irregular phengite layers. This foliation is not generally a plane of splitting. In some outcrops, particularly those in the area west of the Tonale Pass, a foliation and subsidiary compositional banding may be distinguished. The banding is approximately coincident in orientation with the foliation although local dip divergence of up to 30° may be seen.

Poles to foliation are shown in Map 2. The foliation varies in dip from 45°N to 70°S and in strike from 045° to 090°. There has been later f_6 moderate scale open folding along moderately steep to shallow plunging southerly axes. These folds cause the spread in foliation pole orientation. The formation of these folds may be synchronous with the growth of muscovites, which are weakly aligned down the dip of the foliation, and recrystallization and reorientation of quartz.

Minor folds are uncommon in the Stavel Gneiss and, with the exception noted in section 5.31, they refold the

phengite foliation and have an asymmetry which implies a relative southward directed translation. The folds plunge gently southwest and generally have sub-vertical axial planes. The orientation of the fold axes is shown in Figure 17(a). The folds are assigned to the f_5 event. The variation in plunge of the minor fold axes suggests that the strain axes were not constant within the gneiss unit and/or the orientation of the foliation was variable prior to folding. Rarely f_6 kink bands and lines of sigmoidal tensional veins are seen. These features post-date all the above structures.

Apparent rodding lineations of quartz, feldspar and in parts phengite, are abundant in the gneiss. Lineation orientations (f_3) are given in Map 2. In some areas where both compositional banding and foliation can be observed, the lineation represents preferred growth along the intersection of the two planes. This lineation may accord with the extension direction (e.g. T344) particularly near the northern margin of the Stavel Gneiss unit.

5.31 Strain estimates

Within the augen gneiss , microcline-perthite, orthoclase, and albite aggregates show a distinctly ellipsoid form. The major, intermediate and minor axes of the ellipsoid can be relatively accurately determined by inspection. The ratios of these axes are consistent throughout the outcrop but are not exactly orthogonally related to the foliation. Figure 17(b) shows the orientation of the X, Y, and Z axes derived from the feldspar augen in relation to the wavy foliation and later f_5 fold axes and small kink band axial planes (f_6). The graphs in Appendix 3 show the geometrical mean values for 25 augen measurements taken in three planes (75 measurements in total) mutually at right angles and orthogonally related to the X, Y and Z directions. Taking the augen as initially spherical we obtain X:Y:Z ratios of 6.99:2.56:1 with a k value (Flinn, 1962) of 1.11. The good correlation between arithmetical and geometrical means shows that the variation and error in the measurements is small. The results imply that the

Figure 17(a) - Stereogram of f_5 fold axis orientations. The folds have sub-vertical axial planes and a southerly vergence.

Figure 17(b) - Stereogram showing the orientation of X, Y and Z strain axes derived from inspection of feldspar augen. These axes are shown in relation to other structural features at the locality. Note that the shear planes (f_6) lie at approximately 30° to the XY plane.

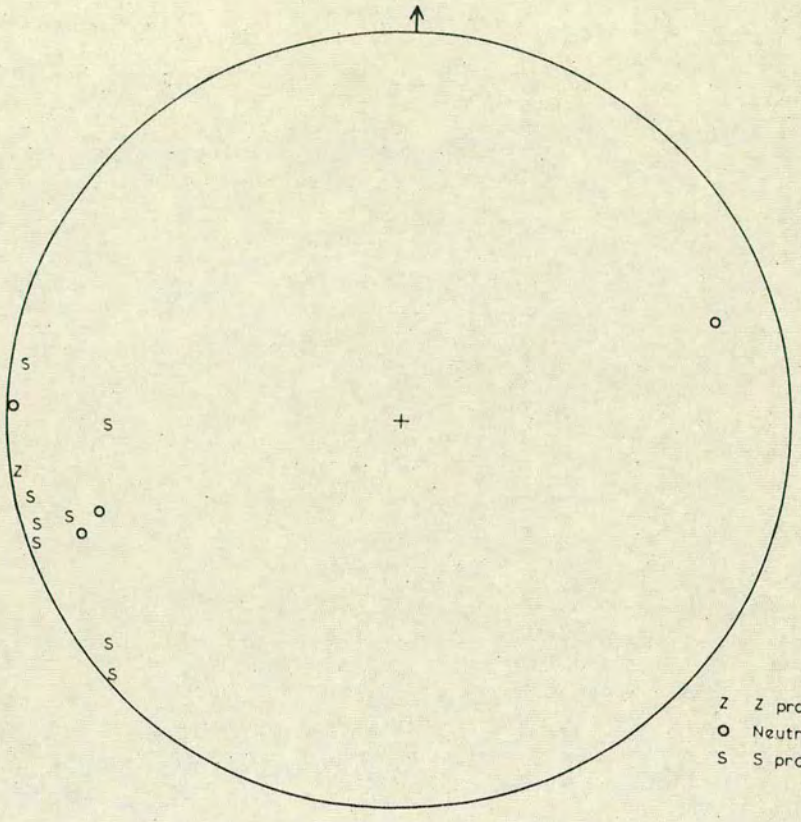
S
S
Z
S
S
S
S
S
S
Z Z profile
O Neutral
S S profile
Minor folds

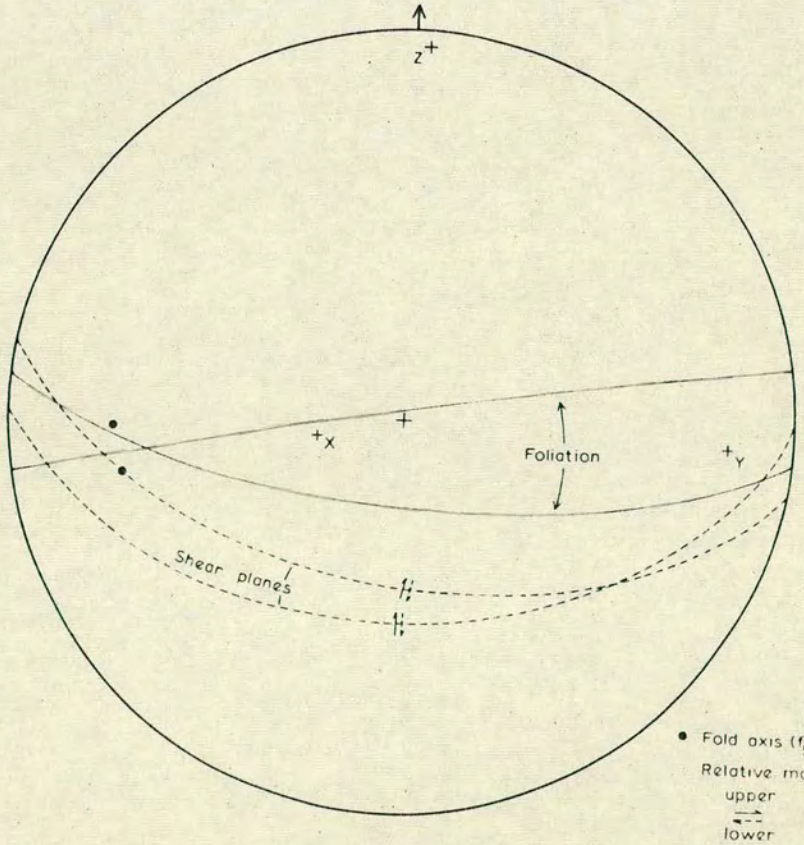
Z+
+X
+Y
Foliation
Shear planes
Fold axis (f_5)
Relative movement across shear plane
upper
lower

strain is close to plane strain.

The values obtained are high considering that feldspar generally shows much reduced strain values compared, for example, with quartz. The undeformed to slightly deformed nature of the aggregates seen under the microscope is also difficult to reconcile with the strain values obtained (c.f. feldspar shapes in mylonite). Even assuming a substantial initial shape factor, the strain values are still too large to be compatible with the microscopic texture of the augen.

The extension of albite and potash feldspar porphyroclasts illustrated in the preceding section show that there is a minimum finite strain of 1.5 to 2 in the direction of the lineation which is approximately coincident with the Y axis of the strain ellipsoid derived from feldspar augen porphyroblast measurements. In the light of this evidence, the feldspar augen porphyroblast measurements cannot be taken as representative of the finite strain in the Stavel Gneiss. They may represent a later part of the total finite strain, or reflect the stress field at their time of growth. This latter possibility is in accord with hydrothermal data on the K mica-feldspar-quartz-fluid system. It also explains the highly consistent augen values. The measurements on fragmented feldspars strongly suggest that the finite strain is of the flattening type (k = 0 to 1).

Although veins are uncommon in the Stavel Gneiss, at T331 a tightly buckle folded aplite vein, with the phengite foliation axial planar to the fold, occurs in the gneiss. Measurements of the vein length indicates shortening of about 75%, coincident with the formation of the phengite foliation. This is compatible with the strain implicit from feldspar elongation taking a $\sqrt{\lambda_1} = \sqrt{\lambda_2} = 2$, and assuming pure flattening (k = 0). Hence we may conclude that phengite foliation formation accompanied a strong flattening strain ($k \sim 0.09 - 0.1$) with 65% to 75% shortening.

5.40 PHENGITE

Phengite is a typical mineral of Alpine metamorphism and its composition and unit cell values have been studied by many workers. (Exner, 1965; Hunziker, 1966; Graeser and Niggli, 1967). It may be used to give some measure of P, T conditions prevailing at its time of formation.

5.41 Chemical and structural formulae

Phengite is a potash di-octahedral mica which forms a solid solution series between the hypothetical end members, pure muscovite $K(Al_2)Si_3AlO_{10}(OH)_2$ and celadonite $K(R_1^{2+},R_2^{3+})Si_4O_{10}(OH)_2$. R_1^{2+} may be Mg, Fe^{2+} and R_2^{3+} may be Al,Fe^{3+}. Hence phengite may be considered as $K_2(Mg,Fe^{2+})(Al,Fe^{3+})_3Si_7AlO_{20}(OH)_4$. Natural phengites generally lie within the range Si_6Al_2 - $Si_{6.9}Al_{1.1}$, the exact composition being dependent on numerous factors. Phengite generally crystallises in a $2M_1$ polymorph (rarely 3T) belonging to the space group C 2/c. Guven (1967) carried out a structural analysis of the phengite $K_{0.87}Na_{0.07}Ba_{0.01}Ca_{0.02}(Al_{1.43}Ti_{0.01}Fe^{3+}_{0.09}Mg_{0.5})(Si_{3.39}Al_{0.61})O_{10}(OH)_{1.92}O_{0.08}$ compared with a fairly pure muscovite $K_{0.86}Na_{0.10}(H_3O)_{0.01}(Al_{1.9}Ti_{0.01}Fe^{3+}_{0.02}Fe^{2+}_{0.05}Mg_{0.06})(Si_{3.02}Al_{0.98})O_{10}(OH)_{1.99}F_{0.01}$. He showed that the deviations in the Si-O and Al-O angles from 120° in the tetrahedral layers was much less for phengite than for muscovite. This, and the substitution of Fe,Mg for Al in the octahedral layer, result in the greater b_o measurements found in phengites, as predicted by Radoslovich and Norrish(1962). The b_o unit cell spacing for phengites has been defined by Chiesa et al (1972) as between 9.025 and 9.049 Å, and by Schwander et al (1968) as between 9.021 and 9.060 Å.

The increased lattice ordering in phengites results in reduced tetrahedral tilt (corrugation of anionic planes) and hence reduced d_{002}. d spacing = d_{002} = $c \sin\beta$ where c_o is the length of the unit cell edge and β is the angle between the basal plane (001) containing a_o and b_o, and c_o.

The difference in d_{002} between the two above micas due to tetrahedral tilt is 0.12 Å. This is the major controlling factor in the d_{002} variation. The octahedral metal - O distance is greater in phengite than in muscovite by 0.024 Å, probably owing to the larger ferromagnesian cations in the phengite lattice. There is only a minor tendency for the muscovite-phengite series to become tri-octahedral (see Chatterjee, 1971) and the sequence is basically di-octahedral.

5.42 Factors affecting phengite composition and unit cell parameters

Assessment of the substitution paragonite ($NaAl_2Si_3AlO_{10}(OH)_2$) and margarite ($CaAl_2Si_2Al_2O_{10}(OH)_2$) in phengite is important to the understanding of its compositional changes with metamorphism. Chiesa et al (1972) suggested that up to 30% margarite substitution may occur in agreement with experimental data (Heinricksen and Schurmann, 1971). Hock (1974) and Cipriani et al (1971) both show conclusively that in natural phengites no regular pattern of Ca substitution occurs, and not more than 4% margarite occurs in phengite. Paragonite substitution is noted by Cipriani et al (1971) and Schwander et al (1968) as being important at higher temperatures (i.e. $>500^{\circ}C.$) where phengites trend towards the muscovite end member. The Na substitution in muscovite with increasing temperature is well known (Eugster and Yoder, 1955; Deer et al, 1962). There is no evidence to suggest that d_{002} and b_o values for phengite vary significantly with Na content. It is interesting to note that paragonite and margarite themselves show very little variation from their ideal formulae (c.f. Muscovite - phengite).

Initial rock composition may exert a considerable influence on the composition of the phengite formed. For example, Na contents of phengites measured in association with paragonite (Hock, 1974; Velde, 1967) show a marginally higher Na content than those measured from non-paragonite bearing rocks (Beran,1969; Chatterjee,1971). In one analysis from a chlorite-glaucophane-phengite-aragonite-

jadeitic pyroxene schist (Ernst,1963) with no free quartz, the phengite contains high Cr, Ba and Li and shows a high Al/Si ratio. Tobschall (1974) has shown, from analyses of 46 phengites in one specimen, that those for albite rich layers differed significantly from those from albite poor layers (higher Na/K, Al^{vi}/Si ratios from albite rich layers). Cipriani et al (1971) have shown that phengite may become Fe, Mg enriched at moderate temperatures and pressures in rocks poor in Fe-Mg, whereas the converse is found for rocks rich in Fe-Mg. This is because Fe-Mg and related elements find it easier to pass into ferromagnesian metamorphic minerals in Fe-Mg rich rocks, but in Fe-Mg poor rocks, they pass into white mica. At higher temperatures (e.g. 500° - 550°C), Fe/Mg ratios for coexisting mineral pairs are almost equal (Ernst et al,1970).

The bulk chemical composition only has an important effect on the substitution $R^{2+}, Si \rightleftharpoons Al^{vi}, Al^{iv}$, where the bulk rock composition is highly aluminous. Velde (1967) has proposed that this substitution is controlled by $P.H_2O$, T conditions. However as shown in Figure 18, phengites occurring for example in the glaucophane schist subfacies, which has a relatively narrow P, T range, have Si values of 3.19 → 3.5. This range covers most of the phengite field. P and T do control phengite composition to some extent. Sassi and Scolari (1974) have shown that the b_o parameter may be correlated with pressure. Values range from 8.99Å for low grade rocks in the Bosost area (C. Pyrenees) to 9.055Å for glaucophanitic parageneses. These conclusions cannot be applied to chlorite, feldspar or carbonate rich rocks.

The following compositional trends are found in phengite (Cipriani et al, 1971),

1) Increase in Fe^{3+} content to about 500°C and then rapid decrease.

2) Overall decrease in Mg and Fe^{2+} with temperature increase. Consequent increase in Al^{vi} content.

Figure 18 shows the Si^{4+} content of phengites plotted against d_{002} for phengites lying in the range d_{002}

Figure 18 - d_{002} - Si^{4+} content for published data showing the Al^{VI} content assuming an ideal phengite formula with 24(O + OH). The data of Velde (1967), Makanjuola and Howie (1972) and Ernst et al (1970) are derived largely from glaucophane schist terrains. No estimates of the error in d_{002} and Si^{4+} are given for much of the data.

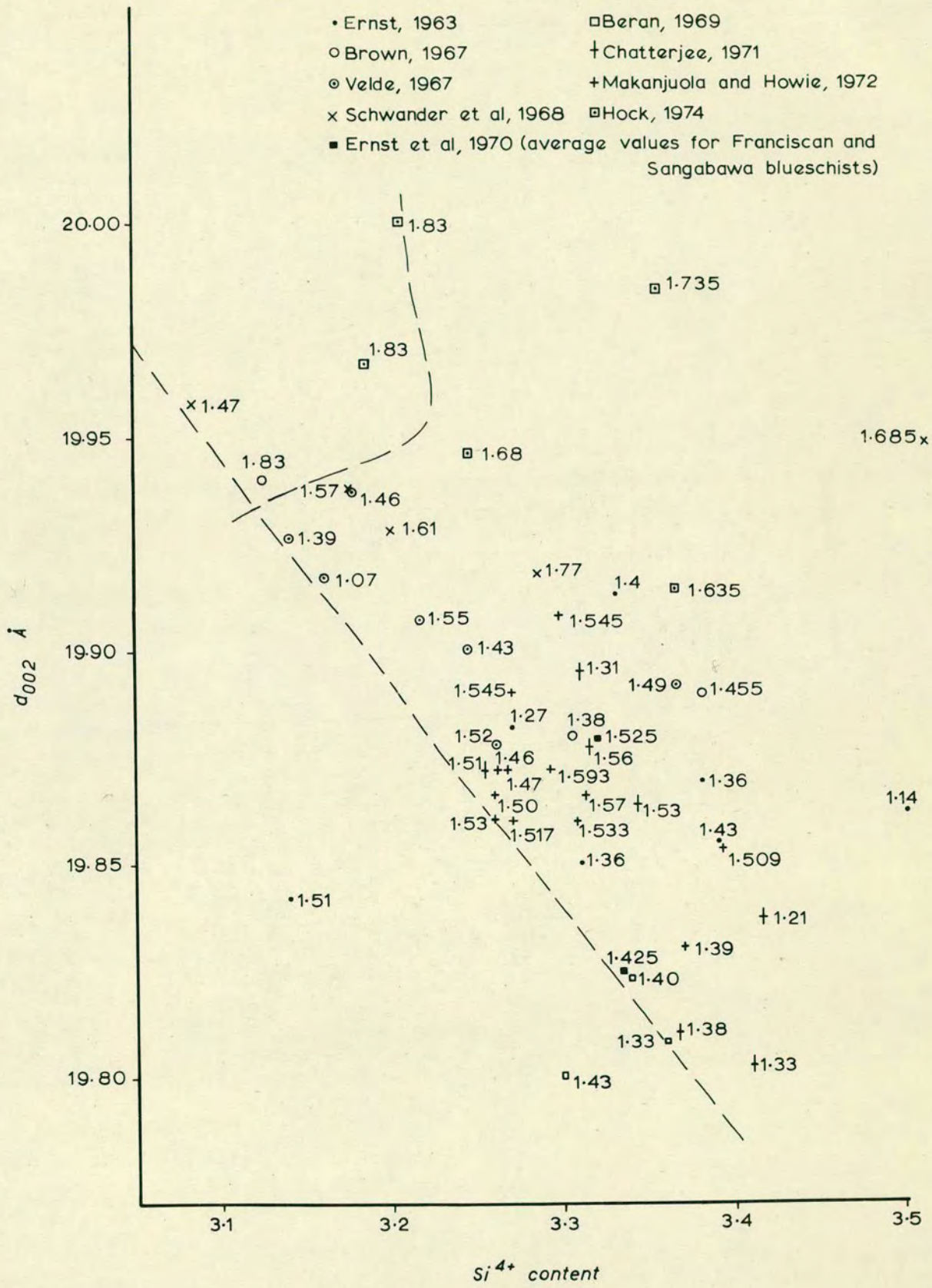
• Ernst, 1963
○ Brown, 1967
⊙ Velde, 1967
× Schwander et al, 1968
▪ Ernst et al, 1970 (average values for Franciscan and Sangabawa blueschists)
▫ Beran, 1969
† Chatterjee, 1971
+ Makanjuola and Howie, 1972
⊡ Hock, 1974
20·00
19·95
19·90
19·85
19·80
d_{002} Å
3·1
3·2
3·3
3·4
3·5
Si^{4+} content
1·83
1·735
1·83
1·47
1·685
1·83
1·68
1·57
1·46
1·39
1·61
1·07
1·77
1·4
1·635
1·55
1·545
1·43
1·31
1·545
1·49
1·455
1·27
1·38
1·52
1·525
1·51
1·46
1·56
1·47
1·593
1·36
1·14
1·50
1·57
1·53
1·53
1·517
1·533
1·43
1·36
1·509
1·51
1·21
1·39
1·425
1·40
1·38
1·33
1·33
1·43

19.75 - 20.00 and Si 3.0 - 3.5. The cations are calculated using 24 (O+OH+F) which means that the values are not controlled by the accuracy of H_2O measurement. Values used are selected from Ernst, 1963; Velde, 1967; Brown, 1967; Schwander, Hunziker and Stern, 1968; Beran, 1969; Ernst et al, 1970; Chatterjee, 1971; Makanjuala and Howie, 1972; Höck, 1974; R.T.C. Frost (pers.comm. 1974) and the authors values from the Stavel Gneiss. It must be emphasized that many micas termed phengite by other authors lie in the muscovite field. The accuracy of most of the values plotted is not known.

The lower limit of points shows a well-defined trend which has an average negative gradient of 0.0533Å/0.1Si. This gradient reflects the change in tetrahedral tilt of the anionic layers and is in accord with d_{002} values of 20Å for pure natural muscovite and synthetic muscovite (Ernst, 1963). The displacement of values above this basal trend depends on a number of factors including (Fe^{2+}, Mg, Fe^{3+}) $\rightleftharpoons$ Al^{vi} substitution. The higher values of substitution give the more phengitic micas and lower d_{002} values. The unit cell parameters are not significantly affected by the nature of the element substituting, since Fe^{2+}, Mg and Fe^{3+} all have similar ionic sizes. Variation in d_{002} does not show a simple relationship to Al^{vi} content (Figure 18) except where phengites are taken from a specific lithology in a small area of uniform metamorphic grade (e.g. Makanjuola and Howie, 1972 - aluminous schists).

5.43 Conditions of phengite formation

The presence of abundant quantities of fluid and a high P H_2O are necessary for the formation of phengite (Ernst, 1963; Velde, 1965). The fluid phase is thus an integral part of the system and such variables as fO_2, pH, composition, and ionic activity become important. Since almost all reactions occur in the presence of quartz, silica activity may be taken as unity. Fluid inclusions in crystalline rocks are dominantly alkali chloride solutions (Newhouse, 1932; Roedder, 1963; Tuttle, 1949) and hence we may conclude that the molar concentration ratio

m KCl/m HCl is the primary factor controlling fluid composition, pH and ionic activity in the K mica - feldspar - quartz - fluid system (Hemley and Jones, 1964) at moderate to high pressurs and low to moderate temperatures.

The effects of f O_2 on phengite stability and composition are not well known. f O_2 broadly increases with temperature as H_2O dissociates (Cipriani et al,1971). Mica becomes more oxidised at higher temperatures as shown by the ratio $Fe^{3+}/Fe^{2+}+ Fe^{3+}$, which increases with temperature. Tobschall (1974) has shown that phengite composition in a layer of specific composition is constant, and suggested that chemical potentials of cations in the co-existing fluid phase are important.

It is well known that certain minerals rapidly undergo ionic exchange with a chloride fluid. For example Orville (1963, 1967) showed that plagioclase equilibrated rapidly with aqueous chloride solution particularly at high temperatures (750$\emptyset^{o}$C). Hemley and Jones (1964) have shown that potash and plagioclase feldspar both readily react with alkali chloride solutions to give K and Na micas and clay minerals. The various controlling factors, T, P, m alkali cations/H^+ ions and activity co-efficients are all considered by Hemley and Jones. Quartz was present in all their experiments and hence silica activity was considered as unity. Variations in P H_2O have a large effect on feldspar - mica reactions at temperatures around 400^{o} - 500^{o}C. Solution density is also very important at these temperatures, and pressures over 1 kb; less dense fluids favouring the stability of mica due to the greater dissociation of water.

The present work has shown that hornblende will readily recrystallise in the presence of fluids at moderate temperatures and pressures (see 7.60 Folds in Amphibolite). A similar relationship can also be inferred for epidote/clinozoisite (see 7.20 Mylonites - Mineralogy.) Hence the minerals K feldspar, K mica (including biotite) Ca amphibole and epidote/clinozoisite will act as buffers to fluid composition and ion activity if present in the gneiss.

* Its large d_{002} range reflects P, T conditions (particularly temperature). A variation from 19.808Å (Lower Greenschist facies - Beran, 1969) to 19.918Å (Lower Amphibolite facies - Schwander et al, 1968) is shown by the rather sparse data.

Using the d_{002} - Si^{4+} diagram, the various minerals associated with phengite may be labelled and their effects noted. The minerals K feldspar, Ca amphibole, chloritoid, paragonite, garnet, quartz and epidote all lie in distinct fields (Figure 19). The influence of these minerals varies from K feldspar which delineates a restricted field, to epidote, which covers much of the phengite field. The boundaries of the fields are tentative and will no doubt be refined as more data become available. Unfortunately many authors fail to give associated mineral parageneses and unit cell data for their analysed phengites. Calcite, albite, rutile, sphene and hematite all appear to exert little influence on composition and d spacing of phengite.

The limited Si range (3.3 ± 0.12) of the K feldspar-phengite paragenesis reflects the strong buffer effect of excess K feldspar on the fluid. * As d_{002} values can easily be measured by scanning across the mica 0010 peak, using αFe_2O_3 as a standard, on the X-ray Diffractometer (Cu Kα radiation, $\frac{1}{4}$ or $\frac{1}{2}^{\circ}$/minute, chart 240 mm/hour), we can then obtain some idea of the metamorphic grade of the rock. The fields of the various minerals can be used to define broad P.T conditions. Hence chloritoid, which is found in the central part of the phengite field, shows that this region is in the Upper Greenschist to Lower Amphibolite facies, with P H_2O between 1.5 and 10 kb and T 400° - 550°C at f O_2 close to F.M.Q. buffer (Hoschek 1969).

The assemblage paragonite-chloritoid (Hock 1974) indicates a highly aluminous bulk rock composition and occupies a field at higher d_{002} values than the normal chloritoid field. In rocks containing margarite the bulk rock composition was extremely aluminous. In both cases the phengite formed has a high Al_2O_3 content. The presence of paragonite limits phengite d_{002} values to above 19.88Å with a maximum concentration around 19.95Å, (Chatterjee, 1971). Margarite limits d_{002} values to above 19.95Å. Hence diffusion rates of concentration of Al^{3+} ions are important controls on phengite composition (c.f.

Figure 19 - d_{002} - Si^{4+} content for published data together with the author's data and that of Frost (pers. comm. 1974). The mineral fields show the range of d_{002} and Si^{4+} content in phengite within which particular minerals coexist with the phengite. Note that some points may have errors in either d_{002} or Si^{4+} values. The true relationship between these parameters and co-existing minerals can only be correctly assessed if the phengite composition is in equilibrium with a stable mineral assemblage.

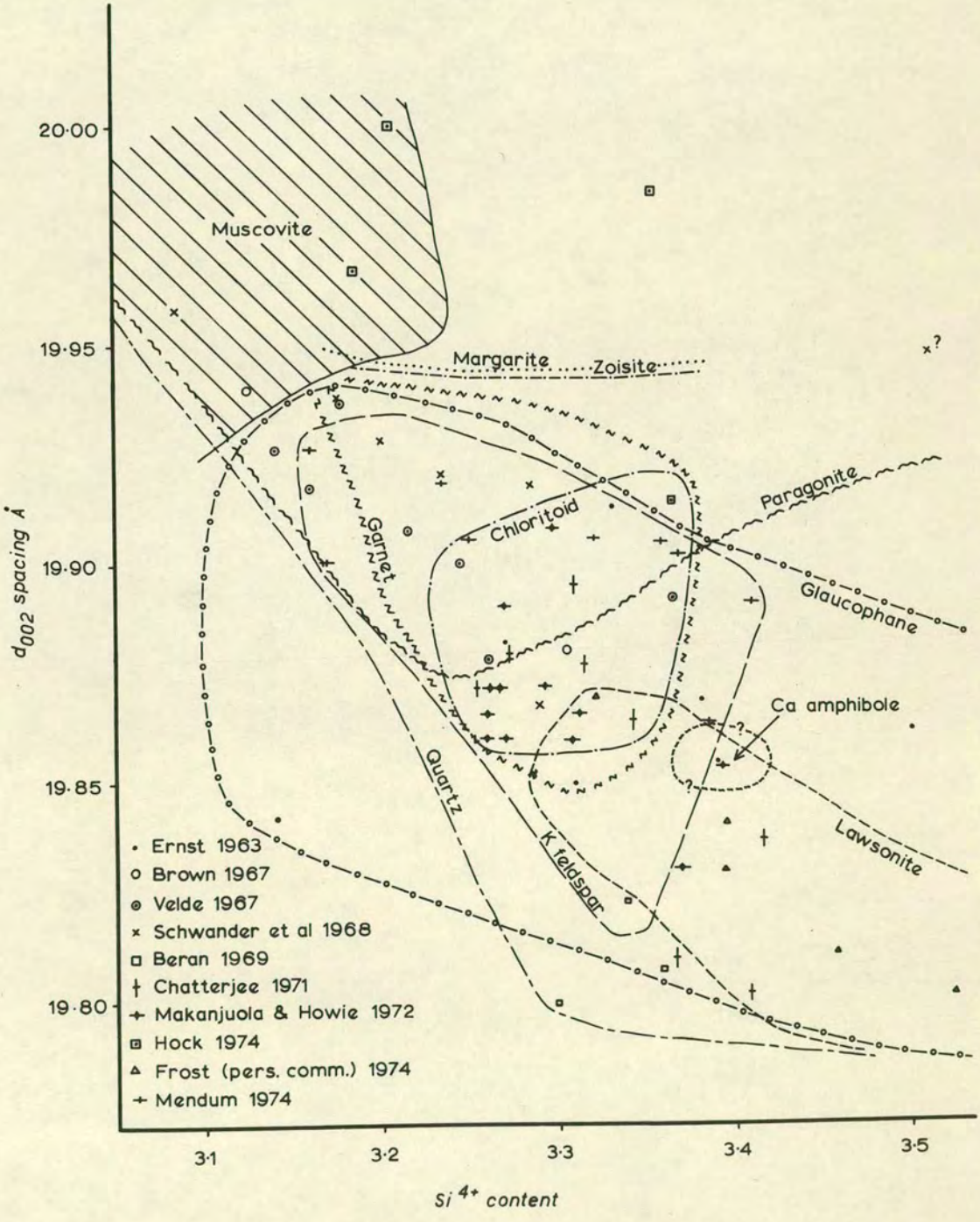
20·00
19·95
19·90
19·85
19·80
d_{002} spacing Å
3·1
3·2
3·3
3·4
3·5
Si^{4+} content
Muscovite
Margarite
Zoisite
Paragonite
Chloritoid
Garnet
Glaucophane
Ca amphibole
Quartz
K feldspar
Lawsonite
Ernst 1963
Brown 1967
Velde 1967
Schwander et al 1968
Beran 1969
Chatterjee 1971
Makanjuola & Howie 1972
Hock 1974
Frost (pers. comm.) 1974
Mendum 1974

zoned plagioclase). Makanjuola and Howie (1972) have shown that paragonite is not a stable mineral at high pressures, and results from the breakdown of glaucophane + chloritoid in the Ile de Groix area of Brittany (but see Thompson, 1974). The presence of zoisite also reflects high alumina bulk compositions and implies that the proportion of CO_2 in the fluid at the time of phengite formation was small (Storre and Nitsch, 1972) and that temperatures lay in the Lower Amphibolite facies (Hörmann and Raith, 1973).

The phengite values given by Velde (1967) may also be used to illustrate another problem. Subsequent work in the Ile de Groix area by Makanjuola and Howie (1972) and Triboulet (1974) has shown that there are two phases of metamorphism represented by the parageneses given by Velde. Hence phengites may have a modified composition and unit cell dimension and may not be in equilibrium with other minerals in the rocks. The values of Makanjuola and Howie (1972) are more consistent within a particular rock type and show better correlation with values from other sources. They may not be representative of phengites from eclogitic facies rocks however. Phengites must be shown to be in equilibrium with at least some of the other minerals in the rock for their composition and unit cell parameters to be used to infer metamorphic grade.

5.44 Chemical composition and d spacing of phengites from the Stavel Gneiss

In Figure 20 chemical compositions, structural formulae, d spacing and mineralogy are given for "muscovites" and phengites from 5 specimens of Stavel Gneiss and 1 specimen from northeastern Greece (R27 - G.Yarwood pers. comm.1973). The compositions were determined using the Cambridge Microscan electron probe (20 kv, 0.3 m.A). The term "muscovite" is applied in this work, with reference to the Stavel Gneiss, to those K micas which are colourless in thin section and form larger plates discordant to the phengite foliation. This is not strictly correct as the analyses show these micas are phengites.

Figure 20 - Chemical compositions and structural formulae of K-micas from the Stavel Gneiss. d_{002} values, % values of the component end members and associated mineralogy are also given.

Specimen Number	M438	M438	M438	T289	T289	T289	T6	T6	T6	T344A	T344A	T344A	T8	T8	R27	R27
Mineral	K mica	Phengite	Phengite	K mica	K mica	Phengite	K mica	K mica	Phengite	K mica	K mica	Phengite	K mica	Phengite	Phengite	Phengite
SiO_2	48.625	50.119	48.936	48.453	48.901	49.380	46.684	49.679	48.809	47.220	46.366	48.582	46.103	48.935	50.760	49.907
TiO_2	0.508	0.152	0.138	0.392	0.462	0.093	0.333	0.628	0.652	0.482	0.394	0.058	0.374	0.730	0.289	0.271
Al_2O_3	30.005	25.644	27.024	32.707	31.492	27.924	32.230	28.904	25.045	32.401	32.717	27.157	31.627	26.822	22.056	22.355
Cr_2O_3	0.009	0.015	0.015	0.029	0.009	-	0.003	0.014	0.019	0.026	0.019	-	0.017	0.014	0.020	0.017
Fe_2O_3	0.635	1.571	2.382	-	-	3.039	1.010	0.655	3.231	0.354	1.434	2.386	1.383	1.038	4.934	6.010
FeO	2.875	3.487	2.500	2.642	3.301	3.804	1.360	2.784	3.129	2.343	1.345	3.294	1.675	5.008	4.398	3.980
MgO	1.359	2.271	2.062	0.704	0.746	1.070	1.082	2.017	2.123	0.764	0.824	1.463	0.868	1.075	2.295	2.041
MnO	0.038	0.038	0.036	0.011	0.033	0.109	0.038	0.088	0.059	-	0.030	0.080	0.023	0.011	0.089	0.106
CaO	-	-	0.004	0.032	0.001	0.013	-	-	-	0.007	-	0.001	-	0.034	0.038	-
Na_2O	0.197	0.066	0.078	0.399	0.336	0.153	0.386	0.149	0.053	0.431	0.425	0.054	0.352	0.082	0.139	0.154
K_2O	10.811	10.948	10.900	10.520	10.731	10.651	10.582	10.507	10.913	10.567	10.631	10.892	10.675	10.697	10.779	10.818
H_2O	4.452	4.388	4.383	4.518	4.505	4.458	4.413	4.475	4.345	4.447	4.426	4.360	4.365	4.370	4.382	4.363
Total	99.514	98.699	98.458	100.407	100.517	100.694	98.121	99.900	98.378	99.042	98.611	98.327	97.462	98.816	100.179	100.022
Si	6.549	6.850	6.696	6.431	6.510	6.644	6.344	6.657	6.737	6.368	6.282	6.682	6.334	6.716	6.946	6.860
Al^{IV}	1.451	1.150	1.304	1.569	1.490	1.356	1.656	1.343	1.263	1.632	1.718	1.318	1.666	1.284	1.054	1.140
Al^{VI}	3.313	2.981	3.054	3.548	3.451	3.071	3.506	3.223	2.811	3.517	3.506	3.084	3.455	3.054	2.504	2.481
Ti	0.051	0.016	0.014	0.039	0.046	0.009	0.034	0.064	0.068	0.049	0.040	0.006	0.039	0.075	0.030	0.028
Cr	0.001	0.001	0.001	0.003	0.001	-	-	0.002	0.002	0.003	0.002	-	0.002	0.001	0.002	0.002
Fe^{3+}	0.064	0.162	0.245	-	-	0.308	0.103	0.065	0.336	0.036	0.146	0.247	0.143	0.107	0.508	0.622
Fe^{2+}	0.324	0.399	0.286	0.293	0.367	0.428	0.155	0.313	0.361	0.264	0.152	0.379	0.192	0.575	0.503	0.457
Mg	0.273	0.463	0.421	0.139	0.148	0.215	0.219	0.403	0.437	0.154	0.166	0.300	0.178	0.220	0.468	0.418
Mn	0.004	0.004	0.004	0.001	0.004	0.012	0.004	0.010	0.007	-	0.003	0.009	0.003	0.001	0.010	0.012
Ca	-	-	0.001	0.005	-	0.002	-	-	-	0.001	-	-	-	0.005	0.006	-
Na	0.051	0.017	0.021	0.103	0.087	0.040	0.102	0.039	0.014	0.113	0.112	0.014	0.094	0.022	0.037	0.041
K	1.857	1.909	1.902	1.781	1.822	1.828	1.834	1.796	1.921	1.818	1.837	1.911	1.871	1.873	1.882	1.897
OH	4.000	4.000	4.000	4.000	4.000	4.000	4.000	4.000	4.000	4.000	4.000	4.000	4.000	4.000	4.000	4.000
% Paragonite	2.7	0.9	1.1	5.4	4.5	2.1	5.3	2.1	0.7	5.8	5.7	0.7	4.8	1.1	1.9	2.1
% Celadonite	28.8	42.4	34.7	20.3	24.5	31.1	17.6	36.1	39.4	19.5	15.0	33.5	17.6	38.8	47.2	42.6
% Muscovite	68.5	56.7	64.2	74.0	71.0	66.7	77.1	61.8	59.9	75.6	79.3	65.8	77.7	59.7	50.6	55.3
d spacing	19.879Å ± 0.003Å	19.863Å ± 0.003Å		19.918Å ± 0.003Å		19.904Å ± 0.003Å	19.905Å ± 0.007Å		19.901Å ± 0.005Å	19.926Å ± 0.008Å		19.890Å ± 0.004Å	19.901Å ± 0.008Å	19.904Å ± 0.004Å	19.860Å ± 0.004Å	
Mineralogy	Quartz, perthite, orthoclase, phengite, muscovite, albite, oligoclase-andesine, minor calcite, limonite, apatite.			Quartz, orthoclase, perthite, microcline, albite, phengite, muscovite, minor apatite, limonite (after pyrite).			Quartz, orthoclase, perthite, albite, phengite, muscovite, minor pyrite, calcite.			Quartz, perthite, albite, phengite, muscovite, minor andesine, apatite, limonite, albite.			Quartz, microcline, orthoclase, albite, phengite, muscovite, minor perthite, apatite, limonite, rutile.		Quartz, albite, antiperthite, phengite, epidote, hematite.	

K mica formulae are calculated for 24(O+OH) with the % H_2O based on the ideal formula of $(OH)_4$. The ferrous content (Fe^{2+}) was calculated from the relationship Fe^{2+} + Mg + Mn = 2 - (Al^{iv} - Ti - Cr - Ca) (R.T.C. Frost, pers. comm. 1974) which assumes ideal dioctahedral occupancy. This approximation agrees well with published analyses (e.g. Chatterjee, 1971). The total number of cations in the octahedral site is never greater than 2.041 and averages 2.011 for the 16 K mica analyses.

There are notable compositional differences between the "muscovites" and phengites. Paragonite solid solution in phengite ranges from 0.7 to 2.1 % whereas in "muscovites" it lies between 2.1 and 5.8%. These "muscovite" values are not compatible with paragonite solid solution values determined by Lambert (1959).

Phengite Al_2O_3 values are considerably lower than those for "muscovite" and Figures 21(a) and 21(b) show the relationship between % Al_2O_3 and % FeO + Fe_2O_3, and % Al_2O_3 and % FeO + Mno + MgO respectively. The specimen points calculated from probe analyses (some which show spurious % SiO_2 values are omitted from the tables in Figure 20) show that the compositions of the two phases are gradational. This is in agreement with the wide 0010 diffraction peaks obtained from phengites and "muscovites" in some specimens. The K micas lie close to the lines % Al_2O_3 = 38.4 - 2.136 (% FeO + % Fe_2O_3) and % Al_2O_3 = 38.4 - 2.206 (% FeO + % MgO + % MnO) in Figures 21(a) and 21(b) respectively. These lines pass through pure muscovite when octahedral occupancy of the Al^{iv} site by Fe^{2+} + Fe^{3+} and Fe^{2+} + Mg + Mn is zero. Miyashiro (1973) has shown that K micas may be used to denote metamorphic grade on the % Al_2O_3/ % (FeO + Fe_2O_3) diagram and his divisions are shown in Figure 21(a). The presence of K feldspar shifts K mica points to lower % Al_2O_3 values. The magnitude of this shift is unknown and it is probable that the points lie in the Greenschist and Almandine Amphibolite zones. Hence the K micas from the Stavel Gneiss appear to reflect a progressive increase in grade as mica growth

Figure 21(a) - Graph showing the relationship between wt.% Al_2O_3 and wt.% FeO + Fe_2O_3 for 11 "muscovites" and 11 phengites from the Stavel Gneiss and from North Eastern Greece. The points from the Stavel Gneiss define a trend line giving the relationship % Al_2O_3 = 38.4 - 2.136 (%FeO + %Fe_2O_3). The variations in % wt. Al_2O_3 and % wt.FeO + Fe_2O_3 in phengites in relation to certain metamorphic zones, (from Myashiro, 1973), are shown.

Figure 21(b) - Graph showing the relationship between wt.% Al_2O_3 and wt.% FeO + MgO + MnO for 11 "muscovites" and 11 phengites from the Stavel Gneiss and from North-Eastern Greece. The points from the Stavel Gneiss define a trend line giving the relationship % Al_2O_3 = 38.4 - 2.206 (FeO + MgO + MnO).

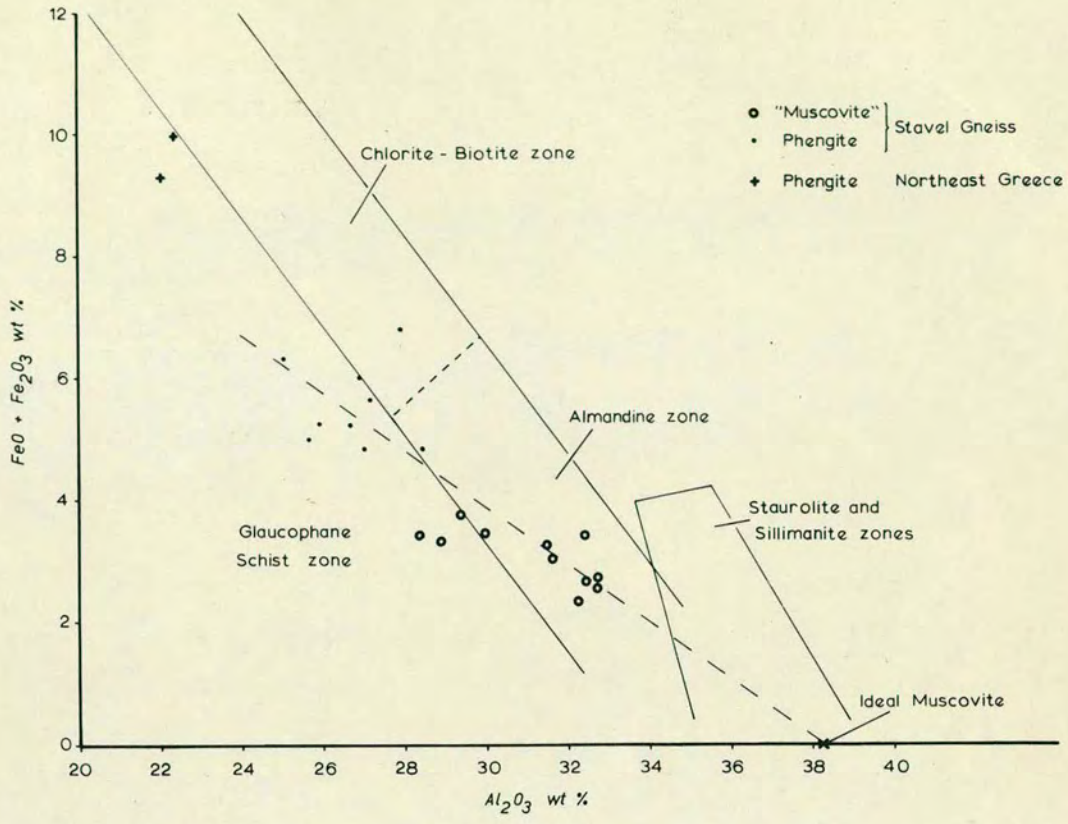
"Muscovite"
Phengite
Stavel Gneiss
Phengite Northeast Greece
Chlorite - Biotite zone
Almandine zone
Staurolite and
Sillimanite zones
Glaucophane
Schist zone
Ideal Muscovite
FeO + Fe2O3 wt %
Al2O3 wt %
0
2
4
6
8
10
12
20
22
24
26
28
30
32
34
36
38
40

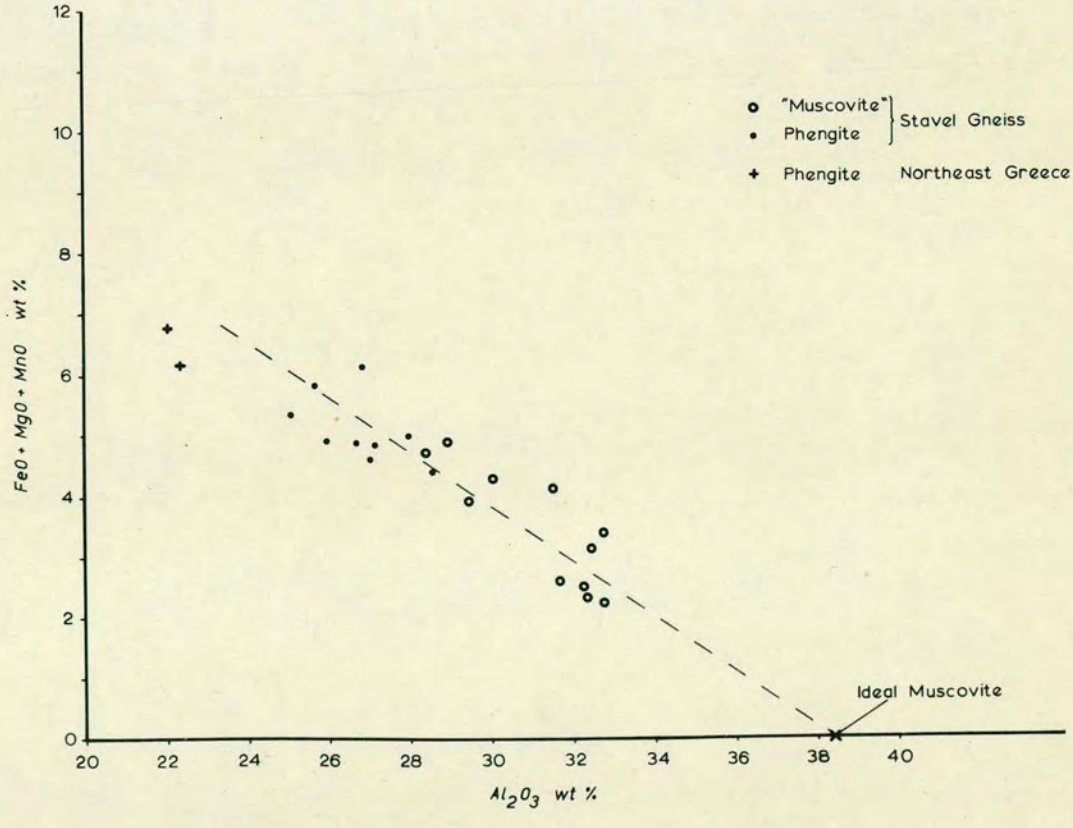
"Muscovite"
Phengite
Stavel Gneiss
Phengite Northeast Greece
Ideal Muscovite
FeO + MgO + MnO wt %
Al2O3 wt %
0
2
4
6
8
10
12
20
22
24
26
28
30
32
34
36
38
40

occurred. The change in composition is better explained by utilization of available biotite and subsequent growth of muscovite under similar or lower pressure conditions.

"Muscovite" - phengite pairs from the Stavel Gneiss show a well-defined d_{002}/Si^{4+} gradient of 0.149Å/0.1 Si^{4+} ±0.008 for the specimens M438, T344A, T289 from the northern parts of the Stavel Gneiss outcrop (Figure 22). The greater difference in phengite and "muscovite" Si^{4+} values between T344A and the other specimens may reflect the degree of deformation of the specimen. The rock contains a very strong linear fabric and this may have facilitated the feldspar-mica reactions at both early and late stages of K mica formation.

The values for phengites from quartz-albite-epidote-glaucophane-lawsonite schist from Eastern Greece (R.T.C. Frost, pers. comm. 1974) define a linear trend of gradient - 0.36Å/0.1Si^{4+}. We may speculate that this gradient represents a constant P, T. line (since mineralogy and bulk composition are constant) which is in accord with the Si^{4+} - d_{002} data from other authors. Provided that this linear trend is constant on the d_{002} - Si^{4+} diagram for different points, the tie lines in the Stavel Gneiss K micas with a lesser negative gradient will represent retrograde metamorphism. The almost horizontal tie lines for T6 and T8 would then correspond to greater reductions of P in accord with the development of larger microcline and perthite porphyroblasts (see Gresens, 1967). Helgeson (1974) has shown that the effects of increased temperature or reduced pressure both affect the feldspar-fluid system in similar manner.

Velde (1965) has given hydrothermal data for phengite ($Si_{3.3}$) stability and shown that it is favoured by high P H_2O, since the density of phengite is high, and restricted to temperatures below about 500°C. Between 400°C and 500°C, minimum P H_2O values are 4 to 6 kb respectively. Although this data is subject to several uncertainties (e.g. uncontrolled fO_2, fluid activity of water only considered) and refers to the reaction,

Figure 22 - Graph showing the relationship between d_{002} and Si^{4+} content for phengite and "muscovite" from the Stavel Gneiss and phengite from N.E. and E. Greece. Note that phengites and "muscovite" for T8 and T6 have similar d_{002} values. These specimens showed notable microcline augen.

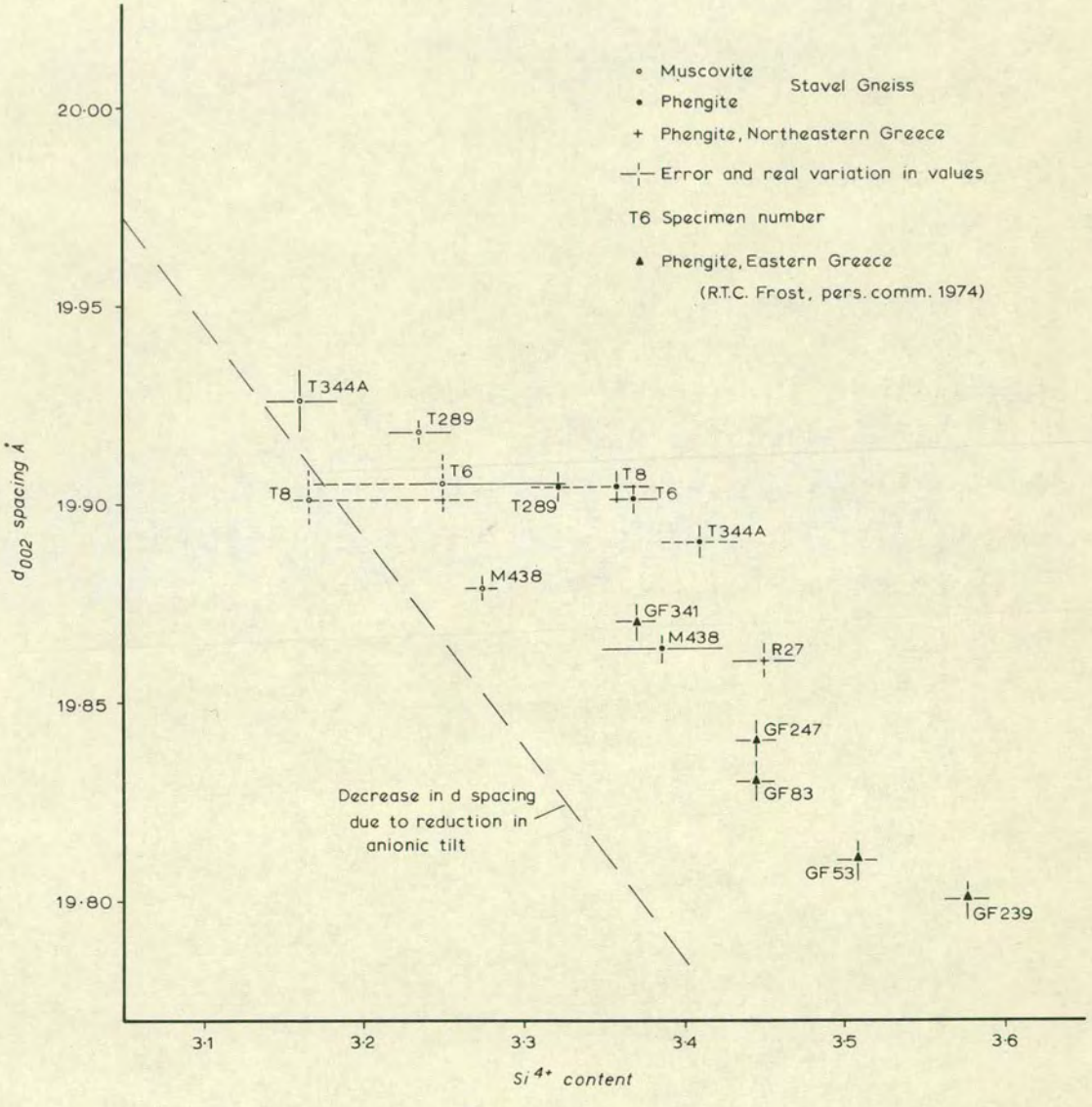
Muscovite
Phengite
Stavel Gneiss
Phengite, Northeastern Greece
Error and real variation in values
T6 Specimen number
Phengite, Eastern Greece
(R.T.C. Frost, pers. comm. 1974)
20·00
19·95
19·90
19·85
19·80
d_{002} spacing Å
T344A
T289
T6
T8
T8
T289
T6
T344A
M438
GF341
M438
R27
GF247
GF83
GF53
GF239
Decrease in d spacing due to reduction in anionic tilt
3·1
3·2
3·3
3·4
3·5
3·6
Si^{4+} content

$$3\text{Muscovite} + \text{Biotite} + 2\text{K feldspar} + 3\text{Quartz} + 2H_2O \rightleftharpoons 6\text{Phengites}$$

it agrees moderately well with stability fields from other co-existing minerals (e.g. chloritoid, paragonite, glaucophane). Many of the experiments carried out by Velde were strongly buffered by K feldspar.

5.45 Chemical composition of feldspars from the Stavel Gneiss

In Figure 23 chemical compositions and structural formulae are given for K feldspars and albites from the specimens used for phengite analysis. In these analyses all iron oxides are assumed to be Fe_2O_3 since Fe^{3+} commonly substitutes for Al. Low SiO_2 values were obtained for K feldspar T8 (b) and high values for K feldspar T289 (b) and albites R27 (a) and (b). These values probably result from incorrectly extrapolated count levels for the Si standard and/or loss of K or Na during probe analysis. The low Mg^{2+} and Mn^{2+} cation values are assumed to be equally divided amongst the end members. The feldspar compositions in terms of the end members Orthoclase (Or), Albite (Ab) and Anorthite (An) are shown graphically in Figure 24(a).

K feldspars have a very consistent composition in the Stavel Gneiss, averaging $Or_{96}Ab_4$. K feldspar T289 (b), a large fractured and veined porphyroblast, has a composition of $Or_{84.2}Ab_{15.7}An_{0.1}$, compatible with temperatures above about 500°C (Wright, 1967). The smaller potash feldspars around this large crystal are clear orthoclase and microcline, suggesting that the large feldspar is a relict from the original gneiss. K feldspar in igneous rocks equilibrates with the surrounding P.T. conditions down to sub-solidus temperatures (Hall, 1967; Leake, 1974) and albite exsolution generally results in the formation of microperthite. The high solubility values of K_2O and Na_2O for pegmatite in aqueous HCl at P = 4 kb and T = 500°C (Clark, 1966) suggest that fluid-feldspar equilibrium will be rapidly reached under high P H_2O conditions.

The presence of microcline in many of the rocks,

Figure 23 - Chemical compositions and derived structural formulae for potash feldspars and albites in Stavel Gneiss specimens. The total values of +100% for the K feldspar T289(b) and the albites R27a, b, are due to high SiO_2 values. These result from minor volatilization of K under the electron beam during analysis.

Specimen Number	M438 a	M438 b	M438 c	T289 a	T289 b	T8 a	T8 b	T6 a	T6 b	T6 c	T344A a	T344A b	R27 a	R27 b
Mineral	K fspar	K fspar	Albite	K fspar	K fspar	K fspar	K fspar	Albite	Albite	K fspar	K fspar	K fspar	Albite	Albite
SiO_2	65.077	65.258	68.238	64.606	67.510	64.984	63.994	67.838	67.928	63.629	64.445	64.725	72.082	71.264
TiO_2	0.026	-	-	0.006	-	0.043	0.004	0.034	-	-	-	0.010	-	-
Al_2O_3	17.637	17.593	18.678	17.911	17.713	18.092	18.151	19.275	19.610	18.167	18.414	18.352	18.787	18.801
Fe_2O_3	-	0.003	0.029	0.042	-	0.039	-	0.053	0.024	0.006	0.029	0.025	0.039	0.047
Cr_2O_3	0.011	0.011	-	-	0.004	-	0.016	0.005	-	0.018	-	-	-	-
MgO	0.026	0.022	0.016	0.015	0.004	-	-	-	0.040	-	0.028	-	0.024	0.008
MnO	0.002	0.013	0.017	0.008	-	0.039	0.005	-	-	-	-	0.011	0.002	-
CaO	0.003	-	0.099	-	0.020	-	-	0.025	0.595	-	0.002	-	0.051	0.241
Na_2O	0.445	0.372	11.559	0.366	1.774	0.514	0.802	11.744	11.395	0.468	0.423	0.505	11.569	11.511
K_2O	15.956	15.958	0.124	16.166	14.451	15.992	15.348	0.089	0.089	15.904	16.128	15.929	0.096	0.074
Total	99.183	99.230	98.760	99.122	101.476	99.703	98.320	99.063	99.681	98.192	99.469	99.557	102.650	101.946
Si	3.026	3.031	3.017	3.011	3.046	3.009	3.000	2.993	2.980	2.994	2.994	3.000	3.054	3.044
Al	0.967	0.963	0.973	0.984	0.942	0.987	1.003	1.002	1.014	1.008	1.008	1.003	0.938	0.946
Ti	0.001	-	-	-	-	0.001	-	0.001	-	-	-	-	-	-
Fe^{3+}	-	-	0.001	0.001	-	0.001	-	0.002	0.001	-	0.001	0.001	0.001	0.002
Cr	-	-	-	-	-	-	-	-	-	0.001	-	-	-	-
Mg	0.002	0.002	0.001	0.001	-	-	-	-	0.003	-	0.002	-	0.002	0.001
Mn	-	0.001	0.001	-	-	0.002	-	-	-	-	-	-	-	-
Ca	-	-	0.005	-	0.001	-	-	0.001	0.028	-	-	-	0.002	0.011
Na	0.040	0.034	0.991	0.033	0.155	0.046	0.073	1.005	0.969	0.043	0.038	0.045	0.951	0.953
K	0.946	0.946	0.007	0.961	0.832	0.944	0.918	0.005	0.005	0.955	0.956	0.942	0.005	0.004
% K fspar	95.98	96.53	0.70	96.68	84.20	95.35	92.63	0.49	0.50	95.69	96.28	95.44	0.52	0.41
% Albite	4.02	3.47	98.80	3.32	15.70	4.65	7.37	99.41	96.71	4.31	3.82	4.56	99.27	98.45
% Anorthite	-	-	0.50	-	0.10	-	-	0.10	2.79	-	-	-	0.21	1.14

Figure 24(a) - Feldspar compositions from the Stavel Gneiss in terms of the end members Orthoclase (Or) - $KAlSi_3O_8$, Albite (Ab) - $NaAlSi_3O_8$ and Anorthite (An) - $CaAl_2Si_2O_8$. The K feldspars and Albites generally show a consistent composition.

Figure 24(b) - Graph showing the phase relationships for K mica, K feldspar, Kaolinite and pyrophyllite for differing temperatures and molar ratios, KCl/HCl. The K feldspar - K mica phase change is shown for P H_2O (= P total) values of 0.3 kb. 1 kb. and 2 kb.

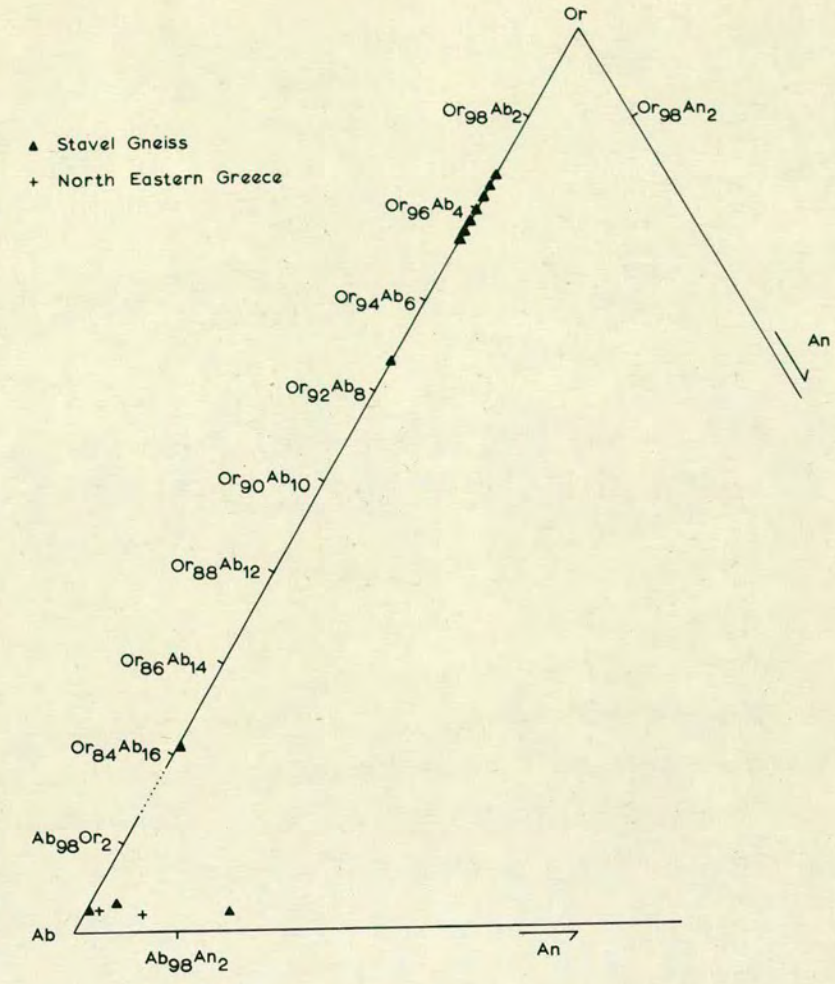
Or
$Or_{98}Ab_2$
$Or_{98}An_2$
▲ Stavel Gneiss
+ North Eastern Greece
$Or_{96}Ab_4$
$Or_{94}Ab_6$
$Or_{92}Ab_8$
$Or_{90}Ab_{10}$
$Or_{88}Ab_{12}$
$Or_{86}Ab_{14}$
$Or_{84}Ab_{16}$
$Ab_{98}Or_2$
An
Ab
$Ab_{98}An_2$
An

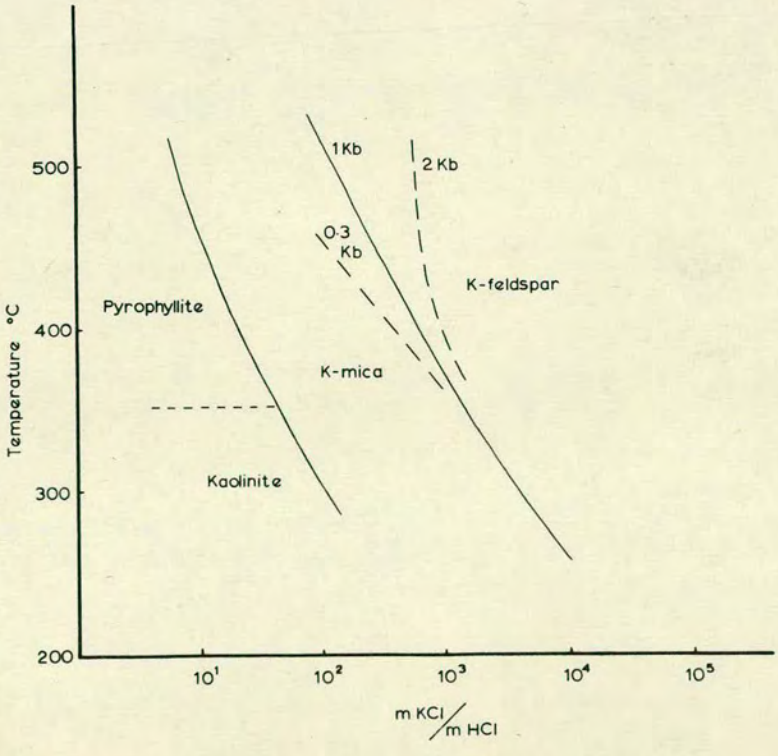
1 Kb
2 Kb
0·3 Kb
K-feldspar
Pyrophyllite
K-mica
Kaolinite
Temperature °C
500
400
300
200
10^1
10^2
10^3
10^4
10^5
m KCl / m HCl

particularly in the augen gneiss, suggests that temperatures lay around the microcline-orthoclase transition. For low Ab contents (approx. 4% Ab) this transition lies close to 430°C at 200 bars (Wright, 1967). At 5 kb P H_2O Martin (1974) has shown that this transition lies near 575°C although the transition is controlled by time and fluid + mineral peralkilinity (molar ratio $Na_2O + K_2O/Al_2O_3$) effects. For higher Ab contents at this temperature perthite or microperthite is formed, and the resultant K feldspar has a composition close to Or_{96} Ab_4. Barth (1962) has shown that perthites formed below 500°C must contain relatively pure end members Or_{95-100}, $Ab_{95.5-100}$. Barth (1969, p.29) states that perthite formation below 500°C will be favoured by a high strain energy and hence tectonically active environment. The presence of unfractured and weakly strained microcline as anhedral grains in the gneiss (particularly in the augen gneiss), and textural evidence (e.g. lack of K mica around the margins) suggesting its late growth, shows that this phase formed at or below the orthoclase - microcline transition temperature. In contrast, phengite formed in equilibrium with orthoclase.

The albites from the Stavel Gneiss lie close to the pure end member as shown in Figure 24(a). They contain consistently low amounts of K_2O but vary considerably in their CaO content (0.595% to 0.025%). This is interpreted to show that albitisation of plagioclase has occurred and equilibration is not complete in some grains. Orville (1972) showed that synthetic plagioclase will equilibrate very slowly with aqueous chloride solutions at 500° - 700°C and 2 kb. If plagioclase takes part in the formation of phengite, as suggested by the petrographic evidence, Na^+ ions will be released. These ions will initially be in low concentration but as reaction proceeds concentration of Na^+ ions will increase. Hence plagioclase-albite changes are to be expected.

Baskin (1956) has shown that authigenic chequer board albite, which commonly forms at temperatures below 150°C and pressures below 1.5 kb, contains less than 0.4%

K_2O and less than 0.2% CaO. The higher K_2O contents obtained from the Stavel Gneiss thus suggest higher temperatures. Barth (1968) showed that albite coexisting with K feldspar formed at temperatures below 500°C.

The albites from the augen gneiss of North Eastern Greece show a slightly lower K_2O content and higher Na_2O content, showing the metamorphic conditions were below those prevailing in the Stavel Gneiss. This is in accord with the phengite d_{002} - Si^{4+} data (Figure 22). A temperature of formation of 350° to 400°C may be estimated for the gneisses from N.E. Greece.

5.50 GENESIS OF THE STAVEL GNEISS

Phengite has been observed in thin section rimming feldspar grains. The corrosion of K feldspar and plagioclase shows without doubt that these two minerals were involved in the formation of phengite in the Stavel Gneiss. It is necessary for a ferromagnesian mineral to be initially present so that the substitution Si + (Mg,Fe) = Al^{iv} + Al^{vi} can occur. No ferromagnesian mineral is seen in the Stavel Gneiss and we can only infer that it was probably biotite. Biotite rich paragneiss is abundant to the north and if the phengite gneiss is considered to be a "metasomatic" equivalent of this gneiss, it is reasonable to infer the initial presence of some biotite. In north eastern Greece near Mt.Olympus, strongly pleochroic green phengite (Fe rich) has formed from epidote + K feldspar (+ chlorite ?). The following reactions may be important:-

1) $11KAlSi_3O_8 + 5H_2O + K(Mg,Fe)_3AlSi_3O_{10}(OH)_2 \underset{\text{Temp.}}{\overset{P\ H_2O}{\rightleftharpoons}}$

K feldspar — Biotite

$3K_2(Mg,Fe)Al_3Si_7AlO_{20}(OH)_4 + 15SiO_2 + 6K^+$

Phengite — Quartz

---

2) $3KAl_2Si_3AlO_{10}(OH)_2 + 3K(Mg,Fe)_3AlSi_3O_{10}(OH)_2 + 7SiO_2 +$

Muscovite — Biotite — Quartz

$4H_2O \underset{\text{Temp.}}{\overset{P\ H_2O}{\rightleftharpoons}} (Mg,Fe)_5Al(Si_3Al)O_{10}(OH)_8 + 4K_2(Mg,Fe)Al_3Si_7AlO_{20}(OH)_4$

Chlorite — Phengite

---

3) $(Mg,Fe)_5Al(AlSi_3)O_{10}(OH)_8 + 18KAlSi_3O_8 + 6H_2O \underset{\text{Temp.}}{\overset{P\ H_2O}{\rightleftharpoons}}$

Chlorite K feldspar

$5\ K_2(Mg,Fe)Al_3Si_7AlO_{20}(OH)_4 + 8\ K^+ + 22SiO_2 + 4(O)^{--}$

Phengite Quartz

---

4) $5KAlSi_3O_8 + 3NaAlSi_3O_8(CaAl_2Si_2O_8)_{0.5}$

K feldspar Andesine (An33)

$K(Mg,Fe)_3AlSi_3O_{10}(OH)_2 + 5H_2O \underset{\text{Temp.}}{\overset{P\ H_2O}{\rightleftharpoons}}$

Biotite

$3K_2(Mg,Fe)Al_3Si_7AlO_{20}(OH)_4 + 9SiO_2 + 3Na^+ + 1.5Ca^{++} + 3(O)^{--}$

Phengite Quartz

By analogy with the experimental data of Hemley and Jones (1964) and Orville (1972), reactions moving to the right to give mica + quartz are favoured by reaction kinetics, oxidation (increased Alkali ion/H^+ ratio) and increased P H_2O. Hence reactions 1), 3) and 4) are considered to be the most likely ones for production of phengite. Reactions 1) and 4) result in ~10% and ~15% volume decrease respectively and probably both participate in the formation of phengite in the Stavel Gneiss (particularly reaction 4). The presence of phengite in shear zones, and fractures in the feldspar suggests that P fluid ≈ P total, since any tectonic movement would then result in brittle fracture and not ductile flow (Sibson, 1973, Tectonic Studies Conference, Newcastle). The production of phengite is envisaged as a relatively rapid metamorphic process, given a large supply of water. A reduction of the alkali ion /H^+ ratio consequent on its formation would favour its development until biotite was utilised in the Stavel Gneiss. Helgeson (1974) showed that ion complexing (e.g. $Al^{+++} \rightarrow Al(OH)_4$) may strongly favour solubility of feldspar at high temperature.

The presence of feldspar (microcline-perthite) which apparently post-dates the phengite and in parts forms augen in the gneiss, may be explained by variation in P H_2O, m KCl/m HCl and T. Gresens (1967) has used the

data of Hemley and Jones (1964) to explain the formation of pegmatites by such variations. This data shows that K mica is favoured over paragonite (Na mica) in the K_2O-Na_2O-Al_2O_3-SiO_2-H_2O system given equal molar concentration ratios of KCl/HCl and NaCl/HCl.

A decrease in pressure (P H_2O) results in reversal of the reaction

K feldspar + Perthite + $H^+ \rightleftharpoons$ K mica + Quartz + (K^+, Na^+).

Hence if uplift occurred at a temperature of about 500°C subsequent to phengite formation, a reasonable assumption if large amounts of a moderate density fluid phase were present, the resultant drop in P H_2O would favour potash feldspar or albite, dependent on relative concentrations of K^+ and Na^+ in the fluid. Concurrent with a reasonably rapid drop in P H_2O, there would be a drop in pH (Gresens, 1967; Helgeson, 1974) and m KCl/m HCl and possible rise in silica activity. Figure 24(b) (from Meyer and Hemley, 1967) shows the effect of increased P H_2O on molar concentration ratio (m KCl/m HCl) and the stability fields of K feldspar and mica at 1 kb. PH_2O. The solubility of K_2O and Al_2O_3 in aqueous HCl solution has been shown by Clark (1966) to be reduced with pressure, possibly as a result of complexing (see Helgeson, 1974). Hence the resultant increased ionic activity would speed up reaction between K feldspar and K mica.

A P H_2O drop may also eventually favour reduced alkali ion/H^+ ratios and hence K mica, due to a decrease in ionisation of HCl <u>relative</u> to alkali chloride (both decrease with lower pressure). A simpler solution is provided by the data of Helgeson (1974) who shows that the solubility of aluminium oxides and aluminosilicates, as a function of solution pH, is a minimum at about 300°C. Hence a temperature reduction favours lower a K^+/a H^+ ratios. The system would gradually revert to the K mica field once more as the reaction

5 K feldspar + $H^+ \rightleftharpoons$ 0.5 K mica + Quartz + K^+

occurred when dissociation of KCl became dominant over the other effects noted above. The K feldspar - K mica

system at~500°C and~4 to~8 kb. P H_2O is very sensitive to molar concentration, silica activity and fluid density values. Sassi (1971) has suggested that isochemical feldspathisation occurs in pelitic rocks due to an increase in pH and alkali and oxygen concentrations in the intergranular fluid when tectonic overpressure is released. Tectonic overpressures are untenable at high P H_2O/P total ratios (near 1) since rock strength is too low to maintain such overpressures (Brace et al, 1970). Alkali ion and oxygen concentration would decrease in absolute terms on removal of pressure (Hemley and Jones, 1964; Barnes and Ellis, 1967).

The large grain size of augen feldspar porphyroblasts is good evidence for their growth under high P H_2O. The activation energy of the mineral is lowered by the concentration of intergranular fluid which enhances diffusion rates. Large crystals or aggregates of spherical or ellipsoidal shape would develop in an attempt to minimise surface energy. Hence the augen measured in the Stavel Gneiss probably reflect the local stress conditions at their time of growth.

The presence of late stage muscovite may be accounted for by a drop in pressure and molar ratios in a low density fluid, or increase in temperature with resultant higher water activity. The lack of available ferromagnesian minerals would preclude the formation of further phengite.

Scotford (1969) has described a similar orthoclase augen gneiss from West Turkey. Detailed studies of the feldspar showed that the gneiss formed at temperatures near 500°C and the gneiss formation was attributed to metasomatism. Scotford reported the presence of a mylonite beneath the augen gneiss zone.

The origin of large quantities of fluid necessary for phengite formation presents a problem. Three tentative possibilities are :-

1) the dehydration of paragneiss associated with subduction in the Early Alpine f_3 deformation phase.
2) magmatic fluid derived from progressive release of

volatiles during the ascent of the plutons of the Adamello massif.

3) Incorporation of connate or meteoric water at depth.

The first possibility is preferred because phengite formation is best explained in relation to the f_3 mylonitic event, and regional uplift occurred at this time. The subsequent well-documented f_5 event may not account for the amount of uplift necessary (although the Peio Line is dominantly an f_5 structure). It is difficult to envisage how the Adamello volatiles can concentrate in a small zone. There is no evidence that meteoric water may penetrate to a depth of about 16 km. except by tectonically controlled processes. The widespread association of phengite with blueschist metamorphism (Ernst, 1963; Chatterjee, 1971; R.T.C. Frost pers. comm. 1974) suggests a genetic relationship between dehydration by subduction and phengite formation in many areas.

6.10 INTRODUCTION

The Central Alps consists basically of paragneiss, in the area mapped. Very minor orthogneiss is present and abundant pegmatite and quartz veins commonly cross-cut the gneissic banding. The unit is bounded to the south by the Stavel Gneiss; a 10 m. to 20 m. mylonite zone marks the contact. The paragneisses of the Central Alps are cut by several thick mylonite zones which sub-divide the area into tectonic sub-units. These are from south to north: Vallazza sheet, Mezzolo sheet, Cadil sheet, Mt.Tonale sheet, Casiole sheet, Albiolo sheet, Viso sheet. The position, lithology and structure of each sheet is shown in Maps 1 and 2. Map 3 shows the more detailed geology of part of the Central Alps. The Mezzolo sheet is only present in the eastern part of the area. In the west the overlying Vallazza sheet transgresses to a lower structural level and the Mezzolo sheet is cut out. The mylonites are zones of very high strain across which there is structural discontinuity.

The Peio Line is a major mylonite zone (Andreatta, 1948) which separates the Upper Amphibolite grade, Caledonian paragneisses to the south (the Tonale Zone) from the Lower Amphibolite to Upper Greenschist grade, Hercynian schists and quartzites to the north. These latter rocks constitute the Viso sheet in the area mapped, and show evidence of only three major deformation events, f_1, f_3 and f_6. The f_o event and m_1 metamorphism are absent. The Peio Line is a site of major Late Alpine differential uplift.

Although the major structure of the Central Alps is simple, the minor structures are considerably more complex. Six separate minor fold sets, f_1 to f_6 are recognised but only the f_3 and f_5 folds have determined the major structure. Only minor normal and reverse faulting has occurred and this has not significantly disrupted the structural pattern. Fault and joint patterns are attributed basically to late stage uplift of the area (c.f. 2.64). This faulting is not discussed in this thesis.

6.20 LITHOLOGY

South of the Peio Line, a sequence of pelitic gneiss, marble and amphibolite with minor quartzite, pegmatites and small granitic intrusives crops out. The sequence is affected by up to 6 fold sets and up to four metamorphic events. North of the Peio Line semi-pelitic schists, quartzites and minor pelitic schists, marbles and ultramafics are present. This sequence is comparable to the Palaeozoic beds of the Tauern window.

The rocks comprising the Vallazza to Albiolo sheets contain significant local variations in rock type. As shown in Map 1, marble and amphibolite are common in the Cadil and Albiolo sheets whereas the Casiole sheet is composed mainly of pelitic gneiss. Within the uppermost part of the Mt.Tonale sheet at T184 a 40 cm. wide, closely jointed bed of grey-purple, fine-grained feldspar porphyry (andesite) occurs in sequence with pelitic gneiss and garnet amphibolite. A 10 cm. bed is also present but this lenses out laterally over a short distance. In thin section ovoid low andesine phenocrysts (average 0.4 mm.long) with small chlorite strain shadows lie in a foliated matrix of sericite (muscovite), biotite, feldspar and magnetite.

In the upper part of the Cadil sheet and lower part of the Vallazza sheet quartzites are locally abundant in the paragneiss. These commonly contain actinolite needles. There was apparently some cyclic sedimentation as shown by the repetition of the sequence marble-pelitic gneiss-quartzite.

The Viso sheet which lies to the north of the Peio Line contains rare thin grey marble and pelitic schist bands but generally the lithology is more uniform than in the Tonale Zone to the south. Around Passo Gavia, 5 km. northwest of the area mapped, large pegmatites are seen, and to the east near Peio these are abundant in the semi-pelitic schist. Intercalated in these sediments are thin highly altered ultramafic lenses (now serpentine + magnesite + talc). Hercynian granitic intrusives are common to the east and northeast of the area mapped. To the north

beyond the Ortler, orthogneiss and paragneiss of the Campo sheet occur showing that lower structural levels are again exposed.

6.30 METAMORPHISM

6.31 Introduction

The paragneiss of the Central Alps contains complex mineral assemblages. In outcrop, sillimanite porphyroblasts up to 2 cm. across are abundant in the pelitic gneiss as shown in Plate 6(a) and grossularite pods up to 6 m. across are common in the marbles. In some areas, folded banded marble changes abruptly along strike into a coarse calcite - grossularite mixture containing no planar or linear structure. These features are attributed to a Caledonian Upper Amphibolite metamorphism. Borsi et al (1973) have obtained a whole rock Rb-Sr isochron of 497 $\pm$ 38 m.y. on similar paraschists in the "Altkristallin" sheet south of the Tauern Window.

The subsequent Hercynian metamorphic event in other parts of the Altkristallin sheet has a minimum age given by biotite and muscovite Rb-Sr and K-Ar cooling ages around 300 m.y. (Borsi et al, 1973; Harre et al, 1968; Schmidt et al, 1967). In the Tonale Pass area this event has generally caused partial to complete modification of the Caledonian assemblages except in the Viso sheet where no Caledonian assemblages are present. This metamorphism was synchronous with the f_1 folding and continued after deformation had ceased. Since the Hercynian event has a variable intensity in this area and lies in the Upper Greenschist - Lower Amphibolite transition zone, it is difficult to distinguish from the Alpine event which is of similar grade.

The metamorphism is considered under three basic rock types; Pelitic and semi-pelitic; Calc-silicate; Amphibolite. A brief synthesis of the metamorphic conditions for each event is given.

6.32 Pelitic and semi-pelitic assemblages

The following assemblages are found in the Central Alps:-

Plate 6

(a) Sillimanite porphyroblasts in pelitic gneiss of the Central Alps. These prominent grey-blue aggregates commonly reach 2 cm. in diameter. (T161 - Mt.Tonale Sheet)

(b) Semi-pelitic gneiss showing a strong foliation defined by biotite and sillimanite. The sillimanite is in the form fibrolite and has largely replaced muscovite. (M222 - Vallazza Sheet).

(c) Pelitic gneiss with garnet porphyroblasts. Biotite has formed in the pressure shadows of the garnets. Two generations of biotite can be seen in the photomicrograph. (T38 - Vallazza Sheet)


2 mm

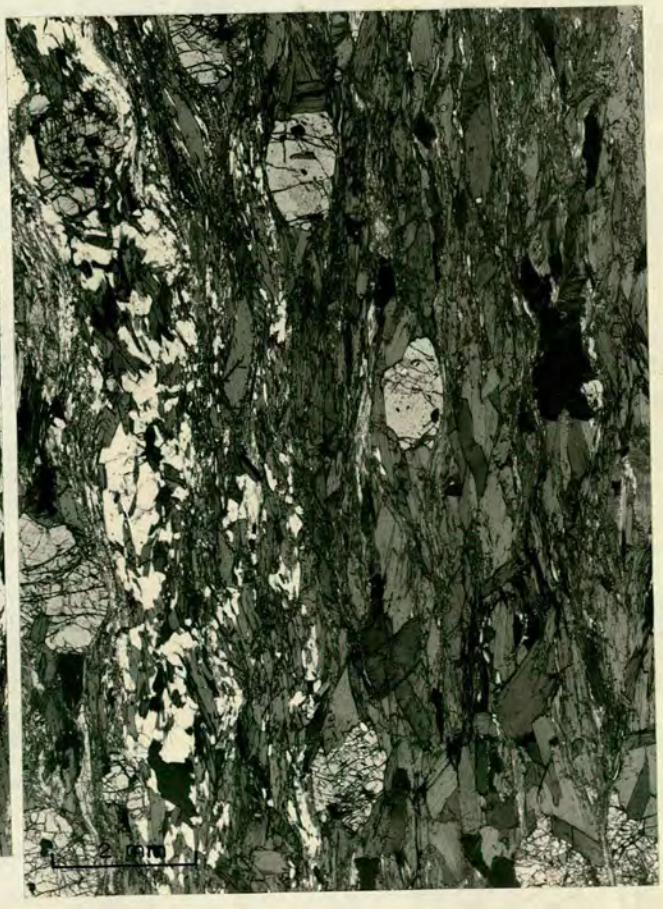
2 mm

Caledonian (m_1)	Accessories
Qz - Pl - Bi - Mu - Ga - Sill	Ap - Mag
Qz - Bi - Sill	Ap-Monz-Ilm-Mag
Qz - Pl - Kf - Bi - Sill - Ga	Mag - Zir
Hercynian (m_2)	
Qz - Bi - Clin - Chl - Pl - Kf - Ser - Mu	Ctd - Mag
Qz - Kf - Pl - Ser - Mu - Chl - Ga	Ap-Ca-Zirc-Mag-Clin
Qz - Ser - Mu - Clin - Chl	Tourm-Mag
Qz - Pl - Ser - Mu - Chl	Mag - Lim
Qz - Mu - Chl - Kf - Pl - Ctd	Tourm

These assemplages are represented on ~~AKF diagrams and~~ a Thompson AFM projection (projection from muscovite on to the AFM face of the AKFM tetrhedron) ~~respectively~~ (Figure 25). All Hercynian assemblages contain excess silica and muscovite (sericite) but only a few Caledonian assemblages contain muscovite and are thus able to be represented on the AFM projection. Phase compositions are taken from Miyashiro (1973).

Quartz and plagioclase (low andesine) may be additional phases in the Caledonian assemblages in the AKF diagram.

The texture of the gneiss is shown in plates 6 (b) and (c). Large ovoid garnets are abundant in pelitic Fe rich gneisses and commonly two generations of biotite can be seen. Where sillimanite (fibrolite) is present it generally occurs in linear zones associated with muscovite. It is difficult to ascertain in the Caledonian assemblages whether sillimanite is replacing muscovite or whether the two phases are co-existing. Since crossed-ties occur on the AKF diagram the former possibility is preferred. Although Thompson (1974) has shown that anatexis should occur in the sillimanite-K feldspar field at moderate pressures, if P fluid$\neq$P total and X CO_2 is high, the temperature of granite melting is substantially increased. The ubiquitous locally "sweated" small quartz veins in the Caledonian gneiss are compatible with the observed assemblages and inferred P, T conditions.

Staurolite may have been present in some pelitic gneisses but replacement by sericite is now complete. The

Figure 25(a) - Thompson AFM projection for "Caledonian" assemblages in pelitic gneiss of the Central Alps. Quartz and Muscovite are additional phases and plagioclase is generally present. The "Caledonian" pelitic assemblages which do not contain muscovite are not represented.

Figure 25(b) - Thompson AFM projection for 'Hercynian' assemblages in pelitic gneiss of the Central Alps. Quartz and muscovite are additional phases and plagioclase is generally present.

Phase compositions taken from Miyashiro (1973).

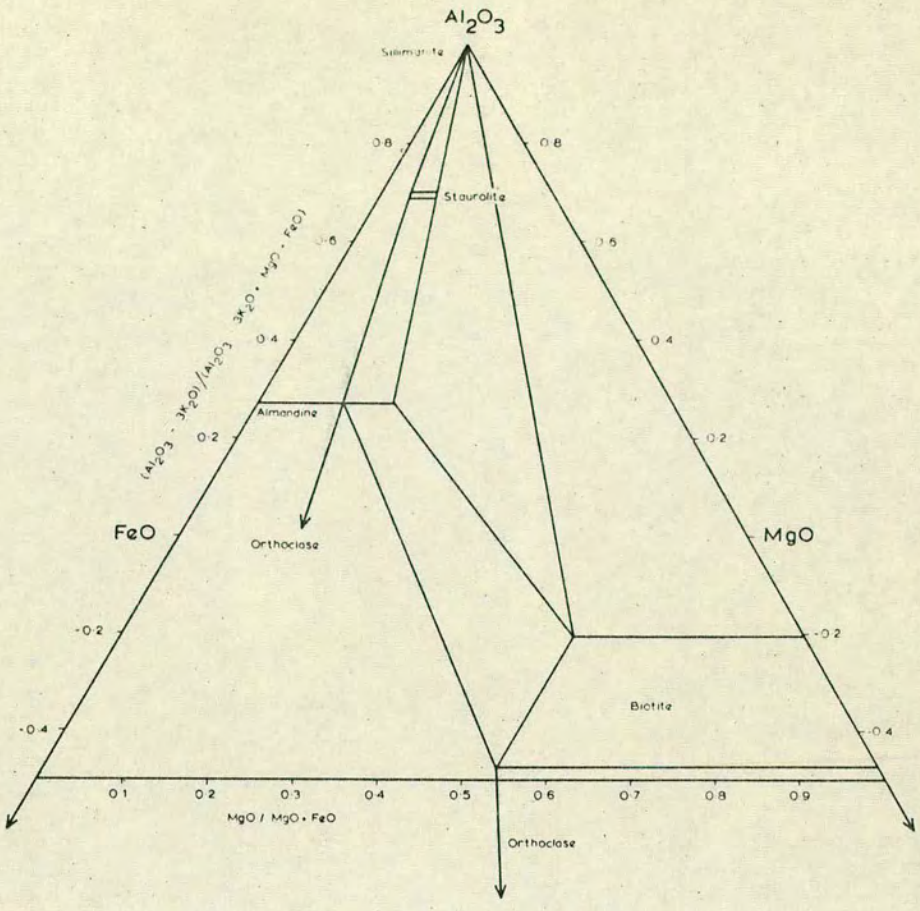
Al_2O_3
Staurolite
Almandine
Orthoclase
FeO
MgO
Biotite
Orthoclase
MgO / MgO + FeO
$(Al_2O_3 - 3K_2O)/(Al_2O_3 - 3K_2O + MgO + FeO)$

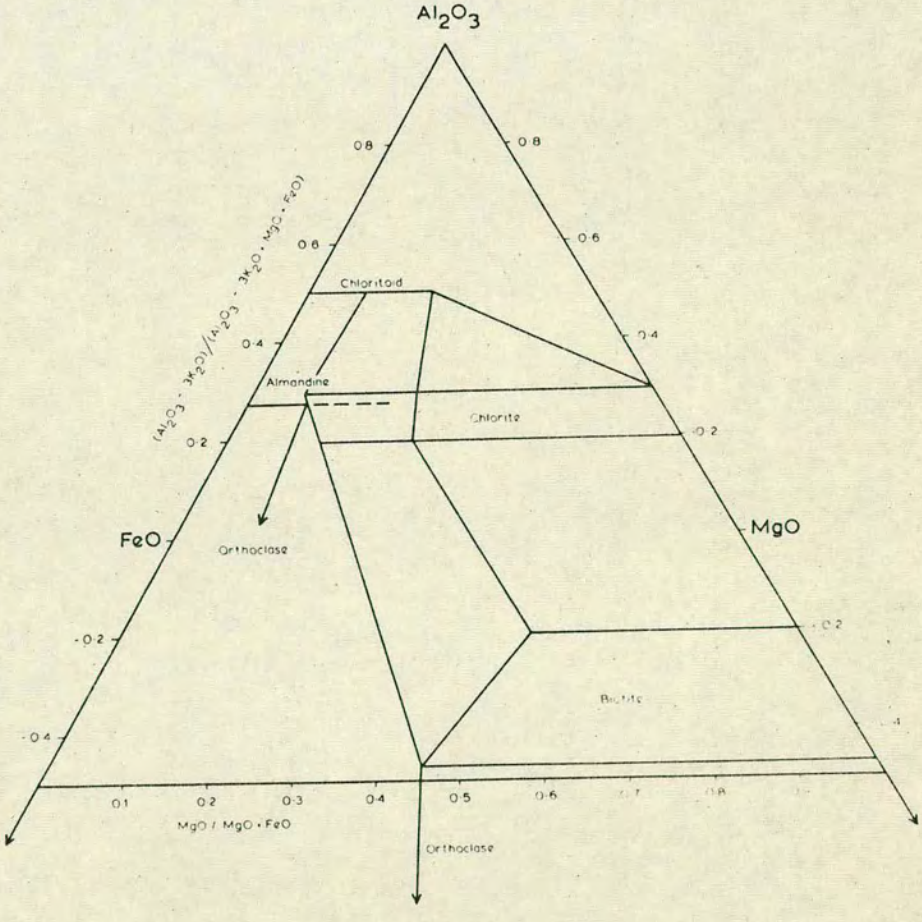
Al_2O_3
Chloritoid
Almandine
Chlorite
Orthoclase
FeO
MgO
Orthoclase
MgO / MgO + FeO
$(Al_2O_3 - 3K_2O)/(Al_2O_3 - 3K_2O + MgO + FeO)$

AFM projection shows that unless the almandine contains abnormally high MgO, staurolite should occur in the sillimanite-almandine-biotite triangle.

Garnet in the more pelitic biotite rich gneiss commonly grows discordantly across the biotite foliation. Some of these garnets result from biotite re-equilibration (less Fe, Ti rich) during the Hercynian metamorphism. This biotite forms an f_1 foliation which at several localities lies slightly discordant to the compositional banding. In parts garnet is partially retrograded to chlorite and magnetite and rarely these porphyroblasts have thin marginal overgrowths. This suggests that the Hercynian event may have increased in grade.

Large muscovite laths commonly cross-cut pre-existing textures defined by partially chloritised biotite. The muscovite pre-dates the mylonitisation (f_2 and f_3) and may be related to the abundant Hercynian pegmatites, adjacent to which large muscovites are very abundant. The period of muscovite growth and pegmatite injection was typified by high water pressures and post-dated the main metamorphism.

The following mineralogical changes are seen under the microscope:-

Caledonian (m_1)	Hercynian (m_2)
sillimanite	sericite
strongly pleochroic biotite	weakly pleochroic biotite chlorite + magnetite (ilmenite) chloritoid
plagioclase (An_{30-34})	plagioclase(An_{5-10}) + clinozoisite sericite (+ clinozoisite) plagioclase(An_{5-10}) + sericite
k feldspar	sericite
garnet	chlorite + magnetite (rarely late garnet overgrowths)

In the Viso Sheet the following assemblage is found in the pelitic schists:-

Qz - Pl - Bi - Mu - Ga - Ctd - (Mag-Pyrite)

The texture of the schists is illustrated in Plate 7(a) and is in marked contrast to the largely retrograded Upper

Plate 7

(a) Garnetiferous quartz-feldspar-biotite-muscovite gneiss with chloritoid growing in biotite - rich zones. The garnets show two stages of growth, the later one at least post-dating the main foliation formation. The foliation is defined by biotite and muscovite. Prominent albite/ oligoclase porphyroblasts are seen in the gneiss (M289 - Viso Sheet).

(b) Forsterite porphyroblast with marginal alteration rims to chondrodite and serpentine. The serpentine is probably of Alpine age. Calc-silicate rock (M423- Cadil Sheet).

(c) Cross-cutting relationships between amphibolite bands. The structure resembles a channel infill with the more northerly band cross-cutting to underlying fine banded amphibolite (T108 - Mexzolo Sheet).

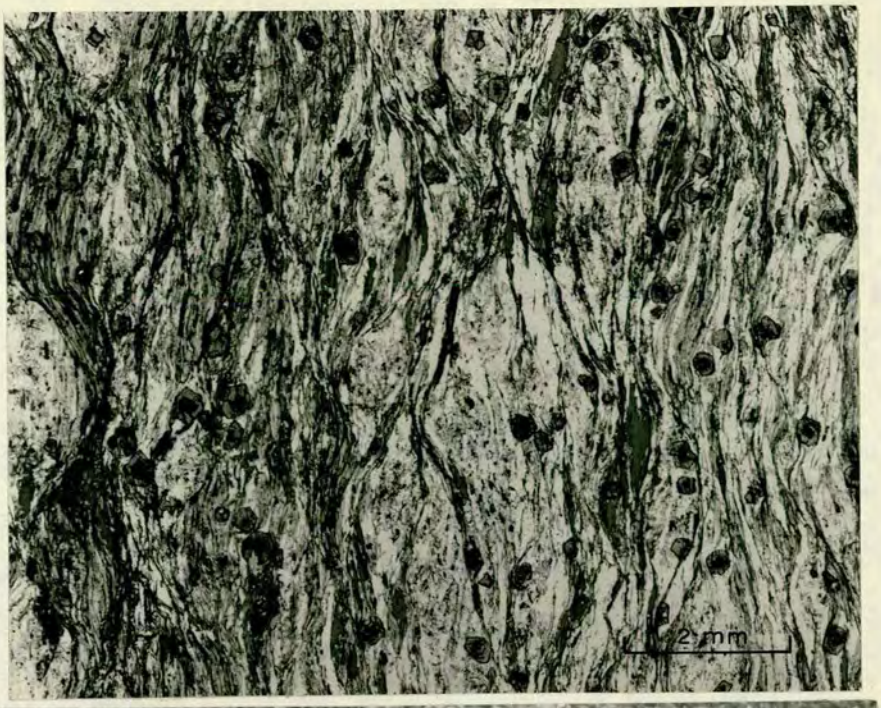
2 mm

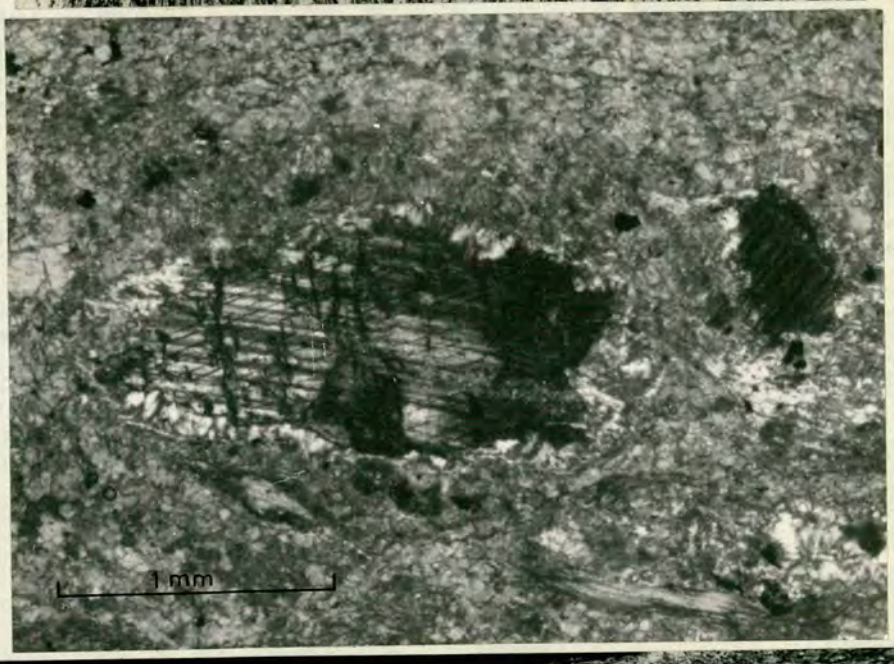
1 mm

Amphibolite gneiss south of the Peio Line. There is no evidence in the Viso sheet of a pre-existing metamorphic assemblage. The 3 to 7 mm. wide plagioclase porphyroblasts consist of albite in the Passo Gavia area and low oligoclase in the Valle di Viso. The euhedral garnets in the schist (average diameter 0.35 mm.) were formed in two growth phases; an early phase in which small biotite, feldspar and quartz inclusions were incorporated; or later phase of clear growth. The Si defined by the inclusions is not parallel to Se, implying that porphyroblast rotation has occurred or that the new schistosity formed at an angle to a pre-existing anisotropy. Since garnets overgrow the biotite foliation in places and f_3 Early Alpine folds post-date this foliation, the former explanation is preferred. The textures in the pelitic schist show that the following growth sequence occurred: 1) biotite-chloritoid, 2) garnet 1, 3) garnet II, 4) plagioclase porphyroblasts, 5) muscovite. Since Hercynian(?) pegmatites and quartz veins cross cut parts of the sequence north of the Peio Line (although these are not well-developed in the areas studied), the initial Bi - Ctd - Ga assemblage is probably of Hercynian age. The garnet II overgrowths, plagioclase porphyroblasts and muscovite may be of Alpine age.

Ultrabasic pods in the Passo Gavia area are altered to a fine grained admixture of calcite (or magnesite)-talc -serpentine with minor magnetite.

Chloritoid + biotite + sericite define the axial plane foliation to an f_1 fold in the lowermost part of the Cadil sheet (T124B). Chloritoid is commonly found in minor quantities associated with Hercynian assemblages in the area between the Peio and Tonale Lines, but is absent from mylonite and "mylonitic" gneiss. It is thus taken as a diagnostic mineral for the Hercynian event in this area.

The Alpine metamorphism is restricted to mylonite zones and areas of strong Alpine deformation. This metamorphism ranges from Lower Amphibolite grade in Early Alpine mylonites to Lower Greenschist grade in the Albiolo

sheet - Peio Line area and Lower Cadil-Vallazza sheet area where the Late Alpine metamorphism is best developed. The assemblages are discussed under Mylonite - Mineralogy.

6.33 Calc - silicate assemblages

The assemblages are as follows:-

	Accessories
Caledonian (m_1)	
Ca - Di - Micro - Gross - Ves	
Ca - Di - Fo - Pl - Micro	Mag
Ca - Di - Kf - Pl - Sph	
Ca - Di - Micro - Phl - Fo - Sph	Mag - Pyrite
Hercynian (m_2)	
Ca - Qz - Phl - Trem(Clin)	Cpyrite - Sph
Ca - Phl - Trem - Clinochl	Cpyrite
Ca - Trem - Clinochl	Lim
Ca - Trem - Clinochl - Clin - Phl - Sph	Lim - (Pyrite)
Ca - Chond - Trem - Phl	Lim - Geoth
Ca - Trem - Kf - Ab - Chond - Clin - Sph	
Ca - Trem - Clin - Kf - Phl - Sph	Norb - Clinochl - Mag
Ca - Trem	Mag - Qz

Calc-silicates are common in the Tonale Pass area and generally contain mixed Caledonian - Hercynian assemblages. Alpine effects are locally strong. The Alpine parageneses are very similar to the Hercynian ones. The plagioclase in all assemblages is albite but Caledonian plagioclases generally contain some associated clinozoisite suggesting that they were initially more calcic.

Caledonian and Hercynian assemblages are projected from calcite onto the SiO_2 - Al_2O_3 - MgO + FeO plane (SAM) in Figure 26 and show a range from commonly Mg - Si rich (dolomite rich) to more rarely Si - Al rich compositions. The two major K bearing phases, K feldspar and phlogopite reflect this compositional difference; K feldspar is generally restricted to Si - Al rich compositions; phlogopite to Si - Mg rich compositions. The more K_2O rich calc-silicates may contain both minerals.

The presence of chondrodite (showing multiple twinning) results from the alteration of forsteritic olivine (av.Fo92). As shown in Plate 7(b) later marginal alteration to ser-

Figure 26(a) - Projection from calcite on to the SAM (SiO_2 - Al_2O_3 - MgO + FeO) plane for 'Caledonian' calc-silicate assemblages in the Central Alps. All assemblages also contain calcite and CO_2. As Phlogopite lies close to the SAM plane tie lines are solid between it and other phases. K feldspar lies a considerable distance away from the SiO_2 - Al_2O_3 join and tie lines to it are dashed.

Figure 26(b) - Projection from calcite onto the SAM /SiO_2 - Al_2O_3 - MgO + FeO) plane for 'Hercynian' calc-silicate assemblages in the Central Alps. All assemblages also contain calcite and CO_2. In this case tie lines drawn to K feldspar and phlogopite are dashed. Fe-Mg ratios in phlogopite and tremolite may mean that a further dimension is given to the projection and tie lines are not as close as appear on the projection.

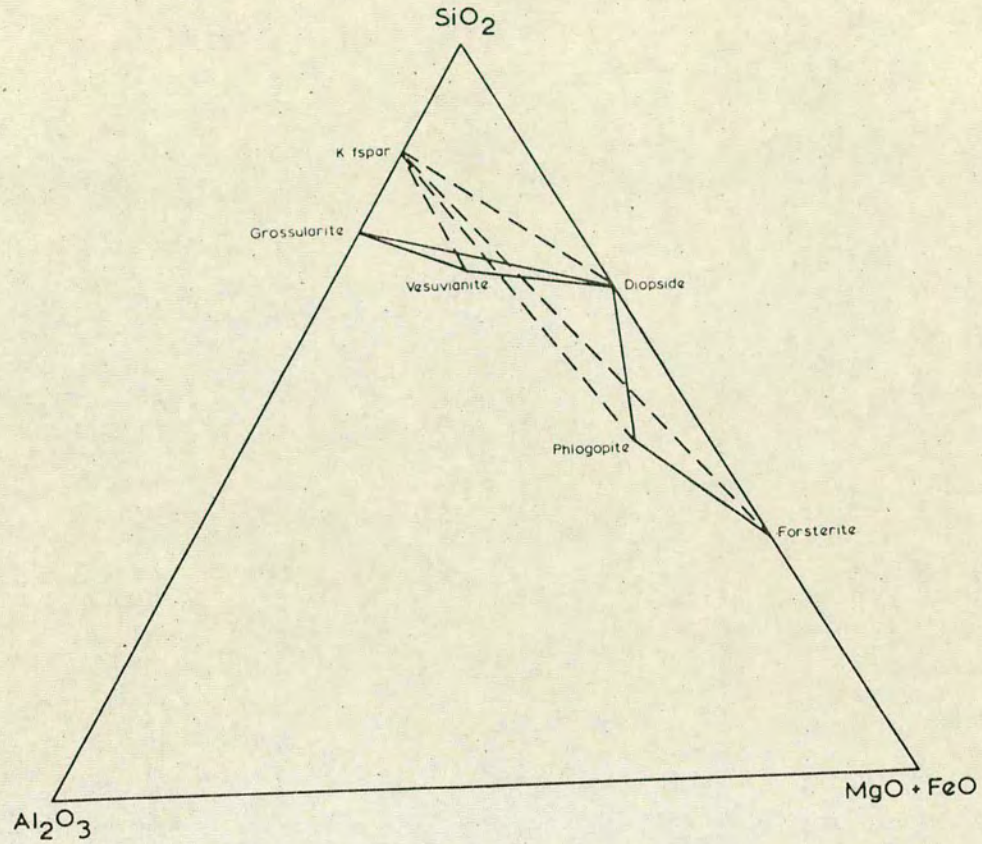
SiO2
K fspar
Grossularite
Vesuvianite
Diopside
Phlogopite
Forsterite
Al2O3
MgO + FeO

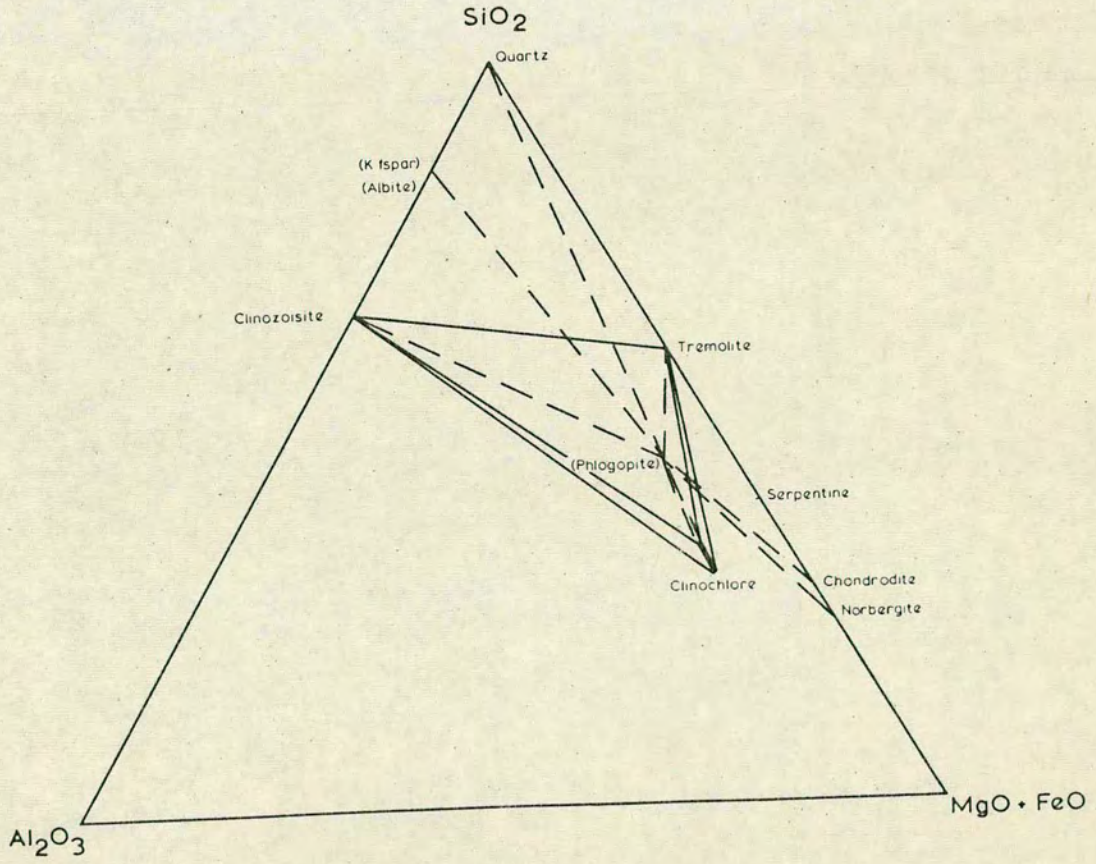
SiO2
Quartz
(K fspar)
(Albite)
Clinozoisite
Tremolite
(Phlogopite)
Serpentine
Clinochlore
Chondrodite
Norbergite
Al2O3
MgO + FeO

pentine (probably of Alpine age) also occurs.

In the Cadil sheet (T77), marble adjacent to 1 m. and 30 cm. amphibolite bands shows development of diopside, 0.7 to 1.5 cm. from the contact. Tremolite partially replaces the diopside and clinochlore is developed adjacent to the tremolite/diopside. This shows that during the Caledonian metamorphism Mg and Si diffusion occurred locally across the marble/amphibolite interface. If the amphibolite was derived from a dolomitic marl, which contained locally excess Mg and Si adjacent to these contacts, then the compositions of the hornblende and feldspar formed would control the amount of Mg and Si in the intergranular fluid. Leake (1972) has shown that once stable metamorphic minerals are formed, then any elements which are discriminated against (e.g. Si and K in chlorite schist) may migrate out of the system. The process would explain the occurrence of diopside adjacent to some contacts only.

McCallum (1974) has shown that dolomitic marble readily undergoes reaction in mylonite zones and that mineral compositions depend to a large degree on H_2O and CO_2 content of the fluid. The readiness of marble to deform by twinning, recrystallization and possibly dislocation climb favours fluid and ion diffusion. Hence large porphyroblasts are common in calc-silicate rocks. Hercynian metamorphic assemblages are abundant and only relict Caledonian assemblages are found.

In the vicinity of Mt.Tonale Orientale, tremolite crystals up to 2 cm. long and 0.5 cm. wide form a strong lineation plunging steeply northeast. This growth alignment may have been controlled by the Early Alpine stress field, in which case the amphibole long axis (c crystallographic axis) will define the Y axis of the strain ellipsoid (see 7.60). The X axis would hence plunge up to 30°SW to W and assuming coaxial strain increments (see Elliot 1972), σ_1 acted subhorizontally in a NNW - SSE plane. These results are in agreement with Early Alpine boudinage and fold axis (f_2) orientations.

If the calc-silicate was quartz rich the reaction

5phlogopite + 6calcite + 24quartz $\overset{P}{\underset{T}{\rightleftharpoons}}$ 3tremolite + 5K feldspar + $2H_2O$ + $6CO_2$ (Hoschek 1973)

may have occurred to form the tremolite. This occurs at temperatures of around 500°C at 3 kb (X CO_2 = 0.2)

6.34 Amphibolite assemblages

Amphibolite assemblages are:-

	Accessories
Caledonian (m_1)	
Hb + Pl (Labradorite) - Ap	Pyrite, Ilm
Hb + Ga + Pl (Andesine) - Ap	Pyrite, Mag
Hercynian (m_2)	
Trem - Ga - Qz - Clin - Pl(Albite) - Chl	
Trem - Ep/Clin - Qz - Pl(Oligoclase) - Kf - Sph	Chl - Ilm - Ap - Ser - Lim
Trem - Clin/Ep - Chl - Qz - Pl(Albite) Ga - Sph - Ser	Ap - Mag

Amphibolite forms bands up to 30 m. thick and shows small scale internal compositional banding. Alpine assemblages are indistinguishable from Hercynian ones. Biotite + magnetite may form locally from Caledonian hornblende during either of these later events. Some diffusion of K_2O may take place from the surrounding pelitic gneiss.

Almandine garnets up to 5 cm. across are common in certain amphibolites particularly in the Vallazza sheet; these porphyroblasts probably result from an initially locally high Fe content in the marl. E.M.Stolper (pers.comm. 1974) has suggested that hornblende composition is very sensitive to bulk rock composition and garnet formation results from excess Fe which cannot be accomodated in hornblende. Since hornblende and plagioclase (and garnet if formed) act as "sinks" for the commonly occurring elements (Ca, Mg, Si, Fe, Al) during high grade metamorphism, a wide range of sediment compositions will result in the formation of amphibolite (Leake ~~and Evans~~, 1964; Orville, 1969). Large almandines are rimmed with feldspar rich zones 2 to 3 mm. wide.

The close relationship of amphibolite to marble and pelitic gneiss, presence of labradorite (high Ca content) and locally variable mineralogy suggest that it was initially

a marl and not a basic igneous rock. Orville (1969) has suggested that amphibolites 1 to 5 m. thick may form by diffusion between pelites and marble. The relationship pelite - amphibolite - marble is not always seen in this area and it is difficult to explain the observed occurrence of amphibolite bands entirely within marble or pelitic gneiss by a diffusion hypothesis. Evidence from marble/amphibolite contacts (see previous section) shows that ionic diffusion is limited to a few centimetres. Similarly, in the upper part of the Cadil sheet almandine garnets are developed in the 2 cm. adjacent to a pelitic gneiss/amphibolite contact in both lithologies. Although this may reflect initial compositional differences it is probable that Fe and Mg diffusion occurred across the contact during the Caledonian event. Cross-cutting structures in amphibolites as shown in Plate 7(c) mimic initial sedimentary structures. Minor feldspathic veins and segregations commonly occur in amphibolites.

Hornblende recrystallization and re-orientation in the presence of fluid has occurred in both the Hercynian and Alpine metamorphic events, as shown by the coincidence of hornblende lineation and fold axis orientations (see 7.60).

In the Cadil sheet, east of Mt.Tonale Orientale, a vein of magnetite-chlorite-brucite (periclase)-serpentine-chloritoid rock occurs in amphibolite. This is probably related to Alpine ultrabasic rocks at depth and represents a retrograde high temperature (+ 600°C), low X CO_2 vein deposit, in which the Late Alpine chloritoid shows a random orientation. The assemblage brucite-serpentine suggests temperatures of around 400°C at 2 to 3 kb. (Hostetler et al, 1966; Evans and Tromsdorff, 1970).

6.35 Conditions of metamorphism

The observed mineral assemblages can be used together with experimental data to define the reactions and pressure temperature limits of the various metamorphic events (Figure 27).

In the Caledonian (m_1) event, sillimanite was commonly formed in the pelitic gneiss of the area mapped although

Figure 27 - Experimental data for some critical pelitic and calc-silicate assemblages from rocks of the Central Alps, showing the probable range of P H_2O - T conditions for the differing metamorphic events. For a key to the mineral abbreviations see 1.50.

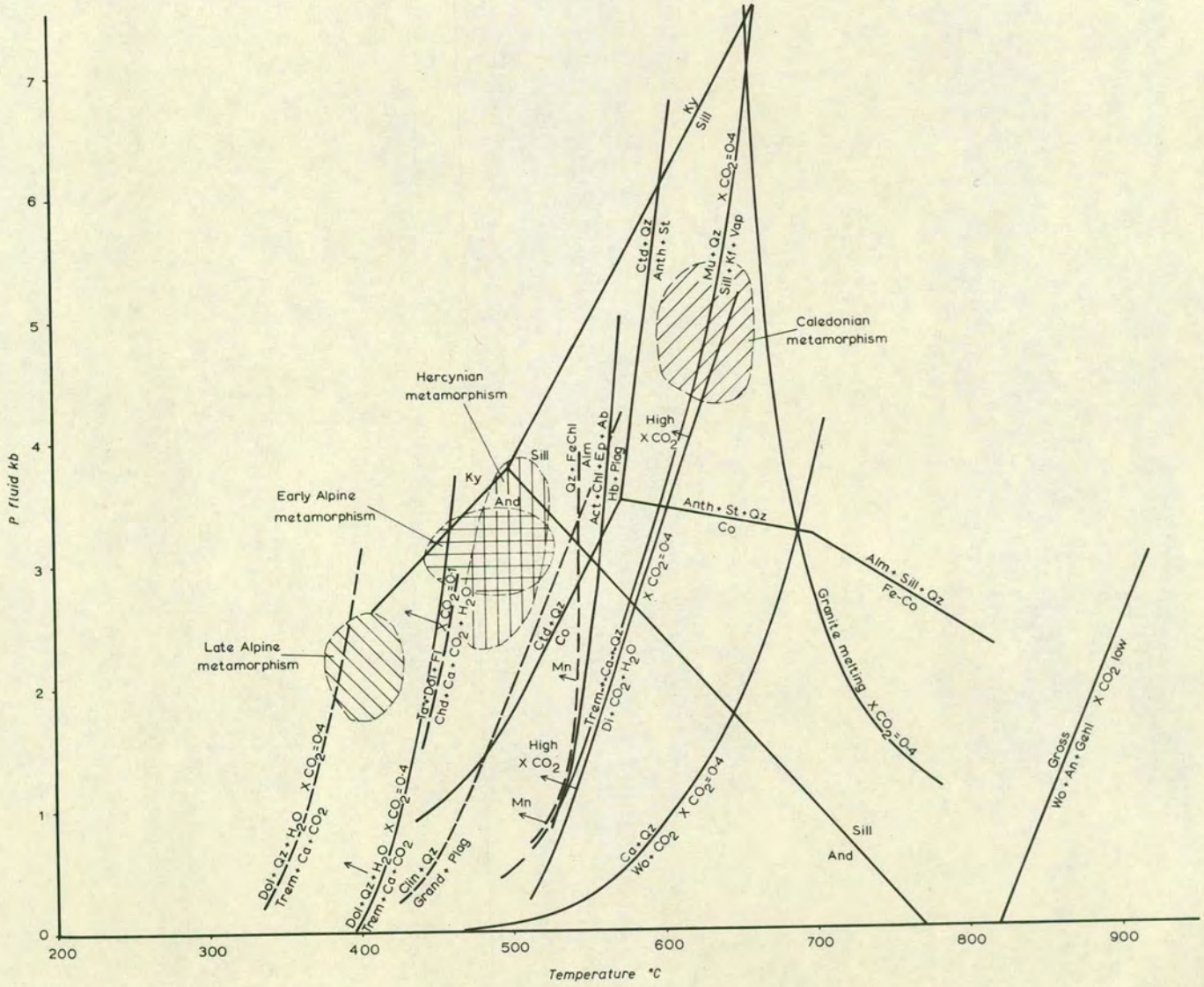
P fluid kb
Temperature °C
Caledonian metamorphism
Hercynian metamorphism
Early Alpine metamorphism
Late Alpine metamorphism
Ky
Sill
And
Mu • Qz
Sill • Kf • Vap
Ctd • Qz
Anth • St
X CO2=0·4
High X CO2
Qz • FeChl
Alm
Act • Chl • Ep • Ab
Hb • Plag
Anth • St • Qz
Co
Alm • Sill • Qz
Fe-Co
Granite melting X CO2=0·4
Grass
Wo • An • Gehl
X CO2 low
Ctd • Qz
Co
Mn
Trem • Ca • Qz
Di • CO2 • H2O
Dol • Qz • H2O
Trem • Ca • CO2
Clin • Qz
Grand • Plag
Co • Qz
Wo • CO2
X CO2=0·1
Chd • Ca • CO2 • H2O
Tr • Dol • F

kyanite has been widely reported from other parts of the "Altkristallin" sheet (Hoernes, 1971; Borsi et al, 1971). Sillimanite formed by the reaction

muscovite + quartz $\rightleftharpoons$ sillimanite + K feldspar + H_2O

and in some rocks the reaction was incomplete. Evans (1965), Kerrick (1972) and Hess (1969) have defined an experimental P, T curve for the reaction (using the seeding method) but (Day (1973) and Althaus (1970) obtained higher temperatures using synthetic starting materials. Kerrick (1972) has shown that increased pressure favours reaction rates and that CO_2 content of the fluid lowers the temperature of reaction. Taking X CO_2 = 0.4 (Hyndman, 1972, p.321) a maximum value for pelite metamorphism, assuming rapid diffusion from adjacent calc-silicates at equilibrium, T = about 560°C at 2 kb P total, and T = 610°C at 4 kb P total. Taking Kerrick's (1972) data for granite melting at X CO_2 = 0.4, then Caledonian metamorphism is fixed at about 4 to 5 kb and 600° to 660°C. The presence of staurolite provides a lower temperature limit of 550°C (Hoschek, 1969) and the lack of cordierite shows that pressures were above 4 kb (Hess, 1969; Dallmeyer and Dodd, 1971).

The presence of labradorite in amphibolite shows that we are in the Upper Amphibolite facies (Wenk and Keller, 1969). Liou (1974) has shown that labradorite (An_{50}) is stable at around 600°C.

The calc-silicate assemblages are consistent with the P, T conditions derived above. The lack of wollastonite, and presence of forsterite as opposed to clinohumite + calcite all suggest that P CO_2 was moderately high (see Kerrick et al 1973). Miyashiro (1973, p.272) has shown that most calc-silicate reactions during prograde metamorphism release CO_2. The diopside-forming reaction (Metz, 1970) shown in Figure 27 takes place at lower temperatures (up to 50°) at high X CO_2 or X H_2O values. Since the reaction produces H_2O, it is favoured by low X H_2O, high X CO_2 and P fluid $\neq$ P total. The reaction

tremolite + 11 dolomite $\rightleftharpoons$ 8 forsterite + 13 calcite + 9 CO_2 + H_2O

lies within 10° of the diopside-forming reaction if the

ratio X CO_2/X H_2O is high. Miyashiro (1973) has also shown that the reaction

talc + dolomite $\rightleftharpoons$ 4 forsterite + 5 calcite + 5 CO_2 + H_2O

occurs at similar temperatures. Grossularite is only stable in quartz-deficient calc-silicates at the temperatures and pressures suggested for the Caledonian metamorphism.

The Hercynian (m_2) metamorphic parageneses imply low X CO_2 values, high X H_2O, and lower P, T values than the Caledonian event. Chloritoid is the typical mineral in pelitic rocks and appears to form by the reaction of biotite with an Al-rich phase. Hoschek (1969) has reported that the assemblage chloritoid + biotite + quartz is rare in nature and using the present experimental data, its stability field lies between 2 and 4 kb and 450° to 500°C f O_2 = F.M.Q. buffer). The stability of the assemblage chloritoid + quartz in equilibrium with the F.M.Q. buffer was recently determined by Grieve and Fawcett (1974).

Plagioclase ranges from albite to oligoclase and Liou et al (1974) have shown that in amphibolite the reaction hornblende + plagioclase $\rightleftharpoons$ actinolite + chlorite + epidote + albite occurs at 550° to 570°C, P fluid = 1 to 7 kb. Chlorite begins to react at temperatures above 475°C and a 75° transition zone occurs between Greenschist and Lower Amphibolite facies assemblages.

The presence of chondrodite after forsterite shows that X CO_2 is less than 0.2 (Kerrick et al, 1973). Experimental work on the stability of chondrodite (Tell, 1974) shows that it reverts to talc + dolomite + fluorine at around 450°C, 2kb (X CO_2 = 0.1).

The reaction

clinozoisite + quartz $\underset{P}{\overset{T}{\rightleftharpoons}}$ grandite + anorthite

has been experimentally determined by Holdaway (1966) but Hyndman (1972, p.316) has stated that the reaction probably occurs at temperatures about 100°C lower when more sodic plagioclase is formed. Liou (1973) has shown that epidote and clinozoisite are not stable at f O_2 values less than the F.M.Q. buffer. Curves for the upper stability of clinozoisite (about 50°< T for epidote)

agree well with those shown by Hyndman (f O_2 = F.M.Q.buffer.)

It is improbable that P fluid equalled P total during the Hercynian metamorphism of the pre-existing high grade gneiss. Water was introduced during metamorphism to cause the observed retrograde assemblages. Local biotite and almandine growth and recrystallization occurred.

The Early Alpine (m_3) metamorphism ranges in grade from Upper Greenschist to Lower Amphibolite facies. Oligoclase-andesine is typical of temperatures in the range 500° to 530°C at 3 kb (see 7.35 for pressure estimates during mylonitisation). Fluid pressure was high within mylonites and zones of strong deformation but in the bulk of the gneiss the Hercynian assemblages are little changed. Some retrogression of chondrodite to serpentine has occurred. This takes place at temperatures between 450° and 500°C at 2 to 4 kb. Growth of large tremolite crystals has also been observed in impure marble (+ 380°C at 2 kb, X CO_2 = 0.1). Almandine porphyroblasts have grown in mylonites and metasediments in the Viso sheet. Hsu (1968) has shown that almandine is only stable above 540°C at 2 to 5 kb (f O_2 = F.M.Q. buffer) unless some manganese is present. If almandine contains 5% spessartine (as for example reported by Cliff et al, 1971, from Peripheral Schieferhulle) stability is extended down to 500°C at 2 to 5 kb.

The Late Alpine (m_4) event, which occurred primarily in the Albiolo, Cadil and Vallazza sheets, is typified by the minerals chlorite, epidote, albite and tremolite. Such minerals are stable in the range 220°C (minimum for epidote - Seki, 1972) to 450°C (Liou et al, 1974), at 1 to 2 kb. The presence of chloritoid growing across the brucite - serpentine fabric in a vein within amphibolite (Cadil Nappe) suggests that temperatures around 400°C were attained and P fluid was greater than 2 kb (Hoschek, 1969). Abundant biotite in some f_5 mylonites also suggests temperatures around 400°C (Turner, 1969, p.118). The presence of limonite and hematite suggest that f O_2 values were greater than the F.M.Q. buffer and lay between the H.M. and N.N.O. buffers.

6.40 STRUCTURE

6.41 Introduction

The regional structure of the Central Alps is controlled by the distribution of large scale folds and mylonites of the f_3 event. Several features in the gneisses of the Central Alps have been used to clarify structural relations in the Central Alps. Discordant Variscan pegmatites and quartz veins in the gneissic sequence are important markers since they cross-cut the earlier f_1 structures but are folded by the later events. The majority of mylonites are developed synchronous with the f_2 and f_3 events. Late stage muscovite in the mylonite zones also provides a useful marker since these 1 to 5 mm. diameter plates are folded by the f_4 and f_5 structures. The andesite-quartz monzonite dykes cross-cut the f_3 and f_4 structures but are deformed by f_5 mylonites.

The paragneisses dip steeply N to NNW adjacent to the Tonale Line, and to the north turn over to dip steeply S to SSE. Further north, the dip shallows to about 50° SSE and north of the Peio Line to about 15° SSE. The overall structure defined by the gneissic banding is a large-scale "back fold" with its axis plunging gently WSW. The structure is similar to that shown in many early syntheses of Alpine geology (e.g. Argand, 1916; Heim, 1922). This is primarily an f_3 structure associated with northward thrusting of the Austro-Alpine Nappes. The later f_5 event has compressed this structure causing the backfold to develop, and differential uplift of the zone between the Peio and Tonale Lines has occurred. This uplift is a maximum at the Peio Line, along which a considerable thickness of mylonite is developed.

The geometry of the structures and their associated metamorphism show that each deformation event occurred at successively lower temperatures and pressures, with the possible exception of the f_3 event. The initial f_0 event occurred under Upper Amphibolite conditions and has resulted in the formation of isoclinal folds and a dominant foliation. The f_5 structures show a geometry of close to parallel folding with slickensiding on the limbs and a

cleavage in suitable lithologies at fold hinges. f_6 kinks are shallow level structures (see Dewey, 1965) and their axial orientations imply some local variation in stress field.

The detailed geometry, distribution and orientation of the structures is given below.

6.42 f_o event

The original sedimentary banding is now reflected by mineralogical banding and grain size. The gneissic banding pre-dates the f_1 structures and in some areas (e.g. Vallazza sheet, T295) poorly defined isoclinal folds may relate to this early f_o event. These structures have amplitudes of 10 to 30 cm., wavelengths of 4 to 12 cm. and angular synformal and rounded antiformal hinges. Fold axes plunge steeply southwest and the gneissic banding is axial planar to the folds. Similar poorly defined isoclinal folds are seen in marble of the Cadil sheet, on the Southern slope of Monte Tonale Orientale (M182). These folds, whose axes plunge gently W, pre-date the metamorphic fabric and may relate to an early event. It must be emphasized that it is very difficult to determine whether these folds represent a folding event prior to the Upper Amphibolite m_1 metamorphism, or if they are f_1 structures. The former explanation is preferred here.

6.43 f_1 event

The gneiss contains abundant thin quartz veins and segregations which generally lie in the plane of the banding. These commonly have a pale blue-grey colour due to abundant minute inclusions. The segregations are folded into minor tight to isoclinal folds, with the banding generally axial planar to these structures. The folds have amplitudes ranging from 1 cm. to 1 m. and wavelengths of 0.3 cm. to 6 cm. The folds have markedly thickened hinges and would correspond to Class 1C folds of Ramsay (1967, p.365). The folds generally have axes plunging east or west (see Map 2).

The gneissic banding is rarely folded by the f_1 event. In such cases the f_1 minor folds are tight to isoclinal with

thickened hinges and approximate to "similar" in profile (Class 2 - Ramsay 1967, p.366). They range from 5 cm. to 1.5 m. in amplitude and from 2 cm. to 2 m. in wavelength. The hinges are more rounded than the quartz vein folds and the folds are generally asymmetric with a short common limb. Only very rarely are multiple folds seen. Although later events may have modified the initial orientations, since later folds (f_3 and f_5 generally) have axes with similar orientations, the degree of modification is probably only small. The folds have a southward vergence where a sense of asymmetry can be determined, implying a south-directed rotation during the Hercynian f_1 event.

In many areas, e.g. the S.E. slope of Monte Tonale Orientale, (central part of Monte Tonale sheet) biotite defines a strong axial plane foliation to the f_1 folds in the gneiss, which is best seen in the fold hinges. Hence biotite growth occurred synchronously with the f_1 deformation. It is interesting to note that tremolite crystals up to 1 cm. long define a strong lineation in parts of the Cadil sheet, also showing that growth was synkinematic with the f_1 event. At T320, above the Saccarana fort on the SE slope of Monte Tonale Orientale, a marked biotite foliation is seen at 2° to the lithological boundary. This small difference in planar orientation may be interpreted to show that a synclinal hinge lies to the north, suggesting that larger scale f_1 folds than those seen in outcrop occur. Similar relationships are seen over many parts of the field area. Since no large scale f_1 folds were detected during the detailed mapping of the area, it is more probable that the Hercynian stress system lay at an angle to the gneissic layering during deformation, since numerous f_1 folds of the banding were seen in the vicinity of T320. Small discontinuous quartz and quartz-biotite-garnet veins and pods, which are interpreted as locally sweated during the Hercynian m_2 metamorphism, cross-cut the biotite foliation. At several localities (e.g. summit of Monte Tonale Occidentale, T177) almandine garnets up to 5 mm. across grow across the planar gneissic layering and also cross-cut the

f_1 folds. In the marble, tremolite and epidote/clinozoisite crystals up to 1 cm. long grow across f_1 structures. These features show that m_2 metamorphism continued after f_1 deformation had ceased.

In the marbles, tight to isoclinal minor folds of calc-silicate and quartz bands are present. Figure 28 shows typical f_1 folds of quartz veins in marble. Grossular crystals are dismembered, folded and boudinaged in some areas and hence the growth of grossular must have occurred prior to the f_1 event, which is here considered to be of Hercynian age. f_1 marble structures have axial planes sub-parallel to the banding and where the folds show asymmetry they have a southerly vergence.

6.44 f_2 event

This event is generally restricted to marble bands thicker than 2 m., and f_2 folds of the gneissic banding result from contact strain effects adjacent to the folded marble bands. The folds have axes plunging moderately SE and axial planes which dip moderately steeply SE to E. They vary from open to tight and occur on two scales; those with a wavelength of 50 to 200 m. and a corresponding amplitude of 20 to 70 m; those with a wavelength of about 40 cm. and an amplitude of about 20 cm. The folds contain no axial plane foliation. Folds are commonly symmetrical but in some areas where asymmetrical folds are present (e.g. Monte Serodine, Vetta d'Albiolo) they show a southwest vergence.

Where f_2/f_3 interference patterns are seen, the later f_3 folds are generally open in style. When two separate fold systems are present, the later system is commonly only weakly developed since higher stresses are required to fold the pre-existing folded layering. Since f_2 structures are found on the shallow S - dipping limbs of large-scale f_3 folds in the Albiolo sheet, but not on the steep northerly limbs, the f2 folds may have developed in part synchronously with the f3 folding. In parts of the Monte Serodine area, the f_2 folds are tight and we may infer that metamorphic and/or stress conditions were more favourable

Figure 28(a) - Tight to isoclinal f_1 quartz vein folds in marble.

Figure 28(b) - Asymmetrical f_3 folds in calc-silicate-marble bands. The large degree of hinge thickening and limb thinning should be noted.

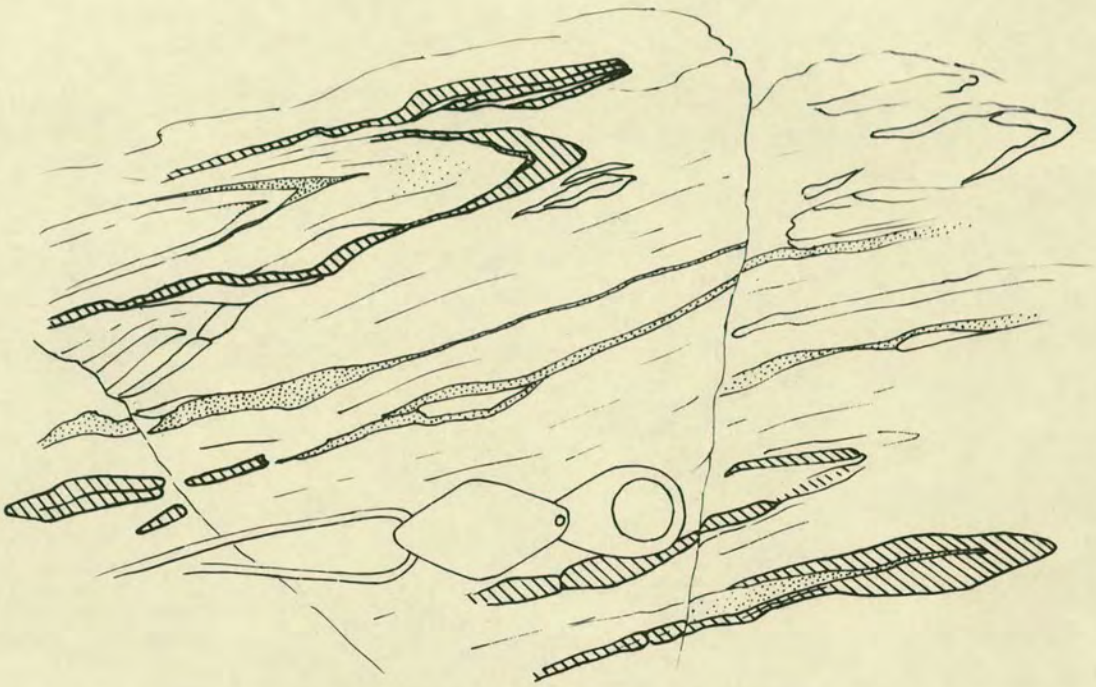

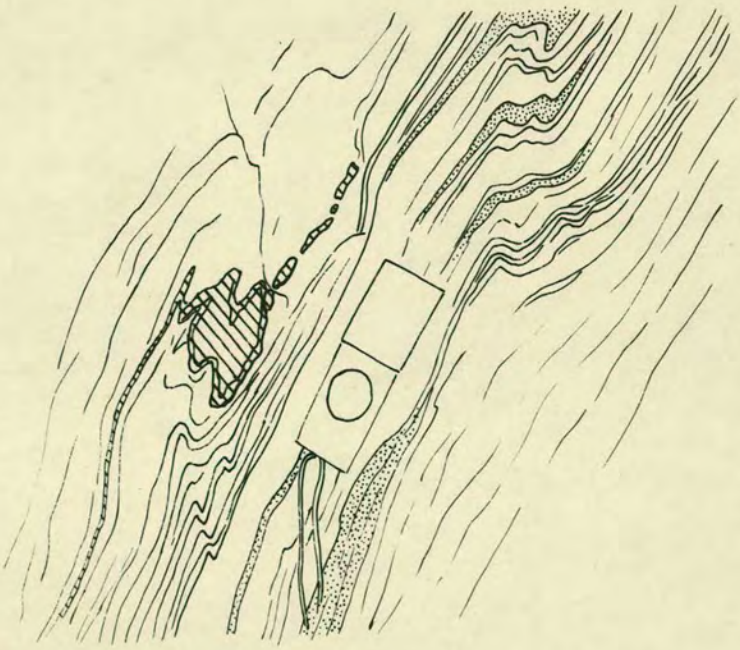

for ductile marble deformation than in the more northerly thrust sheets.

Rutter (1972) has shown that marble will deform in a ductile manner at high pore fluid pressures ($\lambda = 0.9$), moderate confining pressures, and low differential stresses. He showed that the law of effective stress ($\sigma s = \sigma - p$, where σs = effective stress, σ = total stress and p = pore fluid pressure) is a good approximation for marble behaviour under normal geological conditions. In his subsequent work (Rutter 1974) he tentatively extrapolates experimental data to geological strain rates and shows that at differential stresses of about 200 bars, steady state ductile flow will occur at a confining pressure of 1.5 kb. At higher strain rates (e.g. 10^{-8}/sec) and temperatures around 400°C, differential stresses necessary for ductile deformation will be less than 2 kb at $\lambda = 0.1$ and a confining pressure of 1.5 kb. We may infer from mylonitic textures that mylonitisation, and hence probably f_2 and f_3 folding in the Central Alps, occurred under confining pressures of approximately 3 to 5 kb. Minimum differential pressures of 3 to 6 kb are probable in the gneiss under such conditions.

At M361, in the Albiolo sheet, an f_1 lineation on a quartz vein is folded by an f_2 small-scale close fold. The lineation locus is plotted in Figure 29(a) and is similar to those shown by Ramsay (1967, p.468) which result from flattened flexural slip folding, where the Y axis of the strain ellipsoid is not coincident with the fold axis. This suggests that the quartz veins in the marble behave as thin plates with deformation occurring by a buckling mechanism (tangential longitudinal strain). Subsequent flattening has modified the initial buckle fold. This mechanism has been shown to be important in natural deformation in many areas (Hudleston, 1973 a, b; Ramsay, 1967 p.432).

The presence of f_2 folds with axes sub-parallel to the extension direction (as shown by measurements of quartz aggregates in the mylonite zones and f_3 fold

Figure 29(a) - f_1 quartz lineation locus for an f_2 quartz vein fold. The locus suggests that the f_2 fold is a flattened flexural slip fold in which Y does not coincide with the axis of folding.

Figure 29(b) - f_1 quartz lineation locus for an f_3 quartz vein fold in mylonitic gneiss. The locus shows that the f_3 fold formed by heterogeneous compressive strain probably resulting from a combination of buckling and flattening.

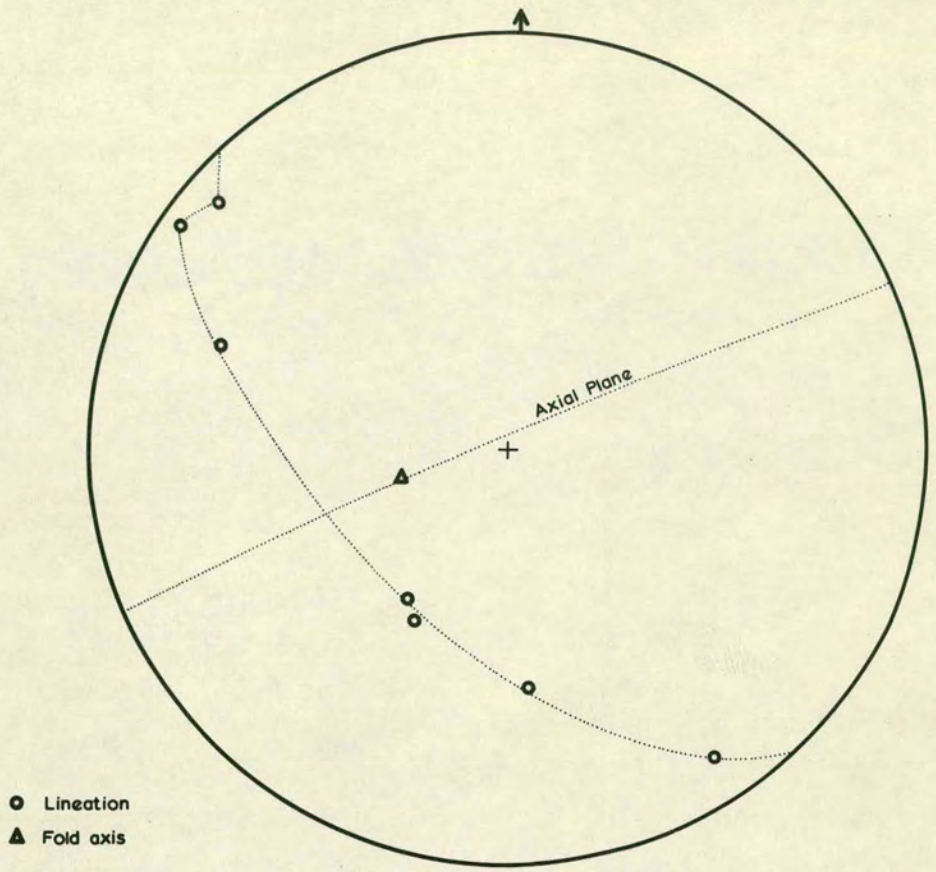
Axial Plane
Lineation
Fold axis

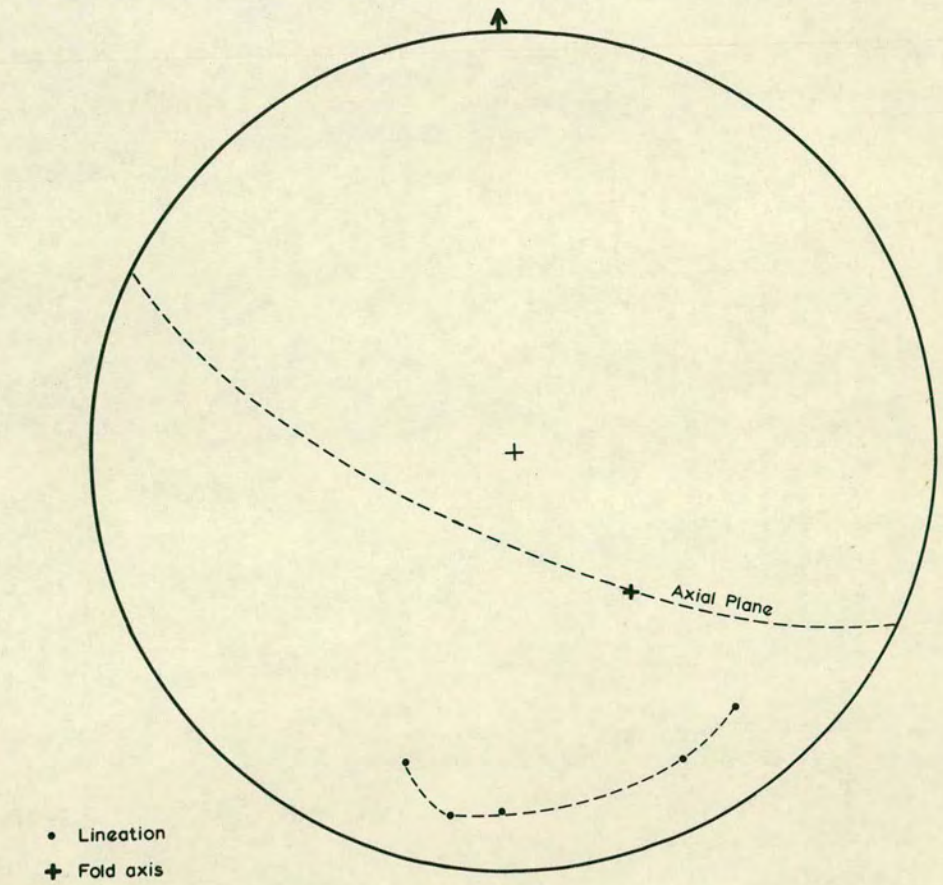
Axial Plane
Lineation
Fold axis

geometry) can be partially explained by rotation of axes, since the strain ellipsoid which is applicable to the f_2 deformation in the marble, is a constriction type ($1 < k < \infty$, Flinn 1962) with high X/Y values (see Sanderson 1973). The fold axes show a constant orientation irrespective of the position of the fold with respect to the marble/gneiss contact. Since there is a change from a constrictional to a flattening ellipsoid as we pass into the gneiss we may expect that axial rotation would be reduced. This is not seen in the field and it is assumed that fold orientation is controlled by the internal strain state in the marble. It is probable that compression occurred along the marble layers to accomodate the high strains in the marble, imposed by the f_3 stress state in the constraining gneiss. Very strong extension would only occur in the X direction which is in accord with tectonic transport directions to the N and NNW derived from f_3 fold geometry. This is also in agreement with the occurrence of cuspate structures with cusp axes coincident with the f_2 folds.

6.45 f_3 event

The f_3 event affects all the rocks of the Central Alps. Axial orientations of f_3 folds are relatively consistent throughout the area and the folds are generally asymmetrical and consistently show northward vergence. The folds are most abundant where mylonite development is greatest (see 7.11 Mylonites - Field Relationships). The folds vary in wavelength from about 2 cm. to about 2 km. and in amplitude from 0.7 cm. to 500 m. The largest folds seen involve the northern part of the Mt.Tonale sheet and the Casiole sheet. A thick mylonite zone is developed along the middle limb. The larger folds are generally open to close in style whereas small scale folds are usually close to very tight. The folds are broadly "similar" with relatively constant thicknesses when measured parallel to the axial plane. f_3 isoclinal folds are found only in mylonite or strongly mylonitic gneiss (see 7.50 Mylonitic Folds). f_3 folds have axes commonly plunging at variable angles to the E or W, although some axes show a spread within the

steep axial surface as shown on Map 2. Axial planes generally dip steeply SSE but may dip steeply NNW owing to the effects of later f_5 folding and shortening. Only in mylonitic zones is a penetrative new axial plane foliation developed. The mylonitic foliation represents the XY plane of the strain ellipsoid for the period of mylonitisation. f_3 folding and mylonitization were synchronous in many areas and the f_3 axial plane and the mylonitic foliation are coincident throughout the area mapped.

The spread of f_3 axes results from the superimposition of a relatively homogeneous stress field, as shown by consistent maxima for mylonitic foliation poles on layering of variable orientation on Map 2. f_3 fold axes for the various thrust sheets show a maximum at about 085° - 265°. The folds show a constant sense of overturning to the N, suggesting an important rotational component in f_3 movements. The fold axes define a partial great circle girdle corresponding to the axial surface, while their rotations are opposite on either side of a minor plane of symmetry. Hansen (1966) and Cliff et al (1971) have formalised this concept for asymmetrical folds with a consistent sense of vergence. The pole to the symmetry plane is the rotation axis which in the Tonale Pass area is horizontal with a trend of 085°. The direction of tectonic transport is defined by the fold vergence and lies where the symmetry plane intersects the axial surface. In the area mapped transport is toward 355°. This transport direction is also seen by displacements on small mylonite zones and by the geometry of minor structures and strain indicators in the mylonites. Howard (1968) has shown that in areas of disharmonic asymmetrical folding the separation angle (the angular section separating the distribution of fold axes whose senses of rotation converge) is a better parameter to use to determine tectonic transport.

The geometry of the f_3 folds in the paragneiss is best illustrated by Figure 29(b) which shows an f_1 lineation locus around a close minor f_3 fold. The locus defines a great circle apart from a small divergence in

its northwest part. This locus is almost identical to that shown by Ramsay (1967 p.485) for folds approximately "similar" in style (Class 1C and 3) formed by heterogeneous compressive strain. Such a strain would result from a combination of buckling and flattening (Hudleston 1973 a,b) or a multi-layer complex.

Minor f_3 folds of amphibolite bands are not common, but where amphibolite bands are less than 2 m. thick, open to close folds (Class 1B to 1C) may be developed. These folds are preferentially developed where the banding dips at moderate angles to the south. The folds have axes plunging gently E or W and axial planes dipping at low to moderate angles to the S or SE. Adjacent to mylonite zones amphibolite is internally folded (see 7.60).

The thick marble bands found in the Central Alps (Vallazza, Cadil, Mt.Tonale and Albiolo sheets) form marked strain and structural discontinuities in the Austro-Alpine Nappes. The role of marble in mylonitisation is discussed later (see 7.13).

At M24, 310 m. S.E. of Mt.Tonale Occidentale, a series of small south dipping imbricate thrusts repeat a 2 m. marble to form a zone about 6 m. thick. These thrusts are geometrically associated with f_3 folds. Northward movement has occurred along the thrusts which cut upwards to the north from the base of the marble. The thrusting is interpreted as a narrow zone of large-scale differential movement across which high strain rates and differential stresses have caused cataclastic fracture along zones of high shear strain. Hafner (1951) and Price (1966 p.93) have given shear stress trajectories for blocks under horizontal compression; zones of maximum shear stress invariably form upward curving trajectories which accord well with observed thrust orientations. The thrusting may also be used to suggest high differential stresses across such thin marble bands since Rutter (1972) has shown that at temperatures of 250° - 500°C, brittle fracture will only occur at effective differential stresses greater than 2 kb.

In the Mt.Tonale sheet, 500 m. southwest of Cima Casiole, a thick marble band forms a locus for large scale f_3 folds with a northward vergence as shown in Figure 30. The marble is structurally repeated by numerous tight, moderate scale (wavelength 20 - 50 m., amplitude 15 - 20 m.) "similar" folds and several steep thrusts. The thrusts lie at 10° to 30° to the banding and fold axial planes. Hence a 50 - 60 m. marble band forms a zone of complex structure several hundred metres thick. Using Rutter's (1972) experimental data, we may suggest that increasing differential stress or strain rate during deformation caused thrusting of earlier ductile fold structures.

Perhaps the most remarkable marble structures occur adjacent to Vetta d'Albiolo. Amidst strongly mylonitic gneiss and retrograde amphibolite, a 1.5 m. marble-calc-silicate band shows northward verging very tight minor f_3 folds. The band has a subvertical orientation and at a higher topographic level it forms an ovoid pod about 12 m. in diameter and about 8 m. thick. The structure is best described as "squeezing toothpaste out of a vertical slit". J Hunziker (pers.comm.1973) has noted similar thickness variations in marble bands of the Pennine Alps. Several marble bands on Vetta d'Albiolo display similar "toothpaste slit" structures with marble pods up to 50 m. in diameter. In this area 30 m. x 6 m. marble "boudins" are infolded with mylonitic gneiss.

In marble bands thicker than 3 m., close to isoclinal, minor folds of calc-silicate, impure marble and quartz are common. Quartz and calc-silicate folds are "parallel" (Class 1B) in style and have rounded fold hinges as shown in Figure 28. Their axes and axial planes are coincident with the north verging f_3 folds in the gneiss. Thin marble bands may contain north verging folds when interbanded with gneiss and amphibolite. Thin quartz veins in marble may show tight to isoclinal f_3 folds, particularly in the Albiolo sheet. These veins are extremely strongly lineated parallel to their axes. It is difficult in areas of strongly mylonitic gneiss to distinguish f_1 and tight to

Figure 30 - Photograph and sketch of a large f_3 folds in a thick marble band 500m. southwest of Cima Casiole. The sketch shows the thrusts // and associated northward verging asymmetrical folds. Ma - marble, Pel.gn - pelitic gneiss. Where exposure is poor thrust lines are dashed.

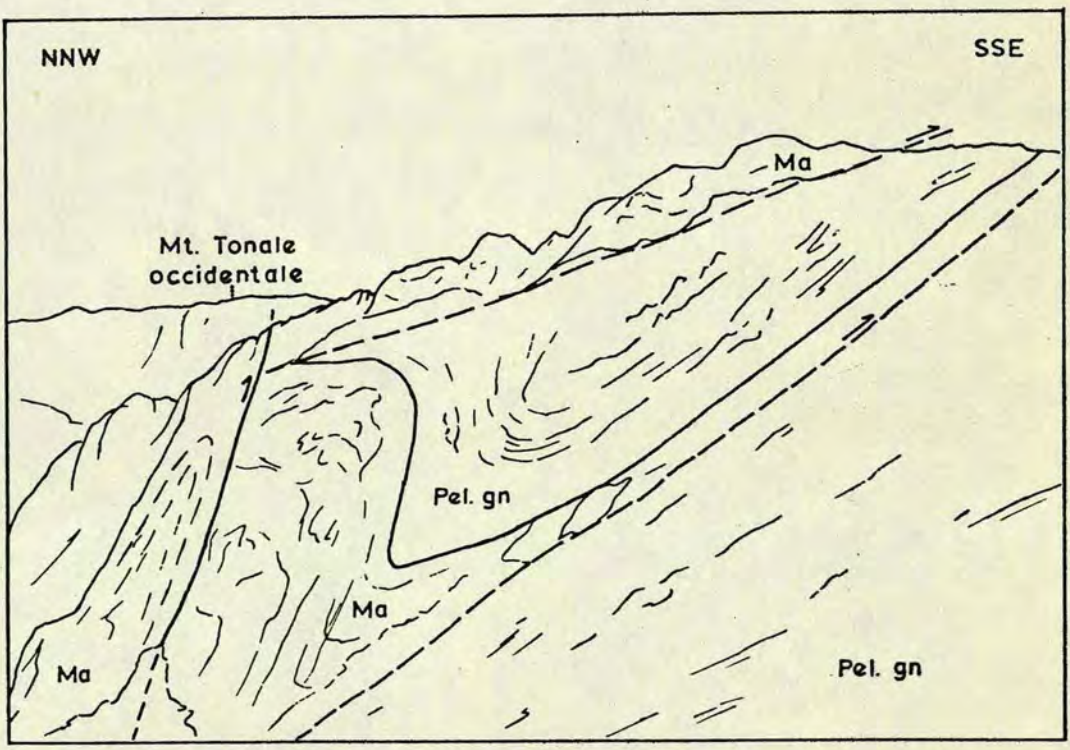
NNW
SSE
Ma
Mt. Tonale
occidentale
Pel. gn
Ma
Ma
Pel. gn

isoclinal f_3 minor folds in marble bands. Some f_3/f_1 interference structures do occur on a small scale.

Within the Cadil and Vallazza sheets (e.g. T76 and T187) the marble becomes finely banded and very fine-grained. The bands define "flow" lines which are commonly closely spaced between adjacent coarsely crystalline marble or pelitic gneiss. The marble has apparently "flowed" in a ductile manner relative to the adjacent blocks. The zones are up to 3 m. wide but average 25 - 30 cm. ~~as shown in Figure 28~~. Associated structures are disharmonic and banding is disrupted.

The field observations of f_3 structures in the marble bands show that it behaves in markedly different ways dependent on; bed thickness; degree of mylonitic deformation (hence possibly strain rate effect); and magnitude of differential stress and pore fluid pressure. The temperature at which f_3 deformation occurred is taken as relatively constant (between 350° and 500°C). It is difficult to explain the presence of northward verging f_3 structures in the gneiss and southward verging f_3 structures in the marble. The two materials have been shown to deform differently under experimental deformation (Griggs et al,1960) and this may possibly be invoked to explain this apparent contradiction. The downward facing marble structures show that relative tectonic transport was to the south and south-east. It is possible that the structures result from gravitational effects. This is inconsistent with the constant style and orientation of the structures and would necessitate volume increase at depth which is difficult to reconcile with other evidence from f_3 folds and probable crustal stress conditions. More probably, the structures result from underthrusting of the gneiss sheets below the marble bands. Such movements would cause a reverse shear couple to that occurring during overthrusting, and result in southward verging folds. This process would require the underlying gneiss sheet to be underlain by a mylonite zone or alternative horizon of translation. Evidence from mylonite zones in the gneiss does suggest that such under-

thrusting has commonly occurred.

The geometry of the structures in the marble shows surprising homogeneity of λ_{mean} strain and generally structural continuity throughout the area mapped. This suggests that the orientation and magnitude of the causative stress state was relatively consistent throughout the f_3 deformation event. Locally differing effects occurred in zones of high deformation, greater pore fluid pressure and large scale rotational strain. The marble bands were zones of preferentially high differential movement (see 7.13) and the amount of f_3 strain undergone by marble is considerably greater than that in the gneiss. This is confirmed by the tightness of f_3 folding and presence of f_2 folds in the marble.

6.46 f_4 event

The f_4 folds are commonly developed in and adjacent to mylonite zones, and in the marble bands. A fine crenulation cleavage lineation occurs in some phyllonite bands. The f_4 folding post-dates the growth of muscovite in the mylonites. This muscovite grows across f_3 lineations and mylonite microstructures.

The fold axes plunge gently to moderately to 070° or 250° and show a remarkable consistency in orientation as shown on Map 2. In contrast the axial planes have very variable strikes and dips. The folds range from chevron to approximately "similar" in profile, from sub-microscopic to 3 m. in wavelength and up to 80 cm. in amplitude. The f_4 folds in mylonite generally show a northward vergence and have a consistent profile along their axes. Locally upward closing folds are abundant in the gneiss and mylonites, and reclined folds are common in the marble. f_4 chevron folds are well developed in the phlogopite rich marbles of the Cadil sheet.

Near the southern margin of the Central Alps in the Val di Strino - Mt.Tonale Orientale area, both large and small scale f_4 folds are present in pelitic gneiss, minor amphibolite and marble. These "crenulation" folds are up to 300 m. in wavelength, and have long straight limbs and

small angular to rounded hinge areas, with only minor hinge thickening. Where such folds affect quartz or pegmatite veins greater than 10 cm. thick, fracturing and dislocation has commonly occurred in the hinge areas. Although the folds are generally asymmetrical with a northward vergence their sense is locally variable.

The consistent axial orientation together with the localised development of f_4 folds probably results from only small principal stress differences during formation. Only areas with a specific banding orientation would then be folded (c.f. f_3 and f_5 folds).

6.47 f_5 event

The effects of the f_5 event are most marked near the Peio Line, but f_5 folds are also developed in the upper Cadil and lower Vallazza sheets. Open to tight folds are particularly common in thick marble bands in this latter region. Phyllonite may also show f_5 minor folds, and in some areas it is difficult to distinguish between f_4 and f_5 minor folds. f_5 folds are almost invariably "concentric" in style. They may be asymmetrical and show a southerly vergence particularly when associated with f_5 shear zones or mylonites.

Open to close f_5 folds range in amplitude from 0.5 cm. to 10 m. and in wavelength from 1.5 cm. to 30 m. The folds have steeply dipping axial planes except where they are very markedly asymmetrical and axial planes dip at low angles. Fold axes generally plunge gently east to north east or west to southwest but show a considerable variation in some areas. f_5 fold axis and axial plane orientations are given in Figure 31(a).

No f_5 quartz lineations were found and in thin section quartz shows abundant strain shadows but no recovery or recrystallization. Minor grain boundary sliding may have occurred. Only in the marble has twin gliding enabled close to tight folds to form.

Slickensides are found on the limbs of several f_5 gneiss folds particularly in the Albiolo sheet. The orientation of these structures shown in Figure 31(a) implies

Figure 31(a) - Stereogram showing f_5 fold axes, axial planes and lineations in the Central Alps. Associated slickensiding on fold limbs in the Albiolo Sheet shows that the 'slip' plane of fold propagation (locus of 'a' directions) trends approximately 015°/Vert.

Figure 31(b) - Stereogram showing the locus of f_2 lineations around an f_5 fold in marble of the Cadil Sheet (see plate 8(a)). The f_5 fold has a lineation locus typical of oblique flexural slip folds. Minor extensional strain has occurred on the outer arc and minor compressional strain on the inner arc. The principal extension direction $\overset{(X)}{\wedge}$ for the 5_5 strain ellipsoid is sub-vertical whereas the 'a' direction plunges moderately NNW. (c.f. Albiolo Sheet results in Figure 31(a)).

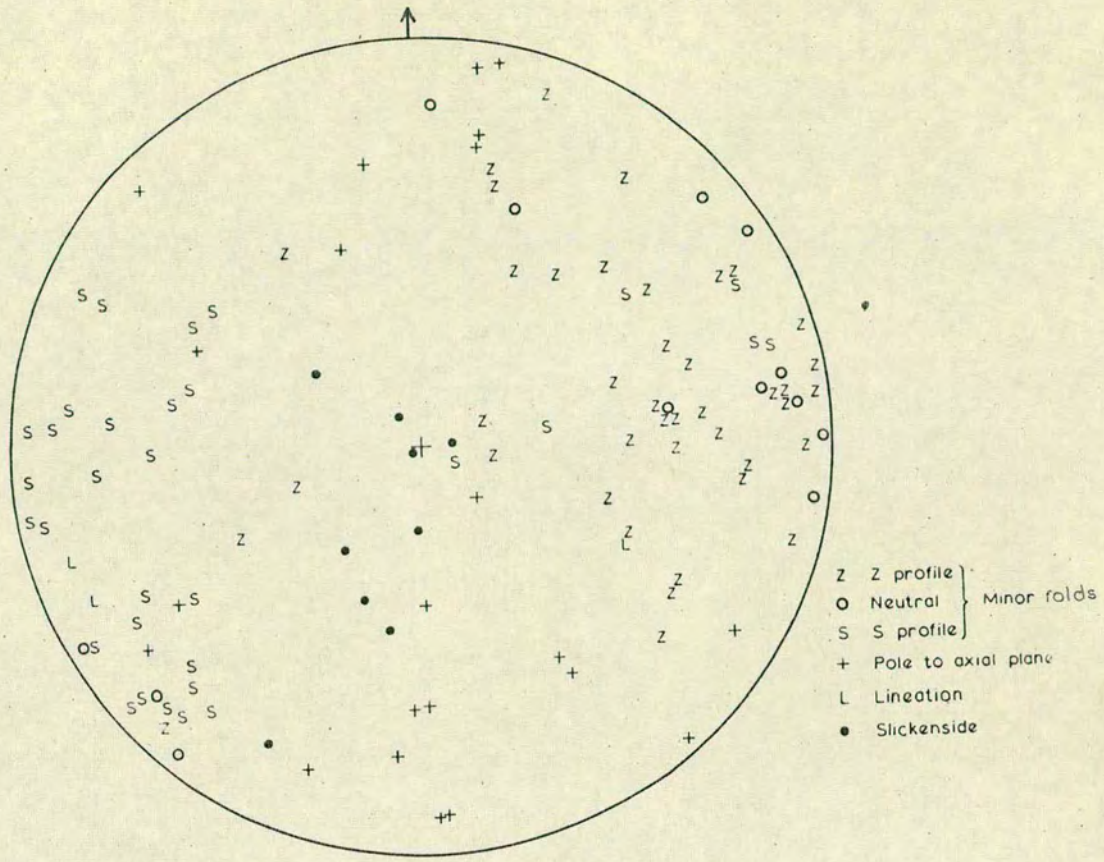
Z Z profile
O Neutral
S S profile
Minor folds
+ Pole to axial plane
L Lineation
• Slickenside

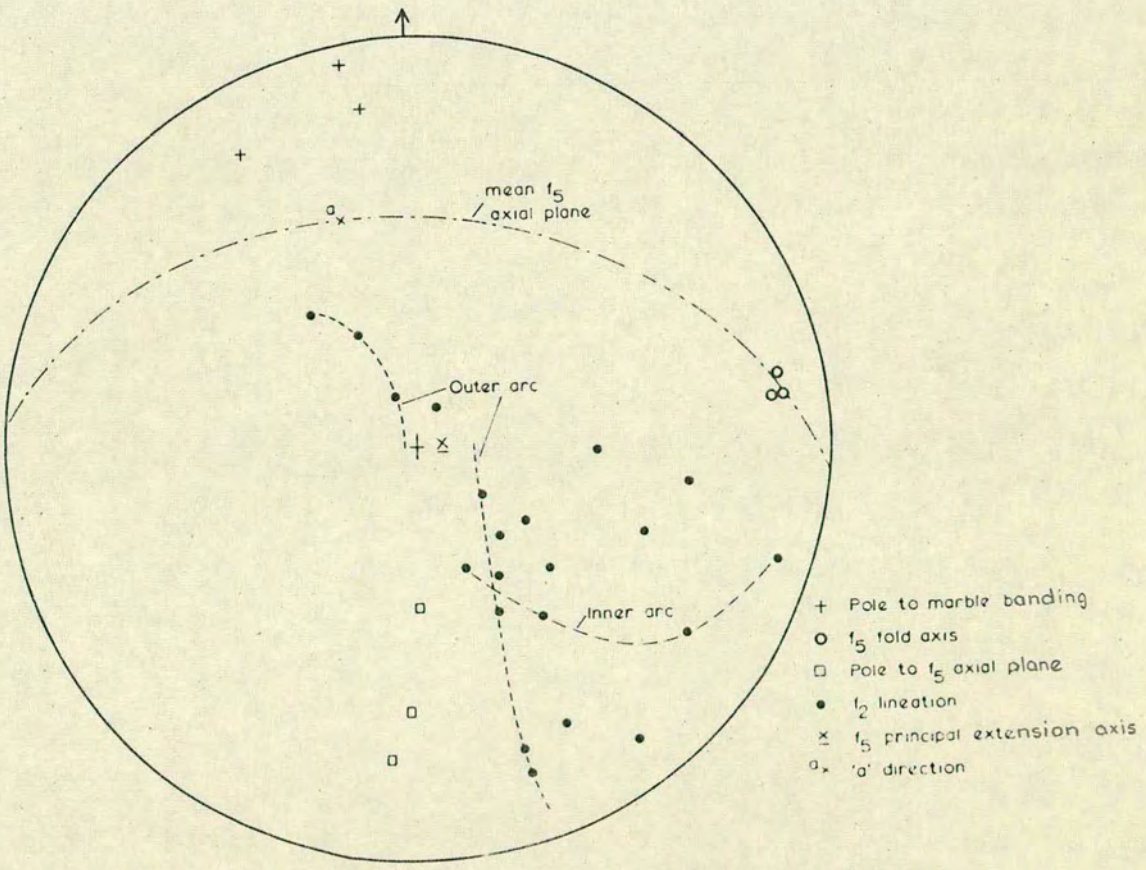
mean f_5 axial plane
a_x
Outer arc
Inner arc
+ Pole to marble banding
O f_5 fold axis
□ Pole to f_5 axial plane
• f_2 lineation
⊻ f_5 principal extension axis
a_x 'a' direction

that the associated X direction lies close to the vertical. Slickensides are also common in steeply dipping mylonite zones where they show a sub-vertical orientation. These result from later f_5 movement along pre-existing mylonites.

As shown in Plate 8(a), f_2 lineations are deformed around f_5 folds in the thick marble band of the Cadil sheet. The measured loci given in Figure 31(b) show that the f_5 oblique flexural slip folds are associated with a strain ellipsoid in which the X direction is sub-vertical. The a direction (direction of fold propagation - see Ramsay, 1967, p.423 - 427), which reflects the initial banding and f_5 axial plane orientations, plunges moderately NNW in accord with the southward vergence of f_5 folds (N.B. lower hemisphere projection). Loci from the outer arc of an f_5 fold show that minor internal extensional strain has occurred in this part of the fold.

At M197 in the Albiolo sheet a very thin discordant feldspar vein is folded implying shortening normal to the steep southeasterly dipping foliation of about 20%. Similar veins in the southern part of the Vallazza sheet show no folding. This shortening value is taken as the minimum bulk strain in amphibolite affected by the f_5 event. Measurements along fold profiles give % shortening values around 40% in mylonites and up to 55% in marble. It must be emphasized that this bulk strain was only significant in areas where f_5 folds are well developed.

6.48 f_6 event

The deformation event has resulted in the formation of small-scale kink bands in two conjugate sets. The amplitude of the kink bands ranges from 1 mm. to 10 cm. and their interlimb angle from 30° to 55°. The kink bands occur throughout the Stavel Gneiss and Central Alps, and show no significant change in orientation. As shown in Figure 32 kink band axes show a scatter about 080° - 260° and about 180°. The plunge and direction of kink band axes results from the intersection of the gneissic banding and kink band axial planes. Kinks are preferentially developed in mylonitic or strongly deformed gneiss where closely spaced

Plate 8

(a) Folded f_2 lineation on an f_5 fold in flaggy phlogopite marble. The lineation locii are given in Figure 31(b). (M136 - Cadil Sheet).

(b) f_1/f_3 fold interference patterns in banded marble. (T43 - Cadil Sheet).

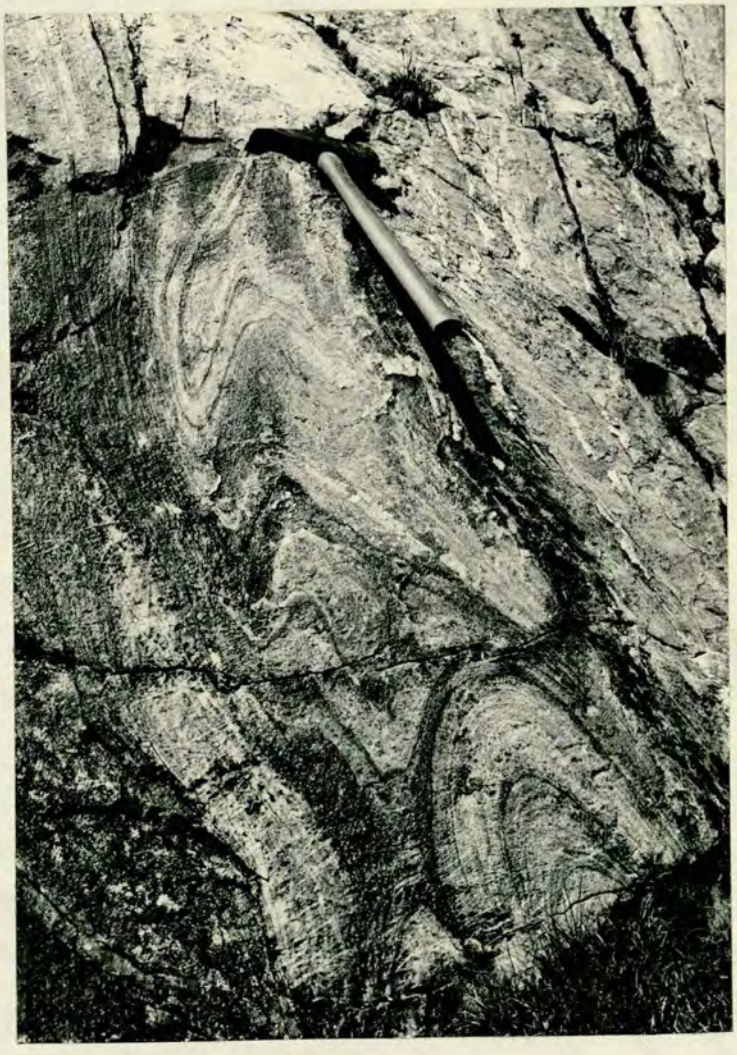

Figure 32 - Stereogram of the kink band axes and axial plane orientations in the Central Alps. The majority of kink bands show a dextral sense when viewed down plunge. Kink bands show concentrations in sub-vertical planes trending approximately north-south and east-west.

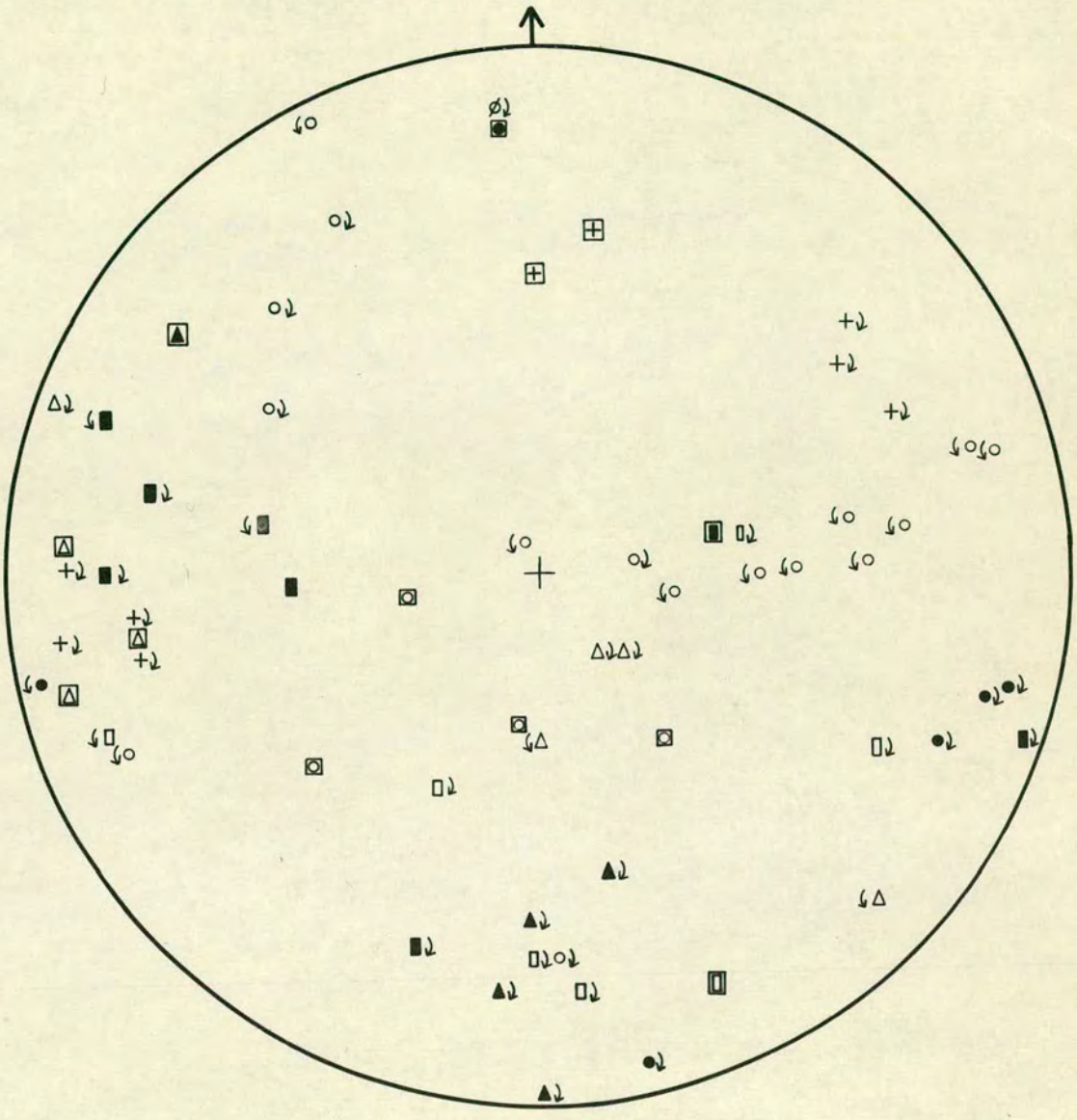

Axis	Axial plane	
●	▣	Viso sheet
+	⊞	Stavel Gneiss
o	⊡	Mt Tonale sheet
△	⧋	Casiole sheet
▲	▲	Albiolo sheet
▯	▯	Cadil sheet
▮	▮	Vallazza sheet
ø		Mezzolo sheet

↳ sense of rotation viewed down axis

layering has been developed. Kink band axial planes generally have an E-W or N-S strike which can be used to define the orientation of the causative stress systems. Some intermediate orientations are also present.

The majority of kink bands with south plunging axes show a dextral sense when viewed down plunge. This results from principal stresses acting at an angle to the layering. The kink band geometry suggests that σ_1 acted in a northeast - southwest plane. Although no interference relationships are seen between the two conjugate sets, it seems probable that the E - W trending kinks were initiated first. The N - S trending kinks are correlated with the large scale very open folds with N - S striking axial planes, which affect all other fold sets. The effects of these f_6 folds is seen in the broadly sinuous outcrop pattern of the major rock units (Map 1). Gansser (1968) and Sassi et al (1974) have all reported horizontal slickensiding along the Insubric Line implying late lateral movement. Laubscher (1971a) has suggested that late dextral movement about steep axes has occurred in the Gotthard massif and Lepontine Alps. These observations agree with evidence of late E.W. relative movements in the Tonale Pass area.

6.49 Interference patterns

Figure 33 illustrates the interference patterns and axial traces at several localities in the area mapped. The majority of interference patterns are caused by the refolding of f_1 folded quartz veins by f_3 folds. Less commonly f_1 banding also shows good refolding structures. Since f_1 and f_3 folds are approximately co-axial and their axial planes lie up to 30° apart, the resultant pattern is a type 1B (Ramsay, 1967, p.531). f_1 banding and folded quartz veins are only refolded where they lie at a moderate angle to the superimposed f_3 stress field and the f_3 deformation is well developed (e.g. mylonite gneiss). More generally pre-existing structures are flattened and f_1 folds became tighter in style.

In banded marbles, up to four sets of folds may be present in a single outcrop. The resultant structure has

Figure 33 Interference patterns.

(a) f_1-f_2-f_3 patterns in banded marble. Vertical face on ridge 875 m. NNW of Mt. Tonale Orientale.

(b) f_1-f_2 patterns in banded marble. Steeply dipping face 100 m. northwest of Mt.Serodine summit.

(c) f_2-f_3 patterns in banded marble. Vertical face 100 m. northwest of Mt.Serodine.

(d) f_1-f_3 and f_2-f_3 patterns in banded marble. Steeply dipping face 100 m. northwest of Mt.Serodine.

Closed interference structures only result when f_2 folds are present in banded marbles. The f_1 and f_3 folds have similar axial and axial plane orientations.

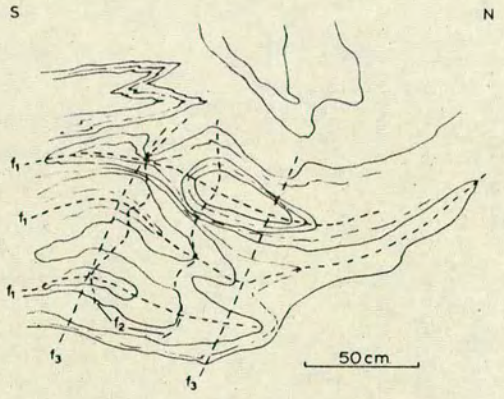

(a)

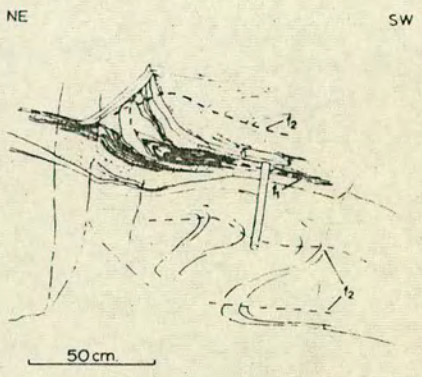

(b)

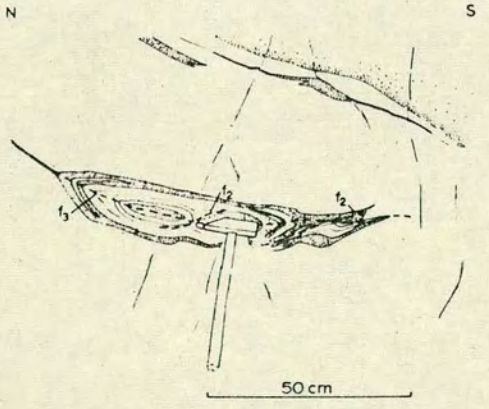

(c)

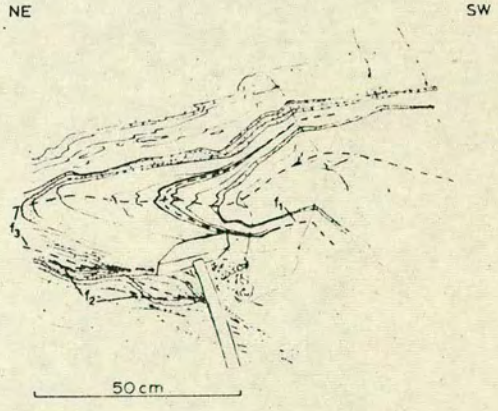

(d)

been termed "schlingen" (vortex) or "wirbel" (spiral) folds (Andreatta, 1953; Schmidegg, 1936) but careful measurements of fold orientations in the Tonale Pass area show a surprising consistency. The observed patterns can thus be simply explained by the geometrical superimposition of several different fold systems.

In the Mt.Serodine area (Cadil sheet) interference patterns f_1/f_4, f_2/f_3 and f_1/f_3 are common in finely banded marble (Figure 32). Plate 8(b) illustrates the f_1/f_3 interference pattern. Figure 34 shows the orientation of the various folds in this area. The rotation of f_1 axes on the limbs of f_2 folds is very noticeable. The spread of f_1 and f_2 axes in a N - S and NW-SE plane may be partly attributed to the effects of f_3 and f_4 folding. f_6 folds are northerly plunging open flexures. Because most of the fold axes are approximately orthogonally related to each other, the geometry of the interference structures does not become particularly complex. f_1/f_3 patterns are type 1B and f_2/f_3 patterns type 2H (Ramsay, 1967, p.531).

In marble of the upper Cadil sheet in the Valbiolo, medium scale "concentric" f_5 open folds refold the smaller scale f_4 chevron folds. More generally only f_4 or f_5 folds are developed in any one area.

Once compositional banding is formed it strongly modifies the orientation of any subsequent stress fields (see 6.71 and Treagus, 1973). The style of later superimposed folds in already strongly folded rocks is more open than that in rocks with only initial planar banding. The stress field must be sufficiently different in type or orientation (e.g. f_3 stress field with a strong rotational component) from that in previous structural events or no interference patterns will result. The f_2 and f_3 fold orientations are controlled in the Tonale Pass area by the local interchange of intermediate and maximum principal stress directions as a result of the specific response of rock type to applied stress (c.f. marble and pelitic gneiss).

6.50 Cuspate structures

These structures develop where two thick beds of

Figure 34 - Stereogram showing the structural data from banded marbles of the Mt.Serodine area. Note the spread of f_1 fold axes along the limbs of f_2 folds. f_1 folds are tight to isoclinal in style and generally have the banding sub-parallel to the axial planes.

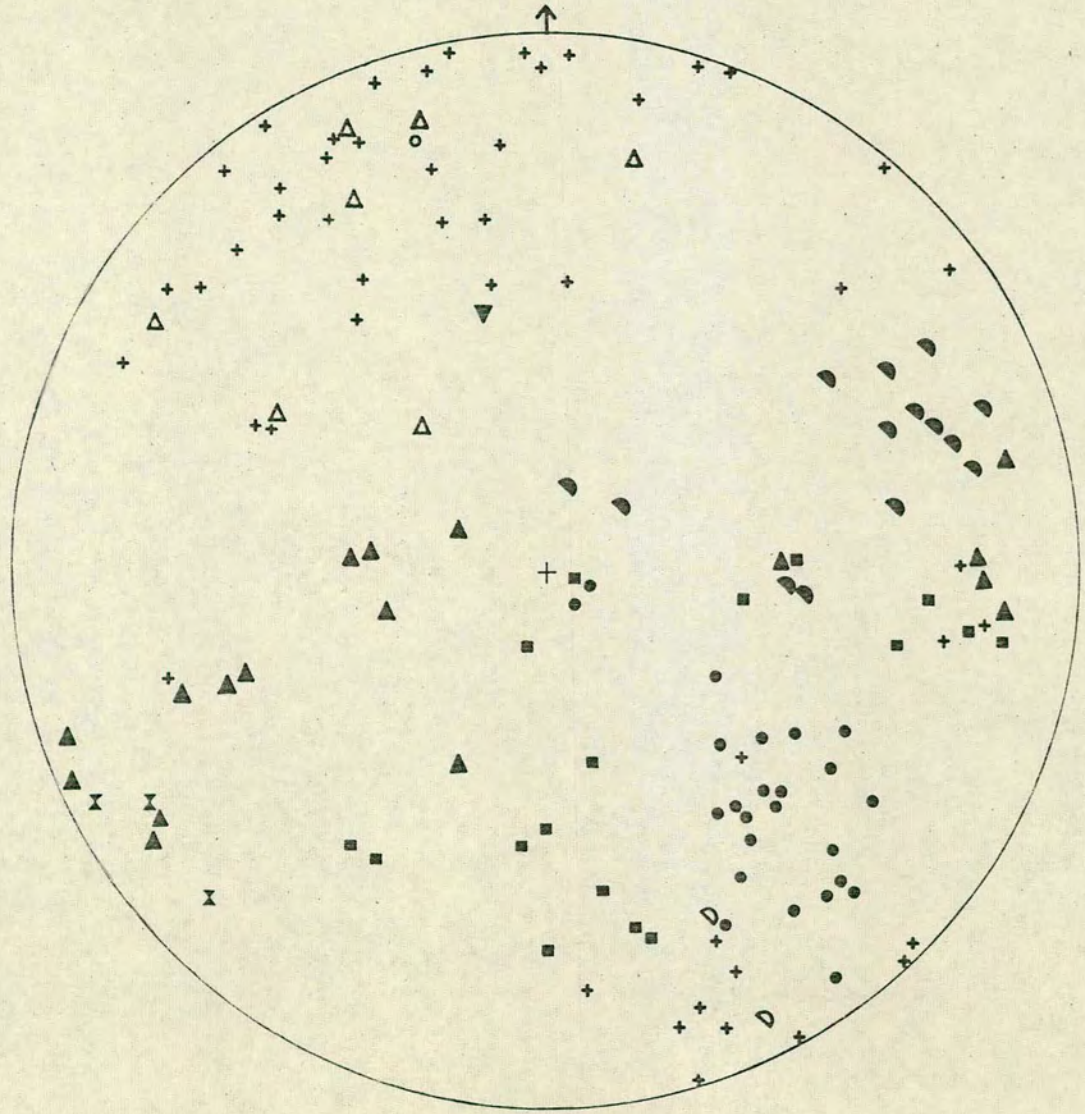

+ Marble banding

■ f_1
● f_2
▲ f_3
◗ f_4
▼ f_6
} fold axes

⧗ f_3 boudin necks

○ f_2
△ f_3
◗ f_4
} fold axial planes

markedly differing viscosity are compressed along the layering. The cusps generally point inwards towards the more viscous material (see Ramsay, 1967, p.383). In the upper part of the Cadil sheet a 1 m. amphibolite band shows cuspate structures at its contact with pelitic gneiss. The cusp axes are horizontal and trend 063°. Similar structures are found at gneiss/pegmatite, gneiss/marble and pegmatite/marble contacts. Using the above criteria the relative viscosity of the different lithologies during the f_2 and f_3 events may be determined. In decreasing order of viscosity they are; feldspar rich veins, amphibolite, pegmatite or quartz, pelitic gneiss, marble.

At the base of the thick marble unit of the Cadil Nappe large upright to overturned cuspate structures 10 to 30 m. wide are common. The sharp anticlinal cusps generally project into the marble in contradiction to the general principle. Siliceous marble replacement occurs at the sharply cuspate areas. The structures plunge moderately to steeply southeast and are assumed to have formed during the f_2 event.

Since f_2 fold development in the marble is attributed to compression in the plane of the banding ~~and~~ we may extend this hypothesis to explain the origin of the cuspate structures. Across the pelitic gneiss/marble contact there is a sharp change in the amount and type of strain. The physical properties of the marble during the Early Alpine deformation have resulted in a constrictional ellipsoid with high % shortening values whereas in the pelitic gneiss a flattening ellipsoid was formed with considerably lower % shortening values. Hence since continuity is maintained, a strain discontinuity develops. The rare occurrence of slaty cleavage axial planar to the cusps in the pelitic gneiss adjacent to the marble/gneiss contact shows that compression in the plane of the layering perpendicular to the cusp axis has occurred. Although this explanation is satisfactory for the development of the cuspate structures, no reason can be offered to account for the anomalous geometry.

6.51 Lineations

Lineations are a common feature in the rocks of the Central Alps. They are generally defined by mineral "rodding" and preferred growth in the pelitic gneisses. Quartz, biotite, chlorite and to a lesser extent muscovite, sillimanite and feldspar may all define such lineations. In many cases there is apparently preferred growth along the lineation. Plate 9(a) shows a deformed pegmatite at M49 (lower Cadil sheet) with well-developed quartz "rodding" pitching 34° to 192°, developed at the intersection of a mylonitic foliation trending 110/40°S and a gneissic banding trending 032/45°SE. Although this is undoubtedly an intersection lineation, some quartz growth has occurred along this line. These lineations constitute the majority recorded during field mapping.

At M247 (lower Mt.Tonale sheet), where a strong intersection lineation with associated minor quartz and muscovite growth is present in highly mylonitic gneiss, deformed garnets show that this lineation is <u>not</u> related to the finite strain axes. Similarly, f_3 lineation orientations (see Map 2) show that they cannot be correlated with stress axes as deduced from boudinage, fold geometry or strain indicators.

Intersection lineations are best developed where the mylonitic foliation and gneissic banding orientations differ by 20° to 50° in dip and 60° to 90° in strike. Exceptionally, in some highly mylonitic gneiss a moderately well-developed lineation may result when these angles are as low as 5°; the initial angular relationships are considerably altered by the bulk strain associated with this deformation. The intersection lineation is probably a direction of minimum stress concentration. In phyllonite, lineations are generally absent and the original gneissic banding is either destroyed, or becomes coincident with the new foliation.

Lineations are generally associated with f_1 and f_3 folds, and less commonly with f_2 and f_4 folds. Crenulation cleavage lineations are associated with some f_4 folds and

Plate 9

(a) Strong quartz rodding lineation in a deformed pegmatite. The lineation results from the intersection of the gneissic and mylonitic foliations. (M49 - lower part of Cadil Sheet).

(b) Boudinage of a thin pegmatite vein in pelitic gneiss. (M418 - lower part of Cadil Sheet).

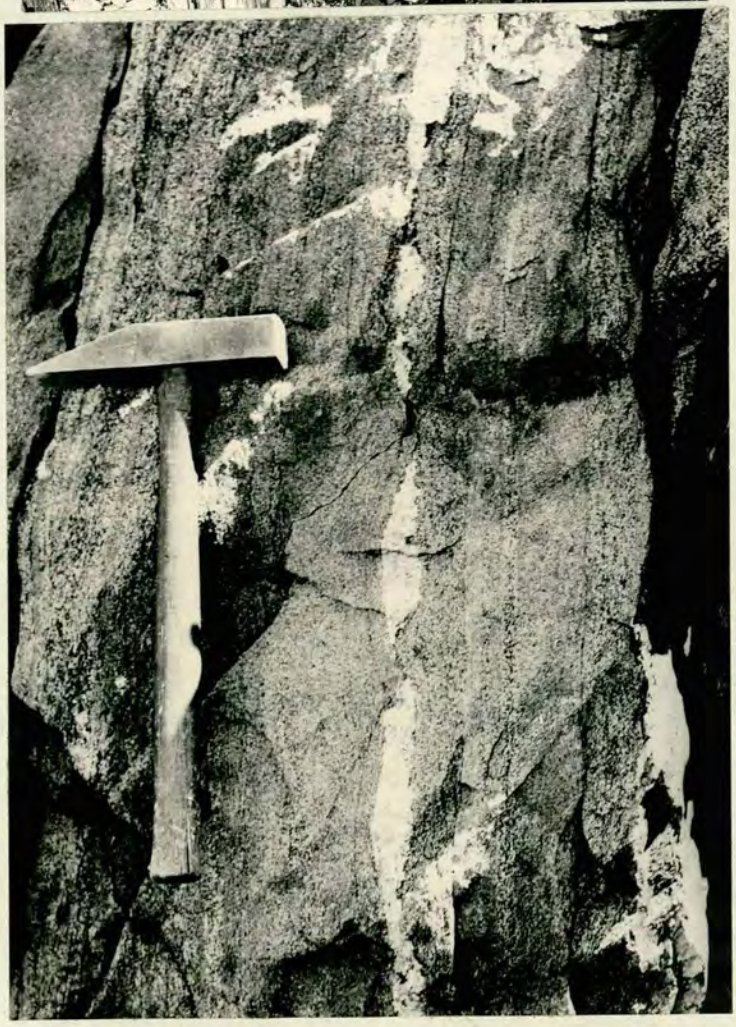

in parts with f_6 kink folds.

In marble, calcite lineations are developed coincident with f_1, f_2 and f_3 fold axis orientations. Where quartz veins or pods are found in marble they show highly developed lineations coincident with f_1 fold axes, if these are present. It appears that the strain in the marble is rapidly taken up by twin gliding and recrystallization but in the quartz slower growth has occurred in the most favourable direction. The resultant lineation is assumed to be the direction of minimum strain in the plane of the quartz vein or pod. This feature is caused by essential continuity across the marble/quartz interface (c.f. cuspate structures, f_2 folds). Similar features were noted by Gansser (1968) in deformed marble from the Tonale Zone in the vicinity of Lake Como.

In amphibolite f_3 hornblende lineations are developed in the direction of minimum strain in the plane of the banding (see Folds in Amphibolite; and Schwerdtner, 1970). This is generally the Y axis of the f_3 strain ellipsoid - the lineation has developed by crystallographic re-orientation of hornblende in the presence of a fluid so that the c crystallographic axis lies parallel to the minimum stress axis. (N.B. in rotational strain the Y axis orientation is constant).

6.60 f_3 STRUCTURAL FEATURES AND STRAIN MARKERS

An attempt has been made to estimate the variable magnitude and type of strain resulting from the f_3 deformation. In the mylonitic gneiss, buckle folded quartz and pegmatite veins have been used to calculate shortening normal to the foliation. Deformed sillimanite porphyroblasts and feldspar pods give a qualitative picture of the shape of the finite strain ellipsoid. Boudinage of quartz, pegmatite and grossularite veins is examined.

6.61 Boudinage

Boudinage is important in the study of the deformed gneiss, since it generally reflects the orientation and nature of the <u>bulk</u> strain that the gneisses have undergone during the f_3 event. Ramberg (1955) has shown that

boudinage is a product of deformation of a pre-existing layer which shows a marked effective viscosity contrast with the surrounding media. Talbot (1970) found that boudinage, even along a single axis, only occurs when the vein undergoes a surface areal increase (i.e.flattening strain). Sylvester and Christie (1968) showed that boudinage in one direction was related to an overall flattening strain.

Boudin style is controlled by 1) the dimensions of the layer and matrix, 2) amount and rate of strain in the boudinaged layer and 3) relative and absolute ductilities of the layer and matrix (Nadai, 1950; Ramberg, 1955; Talbot, 1970). Boudinage will only occur if tensile stress in the layer increases at a greater (or lesser) rate than total stress. Dependent on layer-matrix viscosity contrast, a specific minimum rate of deformation is necessary to initiate necking in a layer of given thickness. Talbot (1970) has shown that boudin shape for a given ductility ratio is related to layer thickness and that sharp necks will develop at short intervals in thick veins, and low angle necks at longer intervals for thinner veins. Such observations are due to the generation of progressively higher tensile stress in the layer as bulk stress increases. When this tensile stress reaches a critical value (dependent on vein thickness) necking commences. Thicker layers remain planar at first and the resulting stress gradient causes sharp necks to develop due to high strain rates. Plate 9(b) illustrates the boudinage of a thin pegmatite vein in semi-pelitic gneiss.

Measurements of boudinaged veins of different composition in the plane normal to the axis of boudinage are plotted against $\log_e$(boudin cross-section area) in Figure 35. These readings were taken from various sheets in the Central Alps. Boudinaged quartz veins have small boudin areas and variable axial ratios. In contrast, pegmatite veins plot in a field with larger boudin areas and moderate axial ratios. From the graph, no simple relationship between style and size, and hence boudin/matrix ductility

Figure 35 - Graph showing the relationship between the aspect ratio of the boudin and the cross-sectional area of the boudin in the plane normal to the axis. The points shown are for several combinations of rock types from the Central Alps. There is a linear relationship between $\log_e$ boudin size and aspect ratio for pegmatite veins in pelitic gneiss and grossular in marble taken from small areas where the strain can be assumed to be approximately homogeneous.

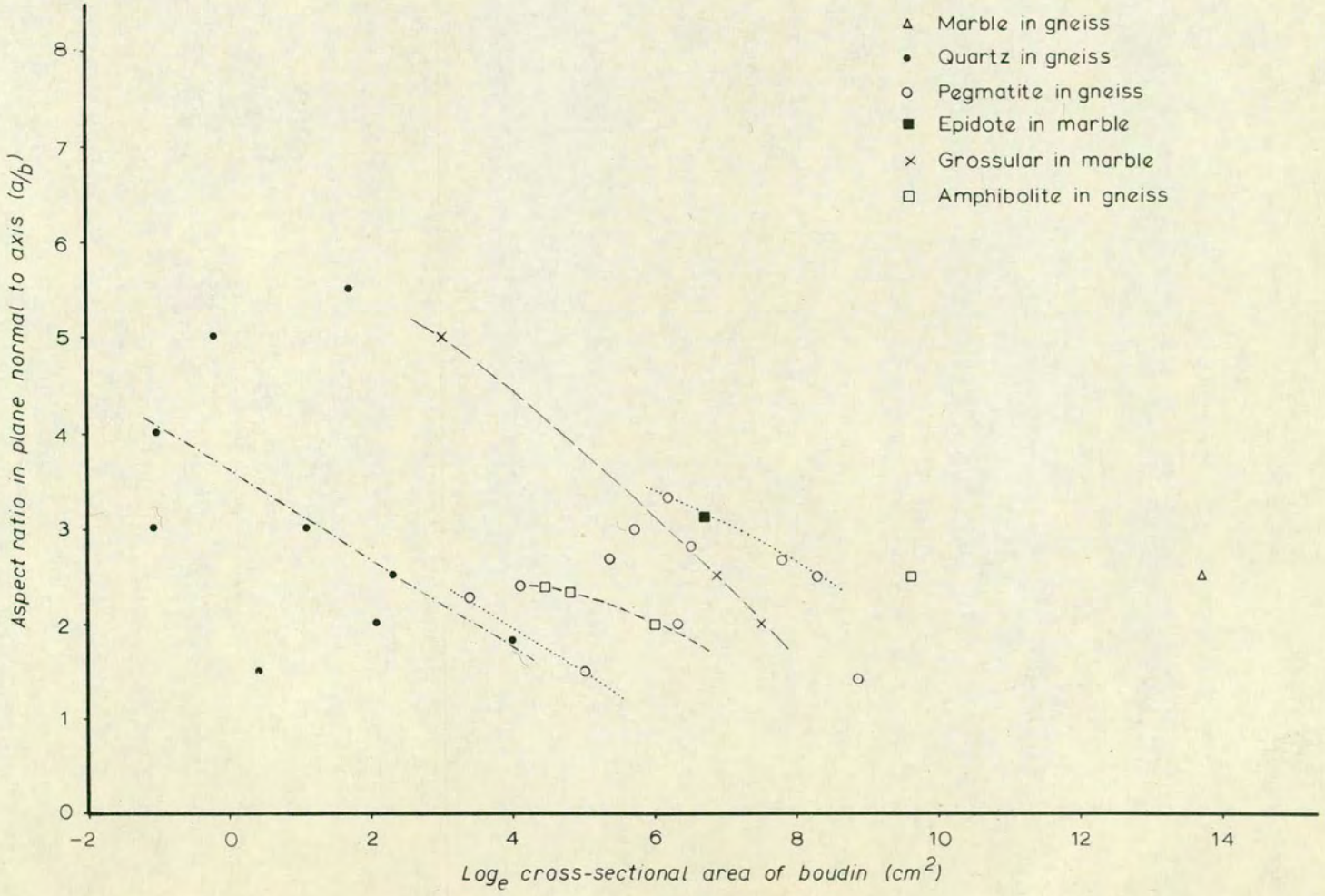
Marble in gneiss
Quartz in gneiss
Pegmatite in gneiss
Epidote in marble
Grossular in marble
Amphibolite in gneiss
Aspect ratio in plane normal to axis (a/b)
Log_e cross-sectional area of boudin (cm^2)
0
1
2
3
4
5
6
7
8
-2
0
2
4
6
8
10
12
14

contrast, can be obtained. For example, marble boudins in gneiss (ductility ratio $\ll 1$) plot in the extreme right of the graph and yet grossularite boudins in marble (ductility ratio $\gg 1$) plot near to them.

Observations in the pelitic gneisses of the Tonale Pass area indicate that pegmatite veins which are thicker than 70 cm. generally show pinch and swell structures. Pegmatite boudins have smaller axial ratios as vein thickness increases. Thus on Figure 35 we can draw a series of lines of negative slope for differing strains, showing an approximately linear relationship between $\log_e$ boudin size (and hence vein thickness) and boudin shape. A steeper line can be drawn for grossular boudins in marble, since all values relate to a small area in which strain was probably relatively homogeneous. Quartz boudin points show a distinct scatter but a general trend can be delineated and a low angle line drawn at a similar gradient to those for pegmatite boudins. It is suggested that these lines reflect layer/matrix ductility ratios with each layer/matrix system having a unique trend under similar metamorphic conditions.

In pelitic gneisses, boudinage and pinch and swell of Hercynian pegmatites, quartz veins, and more rarely amphibolite bands has occurred where the veins lie generally sub-parallel to the gneissic banding. The presence of boudinage axes in two mutually perpendicular directions approximately in the plane of banding in mylonitic gneisses of the Tonale Pass area shows that this is a plane of extension. Figure 36 shows the distribution of boudinage and pinch-and-swell axes, and poles to boudinaged veins or layers in the separate thrust sheets of the Central Alps.

Metallurgical experiments show that steel plates neck both along axes normal to the axis of maximum tension and at about 45° to it, in the plane of maximum shear (Talbot, 1970). If layer thickness is small compared to that of the enclosing medium (< 0.14) necking should develop on these 45° axes (Nadai, 1950 , p.319). Talbot has found that for quartz veins in gneisses, the boudin axes lie

Figure 36 - Stereograms of boudin axis and boudined vein orientations with the orientations of the derived f_3 principal strain axes for differing structural sheets of the Central Alps. It is not possible to assess the degree of strain by the method of Talbot (1970).

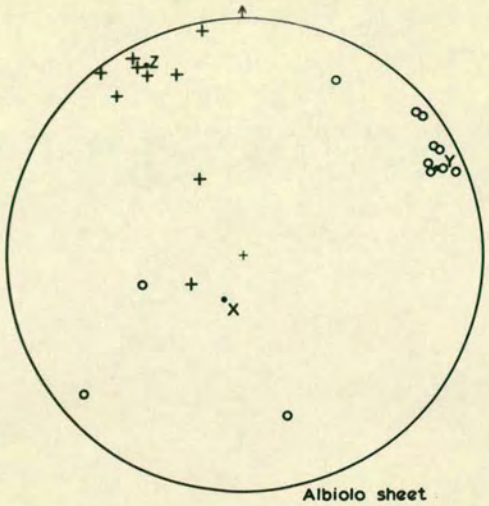

Albiolo sheet

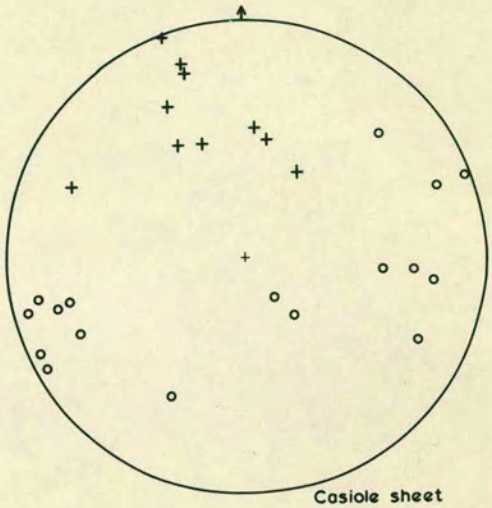

Casiole sheet

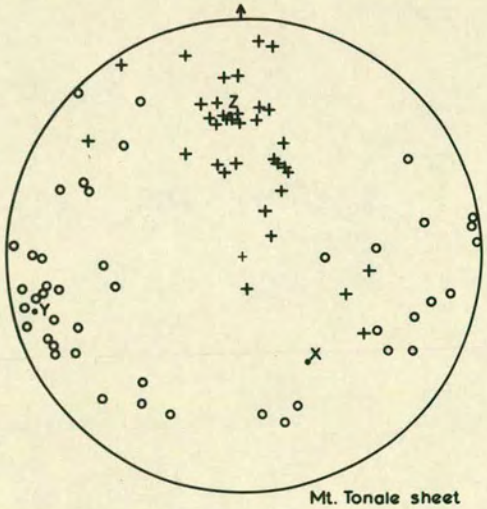

Mt. Tonale sheet

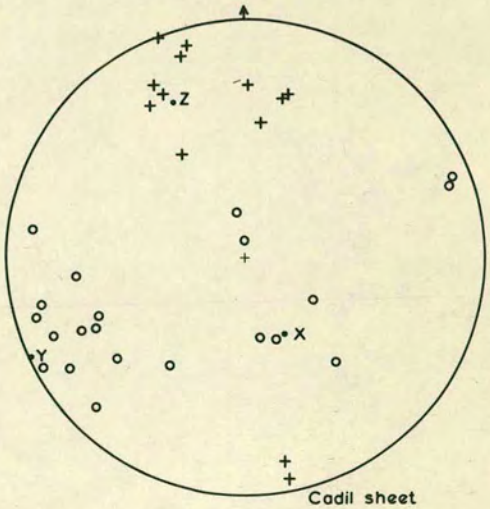

Cadil sheet

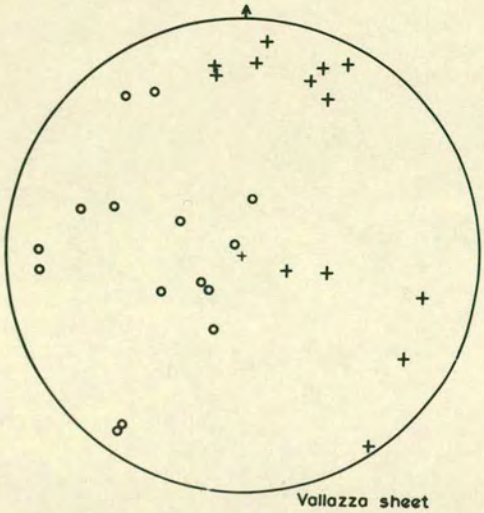

Vallazza sheet

+ Pole to boudined vein
o Boudin axis
• Orientation of strain axis

within 10° of the X or Y axes or midway between these two principal axes. Poles to veins or layers cluster around the Z axis of the finite strain ellipsoid and indicate the size and shape of the extension field. Provided that the strain is homogeneous over the area from which boudinage data are recorded, this extension field will indicate the minimum strain ellipsoid for that area (see Talbot, 1970).

The distributions of boudin axes in the various sheets of the Central Alps are broadly similar. In the Mt.Tonale sheet (Figure 36) a major concentration plunges gently to about 255° and minor concentrations lie at about 45°, about 90° and about 135° to this primary axial direction. Similar results are given by Norris in Cliff et al (1971) for boudinaged quartz and aplite veins in gneisses and amphibolites of the Tauern Window (E.Alps). The spread of boudin axes and poles to boudinaged and pinch-and-swell veins, particularly in the north-south and northwest-southeast planes, is attributed to the effects of f_3, f_4 and f_5 folding. All of these folds have approximately E-W or ENE-WSW axes and hence rotation of pre-existing planes or axes is greatest in a NNW-SSE vertical plane. Because of this later folding, no reliable estimate of a minimum strain ellipsoid can be made. For the Mt.Tonale sheet, 12 of the 35 poles to boudinaged quartz and pegmatite veins cluster around a line plunging 40° to 355°. By analogy with the theory of Talbot (1970), this line represents the Z axis and the clustering of poles reflects a flattening ellipsoid with high X/Z and Y/Z ratios. The measurements are not accurate enough to determine actual values.

In the more southerly sheets of the Central Alps (e.g. Vallazza, Cadil) the boudin axes have a consistently steep plunge, showing there has been little distortion by later folding, and that in parts of the sequence the X-axis of the f_3 strain ellipsoid plunges gently east or west. Thus the X and Y axis orientations may have interchanged in some parts of the Vallazza and Cadil sheets. This is confirmatory evidence that the f_3 strain ellipsoid is generally a strong flattening type ($k < 0.2$) in the Central

Alps. It is significant that boudin axes for the Albiolo sheet lie in a narrow concentration plunging gently to about 064°. The mylonitic and fold structures in this sheet imply that large f_3 strains have occurred. This strong deformation has applied a geometrical restraint to boudin axis orientations and limited them to within about 10° of the Y axis.

For the Mt.Tonale and Albiolo sheets, estimates of the orientation of the X, Y and Z axes of the f_3 finite strain ellipsoid have been made. Boudinaged veins generally lie in the plane of the banding in the various thrust sheets, showing that the orientation of the principal strains is controlled by the pre-existing gneissic anisotropy, and lithological boundaries. The orientation of the boudin axis concentrations in the various thrust sheets is variable. Since this axis is generally parallel to the Y axis of the bulk f_3 strain ellipsoid, there is a variation in Y axis orientation in different sheets. Boudinage is an early formed structure in the f_3 event, since in some areas boudins are folded by f_3 asymmetrical folds. Large translations have taken place across the major mylonite zones which sub-divide the gneisses, marbles etc. of the Central Alps. Relative rotation of the various thrust sheets may have occurred across these mylonite zones if translation has been accompanied by some rotation <u>in</u> the mylonite plane (i.e. movement not in a constant direction). It is suggested that boudinage occurred in the gneisses of the Central Alps while these rocks had an approximately uniform orientation and that later f_3 thrusting, folding, and f_4 and f_5 events have caused the variation seen in the different thrust sheets at present. It is interesting that boudinage is not seen in the mylonites themselves, suggesting that strain is not of the strong flattening type in these zones.

No attempt has been made to estimate strain values for boudinaged vein measurements, since the assumptions involved are thought to be unrealistic. Effective viscosity ratios vary proportional to applied stress, dependent

on material properties, and Biot (1961) has shown that it is invalid to extrapolate a step function method of approximation beyond 25% shortening. Hence no accurate viscous theory is at present applicable to this problem. Norris, in Cliff et al (1971) used Gay's (1968) equation for viscous particles in low concentration in a less viscous medium to relate separation distance between boudins to the amount of strain. Although pegmatite veins are probably more viscous than the surrounding gneiss, quartz veins may, during part of their deformation, be less viscous than the surrounding gneiss. Gay's theory applies to materials with Newtonian viscosity, and experimental work with two-dimensional plasticine models of conglomerate (Mendum, 1972) suggests that such equations cannot be applied to boudinage to give meaningful results.

Boudinage is a feature generally attributed to ductile flattening deformation of a more viscous layer in a less viscous matrix. In the classical examples of boudinage (e.g. Ramsay, 1967, p.105) rectangular shaped boudins are separated by zones of infolded more ductile material. In the Tonale Pass area, the boudinaged veins are generally composed of quartz or pegmatite and lie in a banded pelitic gneiss. More rarely, where grossular boudins lie in marble, the grossular has behaved in a less ductile manner than the marble, and infolded marble lies between the ovoid pods.

During the f_5 event, thin quartz veins were folded in a ductile manner, whereas the enclosing phyllonitic matrix (quartz, K feldspar, plagioclase, biotite, sericite) acted as a brittle material. This deformation occurred under Greenschist facies (biotite grade) conditions, and suggests that in some circumstances quartz behaves as a more ductile material than the surrounding gneiss. The apparently differing ductilities of quartz and pelitic gneiss probably reflects their stress-strain behaviour, with yield points of the two materials differing markedly in time. White (1974 - Chemical Changes Conference, Liverpool) has shown that quartz readily undergoes recovery (or recrystallization) to prevent high dislocation densities developing in

the lattice. The phenomenon of "water weakening" of quartz is well documented by experimental data (Griggs and Blacic, 1965; Tullis et al, 1973). Feldspars and other more complex silicates (e.g. hornblende) develop high dislocation densities on deformation, which inhibits recovery and recrystallization but favours diffusion and metasomatic reactions. Hence it appears that quartz acts as a relatively ductile material under favourable conditions (moderate pore fluid pressure, $T \geqslant 400^{\circ}C$, moderate confining pressure).

Boudinage may be considered as a way in which shape change during deformation minimises the energy of the system. If we take the vein and medium as viscous materials, then, subject to the controlling boundary conditions, a planar vein tends towards a series of discoidal shapes since these are the minimum energy shapes during flattening deformation. The fact that boudins become separated could then be a product of high flattening strain which extended the less viscous quartz or pegmatite boudins. This would explain the lack of low strain areas in many quartz boudin/pelitic gneiss exposures as shown in Plate 9(b).

6.62 Buckle folded quartz and pegmatite veins

In contrast to the abundance of boudinage, buckle folded quartz and pegmatite veins are not common. These veins lay initially at moderate to high angles to the gneissic foliation and hence became buckled by f_3 deformation as shown in Plate 10(a). The axes of such buckle folds show variable plunges in a WSW-ENE direction and their axial planes are coincident with the mylonitic foliation. Close to tight folds affect veins 1 mm. to 5 cm. wide, but in thicker veins (5 to 20 cm. wide) the folds are generally more open in style. In strongly foliated mylonitic gneiss at M51, adjacent to the major Cadil/Mt.Tonale mylonite, a 3 to 7 cm. wide quartz-K feldspar vein cross-cuts the banding and is tightly folded by the f_3 deformation. Plate 10(b) shows that hinge thickening and limb attenuation have occurred resulting in cuspate hinge folds and boudinaged limbs. The features show that

Plate 10

(a) Buckle folded pegmatite vein in sillimanite - rich pelitic gneiss. The gneiss shows a weakly developed mylonitic foliation with a differing orientation to that of the composition banding. (Banding 040/86°S ; Mylonitic foliation 047/80°S). M332 - Lower part of Casiole Sheet.

(b) Folded quartz - K feldspar vein in strongly mylonitic gneiss. Note the boudinage on the limb to the right and cuspate nature of the fold hinges. Layering shortening is dominant over buckling in this instance. (M51 - Lower part of Cadil Sheet).

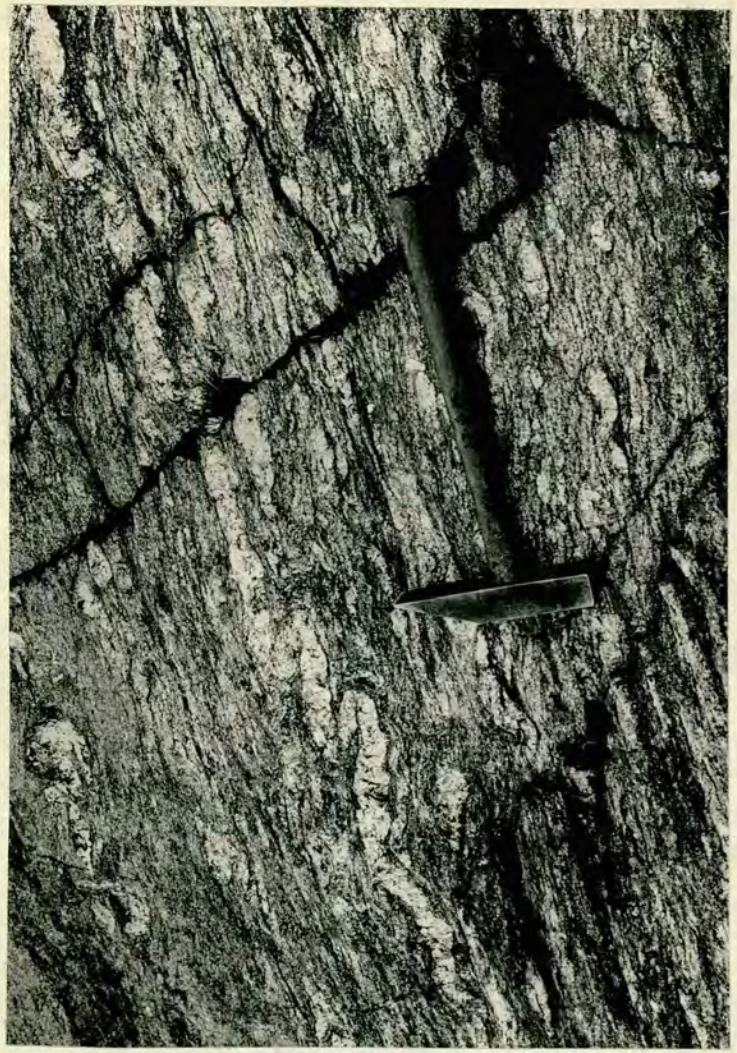

extension has occurred in the X direction and strong compression in the Z direction (c.f.conclusions drawn from boudinage - probably moderate to strong flattening strain). In thick veins, fold initiation does not occur according to thin plate theory, but layering shortening occurs. It is not known at what thickness layering shortening becomes dominant over buckling.

Buckle folding can only occur when less ductile veins of limited thickness lie in a more ductile matrix. Initial perturbations in the vein will control the position of the resultant buckle folds on deformation (Cobbold et al,1972; Hudleston and Stephansson, 1973). If the vein is more ductile than the matrix, for example lamprophyre dykes in gneiss, compression along the layering results in a series of strongly cuspate folds (C.J.Talbot, pers.comm.1974). The majority of veins in the Tonale Pass area rarely show hinge thickening and where this occurs it appears to result from homogeneous flattening of an initial buckle fold. Fold hinges are rounded, profiles broadly consistent at both sides of the vein (i.e. "parallel" folds close to Class 1A), and the fold trains show reasonably consistent amplitudes and wavelengths. These features are all consistent with buckling of a planar layer by tangential longitudinal strain in accordance with thin plate theory. There is no field evidence to suggest that marginal or boundary slip has occurred, and I consider that this factor is not significant. Hence an estimate of shortening normal to the f_3 foliation can be made by measurements along the fold profiles perpendicular to their axes. Hudleston (1973) and Hudleston and Stephansson (1973) have shown that a "parallel" folded layer shows a greater ductility contrast with its enclosing medium than a "similar" folded vein. This conclusion suggests that quartz and pegmatite veins initially act as highly competent layers, and that Biot's theory is valid in this area.

Biot (1961) developed a theory of fold initiation and amplification for a single layer. He showed that for a more viscous vein in a less viscous medium, buckles will

be formed with wavelength, $\lambda = 2\pi t \sqrt[3]{\frac{\eta}{6\eta_1}}$ where t is the vein thickness, η is the effective viscosity of the vein and η_1 is the effective viscosity of the medium. This simple relationship contains numerous limitations which were stated by Biot. The expression has a lower limit of accuracy of $\lambda = 15t$. Gravity is neglected if the veins are thin. The model is made by step approximations to 25% shortening, at which value differential stress is small and a maximum rate of fold amplification has occurred. At higher stresses the differential stress necessary to cause folding increases as the fold further amplifies. If we deform a viscous material by a compressive strain rate, $-\dot{e}$, then $-\dot{e} = f(\sigma)$ where f is a function and σ is stress. Biot shows that $\frac{1}{4\eta} = -\frac{d\dot{e}}{d\sigma} = \frac{df(\sigma_o)}{d\sigma}$ for a stress σ_o and small increments $d\sigma$, $-d\dot{e}$. If the material is non-Newtonian (i.e. σ not directly proportion to $\dot{e}$) then the time for 25% shortening is greater than for Newtonian material by a factor $\frac{df}{d\sigma} \cdot \frac{\sigma}{f}$. De Caprariis (1974) has shown that deviation from Newtonian behaviour by>2% causes the wavelength selection process to break down. For large λ/t ratios (>30) Biot's equation was shown to be a reasonable approximation provided that the viscosity ratio was initially greater than 100. The result of these considerations is that effective viscosity coefficients in the vein and medium decrease as stress increases when shortening proceeds above 25%. The main use of Biot's equation is for calculation of effective viscosity ratios at the time of fold initiation, for known vein thicknesses and fold wavelengths.

The attempt of Sherwin and Chapple (1968) to modify the theory of Biot (1961) to higher strain fails to take into account the variation in absolute or relative effective viscosity and appears to give reasonable η/η_1 values only for folded quartz veins in slates. An estimate of the size of an initial perturbation is necessary for Sherwin and Chapple's theory, and the value for amplification relies entirely upon this estimate. Hudleston and Stephansson (1973) have shown that for small viscosity

ratios between layer and matrix (e.g.10) the resultant folds show strong hinge thickening dependent on the orientation of parts of the folded layer. (N.B. fold profiles may result from quartz migration down the mean stress gradient). The final wavelength is dependent on initial irregularities rather than on dominant wavelength. These deductions all apply to similar type folds however, whereas almost all folds in the Tonale Pass area show no measureable hinge thickening.

Application of Biot's equation to the buckled veins in the Tonale Pass area gives vein/gneiss effective viscosity ratios (η/η_1) of between 30 and 200, and in two rare cases 370 and 63,500. If extension has occurred along the fold axis, as would be the case in flattening strain, then these ratios would be considerably reduced. Taking such ratios as an approximation, the amount of layer parallel shortening prior to buckling is insignificant. Although the calculated effective viscosity ratios may be meaningless in terms of true viscosity values or even ratios (e.g. viscosity ratio <1 if quartz vein is more ductile than gneiss), the conclusion that there is insignificant layer parallel shortening is taken to be valid. Figure 37 shows the values of % shortening calculated for various pegmatite and quartz veins in pelitic gneiss. The paucity of buckle folded quartz or pegmatite veins on suitably orientated surfaces results in only a small number of measurements. Since the buckle folds show consistent wavelengths along the fold train, it is a reasonable assumption to consider the pelitic gneiss as a homogeneous viscous medium (see Cobbold et al, 1972). The % shortening values can be directly related to the degree of development of mylonitic foliation.

Several features of the data shown in Figure 37 require explanation. For those veins in the Vallazza sheet, where the gneiss is biotitic and contains no sillimanite and less feldspar than the more usual pelitic gneiss, the values of % shortening are higher for a similar state of foliation development than those in the

Figure 37 - Table showing values of percentage shortening derived from quartz and pegmatite veins in high grade pelitic gneiss. The values of percentage shortening are broadly related to the degree of mylonitic foliation development. The general lack of hinge thickening in the folded veins suggests that homogeneous shortening prior to buckling was negligible.

Locality number and tectonic unit	Vein and host rock	Average vein thickness (variation in brackets)	Measured vein length	Length of fold train	Average wavelength	Effective viscosity ratio (Biot, 1961) η vein/η host	Percentage shortening	Degree of mylonitic foliation developed	Other comments
M419 Vallazza Sheet	Medium-grained quartz-feldspar-muscovite pegmatite vein in fine-grained quartz-feldspar-biotite-garnet gneiss.	2.274 cm. (1.4 to 3.1 cm.)	154.5 cm.	58.5 cm.	30.9 cm. (26.74 cm. allowing for late homogeneous strain)	39.3 (using wavelength values allowing for homogeneous shortening)	81.4% (including homogeneous shortening and assuming plane strain)	Moderately strong	Homogeneous strain caused hinge thickening and limb thinning subsequent to buckle fold formation. Viscosity ratio and % shortening assume plane strain (no extension along fold axes). See appendix
M421 Vallazza Sheet	Medium-grained quartz-feldspar-muscovite pegmatite vein in poorly banded medium-grained quartz-feldspar-biotite gneiss.	2 cm. (1 to 8 cm.)	138 cm.	9.6 cm.	17.92 cm. 276 cm.	17.4 63,544	93.04% -	Moderately strong	Two sizes of fold are present, i.e. 
M414 Mt.Tonale / Casiole Mylonite	Thin quartz vein in a striped mylonitic gneiss (quartz-feldspar-biotite-sillimanite-muscovite gneiss.)	4 mm. (1 to 8 mm.)	43 cm.	7.3 cm.	5.93 cm.	78.75	83%	Striped very strongly mylonitic gneiss	
M332 Casiole Sheet	Medium-grained quartz-feldspar-muscovite pegmatite vein in a medium-grained quartz-feldspar-biotite-sillimanite-muscovite gneiss.	2 cm. (1 to 3 cm.)	209 cm.	129.5 cm.	29.86 cm.	33.9	38.04%	Weak	Stress refraction in layer assumed.
M130 Casiole Sheet	Fine-grained quartz-feldspar-muscovite vein in strongly foliated quartz-feldspar-biotite-sillimanite-muscovite gneiss.	2 mm. (1 to 3 mm.)	33.8 cm.	21.2 cm.	3.65 cm.	147.5	70.2% (allowing for orientation factor)	Strong	Values of 37.3% shortening are obtained from the measurements unless we take into account the angular orientation of the vein relative to X.
M357 Southern part of Albiolo Sheet	Medium-grained quartz-feldspar-muscovite pegmatite vein in well-banded quartz-feldspar-biotite-muscovite gneiss. Minor sillimanite.	0.5 cm. (0.2 to 1 cm.)	126 cm.	57.4 cm.	10 cm.	193.4	54.4% (assuming stress refraction)	Moderate	1 m. to the north a 25 cm. thick pegmatite shows only very open folds. Only slight stress refraction is necessary here.
M369 Northern part of Albiolo Sheet	Medium-grained quartz-feldspar vein in quartz-feldspar-biotite-muscovite gneiss.	4 cm. (3 to 5 cm.)	118 cm.	55 cm.	236 cm.	4,965	53.4%	Moderate	

Mt. Tonale, Casiole and Albiolo sheets. The pelitic gneiss in these latter sheets contains abundant sillimanite, muscovite and feldspar with some garnet in parts.

The foliation development in pre-formed gneiss is strongly dependent on both strain and mineralogy. It is interesting that shortening values are of the same order as those obtained by Cloos (1949, 1971) for cleavage development in oolitic limestones, and by Maxwell (1962) for slaty cleavage. The results suggest that foliation development commences in quartz-feldspar-biotite-sillimanite-garnet-muscovite gneiss at about 35% shortening. Etheridge (1973) has shown by the experimental deformation of phlogopite ($P = 3kb$, $T = 500^{o}C$, $\dot{e} = 2 \times 10^{-4}$) that shearing will only occur after 30% to 35% shortening; at this value preferred orientation and mica yield are exhausted. This conclusion contradicts the statement of Sherwin and Chapple (1968) that slaty cleavage develops only after about 75% shortening.

The presence of two fold generations at M421 gives two widely differing values of effective viscosity ratio. Biot (1961) shows that large amplitude folds will develop rapidly, and on their limbs smaller amplitude and wavelength folds will develop on further deformation (c.f. generally accepted theory for minor folds which postulates the reverse order of development - Ramsay, 1967). This illustrates the change of effective viscosity ratio with increasing strain, if we accept that thin plate buckling theory is applicable.

In M419, hinge thickening has occurred and hinge and limb thicknesses were measured to give a value for homogeneous shortening after the method of Norris in Cliff et al (1971). Differing values of homogeneous strain are obtained, assuming 1) plane strain ($k = 1$), 2) flattening strain ($k = 0.1$), 3) pure flattening strain ($k = 0$). The values are combined with the shortening value obtained from the buckle fold measurement, and given in Figure 37. If we assume that a homogeneously flattened buckle fold may be divided into two separate events, a primary buckling

and then a subsequent flattening, then for M419 buckling ceases to be dominant after 56% shortening. Hence the presence of isoclinal folds in any gneissic sequence implies that there have been large amounts of homogeneous flattening, subsequent to buckling. Measurements on an isoclinally folded quartz vein in the Casiole/Albiolo mylonite (T368) give homogeneous shortening values of 75%. The resulting fold shape which may then be reconstructed is unrealistic. This suggests that there is a period of synchronous buckling and flattening between the two extreme processes of buckling at low shortening values and homogeneous flattening at high shortening values. Thus the shortening values given in M419 may be too large since a simple two stage process is not a realistic interpretation for the mode of formation of flattened buckle folds.

Many of the veins measured lie initially at an angle to the Z direction of the f_3 strain ellipsoid. If the shortening along the vein is calculated, we can recalculate the maximum shortening in the Z direction based on the angular difference between the vein and mylonitic foliation trace. Reasonable values are obtained for M130, where the quartz vein is only 2 mm. thick and has acted as a "passive" marker in accordance with the above theory. In contrast, for M332 where the vein is 2 cm. thick, somewhat improbable high shortening strain values result. Treagus (1973) has shown that for single layer buckling where the layer is not parallel to the principal stress, stress refraction is a necessary condition. Hence a layer at up to 45° in plane strain, will have the principal stress acting at only a few degrees to the layer-medium interface provided that the effective viscosity ratios for the layer/medium system are high enough for buckle folding (i.e. η/η_1 about 30). The consequences of this system are that greater stress is required to initiate buckling, but the dominant wavelength formed is independent of the angle between the layer and the principal stress. Although Newtonian viscosity was used by Treagus (1973), this approximation should not invalidate the general qualitative conclusions. In the

case of strong finite flattening strain, such refraction may occur up to 70° or 80° from the Z direction, since the field of compression is very large if the infinitesimal strain ellipsoid reflects the finite strain ellipsoid during deformation (i.e. linear strain path). This hypothesis depends on the assumption that the strain is strong or pure flattening. The values measured on these angular veins may be minima as the buckling may not reflect the total shortening strain which has occurred normal to the foliation.

6.63 Deformed sillimanite porphyroblasts and pegmatite feldspars

Sillimanite porphyroblasts are common in the mylonitic gneiss and the porphyroblasts are deformed by the f_3 event. At M150, deformed sillimanite porphyroblasts are well-exposed 3 metres apart in weakly and strongly foliated mylonitic gneiss. Measurements of the three dimensional shapes of 4 porphyroblasts at each exposure gave the very consistent values given in Appendix 4(a). The strain ellipsoid calculated for these measurements is X : Y : Z = 4.45:3.75:1 (k = 0.068). These results imply that the strain is near to pure flattening. The amounts of shape change given by the figures are meaningless regarding the absolute value of the finite or even partial finite strain ellipsoid, because even the less deformed porphyroblasts show considerable strain. Although few measurements were taken, the consistent shape difference shown does reflect the type of strain. The mechanism of deformation, effect of sillimanite structure (i.e. lattice ordering) and influence of initial shape are all factors which must be more fully understood in order to determine true strain values for such porphyroblasts.

Large pegmatite veins and pods, ranging from 2 m. to 50 m. in width, commonly contain a superimposed mylonitic foliation. In some pegmatites, potash feldspar pods are deformed to ovoid shapes and, assuming an average initial equidimensional shape, we can calculate the shape of the

finite strain ellipsoid. 6 measurements in each of two planes orthogonally related to the foliation and lineation in the mylonitic pegmatite at M368 (Appendix 4 (b)) gave X : Y : Z values of 1.84 : 1.64 : 1 (k = 0.187). The X direction is parallel to the lineation in the pegmatite and pitches 8° to 090°. Hence in this area the orientations of the X and Y directions of the f_3 finite strain ellipsoid are interchanged compared to those further south.

6.64 Discussion

The measurements of strain and structural features in the mylonitic gneiss imply that flattening (k = 0 to 0.2) is the dominant bulk strain in the rock. The intensity of this strain increases as we approach the mylonite zones. Phyllonitic lamellae in the mylonitic gneiss occur close to mylonite zones, and are interpreted as planes of high resolved shear stress along which shear strain (γ) is greater than 1.9. There is a marked contrast in the type of strain in the mylonite and mylonitic gneiss. Several features strongly suggest that moderate water pressures (P H_2O) existed in mylonite zones. Hence a gradient of P H_2O would be expected away from the mylonite, decreasing into the surrounding gneiss. The intensity of mylonitic foliation seen in the gneiss is attributed to the effects of high confining pressure on gneiss with a moderate to low P H_2O. This explains the observed distribution of mylonite, and mylonitic gneiss. Most minerals require the presence of some form of fluid (e.g. P H_2O, P CO_2) before deformation and/or recrystallization can occur (Griggs and Blacic, 1965, Griggs, 1967).

6.70 QUARTZ PREFERRED ORIENTATION

The quartz c-axis diagrams for 7 specimens shown in Figure 38 are constructed from 1400 measurements using standard universal stage methods. Assuming orthorhombic symmetry, three planes are defined and their intersections termed X, Y and Z (N.B. not strictly equivalent to the X, Y and Z of the finite strain ellipsoid). The c-axis diagrams basically reflect the latest penetrative

Figure 38 - Stereograms showing 200 quartz c-axis orientations for each of 7 specimens taken from various parts of the Tonale Pass area. The orientation of the principal strain axes, foliation and lineation are given for each specimen. All data relates to the present orientation of the rocks in situ.

T325B - Pelitic gneiss, Vallazza Sheet, Central Alps.

T344A - Lineated phengite gneiss, Stavel Gneiss.

T246A - Late Quartz pod in mylonitic gneiss, Tonale/Casiole mylonite.

T211C - Quartz pod in pelitic schist, Southern Alps.

T362 - Phyllonite, Mt.Tonale/Casiole mylonite.

T8B - Feldspar - phengite gneiss, Stavel Gneiss.

T239A - Lineated pelitic gneiss, Mt.Tonale Sheet, Central Alps.

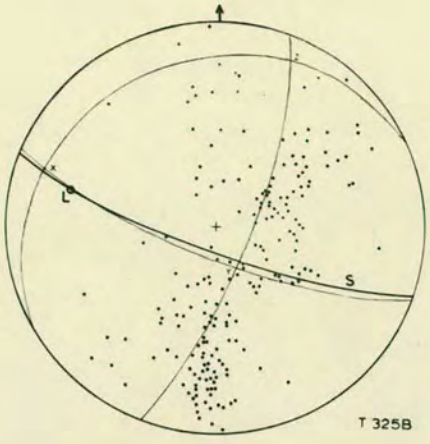

T 325B

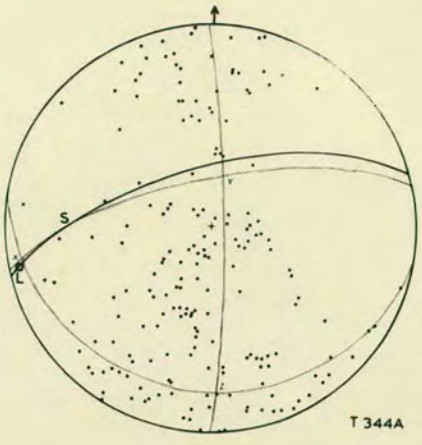

T 344A

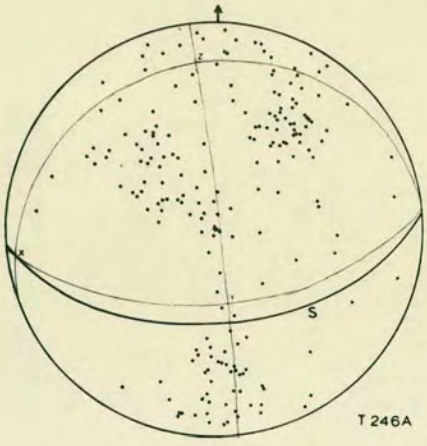

T 246A

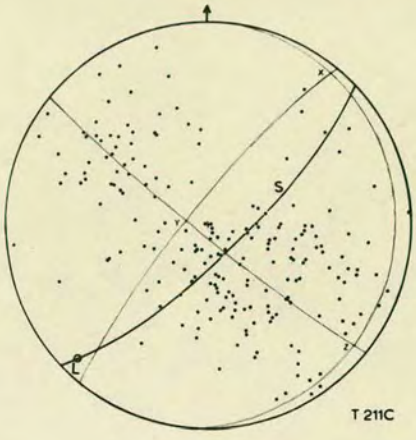

T 211C

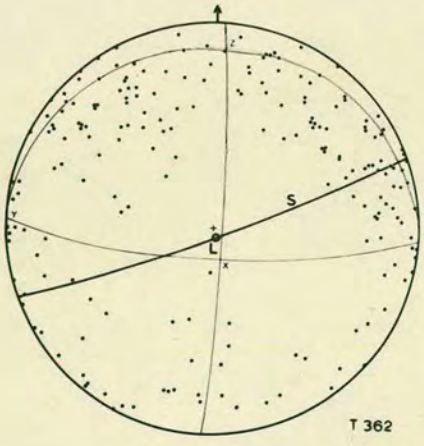

T 362

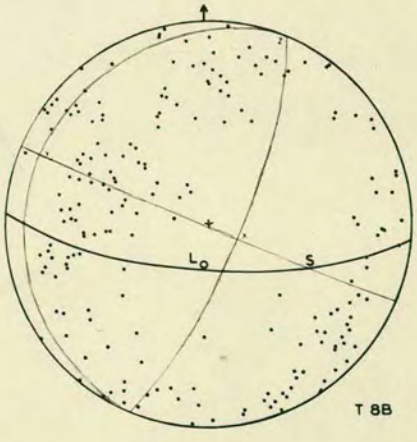

T 8B

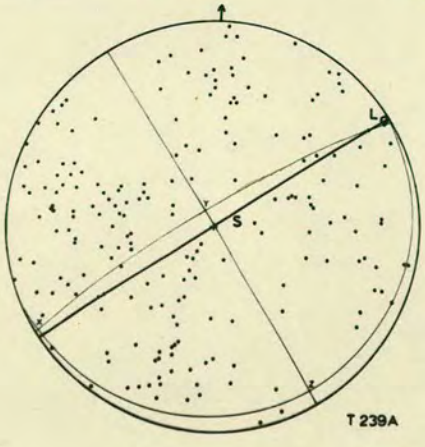

T 239A

deformation phase in which quartz recrystallization occurred. Subsequent or prior events may modify this basic pattern.

6.71 Quartz c-axis patterns and their interpretation

Diagrams T325B, T344A and T211C all consist of a pseudo-two girdle pattern in which the girdle intersection lies close to the vertical. The two girdles lie at a maximum angle of 60° apart. Diagrams T362B and T8B show peripheral pseudo-two girdle patterns. In T362, the two girdles coalesce to form one diffuse girdle. In T239A the pseudo-two girdle pattern is weakly defined and the inter-girdle angle increases to approximately 90°.

Although other interpretations may be made of the above patterns, they are probably best considered in the light of the work of Hara et al (1972) and Hara and Paulitsch (1971). These authors showed that a stable fabric pattern developed by both progressive pure and simple shear (above $\gamma = 1.8$). This pattern consists of two crossed girdles (in some cases best described as small circles, in others as great circles) cutting the XZ plane at up to 35° from Z, and whose intersections lie in the YZ plane at about 35° from Y. In simple shear two maxima may develop at the girdle intersections.

Although many writers have reported the presence of crossed girdles (e.g. Sander, 1970; Sylvester and Christie, 1968; Turner and Weiss, 1963, p.428), in most cases the girdles cannot be accurately matched either to small or great circles. Hara et al (1972) showed conclusively that rotational strain gives rise to an approximately orthorhombic fabric which merely reflects the nature of the stress system. Christie (1963) showed that quartz mylonite from the Stack of Glencoul gave a perfectly orthorhombic pattern with two well-defined maxima. More recent work by Riekels (1973) on the same specimen showed that the refracting planes $10\bar{1}1$, $11\bar{2}0$, $20\bar{2}0$ and $11\bar{2}3$ have a strong monoclinic symmetry plane containing the lineation and perpendicular to the foliation (i.e. XZ plane of simple shear). The c-axis maxima suggest that high γ values are present, in

complete accord with the conclusions of Hara et al (1972).

The experimental data of Green et al (1970) and Tullis et al (1973) show that for low strain rates (10^{-6} to 10^{-8}/ sec.) small circle girdle fabrics lying at about 45° to σ_1 result from syntectonic recrystallization at high temperatures. These fabrics can be correlated with some natural examples (e.g. see Sander, 1970). Crossed girdle fabric patterns were experimentally produced by Green et al (1970) in two non-axially deformed quartzites. The girdles intersect at the σ_2 axis and are bisected by the σ_1 and σ_3 axes. Hobbs (1968), in experimental studies of single quartz crystals, has shown that recrystallized quartz grains develop with c-axes in a plane containing σ_1. Annealing produces only slight changes in the preferred orientation in the α quartz field. Tullis et al (1973) found that differential stresses of about 1 kb are sufficient to deform quartzite when recovery processes keep pace with deformation (800°C at 10^{-7}/sec). These conditions may be extrapolated to 400°C at 10^{-11}/sec. Quartz grains with c-axes orientated parallel or perpendicular to σ_1 tend to remain undeformed whereas recrystallization and sub-grain development is abundant in grains with intermediate orientations.

Wilson (1973) and Suzuki (1970) have shown that preferred orientation patterns may vary with metamorphic grade. The patterns in the Tonale Pass area were generally formed in the Early Alpine, Upper Greenschist - Lower Amphibolite facies event.

The fabric of T362A, a phyllonite from the Mt.Tonale/ Casiole mylonite, is used to determine the orientation of X, Y and Z. The results agree with other structural and strain data from the mylonite zone. The lack of well-defined maxima is attributed to the effects of sericite, clinozoisite, magnetite and feldspar grains, all of which inhibit grain growth and influence the local stress system. (see Hobbs, 1966). The response of grains to free energy differences caused by differential stress is modified by quartz-impurity interfacial effects, with a reduction in

the ease of grain boundary migration. The diffuse girdle pattern occurs on all scales, in contrast to the results of Eisbacher (1970) who reported local fabric homogeneity in thin sections of mylonitic granite. Wilson (1973) illustrates similar effects in quartzites from the Mt.Isa area, Australia.

The quartz preferred orientation pattern for T246A, a quartz pod which cross-cuts the mylonite foliation, probably reflects the f_4 event and is markedly different from the adjacent T362A. There is basically an interchange of X and Y axes. It must be remembered that these axes do not reflect finite or even partial strain orientations but merely partially reflect the f_3 and f_4 stress fields.

Specimens T8B and T344A are both taken from the Stavel Gneiss unit. T344A shows a median pseudo-two girdle pattern which correlates with feldspar dislocation features in thin section and the dominant sub-horizontal linear fabric in the gneiss (all features imply that the maximum extension direction plunges gently west southwest). The contrasting peripheral pseudo-two girdle pattern in T8B implies a steeply dipping X axis which can be correlated with the strain axes derived from spindle shaped feldspars measured at this locality. The positions of the Y and Z axes are poorly defined but both c-axis patterns show that approximately N - S compression occurred during the late f_3 event. Some spread in the diagrams is interpreted as due to the effects of later f_5 deformation and m_4 metamorphism.

T239A shows a weak near symmetrical crossed girdle pattern and is assumed to reflect the abundant elongate mica and clinozoisite crystals which inhibit grain boundary migration and preferred orientation development. The pattern is related to the f_3 event.

Pattern T325B was obtained from a non-mylonitic gneiss and shows clearly the typical crossed girdle pattern associated with many metamorphic tectonites. Only recrystallized grains (formed in f_3 and f_4 events) were measured, although the large remnant grains show similar c- axis orientations.

The pattern probably reflects the co-axial nature of the f_1 and f_3 deformations. Hobbs (1968) and Hu (1969) found that sub-grain growth and ultimately recrystallization is partly host controlled. New grains with c-axes at 20° to 40° to that of the host grain grow preferentially.

A similar process of host control is seen in T211C, a section from a quartz pod in pelitic schist of the Southern Alps. Ribbon-like quartz grains with average axial ratios of 6:2:1 have highly dentate boundaries and have formed from larger strained grains. The remnant grains commonly contain deformation lamellae whose trace is approximately perpendicular to the grain elongation and strain shadows. The new quartz growth (by recovery and minor recrystallization) is a product of contact metamorphism related to the nearby Adamello massif. The subsequent f_5 deformation has resulted in the formation of deformation lamellae, strain shadows, and a minor strain slip cleavage (f_6). The preferred orientation primarily results from the f_3 event but some modification has occurred, associated with the subsequent grain growth and lattice strain.

The correlation of X and the lineation in many of the patterns suggests that mineral growth occurs along the minimum stress axis in the foliation plane (generally very close to σ_3) assuming co-axial strain increments. This lineation and preferred orientation pattern do not necessarily reflect finite strain axis orientations. Magnetic anisotropy values and orientations, and their relationship to finite strain illustrate the fallacy of always assuming coincidence of lineation and finite extension direction (X). In many of the diagrams shown, there is however a convincing correlation between the inferred X direction and the lineation, where both the quartz preferred orientation and the lineation can be assigned to a particular deformation event. The gneissic foliation and cleavage also shows a close correspondence with the inferred XY plane.

It is interesting to consider the shape of girdle patterns in the light of the concept of strain fields.

Assuming that the line of no finite elongation is important in determining c-axis orientation patterns, then migration of these axes until they lie perpendicular to this zone would result in the observed patterns. The pseudo girdle patterns shown here and those presented in the literature can be readily explained by this means. The girdle position would be controlled by the intensity of the differential stress, particularly in the later part of the deformation and metamorphic event. It would <u>not</u> directly reflect the amount of finite strain. Hence mylonites may be expected to give a single diffuse girdle and a banded gneiss to give a distinct crossed girdle. The maximum angle between the girdles may also reflect temperature and strain rate differences since Tullis et al (1973) showed that these parameters have an important effect on experimentally produced girdle orientations. Variations in geological strain rates and temperatures are however, not thought to be large enough to significantly affect the quartz preferred orientation patterns in the diagrams shown.

6.72 Mechanism of quartz preferred orientation

Only a brief sketch of the probable mechanisms is given in this section; for a full summary see Wilson (1973) and Spry (1969).

Kamb (1959) found that quartz c-axes are thermodynamically stable when they lie in a small circle girdle under some stress conditions. Flinn (1965) states that the direction of maximum compliance in α quartz lies at 45° to σ_1. Macdonald (1960) showed that chemical potential differences used by Kamb are four orders of magnitude less than the activation energies of most geological processes. Hobbs (1968) pointed out that this approach also neglects grain boundary effects such as structural and interfacial energy.

Hobbs concluded from experimental observations of recrystallization in single crystals that the stored energy of deformation (elastic lattice strain) was the basic cause of recrystallization. Sub-grain growth and progressive misorientation result in new grain formation.

The effects of twin gliding in quartz are difficult to assess. Small circle girdles may be readily explained by the work of Thomas and Wooster (1951) who showed that dauphiné twinning maximises elastic strain energy, and results in a change of crystallographic orientation. Tullis (1968) has shown that such twinning does occur in experimentally deformed quartzite. Dauphiné twinning tends to occur on relief of stress (C.J.L.Wilson pers.comm.1973), and it cannot be inferred to explain the orientation of recrystallized grains (see also Tullis et al, 1973; Riekels 1973). It is possible, using the various quartz slip systems, to predict almost any preferred orientation pattern but the validity of this process is doubtful.

The present work in the Tonale Pass area strongly suggests that recrystallization is a strain assisted nucleation process at or near grain boundaries, where dislocation densities are probably high. Further strain causes more widespread sub-grain development and progressive misorientation results in a recrystallized quartz aggregate. Cross-slip and grain boundary migration are important although impurities (mica, chlorite, clinozoisite, magnetite generally) inhibit this process and partially control grain shape and orientation. The quartz preferred orientation patterns presented here are primarily due to these mechanisms of recrystallization which in turn are controlled by the orientation of the applied stress system. Stable patterns of preferred orientation will only occur when grain growth and mutual boundary adjustments have reached an equilibrium state (Wilson, 1973; Vernon, 1970). Where differential stresses are important, this pattern is probably a two point maxima as shown by Christie (1963) and Hara et al (1972). At temperatures and pressures above the Lower Amphibolite facies, rock viscosity is probably lowered and differential stresses may be assumed to be very small. In such a situation grain coarsening occurs and a more random c-axis pattern develops as "superindividuals" (Sander, 1970) become dominant (see Wilson, 1973).

6.80 MAGNETIC ANISTROPY OF MYLONITE AND MYLONITIC GNEISS

Cylinders with approximate lengths and diameters of 2.5 cm. were cored from four orientated specimens of mylonite, mylonitic gneiss and relatively undeformed pelitic gneiss. These cores were then placed in a computer-linked slow spinner magnetometer modified by L.Molyneux, and the principal axes of the magnetic susceptibility ellipsoid determined to a high degree of accuracy and repeatability. Dr.R. Thompson carried out these measurements at the Physics Department of the University of Newcastle-upon Tyne. The susceptibility differences are measured in three mutually perpendicular directions and the resulting measurements evaluated to give the principal axes.

The specimens used were :-

M156 (2) Banded quartz-feldspar-biotite-muscovite-sillimanite gneiss with minor very weak mylonitic foliation.

M427 C Two cores (1 and 2). Quartz-feldspar-biotite-sericite gneiss with a moderately well-developed mylonitic foliation. The gneissic banding has not been completely obliterated although abundant quartz recrystallization, fracturing of feldspar and growth of clinozoisite, sericite and minor chlorite has occurred. Gneissic banding/mylonitic foliation angle is 15°.

M93 Banded quartz-feldspar-biotite-muscovite gneiss with a moderately strong mylonitic foliation. Gneissic banding/mylonitic foliation angle is 30°.

M247 Striped strongly mylonitic quartz-feldspar-biotite-garnet gneiss. Original gneissic banding has been virtually obliterated. Mylonitic foliation dominant, containing a strong intersection lineation. Oblate ellipsoidal garnets and feldspars.

The gneissic banding/mylonitic foliation angle refers to the difference in dip between these two planar structures.

6.81 Results

The values of magnetic susceptibility are attributed, on their saturation characteristics, to disseminated magnetic particles in the specimens. These values and related ratios, m and H values are given below.

	Magnetic susceptibility differences			Bulk magnetic susceptibility					
	k max	k int.	k min	K max	K int	K min	m	m($\frac{K\,min}{K\,int}$)	H
M156(2)	+3.24	+2.72	-0.006	19.9	19.3	16.6	0.19	0.164	0.19
M427C,1	+6.277	+3.936	-0.308	24.6	22.2	18.0	0.55	0.448	0.35
M427C,2	+5.743	+3.575	-0.669	27.4	25.2	20.9	0.51	0.425	0.29
M93	+4.66	+2.87	-0.107	22.9	21.2	18.2	0.60	0.517	0.26
M247	+3.098	+2.705	-0.052	14.7	14.3	11.6	0.14	0.114	0.27

Since the torque meter measures magnetic susceptibility differences to a much greater precision than bulk speciman susceptibilities, the differences are used to compute the parameters m and H. $m = \frac{k\,max - k\,int}{k\,int - k\,min}$ and $H = \frac{k\,max - k\,min}{K}$ where K is the specific bulk susceptibility. The m value is hence more accorate than the m(K min/K int) and H values. The m value specifies the shape of the magnetic ellipsoid; m = 0 for oblate ellipsoidal fabrics and m = ∞ for prolate ellipsoidal fabrics. Note that for this value to be equivalent to Flinn's (1962) k value, the m value must be multiplied by $\frac{K\,min}{K\,int}$. Hence for plane strain (k = 1) $m = \frac{K\,int}{K\,min}$. For different specimens the m values are not strictly comparable and the m ($\frac{K\,min}{K\,int}$) values are used. This value is not as accurate as m, since bulk susceptibility values must be used. The H value specifies the strength of anistropy.

6.82 Interpretation

Figure 39 shows the relationship of planar and linear structures of the various specimens and the principal magnetic susceptibility axes. The major errors in the orientation of magnetic axes result from problems in accurate orientation of the cores. The axes for M93 show a constant error which is due to misorientation. M247 also appears to show a systematic error in maximum and minimum axis orientations. Some errors are also present in the

Figure 39 - Stereogram showing the orientations of planar and linear structures of the various specimens and the principal susceptibility axes. Generally there is a good correlation between the foliation and the plane of maximum and intermediate magnetic susceptibility axes.

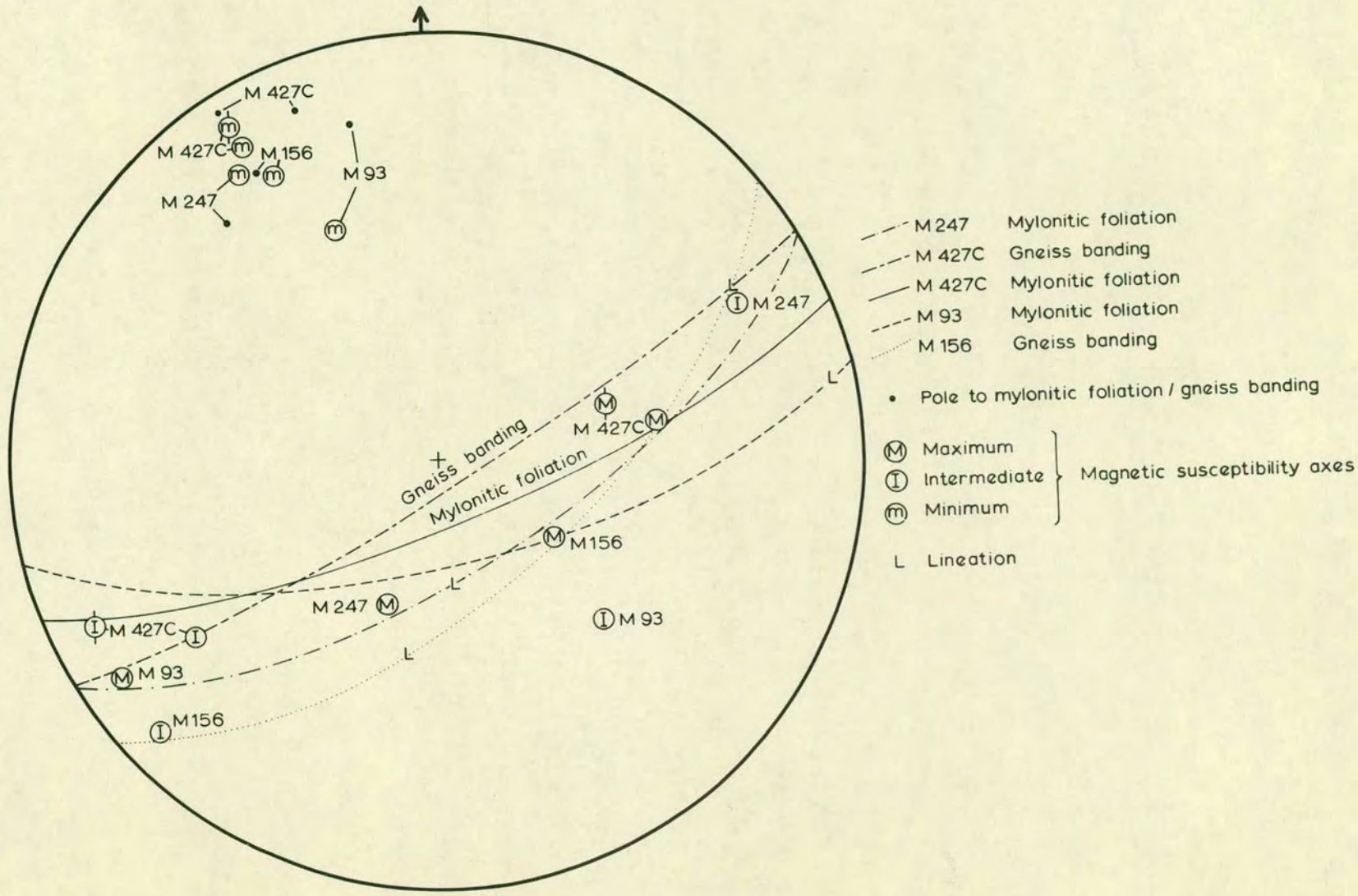
M 427C
M 427C
M 156
M 93
M 247
M 247
M 427C
M 427C
Gneiss banding
Mylonitic foliation
M 156
M 247
M 93
M 427C
M 93
M156
L
L
L
L
M 247 Mylonitic foliation
M 427C Gneiss banding
M 427C Mylonitic foliation
M 93 Mylonitic foliation
M 156 Gneiss banding
Pole to mylonitic foliation / gneiss banding
Maximum
Intermediate
Minimum
Magnetic susceptibility axes
L Lineation

magnetic axis orientations, as shown by the angles determined between them which range from 70° to 90°. Specimens M156(2) and M247, which show low m values (highly oblate ellipsoids) have the minimum angular variations from 90° for the magnetic axes. The magnetic minima show good agreement with the poles to the mylonitic or gneissic foliations. Although there is broad agreement between the magnetic axes and f_3 and f_1 strain axes derived, for example, from boudinaged veins and fold axes in the sheets of the Central Alps, in detail there is no systematic correlation between X and Y strain axes and magnetic maximum and minimum axes. The fact that the magnetic axes can be related to the mylonitic foliation within reasonable bounds of error shows that the bulk magnetic anistropy reflects the orientation of the f_3 strain ellipsoid. Sanderson (Leeds Conf. March 1974) has shown that magnetic principal axes may be closely related to strain axes in deformed slates from North Devon and Cornwall.

The relationship of principal mineral anisotropy axes to lineation is obscure. Several examples have been presented in which a well-defined magnetic maximum coincides with a strong lineation which may not be related to regional strain axes. In the Bergell granodiorite, S.E. Switzerland, Henry (Leeds Conf. March 1974) has shown that a magnetic maximum defines a direction in intrusive veins which is coincident with a prominent lineation in the surrounding rocks. This lineation does not correspond to the regional X strain axis. W.H.Owens has obtained similar results from specimens of mylonite from the Valle d'Ossola, N.W.Italy (M.R.W. Johnson pers.comm.1973) but in these specimens the magnetic maxima do coincide with a strong stretching lineation. In M247, the most strongly deformed mylonitic gneiss, there is good agreement between the orientations of the strong intersection lineation plunging 53° to 191° and the magnetic maximum. Ovoid feldspars and garnets indicate that the X axis of the strain ellipsoid in this specimen plunges approx. 62° to 127°. Hence it appears that the intersection lineation forms a penetrative anisotropy which is reflected in the magnetic results. In

contrast, the mylonitic foliation/gneissic banding intersection lineation, which is quite marked in M427C and M93, is not reflected in the magnetic results for these specimens. The maxima in M427C and M93 lie at orientations apparently unrelated to any structural linear features in the rocks. In M156 (2) which is only slightly deformed, the gneissic and mylonitic foliations are approximately coincident and the magnetic axes may coincide with f_1 strain axes, although no observation could be made in the field to confirm this.

The m value which defines the magnetic ellipsoid shape, shows a low value (m = 0.19) for the relatively undeformed gneiss. This is an oblate ellipsoid with the gneissic foliation containing the two larger axes (K max. K int). In M427C (1) and (2), the m values are 0.51 and 0.55 respectively and similarly in M93 the value is 0.60. These moderately oblate magnetic ellipsoids occur in rocks which contain no dominant planar structure in hand specimen. In M93, the gneissic banding/mylonitic foliation angle is 30° and in M427C, 15°. If we initially take a pre-existing strongly oblate magnetic ellipsoid as is found in M156, and then superimpose a mylonitic oblate ellipsoid such that these later strain axes (particularly Y and Z) lie in different planes, we may expect the ellipsoid to be modified towards (in this case) a more constrictional shape. Such a mechanism has been proposed by Thakur (1973) to account for the presence of prolate ellipsoidal pebbles in a conglomerate deformed by two separate flattening strains. For M93, in which this angular difference is markedly greater than in M427C, the magnetic ellipsoid is hence modified by a greater amount. In M247, in which the gneissic banding and mylonitic foliation are sub-parallel, the prominent fissility and oblate ellipsoidal garnets and feldspars are reflected in the low m value. This value is considered to be about as low as is obtainable from the mylonites of the Tonale Pass area. The more fissile phyllonitic mylonites were not suitable for coring and hence no magnetic measurements

could be obtained for these rocks.

The H values, which specify anisotropy strength, show a minimum (19%) in the slightly deformed gneiss but the four mylonitic specimens give similar values (29%, 26%, 27%, 35%). Specimens M427C (1), (2), and M93 show higher values of bulk susceptibility, suggesting that some magnetite is formed by local Upper Greenschist or Lower Amphibolite metamorphism during mylonitization. There is no regular marked increase in H with degree of mylonitisation, as has been shown by M.R.W. Johnson (pers.comm.1974) from mylonites of the Valle d'Ossola, N.W. Italy.

6.90 INTRUSIVE IGNEOUS ROCKS

6.91 Andesite dykes

In the Central Alps a number of small andesite (microdiorite) dykes cross-cut f_3 asymmetrical folds. They range from 5 cm. to 3.5 m. in width. In the Vallazza sheet the dykes cross-cut strongly lineated paragneiss (including f_4 lineations) but are themselves structurally undeformed.

A similar series of dykes in the Ortles area has been described by Andreatta (1953). There are several dyke "centres" within the "Altkristallin" sheet, particularly north of the area mapped. Alpine dykes have also been reported in the Italian Zillertaler Alps by Borsi et al (1973).

The dykes are deformed by f_5 mylonites in parts of the Casiole sheet where they become strongly foliated and mineralogically changed. The orientation of dykes is shown in Figure 40(a). Most of the dykes strike NE-SW, dip gently SE and appear to be unrelated to the inferred N-S directed Alpine stress system. The orientation of some dykes is controlled by the gneissic banding.

At Passo di Contrabandieri (T370) numerous dykes, ranging from medium grained to fine grained andesite, cross cut coarse grained pelitic gneiss. Figure 40(b) is a sketch of the field relationships. Dykes were observed to change orientation from 177/56°E (sub parallel to the

Figure 40(a) - Stereogram showing the orientation of andesitic dykes and associated hornblende lineations. These lineations are igneous flow textures generally found at the margin of the dykes.

Figure 40(b) - Sketch of the relationships between andesitic dykes and pelitic gneiss at Passo di Contra bandieri (T370). Note that the dykes perpendicular to the pelitic gneiss banding lens out rapidly.

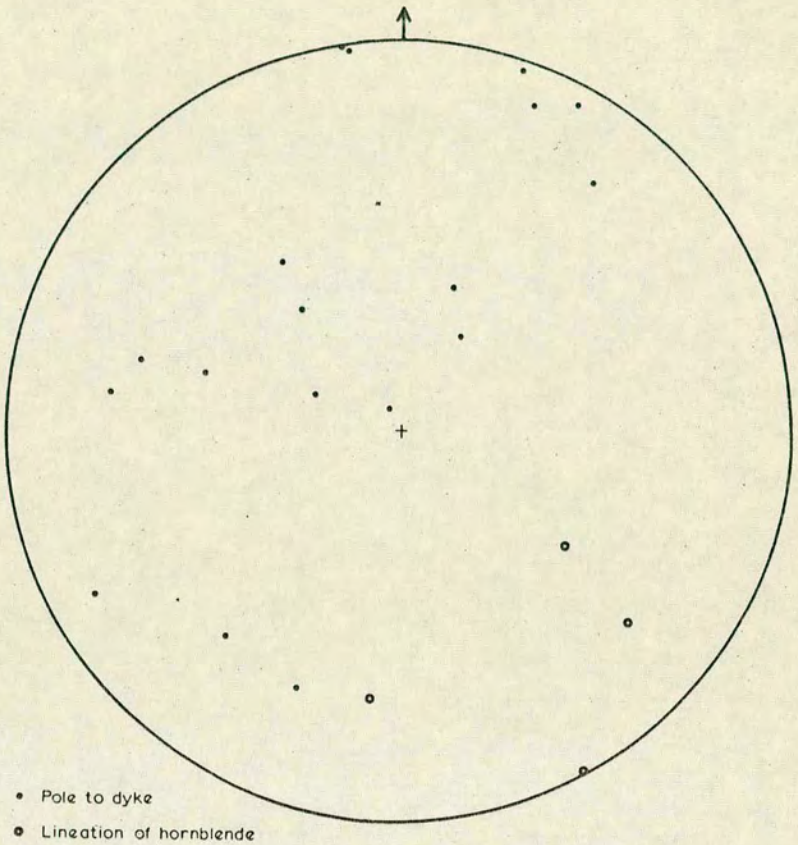
• Pole to dyke
o Lineation of hornblende

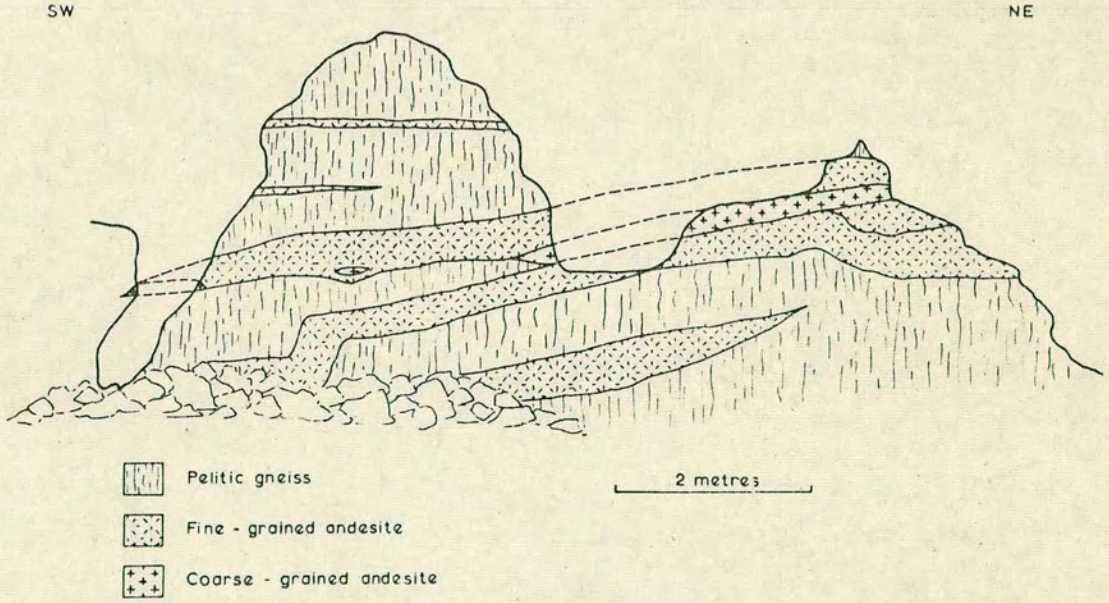
SW
NE
Pelitic gneiss
Fine - grained andesite
Coarse - grained andesite
2 metres

gneissic banding) to 121/23°SW. When close to this latter orientation they rapidly lens out laterally. Contact metamorphic effects are best developed in the steeper dipping sections (2.5 cm. of dark grey material) and are minimal in the more gently dipping parts. N.J.Price (1971, pers.comm.) has shown that thin dykes are injected and solidify in a short period of time, e.g. approx. 35 mins. for a 20 cm.wide dyke.

Minor faulting has commonly occurred along dyke/gneiss contacts and chlorite fibres (see Durney and Ramsay, 1972) imply movement of the uppermost block to the north (006° to 016° range) across small reverse faults.

The dykes range from medium grained porphyritic microdiorite to fine grained grey homogeneous andesite. At Passo di Gavia, a few kms. northeast of the area mapped, a 3.5 m. porphyritic andesite dyke cross-cuts schists and quartzites of the Viso sheet. Under the microscope this rock consists of 0.1 to 3 mm. long, zoned, green, strongly pleochroic, euhedral hornblende and 2 to 5 mm. long altered andesine phenocrysts in a fine-grained matrix of plagioclase, (some albite) K feldspar, apatite and minor pyrite, ilmenite and cancrinite. This dyke has undergone considerably less alteration than those found to the south of the Peio Line.

In thin sections of medium-grained microdiorite from Passo di Contrabandieri (T370A), subhedral brown-green hornblendes (average 1 mm.long) lie in a matrix of plagioclase, chlorite aggregates, clinozoisite, quartz and minor orthoclase (sanidine ?), calcite, sphene and apatite. Sericitic alteration of plagioclase has occurred. The plagioclase laths are generally oligoclase - andesine but more rarely equant crystals show well-developed normal zoning (andesine → albite). Opaques are generally very sparse in the fine grained dykes. Hornblende is commonly fractured and partly altered to chlorite + calcite. These mineral assemblages suggest that Greenschist grade metamorphism has occurred subsequent to dyke intrusion.

Since the field, petrographic and compositional evidence shows that these dykes were emplaced between the

Early and Late Alpine events, it is tempting to correlate them with the Adamello massif. Although the dykes cannot be structurally related to this massif, they probably formed by an approximately coeval magmatic event to the north. They may be equivalent to the hornblende porphyry dykes described by De Sitter (1949) and Gansser (1968) in the Bergamasque Alps.

6.92 Ultramafic rocks

Ultramafic rocks have been mapped in the Tonale Pass area by Hammer and Trener (1908) and Bianchi, Dal Piaz et al (1940); these rocks crop out about 600 m. north northwest of Mt.Tonale Orientale. The lithology weathers to a massive brown rock and breaks up into large prominent rectangular blocks which have been transported by glacial action up to 2 km. down the Valbiolo.

The dunite body has an approximately rectangular outcrop 500 m. by 270 m. (area 0.135 sq.km.). The body lies with its long dimension approximately concordant with the regional strike of the surrounding gneisses of the Mt. Tonale sheet. Its southern margin is faulted. Locally highly discordant contacts and large marble xenoliths in the dunite suggest that the dunite has been intruded into the surrounding rocks. Although the marginal serpentine phase exhibits a "crenulation" cleavage in parts, the body is generally undeformed. The crenulations have axes plunging 0° to 069°, and show a north facing asymmetry. These crenulations result from late northward or upward directed movements (f_4 or f_5) which have been concentrated along the weak bounding serpentinite layer. The dunite body is bounded to the south by coarse-grained quartz-feldspar-biotite-muscovite-sillimanite gneiss containing abundant pegmatites, and 1 cm. to 2 mm. thick phyllonite bands. Marble lies above the body and some stoping has apparently occurred in this region. Small dunite pods lie within the marble, and in places a complex marble-serpentine admixture is seen. These observations show that we are seeing the topmost part of the intrusive ultramafic body. To the north, the dunite is bounded by a 1 m.

grossularite marble in parts, but more generally by quartz-feldspar-biotite-muscovite gneiss with abundant quartz pods. Figure 41(a) shows the general relationships of part of the ultramafic body to the surrounding rocks, and the position of the various contact lithologies.

In thin section, the dunite consists of large rounded olivine crystals up to 1 cm. in diameter with well-developed equilibrium angle boundaries. The olivine is biaxial -ve with a 2V of almost 90° (Fo 85-90). The olivine has a typical well-developedfracture system, with bowlingite (chlorite and goethite) and iddingsite commonly developed. Iddingsite is a brown pleochroic, high relief, hydrated Mg-Fe silicate, which appears to form by diffusion of H^+ atoms into the olivine structure in the solid state (Deer, Howie and Zussman, 1966). Anthophyllite occurs in aggregates of long prismatic crystals, each up to 6 mm. long. The crystals cross-cut the olivine grains and their fracture systems. The anthophyllite shows parallel extinction, is biaxial -ve with a 2V of about 65°, implying that it lies close to the magnesium rich end member in the anthophyllite -gedrite solid solution series. Plates of low birefringent biaxial +ve (2V,10° to 20°), colourless chlorite either 0.1 mm. wide or 0.8 mm. wide (pale green in hand specimen) are abundant in the olivine. They occur as individual crystals and rounded finely felted masses in the olivine. Optical properties show that the chlorite lies in the magnesium sheridanite field on the chlorite diagram (Deer, Howie and Zussman, 1966) with an approximate composition of $(Mg_9\ Fe_{0.5}Al_{2.5})(Si_{5.5}Al_{2.5}O_{20})(OH)_{16}$.

Spinel is invariably associated with this chlorite (magnetite or more commonly chromite - brown at thin edges). Veins 0.5 to 2 mm. across composed of chlorite, anthophyllite, talc and a carbonate (probably magnesite) are present in the olivine. Anthophyllite is in part altered to talc in these zones. Talc is abundant in certain zones in the dunite, and forms highly birefringent felted masses. Minor phlogopite and rare tremolite are present in the larger talc zones. Dark grey-green serpentine (pale green in thin

Figure 41(a) - Detailed sketch map of the dunite body showing its relationships to the surrounding gneiss and contact lithologies.

Figure 41(b) - Stereogram showing poles to joints in dunite. The joint sets are orthogonally related to one another and are typical of undeformed igneous bodies.

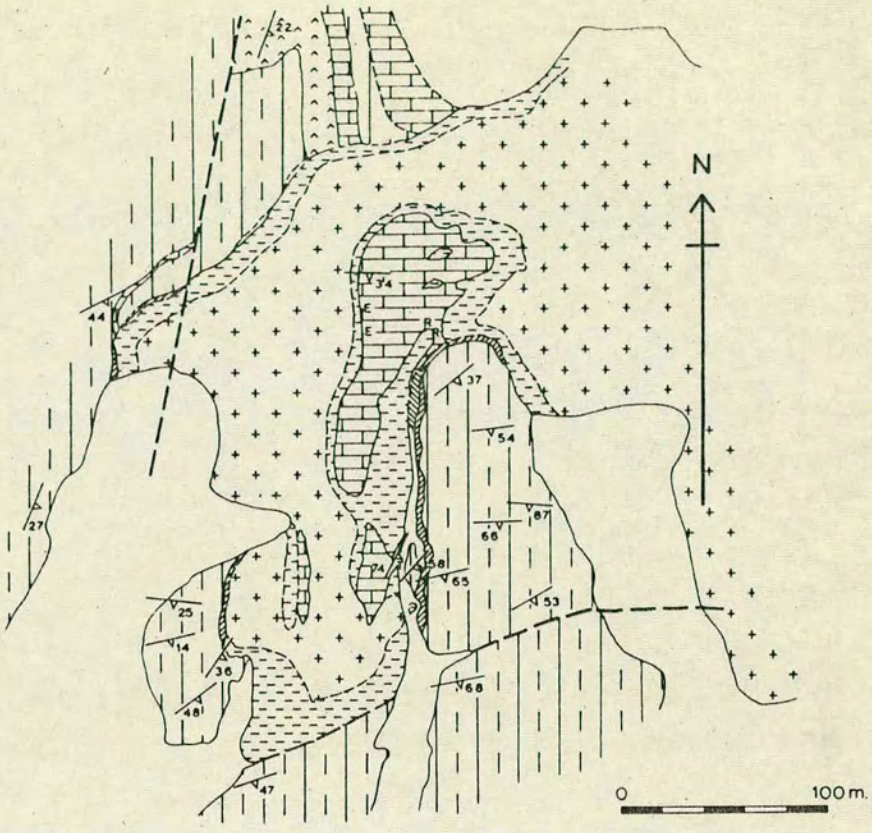

Dunite

Mg chlorite - serpentine rock

Talc - magnesite rock

Actinolite

Pelitic gneiss

Marble

Amphibolite

Geological boundary

Geological boundary - position approx.

Fault - position approx.

Strike & dip of compositional banding

EE Epidote-clinozoisite

RR Rodingite

TT Tremolite

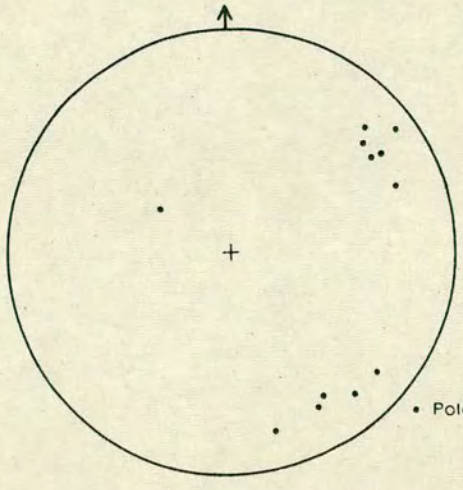

section) showing anomalous bluish birefringence (uniaxial -ve or biaxial -ve with very low 2V) occurs in only very minor quantities in a series of thin sigmoidal dilation veins in a small shear zone. Similar material is described by Cady, Albee and Chidester (1963) as aluminous antigonite. These serpentine veins cross-cut all other mineralogical boundaries in the rock.

The minerals in the dunite are the products of several hydration reactions which occurred during the cooling of the dunite in the presence of water. All these reactions involve an increase in the Si/Mg ratio and addition of H_2O. Anthophyllite, chlorite and chromite precede talc, magnesite, phlogopite and tremolite, and serpentine is the latest product. The presence of anthophyllite-talc aggregates at regular intervals in the dunite, and the association chlorite-magnetite-chromite suggest that these minerals may have formed by hydration of enstatite, at least in part. Chromium is a commonly substituted element for magnesium in enstatite.
The reaction

$$\underset{\text{enstatite}}{7\ Mg(FeCr)SiO_3} + SiO_2 + H_2O \rightleftharpoons \underset{\text{anthophyllite}}{[Mg(FeCr)]_7Si_8O_{22}(OH)_2}$$

is relevant to this hydration. Pressure (P) and temperature (T) relations for the various phases found in the hydration of forsterite and enstatite are shown in Figure 42 (after Evans and Trommsdorf, 1970; and Fawcett and Yoder, 1966).

The presence of abundant magnesium chlorite in the dunite is important since it implies that hydration has occurred at temperatures above the stability limit of serpentine (400° - 520°C). Fawcett and Yoder (1966) have shown that Mg chlorite is stable up to temperatures of 750°C at 2 kb water pressure (P H_2O) and 700°C at 1 kb P H_2O. A reaction for the hydration of olivine and enstatite consistent with thin section evidence would be

Figure 42 - Pressure - temperature relations for reactions between minerals found in the Dunite body in the Tonale Pass area. The data is taken from Evans & Trommsdorf (1970) and Fawcett and Yoder (1966).

Serp - Serpentine
Enst - Enstatite
Sp - Spinel

All other abbreviations are given in section 1:50.

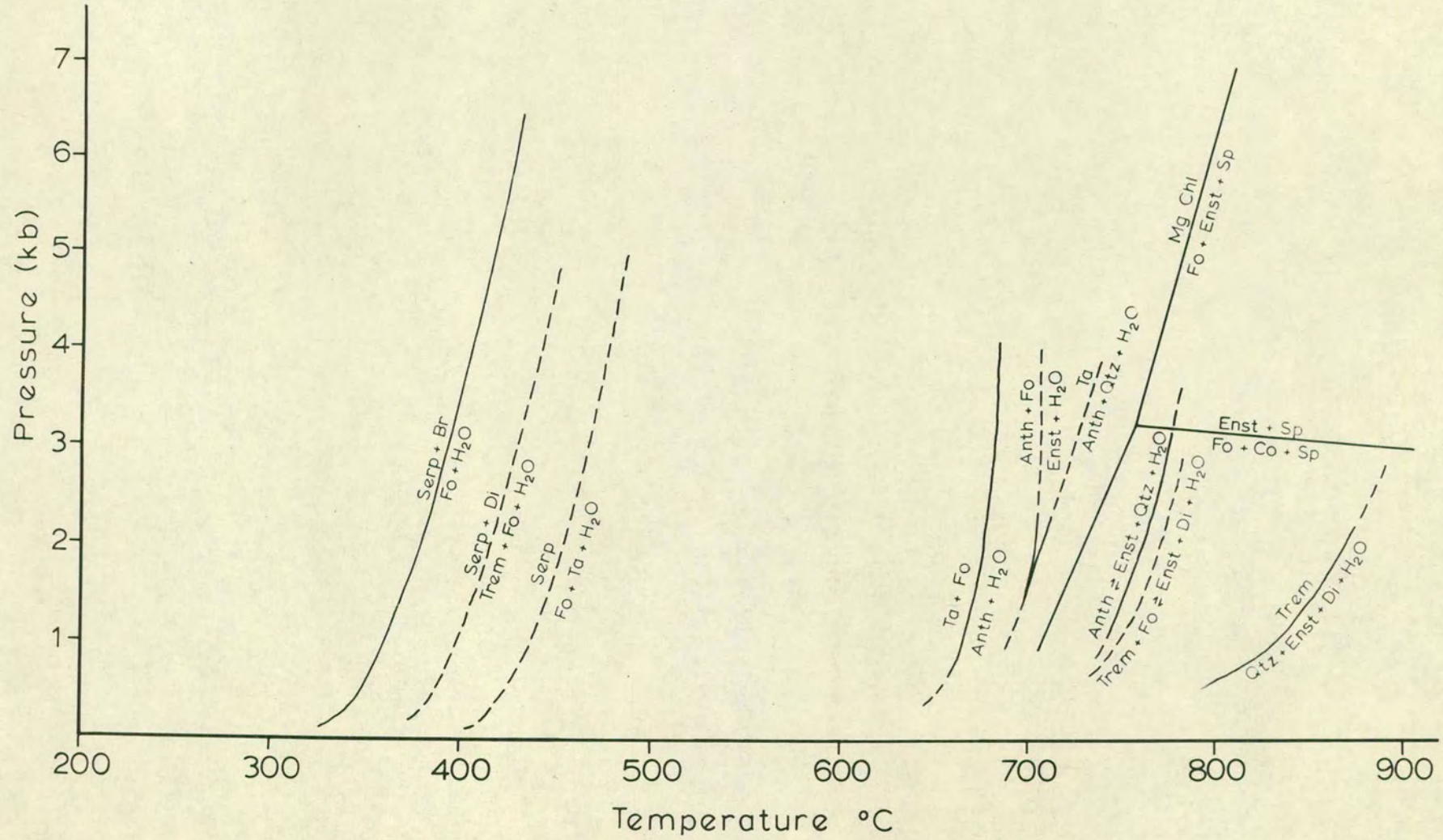
Pressure (kb)
1
2
3
4
5
6
7
200
300
400
500
600
700
800
900
Temperature °C
Serp + Br
Fo + H2O
Serp + Di
Trem + Fo + H2O
Serp
Fo + Ta + H2O
Ta + Fo
Anth + H2O
Anth + Fo
Enst + H2O
Ta
Anth + Qtz + H2O
Mg Chl
Fo + Enst + Sp
Enst + Sp
Fo + Co + Sp
Anth ⇄ Enst + Qtz + H2O
Trem + Fo ⇄ Enst + Di + H2O
Trem
Qtz + Enst + Di + H2O

$$4.475(Mg_{1.8}Fe_{0.2})SiO_4 + (Mg_{0.95}Fe_{0.04}Cr_{0.01})SiO_3 +$$
Forsteritic Olivine — Enstatite

$$2.5Al_2O_3 + 10.192H_2O \rightleftharpoons (Mg_9Fe_{0.5}Al_{2.5})(Si_{5.5}Al_{2.5})O_{20}(OH)_{16}$$
Introduced in fluid — Mg chlorite

$$0{\cdot}005FeCr_2O_4 + 0.143Fe_3O_4 + 4.384(H^+)$$
Chromite — magnetite

The resultant H^+ would be used for transforming olivine to iddingsite. If spinel is changed together with olivine and enstatite, then taking simpler formulae, Yoder and Fawcett (1966) get

Forsterite + Enstatite + Spinel = Mg chlorite

Reactions for the hydration of forsteritic olivine alone give unrealistic values for several components e.g.

$$9Mg_{1.8}Fe_{0.2}SiO_4 + 2.75Al_2O_3 + 21.75H_2O \rightleftharpoons$$
Olivine — introduced

$$1.8(Mg_9Fe_{0.5}Al_{2.5})Si_5Al_3O_{20}(OH)_{16} + 0.3Fe_3O_4 + \underline{27.5}(H^+)$$
Mg chlorite — Magnetite

The dunite is widely jointed and Figure 41(b) shows the orientation of poles to major joints. Two distinct concentrations at 90° apart are present, and these are assumed to be cooling joints. More rarely, gently dipping joints are present. No slickensiding or vein infillings were observed in the joints. As the joints intersect in a line dipping west, the intrusion may extend at depth in this direction.

Surrounding the intrusion is an inner zone of serpentine - chlorite rock, and an outer zone of mid-green serpentinite, together totalling 2 to 40 m. in thickness. Thin cross-cutting chrysotile veins are common in both zones. The serpentine contains banding (magnetite grains ?) which follows the marble/serpentine contact. Thick veins of chlorite-serpentine cut through marginal parts of the dunite body. Under the microscope this chlorite-serpentine rock (M263) consists of corroded tremolite-actinolite crystals and aggregates of optically positive grey birefringent chlorite (as found in the dunite), lying in a felted mass of anomalous blue birefringent aluminium serpentine fibres (optically -ve). X.R.D. traces confirm

the presence of serpentine and chlorite (Mg sheridanite). The serpentine undoubtedly post dates the amphibole and chlorite. The optical and structural properties of serpentines and chlorites are very similar and it is often difficult to distinguish between the two minerals. Generally the term serpentine applies only to a limited compositional range with a simple lattice arrangement and 7Å d spacing. Chlorites on the other hand show a wide range of composition (complex substitutions common) and a 14Å d spacing. Many materials previously identified as serpentine may in fact be Mg chlorites. This has important implications when discussing emplacement and hydration of ultramafics.

The marginal serpentine envelope is in contact with marble and pelitic gneiss. In the marble, single diopside crystals up to 4 cm. across show marginal alteration to tremolite. Zoisite pods up to 10 cm. across, grossular (or hydrogrossular ?) pods averaging 40 cm. and up to 1 m. across, and large clinozoisite pods are common. The minerals only occur near the upper contact of the dunite however, and at the margins small tremolite (?) spots up to 2.5 cm. wide are locally developed at up to 30 cm. from the serpentine-marble contact. The calc-silicate zone has a maximum thickness of 3 m. Rarely a 1 to 2 m. band (M259) of massive pale grey-green-white serpentine-talc-tremolite rock (XRD trace) is present around the outer margin of the calc-silicate zone. This rock type weathers to grey-green and pink. Finely banded quartz-feldspar-actinolite-chlorite gneiss forms the outermost part of the zone of alteration around the ultramafic intrusion. These latter zones are consistent with magnesium metasomatism of the country rock.

At the serpentine/gneiss contact, pods and veins of coarsely crystalline actinolite up to 3 m. across are common. Large phlogopite plates are often associated with the actinolite. Similar pods and veins of actinolite-phlogopite are found at several localities (T155, M313, T68, T245), close to mylonite zones in the Tonale Pass

area. For example at T155, 2 m. thick pods up to 30 m. long occur in mylonitic gneiss in association with a thin marble band. At M313, 100 m. north of the ultramafic outcrop, actinolite-phlogopite pods are associated with small serpentine pods. The actinolitic pods are undeformed and hence must post-date the mylonitic event. This suggests that ultramafics are present below the present level of outcrop and that magnesium rich fluids have caused some metasomatism. In some cases actinolite pods may result from diffusion between the calcic and aluminium rich phases (marble/gneiss) during metamorphism, although this phenomenon is not generally seen in the Tonale Pass area.

A small body of harzburgite (peridotite) occurs about 20 km. north east of the area mapped (R.F.Cheeney, pers. comm.1972). This is part of a lenticular body about 4 km. long and 100 m. wide mapped by Bianchi, Dal Piaz et al (1940). Under the microscope, this ultramafic consists of an aggregate of fractured olivine crystals (Fo 85-90) averaging 1-5 mm. in diameter, with about 12% of kinked, twinned enstatite crystals. Picotite is the major accessory. Fracture zones up to 1 mm. wide consisting of olivine fragments, bowlingite, iddingsite, magnetite and minor talc are abundant in the rock.

The problems of the origin and emplacement of ultramafic bodies are complex and only a brief discussion relevant to this intrusion will follow. It must be emphasized that a considerable body of evidence (Thayer, 1966, 1967; Coleman, 1967; Cady et al, 1963; Ernst, 1965) suggests that partly sheared and serpentinised dunite and peridotite are emplaced at low temperatures (250°- 500°C). Bowen and Schairer (1936) have shown that forsterite begins to melt at 1600°C and melting is complete at 1890°C. Allowing for the presence of 10% fayalite and some 5% silica, and postulating the presence of a fluid ($NaCl - CO_2 - H_2O - SiO_2$) will only reduce this temperature to about 1300°C for partial melting. Green (1967) has described several ultramafic intrusions from which there is good evidence for a high temperature of intrusion.

Orthopyroxene occurs in the inner parts of their metamorphic aureoles. The high alumina compositions of the ortho- and clinopyroxenes and coexistence of orthopyroxene -clinopyroxene exsolution lamellae (Mackenzie, 1960) suggest temperatures in the order of 800° - 1200°C for the Tinaquillo ultramafic intrusion in Venezuela. Green (1967) has shown that the well-documented high temperature peridotites and dunites contain significantly higher Al_2O_3, CaO, and Na_2O than the average compositions for such rocks.

The dunite intrusion in the Tonale Pass area shows good olivine equilibrium textures and there is no evidence of shearing or deformation textures in the olivines. The apparent stoping at the top of the intrusion suggests that it was essentially mobile (but not fluid) during its intrusion and that it was a high temperature intrusion. As ultramafic masses are initially almost anhydrous by virtue of their depth of origin, they will initiate a diffusion gradient of water from the surrounding rock as they rise. Hence, dependent on pressure and temperature, a thin envelope of hydrated magnesium silicates (i.e. talc, Mg chlorite, anthophyllite or, if CaO present, actinolite) would be expected to develop during the ascent of the ultramafic body. The rate of ascent of the dunite mass would depend on the rate of cooling of the ultramafic, its density and viscosity relative to the surrounding rock, and amount of assimilation of country rock. The growth of talc, chlorite, actinolite, etc. may aid the ascent by providing a shearing surface at its perimeter and a zone through which fluid transfer and hence rapid heat loss may be inhibited.

Taking Jaegers' (1959, 1957) approximate values for cooling of an intrusive sheet as being valid, we may postulate a contact temperature of about 700°C (for melting range 1400°-1300°C, conductivities as from Clark (1966) for 200°C, latent heat of solidification 80cal/gm) for dry country rock or slightly less for wet rock. At about 100 to 250 m. from the intrusion (270 m. wide dunite sheet)

this temperature would drop to about 150°C, dependent on water content and porosity of the country rock. These temperatures would all be additional to those prevailing in the country rock. However, the parageneses and field relations imply only slight marginal heating except at the top of the intrusion, where large zoisite and diopside crystals occurring up to 3 m. from the intrusion margin suggest the temperatures were in the Hornblende Hornfels facies (Winkler, 1967). Upper limits are defined by the stability of tremolite, which is locally the only new mineral formed close to the sides of the intrusion. The lack of wollastonite, orthopyroxene and calcic plagioclase suggest that temperatures were never much above 600°C in this calc-silicate zone. The occurrence of zoisite suggests that X CO_2 never reached values greater than about 5 mol.% assuming a maximum P H_2O of 5 kb (Storre and Nitsch, 1972). The reaction

tremolite + 3 calcite + 2 quartz $\rightleftharpoons$ 5 diopside + $3CO_2$ + H_2O

is relevant to this zone on the basis of thin section observations. Metz and Winkler (1964) show that equilibrium temperatures for this reaction are 520° to 540°C at 1 kb total pressure, dependent on the partial pressure of CO_2 and water (P H_2O + P CO_2 = P total). The alteration of zoisite to sericite and marginal alteration of diopside to tremolite show that some retrogression has occurred.

Serpentinization involves the addition of water to forsteritic olivine, the formation of magnetite and serpentine, and removal of excess magnesium, silica and hydrogen (Thayer, 1966). The reaction proposed is

$$5(Mg_{0.9}Fe_{0.1})_2SiO_4 + 4.15H_2O \rightleftharpoons \underset{\text{Serpentine}}{1.87Mg_3Si_2O_5(OH)_4} + \underset{\text{Magnetite}}{0.333Fe_3O_4} + 3.4MgOaq + 1.3SiO_2aq + 0.4H_2$$

Forsteritic olivine

The association of magnetite with serpentine is commonly seen in thin section. The presence of methane and hydrogen gas seeps with younger peridotite intrusions in the Philippines (Thayer, 1966) and New Zealand (Wood, 1972) suggests that hydrogen is a product of serpentinization.

It is difficult to reconcile the production of excess silica with thermodynamic and field considerations however, since we might expect a diffusion of silica <u>into</u> the ultramafic body. The more classic reaction quoted is

$$3Mg_2SiO_4 + 4H_2O + SiO_2 \rightleftharpoons 2Mg_3Si_2O_5(OH)_4$$

would involve a volume increase of 67%. Hostetler et al (1966) have reported the presence of about 5% brucite in many serpentines and conclude that this is evidence for the reaction ;-

$$9(Mg_{0.92}Fe_{0.08})_2SiO_4 + Mg_{0.92}Fe_{0.08}SiO_3 + 12.595H_2O$$

Forsteritic Olivine — Enstatite

$$+ 0.088SO_2 \rightleftharpoons 5(Mg_{0.96}Fe_{0.04})_3Si_2O_5(OH)_4$$

Serpentine

$$+ 2.595(Mg_{0.85}Fe_{0.15})(OH)_2 + 0.177Fe_3O_4 + 0.874MgO$$

Brucite — Magnetite

This would involve a 42% volume increase which, according to Hostetler et al (1966), is taken up by tectonic movements. Thayer's (1966) equation is favoured by the geological evidence but a modification may be made to remove the excess silica and introduce some brucite. The calculated reaction would be:-

$$5(Mg_{0.9}Fe_{0.1})_2SiO_4 + 6.83H_2O \rightleftharpoons 2.5Mg_3Si_2O_5(OH)_4$$

Forsteritic Olivine — Serpentine

$$+ 0.33Fe_3O_4 + 1.5Mg(OH)_2 + 0.33H_2$$

Magnetite — Brucite

If some magnesium is carried away in solution, the brucite quantities are diminished. The equation may be further refined to account for variations in Fe content of brucites and serpentines reported by Hostetler et al (1966).

Chrysotile has been shown by Bowen and Tuttle (1949) to be stable only below 500°C, although antigorite may be stable to slightly higher temperatures (Evans and Trommsdorf, 1970). Temperatures of up to 540°C may be expected from thermodynamic considerations. If brucite is present, a maximum temperature of 400°C is fixed for serpentine by experimental data (Johannes, 1968; Hostetler et al,1966).

Concurrent with serpentinization, there is a movement of CaO into the adjacent country rock (Hess and Otalora,

1964; Coleman, 1967; Thayer, 1966) from the serpentine. The serpentine only retains about 14% of the CaO normally present in dunites. It is important to find out if some of this calcium migrates before serpentinization since it is not known if talc, anthophyllite or chlorite can hold much calcium in their structures. Thayer (1966) has associated serpentinization with the development of rodingite.

Rödingite is the term applied to the calcium aluminium silicates (generally hydrogrossular, clinozoisite, prehnite, idocrase, diopside etc.) which are developed in amphibolites, marbles, gabbros and basaltic rocks adjacent to serpentinized ultramafic bodies. There is little doubt that the serpentinite-rodingite association is valid in many cases (Coleman,1967). Barnes et al (1972) have shown from chemical studies of water associated with recent serpentinites, that a Ca^{2+}-OH^{-1} fluid migrating <u>across</u> the ultramafic country rock boundary may form rodingite in siliceous country rock. Fluid buffered by partial reaction with the ultramafic and siliceous country rocks flow <u>along</u> the contact. These latter fluids are supersaturated with regard to talc and tremolite at moderate temperatures. It is difficult in the Tonale Pass area to reconcile the mineralogy, implied P, T conditions, and field relationships of the rodingite, with serpentinization. The development of these minerals is best explained by movement of SiO_2, Al_2O_3, CO_2 and NaCl rich fluids from the country rock (pelitic gneiss generally) towards the ultramafic; marginal penetration, heating, and subsequent upward movement causing moderate temperature metasomatism of the overlying marble. As Moores and Macgregor (1968) have shown, contact effects at ultramafic margins are largely dependent on the level of exposure now seen, and initial level of intrusion. The presence of 1 to 3 m. wide actinolite pods and veins marginal to the body represents a diffusion reaction between the MgO rich phases of the hot ultramafic and the CaO and Al_2O_3 rich phases of the pelitic gneiss. The retrogression of the rodingite minerals (zoisite → sericite, diopside → tremolite) shows that metasomatism

continued to relatively low temperatures (300°-400°C). The large size of the rodingite minerals is compatible with this metasomatic hypothesis, since abundant metasomatic fluids inhibit nucleation and supply constituents to the already growing grains.

Shieh and Taylor (1969) have shown that granite plutons with well-documented contact temperatures (525° - 625°C on O^{18}/O^{16} and D/H isotope ratios on various mineral pairs), have very localised metamorphic aureoles. Isotopic evidence shows that water moves <u>towards</u> the pluton and then rises upwards as a hot fluid.

6.93 Granitic intrusives and pegmatites

In the area mapped orthogneiss only occurs in the uppermost part of the Mt.Tonale sheet (T145) where pods of aplitic granite 10 to 20 m. across, cut discordantly across banded pelitic gneiss. The pink, leucocratic rock consists of quartz, K feldspar and minor plagioclase and muscovite. It lies within a wide mylonitic gneiss zone and shows a strong foliation. It is probably related to the Hercynian pegmatites.

Pegmatite veins, a few mm. to about 60 m. thick are very abundant in the paragneiss of the Tonale Zone (S. of Peio Line), although they are rare in the Viso sheet to the north. They may discordantly cross-cut the gneissic banding and f_1 folded quartz veins (commonly "blue" quartz), but more generally lie broadly concordant with the regional banding. The pegmatites are deformed by the Early Alpine deformation and in areas of high strain have become internally foliated.

In the 10 to 20 cm. adjacent to some pegmatites (particularly the more feldspar-muscovite rich types) large muscovite flakes have grown suggesting that outward diffusion of a saturated K^+ - H_2O rich fluid has occurred. The pegmatites range in composition from quartz with very minor K feldspar and muscovite, to a quartz-k feldspar-muscovite-garnet rock akin to granite. They are generally medium to coarse grained. Although the rare occurrence of biotite-garnet rich pegmatite in pelitic gneiss is

suggestive of local sweating, the general composition and occurrence suggests that they are related to Hercynian granitic intrusives at depth.

Rarely (e.g. T353) undeformed fine-grained monzonite dykes cross-cut the pelitic gneisses. These dykes are probably related to the Adamello massif to the south or to similar Alpine calc-alkaline intrusives at depth.

7.00 MYLONITES

7.10 INTRODUCTION

In the Tonale Pass area, several mylonite zones ranging from a few mm. to 50 m. wide have been delineated in the paragneisses of the Altkristallin sheet of the Central Alps. There is generally a change in orientation of the gneiss across these zones. The structural features in the gneiss such as quartz veins, pegmatites and pre-existing tight to isoclinal folds may be traced into the mylonite zones, and their progressive deformation observed. The coarse to medium-grained paragneiss undergoes grain size reduction, recrystallization and a change in mineralogy. Plate 11(a) shows the typical appearance of phyllonite in the field. Estimates of the amount and type of strain in mylonite zones in this area are given, and an attempt made to explain the observed structural features in this context. The gradation from non-mylonitic paragneiss to phyllonite is seen in several areas.

The term mylonite (Greek, mylos-mill) was introduced by Lapworth (1885) who described it as a rock in which "old schistosity planes are obliterated and new ones developed, the original crystals are crushed and spread out and new secondary minerals, mica and quartz, are developed". He thought this rock formed when "the most intense mechanical metamorphism occurs along the grand dislocation (thrust) planes, where the gneisses and pegmatites resting on these planes are crushed, dragged and ground out into a finely-laminated schist, ... the laminations are defined by minute inosculating lines (fluxion lines) of kaolin or chloritic material and secondary crystals of mica". Although this definition is largely correct, it cannot be applied to all mylonites.

Subsequent work on mylonite zones from many parts of the world, e.g. Alpine Fault, New Zealand (Reed, 1964), the Moine Thrust belt, N.W. Scotland (Johnson, 1961, 1963; Christie, 1963; Soper, 1971), Grenville Front, S.E.Canada (Dalziel and Bailey, 1968) and the Brevard Zone, S.Appala-

Plate 11.

(a) Typical dark-grey fissile mylonite with tight to isoclinal quartz vein folds. The mylonite foliation forms the penetrative 'cleavage' which is the dominant planar structure. (M52 - Cadil/Mt.Tonale Mylonite).

(b) Garnets from the Vallazza/Cadil Mylonite (T136B).

New 'Alpine' garnets developed syn- and post-mylonitization. In parts these overgrow the mylonite foliation and minor folds. The photo shows a rotation trail defined by magnetite in the upper garnet.

Old 'Hercynian' garnet showing retrogression to chlorite and magnetite and minor fragmentation. In general these garnets are larger than the later 'Alpine' garnets and in part deflect the foliation.

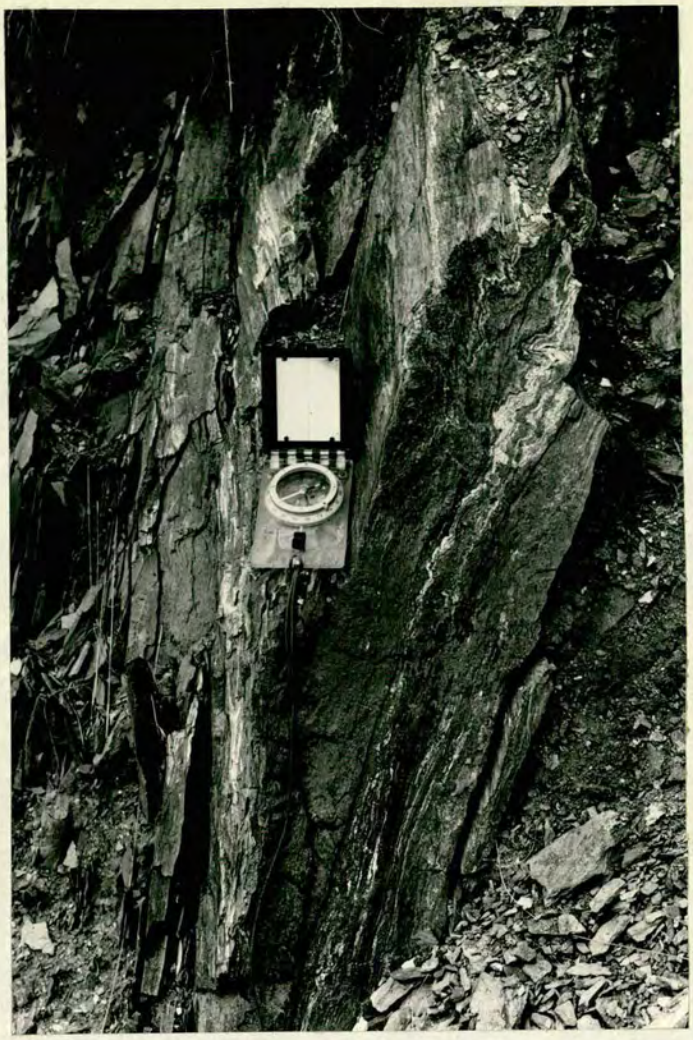

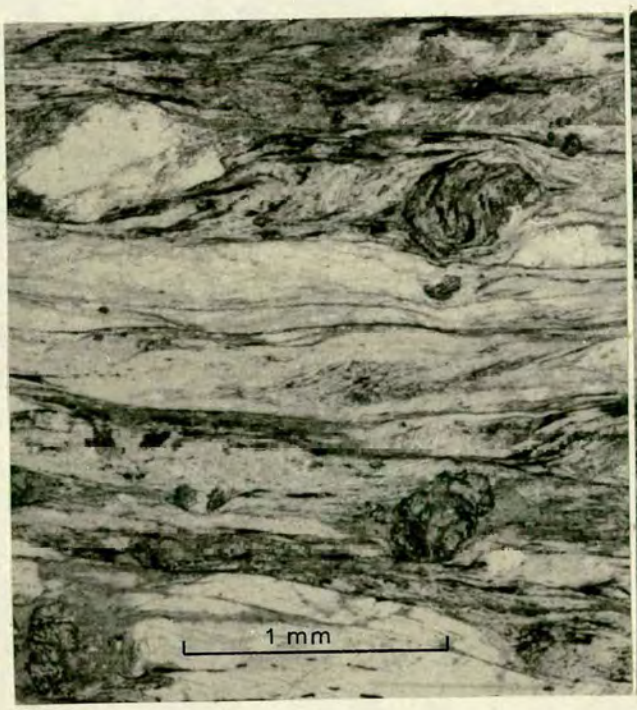
1 mm

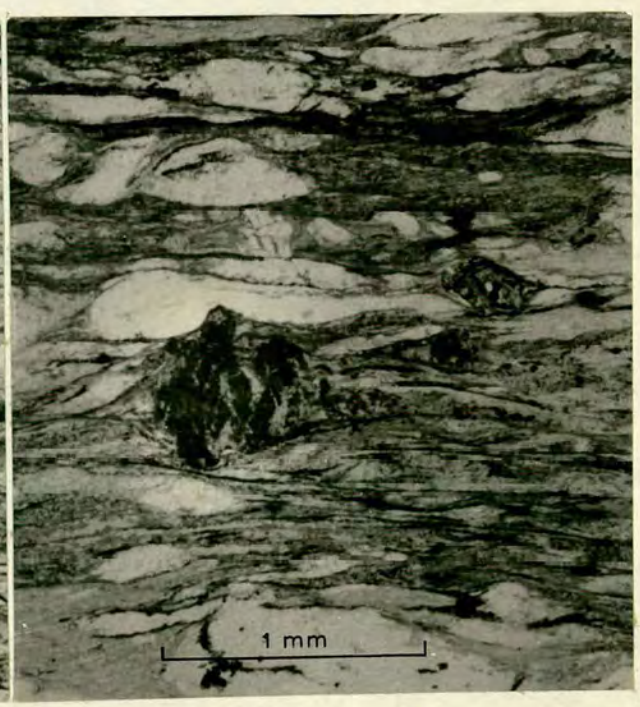
1 mm

chians (Higgins, 1971), has shown that each zone displays unique characteristics, but they are all narrow planar zones of strong deformation and sites of large scale differential movement. Higgins (1971) has discussed the various classifications of mylonite types and summarised descriptions up to 1971.

There has been little work carried out on mylonite zones in the Alps except in small areas (Cliff et al,1971; Johnson, 1973). Up to 1 km. of mylonite and mylonitic gneiss (Rimellaschiefer) is present in the Western Alps adjacent to the Insubric Line (Johnson, 1973) implying that significant tectonic changes occur across and within this zone. The present work in the Tonale Pass area has shown that mylonites are common in the paragneiss of the Austro-Alpine Nappes and a minimum estimate of total relative movement across the zones is approximately 4.2 km. The mylonites are of at least two distinct ages (f_3 and f_5) since they are cut by undeformed hornblende trachyte dykes which in turn become locally mylonitised. These late f_5 mylonites are finer-grained and have assemblages of Greenschist grade (albite-chlorite-epidote) as compared to the Lower Amphibolite grade of the f_3 mylonites (oligoclase/andesine, biotite, clinozoisite). The Peio Line (Andreatta, 1948) which forms the northern tectonic boundary to the high grade paragneisses is largely related to this f_5 event.

7.11 Field Relationships

The mylonites are closely related to the geometry of the f_3 northward facing folds. Figure 43 shows three sections across parts of the paragneiss illustrating this relationship, and also shows the effects of differing rock types. The mylonites are developed in quartz-rich rocks, generally in the pelitic gneiss. Consistently thick mylonite zones are only located at or near major lithological boundaries, showing that lithology and hence ductility variation plays an important part in the determination of the position of mylonites. Where mylonite and phyllonite zones are developed within the pelitic gneiss,

Figure 43 - Three sections across f_3 mylonites and related northward verging folds.

(a) North slope and southeast ridge of Cima Casiole.

(b) Ridge between Punta d'Albiolo and Mt.Tonale Orientale.

(c) Southern end of the south southeast ridge of Vetta d'Albiolo.

Section (c) shows the way in which pegmatite acts as a locus for mylonite development.

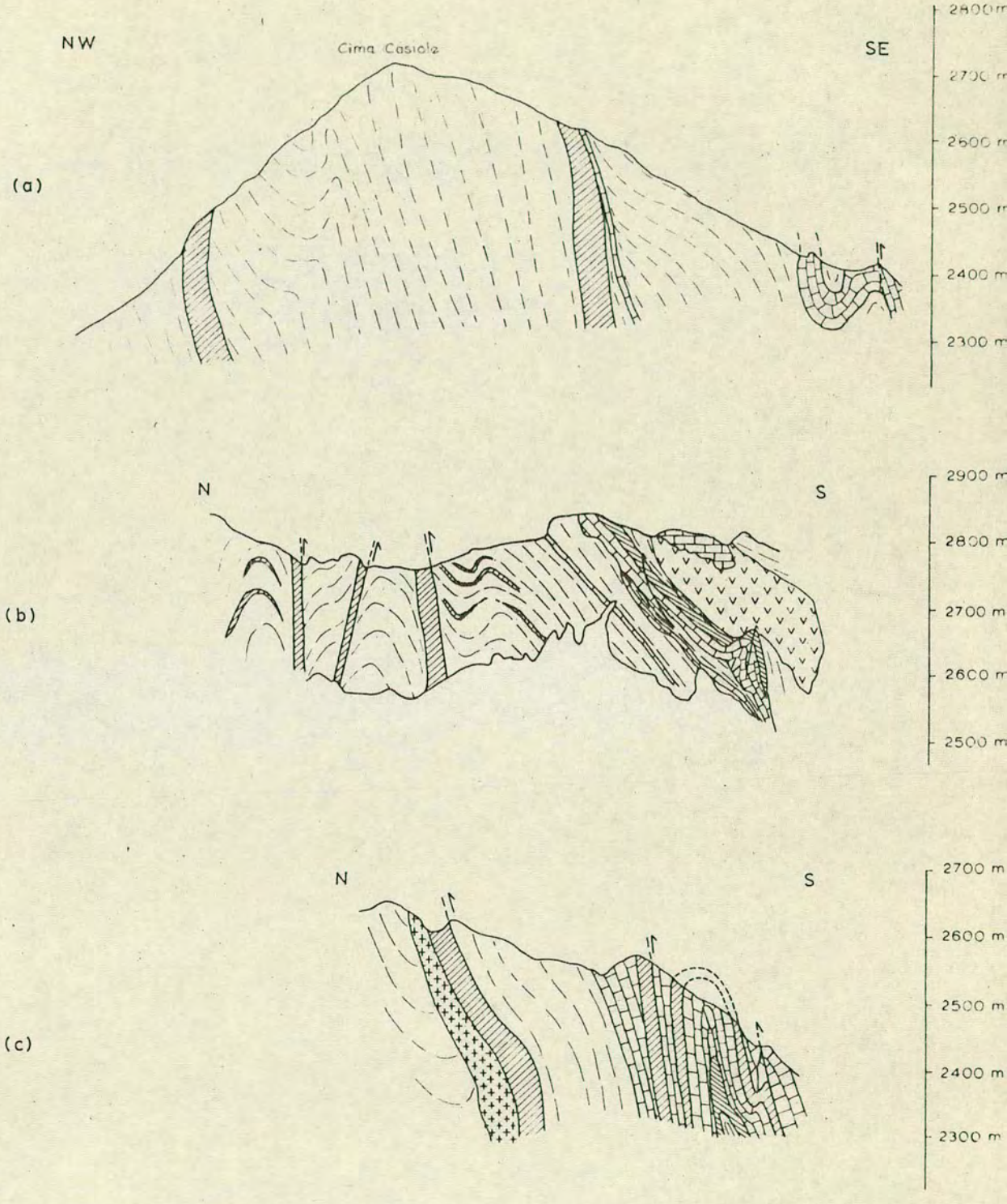
NW
Cima Casiola
SE
(a)
2800 m
2700 m
2600 m
2500 m
2400 m
2300 m
N
S
(b)
2900 m
2800 m
2700 m
2600 m
2500 m
N
S
(c)
2700 m
2600 m
2500 m
2400 m
2300 m
Pelitic Gneiss
Marble
Mylonite
Amphibolite
Pegmatite
Ultrabasic

they have a variable thickness along the strike. Generally, they become sub-divided into several smaller zones whose thicknesses also diminish laterally. New mylonite zones are then developed in adjacent parts of the pelitic gneiss.

The mylonitic gneiss foliation is axial planar to the f_3 asymmetrical folds, and this foliation may be traced into the phyllonite zones where it is the dominant structure. In several parts of the Central Alps, f_3 folds fold mylonite bands, for example in the Casiole sheet at M94, a medium-scale, north facing f_3 fold has folded thin phyllonite bands in the partly mylonitic gneiss. More rarely, in the Albiolo sheet, f_2 folds also fold the mylonitic fabric. These observations suggest that folding has post-dated mylonitisation in some areas, but that the two events were synchronous over much of the area mapped.

Within the pelitic gneiss, thick Hercynian pegmatites form a locus for mylonite development. Pegmatites, quartz veins and dykes have been noted by Higgins (1971, p.35) to be sites of mylonite development and it is apparent in the area mapped that pegmatites and thick quartz veins act, either as more viscous zones adjacent to which mylonites are formed, or as less viscous zones along which yield preferentially occurs. Treagus (1973) has shown that if the principal stress acts at an angle of up to 45° (assuming plane strain) to a viscous layer, it will be refracted to act at a low angle to the layer boundary. The actual angle is dependent on viscosity contrast, assuming Newtonian flow. Since quartz is known to have a very sharp yield point in a hydrous environment, as shown by the experimental work of Tullis et al,(1973) and Griggs and Blacic (1965), it is probable that it initially acts as a highly viscous sheet creating a zone of contact strain around the pegmatite.

At M153, in the central part of the Casiole sheet, a 1 to 3 m. pegmatite dipping 60° N contains a moderately strong mylonitic foliation. The gneiss for 50 cm. each side of the pegmatite is strongly foliated (f_3) and

contains close to tight f_3 folds. The tightness of the folds increases towards the pegmatite-gneiss contact. The fold axes plunge moderately west and their axial planes lie at a low angle to this contact. When viewed down plunge, the folds have an S-profile north of the pegmatite and a Z profile to the south. It can be seen from Figure 44(a), showing hypothetical shear stress trajectories associated with an inclined layer for a layer-matrix viscosity ratio of 35 (after Treagus 1973), that maximum shear stress trajectories lie sub-parallel to the layer margins, providing that the layer is initially inclined at an angle to the principal stress directions. The value for the layer/matrix viscosity ratio is an average value taken from analysis of pegmatite buckle folds in the Tonale Pass area. The use of lower values (c.f. Cliff et al, 1971) causes no significant change in the conclusions. This stress distribution would explain the observed field relationships. The nature of the associated f_3 asymmetric folds suggests that the principal stresses did lie at a considerable angle to the layering, and that the maximum principal stress acted in a north-south direction plunging gently south.

Although mylonites generally form in quartz-rich rocks, similar structures have been reported from ultra-basic and basic igneous rocks; for example in dunite at St.Paul's Rocks (Tilley, 1947), and from metadolerite in the Bear Tooth Mountains, Montana (Prinz and Poldervaart, 1964).

7.12 Development of mylonites in pelitic gneiss

During the mylonitisation of the paragneiss in the Tonale Pass area, initial shear strain will be taken up by mica yield (Etheridge and Hobbs, 1973) which can occur at low differential stresses and moderate temperatures and confining pressures. Subsequent deformation and possible associated minor fracturing promotes the movement of fluid along these zones, which in turn causes a lowering of shear strength, particularly in quartz. This results in the formation of a mylonite zone. In gneiss in which mica yield only occurs to a minor degree, microfracturing and

Figure 44(a) - Hypothetical shear and normal stress trajectories with a viscous inclined layer. The trajectories are drawn using the data of Treagus, 1973, and show the concentration of shear stress within and adjacent to a viscous layer.

Figure 44(b) - Stress distribution for a block under horizontal compression (Hafner, 1951). a is an arbitrary constant which may be calculated from the stress equations given the stress values (see Ramsay, 1967, p. 303-5). The position of the maximum shear stress trajectories in the lower diagram may delineate the position at which thrusts will initially develop.

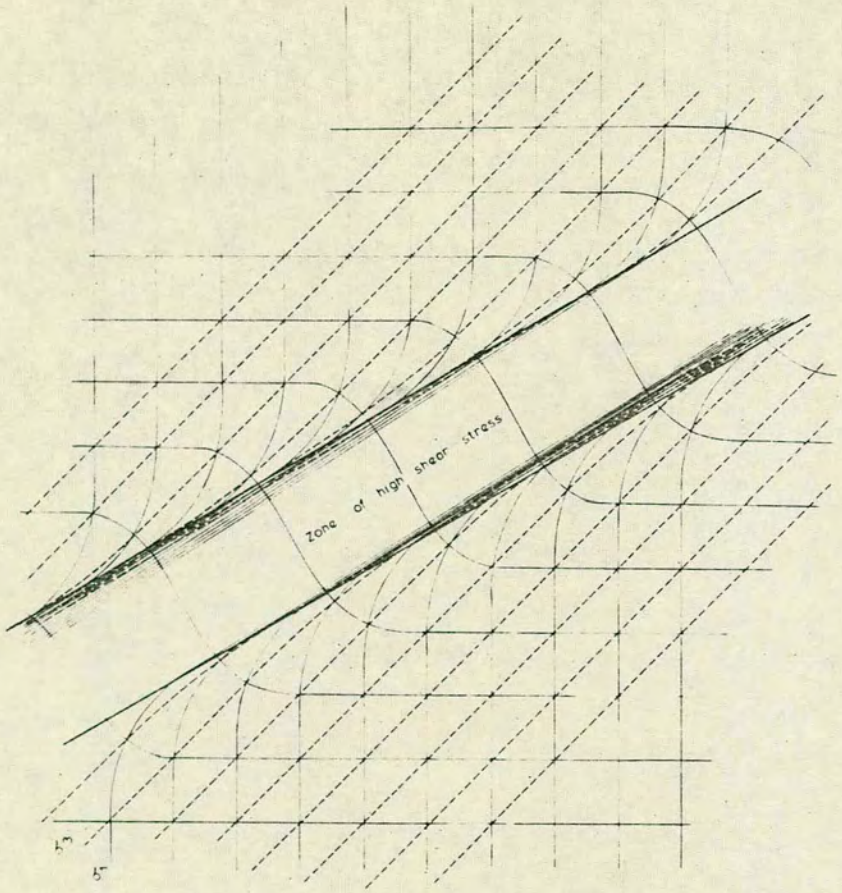
Zone of high shear stress
σ3
σ1

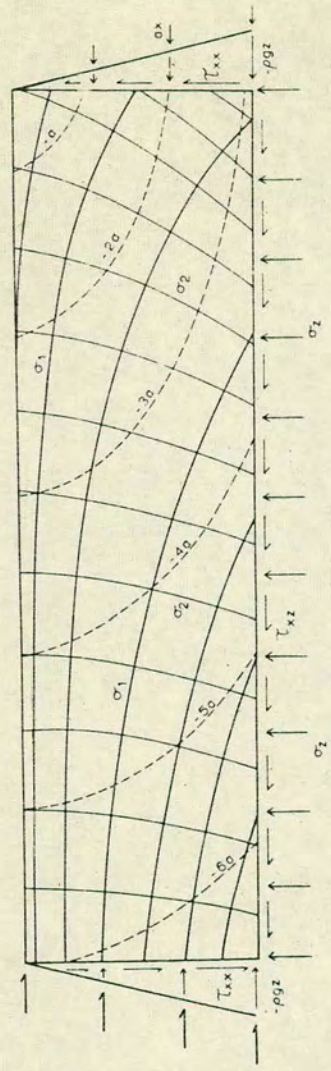
σx
τxx
ρgz
σ1
σ2
σ3
τxz
-σ
-2σ
-3σ
-4σ
-5σ
-6σ

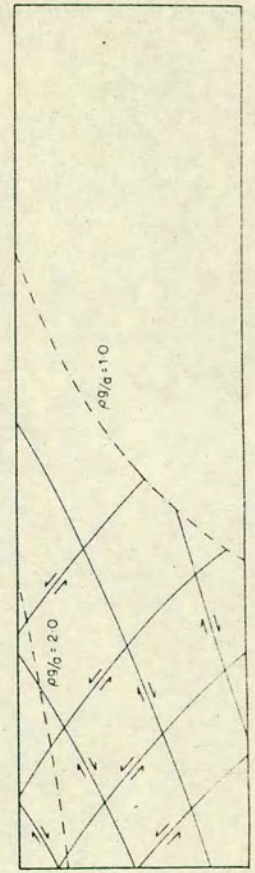
ρg/σ=10
ρg/σ=20

hence pseudotachylite development may occur, particularly in areas of low fluid pressure. Different mylonites examined from the Tonale Pass area show that the effects of fluid pressure were not consistent. Gneisses with a high mica content may never build up high differential shear stresses, which explains the % shortening variations from buckled pegmatite veins in biotite-rich and non-biotite rich gneiss. Strain rates will be lower in the biotite-rich gneiss, fluid diffusion rates greater, and the lower differential stresses will favour ductile deformation of quartz. This deformation may occur by recrystallization, sub-grain development (dislocation climb), grain boundary sliding and possibly intra-crystalline slip (Bell and Etheridge, 1973; Wilson, 1973). The various mechanisms are discussed in the section on quartz preferred orientation.

7.13 Role of marble, amphibolite and pegmatites in mylonite formation

Some major mylonite zones are marked by a change in regional orientation of the gneissic banding. Where a thick marble band occurs adjacent to one of these major structural breaks, no mylonites are developed. The translative movement is taken up in the ductile marble layer, presumably by a combination of recrystallization, twin gliding and other ductile deformation mechanisms (e.g. grain boundary sliding, dislocation climb). The f_3 structures in the marble bands conclusively show the ductile nature of this material during the Early Alpine event. At T132, 300 m. S.E. of Cima Casiole, a 1 to 2 m. band of crystalline marble lies immediately above a thick mylonite zone. The band consists of a single fold with its axis plunging 35° to 242°, and its axial plane parallel to the adjacent gneiss and amphibolite banding. The fold is consistent with a "flow" movement to the south (c.f. f_3 folds in marble).

Thin marble bands are commonly associated with major mylonites, where the marble appears to act as a highly ductile material. It is not possible to assess the

amount of translative movement which has taken place along these bands. It is interesting that Peach and Horne (1907) and Wilkinson (1956) have described a coarsly-crystalline marble within the Moine mylonite zone in the area east of Loch Eriboll, N.W. Scotland. Milnes (1968) has shown that marked changes of orientation of the principal strain axes take place across thin marble bands in the Lower Pennine Nappes of the Ticino. The role of marble as a "movement" horizon is well shown at the base of the Glarus Nappe, in the Helvetic Nappes of central Switzerland. Here, the Lochseitenkalk forms a horizon of large-scale differential movement which has occurred under Lower Greenschist metamorphic conditions.

Amphibolite in mylonite zones in the Tonale Pass area has recrystallized to form strongly lineated bands, which in parts contain tight asymmetrical folds. These features are described in a later section (see 7.60). Rarely, as at M197 in the Albiolo sheet, 500 m. N.W. of Cima Casiole, the amphibolite does form small mylonite zones, but this is exceptional in the Tonale Pass area.

At M356, in the northernmost part of the Casiole Sheet, 250 m. S.S.E. of Vetta d'Albiolo, several 1 to 5 m. phyllonite zones occur in mylonitic muscovite-sillimanite rich paragneiss. The structures in the gneiss show that underthrusting to the north has occurred along these zones. Figure 44(b) shows the stress distribution given by Hafner (1951) for a block under horizontal compression. The maximum shear stress trajectories form a family of curves which slope upwards at a shallow angle towards the unrestrained upper surface of the block. Assuming that the paragneiss sheets of the Austro-Alpine Nappes may be considered as "elastic" bodies, these curves delineate the position at which thrusts will develop. Once a primary overthrust has occurred, the stress distribution will change and local factors, such as the degree of penetration of fluids and disposition of lithological boundaries, will assume more importance. Hence under-thrusting may

well occur in conjunction with overthrusting during the mylonitic event.

In some areas, pegmatite veins may be traced laterally into mylonite zones where they become greatly reduced in thickness. For example, at T372 a 3 m. medium-grained quartz-feldspar-muscovite-garnet pegmatite may be traced into the adjacent Casiole/Albiolo mylonite, where it is only 15 cm. thick. Hence shortening values are of the order of 95%. At M387, in the Casiole sheet, an aplite vein 50 cm. thick passes laterally into a mylonite zone where it is strongly folded on a large and small scale, and a strong axial planar mylonitic foliation is internally developed. These structures show that mylonites are typified by high strain values and that this deformation is of a ductile nature.

7.20 MINERALOGY

As almost all mylonites are derived from the quartz-feldspar-biotite$^{\pm}$muscovite$^{\pm}$garnet$^{\pm}$sillimanite gneiss, the gradual mineralogical changes which occur as we pass into a mylonite zone are retained in the gneiss (c.f.marble, amphibolite). These changes imply that pore fluid pressure (P fluid) was high during mylonite formation since the most important changes are due to extensive hydrolysis. More rarely in mylonites the original mineralogy is largely retained and the abundance of small scale pseudotachylite zones suggests that P fluid was low. Although distinctive textural changes occur in the latter type of mylonite there are only minor mineralogical modifications. Only changes in "wet" mylonites are discussed in the following section.

The mylonites in the Mt.Tonale, Casiole and Albiolo sheets show evidence of two distinct metamorphic events; an earlier Upper Greenschist - Lower Amphibolite grade event which prevailed during the major f_3 movement; a Greenschist grade event which accompanied a later uplift (f_5) centred on the Peio Line. The f_3 mylonites show a systematic decrease in metamorphic grade to the south with

chlorite and albite present in the Vallazza sheet.

Specimen T130, from a minor mylonite zone in the lower part of the Mt.Tonale sheet, shows a gradation from partly deformed paragneiss to phyllonite. Quartz undergoes recrystallization and concomitant grain size reduction. In quartz rich parts, new growth of small mica flakes 'pins' quartz grain boundaries and hence controls their size and shape. The hydration of potash feldspar by the reaction

$$\underset{\text{K feldspar}}{3KAlSi_3O_8} + H_2O \rightleftharpoons \underset{\text{Muscovite}}{KAl_2Si_3AlO_{10}(OH)_2} + 2(K^+) + \underset{\text{Quartz}}{6SiO_2} + O^{--}$$

results in formation of mica aggregates showing optical continuity. This reaction, which occurs extensively in all mylonite zones in the Tonale Pass area, must largely control the fluid composition. The reaction is accompanied by a volume reduction of 13.4%. Excess K^+ ions favour the production of K-mica (Hemley and Jones, 1964) and oxidation occurs. The presence of limonite and hematite in mylonites shows that such oxidation has occurred. In parts, small potash feldspar porphyroclasts are present and these show only minor white mica alteration. Plagioclase changes from mid andesine to oligoclase/andesine (An_{30}) and shows some alteration to white mica. Generally it fragments and forms porphyroclasts. Initially large muscovite flakes which show a variable optical orientation in the gneiss are also changed into aggregates of very fine-grained white mica flakes which show optical continuity. These micas all lie with the basal planes approximately parallel to the mylonitic foliation and also have similar axis orientations. New small biotites have grown in the partially mylonitic gneiss and minor clinozoisite has also formed.

Garnet in the pelitic gneiss becomes progressively fragmented as it is traced into the phyllonite zones. In some mylonites (e.g. T140 - lower part of the Cadil sheet) partial retrogression of garnet to chlorite and

magnetite has occurred. The event preceded the major translation, as fragmented garnet and the retrograded products are commonly spread out along the mylonitic foliation.

Specimen T136B, from the Vallazza/Cadil mylonite zone, is a phyllonitic mylonite with an average matrix grain size, of 0.07 mm., in which two distinct types of garnet are seen. Partially retrograded garnets (to chlorite + magnetite) are flattened, fragmented and in places drawn out along the foliation. These garnets and their retrogression predate the major mylonitic event. Later 0.25 mm. diameter euhedral garnets of very constant size overgrow mylonitic fold hinges in the chlorite-rich bands. Plate 11(b) shows the two types of garnet. Chlorite almost completely replaces biotite in this rock. Several of the later garnets contain true rotation trails (Powell and Treagus, 1967; Cox, 1969) which show that rotation of 50° to 80° about gentle westerly plunging axes. Hence rotational strain occurred during garnet growth (Elliot 1972) and this growth probably occurred in the final stage of mylonitisation in this area. Muscovite (phlogopitic in part) growth and quartz recrystallization occurred subsequent to garnet growth and mylonitisation.

Clinozoisite and more rarely epidote are common in mylonite zones. Their presence is confined to these zones and areas of mylonitic gneiss, and most probably results from the alteration of plagioclase. The reaction: basic plagioclase + water $\rightleftharpoons$ plagioclase + white mica + clinozoisite, has been studied by Ackermand and Karl (1972) who show that this moves from left to right at P H_2O = 2 kb to 4.5 kb and T = 350°C to 500°C respectively. The reaction is best expressed as:-

$$8(NaAlSi_3O_8)_{0.6}(CaAl_2Si_2O_8)_{0.4} + 3KAlSi_3O_8 + 2.5H_2O \rightleftharpoons$$

Andesine K feldspar

$$4(NaAlSi_3O_8)_{0.7}(CaAl_2Si_2O_8)_{0.3} + 2KAl_2Si_3AlO_{10}(OH)_2 +$$

Oligoclase/Andesine Muscovite

$$10SiO_2 + Ca_2Al_3Si_3O_{12}(OH) + 2Na^+ + K^+ + 1.5(O^{--})$$

Quartz Clinozoisite

The reaction has a volume reduction of approximately 6.9% solid components and hence would be favoured by increased P H_2O. An alternative reaction for clinozoisite growth is

$$6CaAl_2Si_2O_8 + K^+ + 2H_2O + (OH)^- \rightleftharpoons 3Ca_2Al_3Si_3O_{12}(OH) + KAl_3Si_3O_{10}(OH)_2$$

Anorthite → Clinozoisite; Muscovite

(Cliff et al, 1971).

The volume reduction is 5% for An_{50}. Possibly a more realistic reaction in the Greenschist grade f_5 mylonites where epidote, albite and chlorite are the typical minerals is:-

$$3K(Mg,Fe)_3Si_3AlO_{10}(OH)_2 + 20(CaAl_2Si_2O_8)_{0.4}(NaAlSi_3O_8)_{0.6} + 6H_2O + 2(O^{--}) \rightleftharpoons 12NaAlSi_3O_8 + 4Ca_2AlFe^{3+}AlSi_3O_{12}(OH) + 3KAl_2(Si_3Al)O_{10}(OH)_2 + (Mg,Fe)_5Al_2Si_3O_{10}(OH)_8 + SiO_2.$$

Biotite; Andesine → Albite; Epidote; Muscovite; Chlorite; Quartz

The reaction results in a volume decrease of 1.87% solid components. Liou (1973) has shown that epidote stability is strongly favoured by high f O_2 which is consistent with the feldspar - mica reactions in the mylonites. High P H_2O favours reactions to give epidote and also promotes its rate of nucleation. Similar reactions for epidote and clinozoisite formation from Morteani and Raase (1974) are given below:-

1) $$10(CaAl_2Si_2O_8)_{0.4}(NaAlSi_3O_8)_{0.6} + KAlSi_3O_8 + 2H_2O \rightleftharpoons 2Ca_2Al_3Si_3O_{12}(OH) + KAl_2Si_3AlO_{10}(OH)_2 + 2SiO_2 + 6NaAlSi_3O_8$$

Andesine; K feldspar → Clinozoisite; Muscovite; Quartz; Albite

Volume reduction of about 4.8% solid reactants.

2) $$30(CaAl_2Si_2O_8)_{0.4}(NaAlSi_3O_8)_{0.6} + 2K(Mg,Fe)_3AlSi_3O_{10}(OH)_2 + 4KAlSi_3O_8 + 7H_2O + 3(O^{--}) \rightleftharpoons 6Ca_2Al_2Fe^{3+}Si_3O_{12}(OH) + 6KAl_2Si_3AlO_{10}(OH)_2 + 6SiO_2 + 18NaAlSi_3O_8$$

Andesine; Biotite; K feldspar → Epidote; Muscovite; Quartz; Albite

Volume reduction of about 3.5% solid reactants.

3) $30(CaAl_2Si_2O_8)_{0.4}(NaAlSi_3O_8)_{0.6} + 6K(Mg,Fe)_3AlSi_3O_{10}(OH)_2$

Andesine Biotite

$+ 3H_2O + 3(O^{--}) \rightleftharpoons 6Ca_2Al_2FeSi_3O_{12}(OH) +$

Epidote

$6KAl_2Si_3AlO_{10}(OH)_2 + 6SiO_2 + 6Fe_2O_3 + 18NaAlSi_3O_8$

Muscovite Quartz Hematite Albite

Volume reduction of about 2.5% solid reactants.

Clinozoisite, epidote and Mn-zoisite porphyroclasts up to 3 mm. long (generally 0.5 - 1 mm.) are found in mylonites. These porphyroclasts are fractured and have trails along the mylonitic foliation as shown in Plate 12(a). Epidote/clinozoisite growth is ascribed to a period of retrograde metamorphism under moderate fluid pressures which immediately preceded mylonitization in many areas. Specimen T362, a fine grained phyllonitic mylonite from the Casiole/Albiolo mylonite zone, contains a Lower Amphibolite facies mineralogy. Small tabular clinozoisite crystals have a preferred orientation with their prism sections lying sub-parallel to the Y axis of the finite strain ellipsoid.

The strict relationship between the mylonites and clinozoisite is well seen in specimen T262A, from the lower part of the Vallazza Nappe. Mineralogical changes of the original quartz-feldspar-biotite-garnet gneiss have occurred in small pervasive f_3 shear zones, whose orientation is coincident with the original biotite foliation. Grain size reduction of quartz has occurred by partial recrystallization, and chlorite, sericite and small clinozoisite laths have formed along these zones. Garnet is partially retrograded to chlorite and magnetite. A small mylonite zone 3.4 cm. long occurs within the rock, and within this sharply bounded zone fine grained (0.02 mm. average diameter) quartz, albite, clinozoisite, sericite and opaques are present. There is no trace of the original mineralogy but some compositional variations (e.g. bands rich in sericite or clinozoisite) are present. The texture and mineralogy in the zone are identical to those seen in many thick phyllonites in the Tonale Pass area.

Plate 12

(a) Ovoid clinozoisite porphyroclast with fragment trails sub-parallel to the mylonite foliation. The foliation is defined by sericite and quartz with minor feldspar. (T252 Mt.Tonale/Casiole Mylonite).

(b) Very fine grained mylonite found at the Peio Line (M294). The assemblages are greenschist grade (albite, epidote, chlorite, quartz, sericite) in this mylonite.

(c) Typical finely-banded phyllonitic texture showing zones of strong differential movement (defined by darker bands). The zones lie at a low angle to the mylonitic banding. (T252 - Mt.Tonale/Casiole Mylonite).

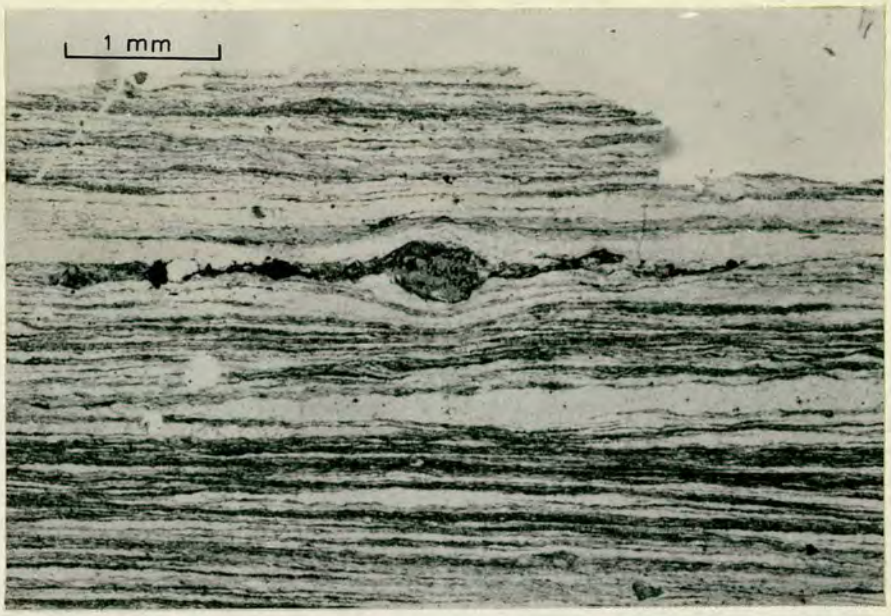
1 mm

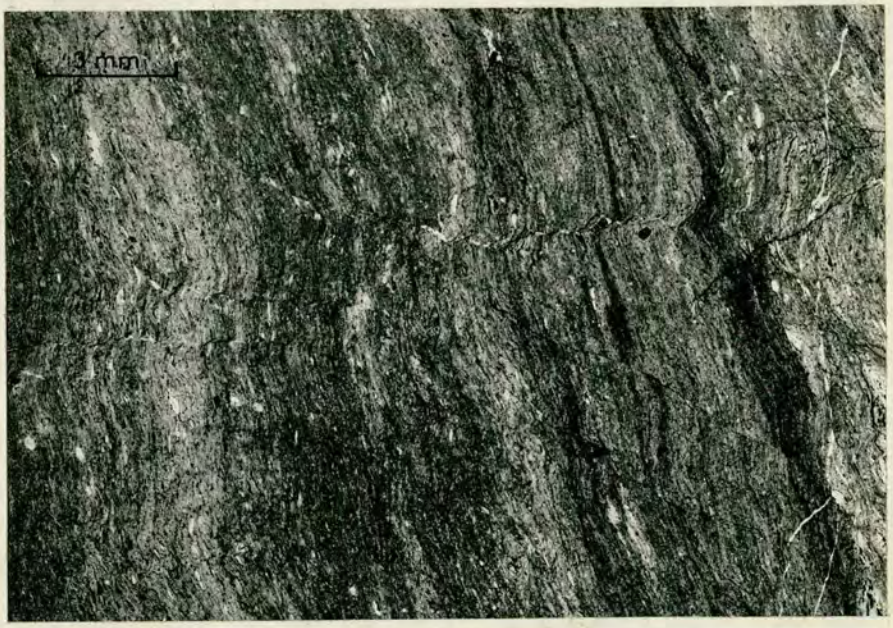
1 mm


2 mm

Where original sillimanite is present in the marginal parts of mylonite zones, it is extensively altered to white mica. The mineral is only found in partly mylonitic rocks and "dry" mylonites. Possible hydrolysis reactions for sillimanite are:-

1) $Al_2SiO_5 + KAlSi_3O_8 + H_2O \rightleftharpoons KAl_2Si_3AlO_{10}(OH)_2 + SiO_2$
Sillimanite K feldspar Muscovite Quartz

2) $Al_2SiO_5 + 3SiO_2 + H_2O \rightleftharpoons Al_2(Si_4O_{10})(OH)_2$
Sillimanite Quartz pyrophyllite

Equation 1) results in a 3.3% volume increase and equation 2) 4.6% increase. The natural instability of anhydrous Al-silicates in a moderate fluid pressure - moderate temperature environment and exothermic nature of the above reactions will counteract the effects of volume increase.

Where amphibolite occurs in or adjacent to large mylonite zones (e.g. Albiolo sheet), blue birefringent clinozoisite and oligoclase/andesine (An_{30-33}) replace the original andesine - labradorite assemblage. In parts of the Albiolo sheet, plagioclase is completely replaced by clinozoisite (M337) and the original albite twins are preserved. 0.5 to 1 mm. wide albite porphyroblasts have grown in this rock. Tremolite partially to completely replaces green hornblende in these amphibolites, although the tremolite is subsequently commonly bent and fractured. The reaction :-

Calcic plagioclase + hornblende + quartz + water $\rightleftharpoons$ tremolite + less calcic plagioclase + clinozoisite may have been important where tremolite is well developed.

In some zones, clinozoisite + white mica + quartz + tremolite + minor hornblende constitute the major proportion of the amphibolite. This assemblage is a result of alteration of plagioclase + hornblende in the presence of H_2O and K^+ rich fluids. Calcite and Mg chlorite are also common. This alteration is generally restricted to planar zones in the amphibolite along which fluid penetration has occurred (shear zones ?). Lenticular areas of unaltered amphibolite 1 mm. to 10 m. long (the feature occurs on all scales) remain, although these become progressively smaller

as the degree of mylonitic deformation increases.

In amphibolite mylonite, fractured, bent and recrystallized aggregates of tremolite and rounded oligoclase/andesine porphyroblasts lie in a fine-grained foliated matrix of tremolite, clinozoisite, white mica, and minor quartz, magnetite and oligoclase/andesine. Recrystallization of tremolite to medium to fine-grained aggregates has occurred in the matrix. The mylonitic banding, defined generally by lines of disseminated opaques, is tightly folded.

Large muscovite plates up to 5 mm. across (average 2 mm.) are common in mylonite zones, particularly in the Mt. Tonale/Casiole and Casiole/Albiolo mylonites. The muscovite is absent from the finer-grained f_3 mylonites. The plates grow across the f_3 mylonite fabric and cross-cut isoclinally folded quartz veins. The crystals are themselves fractured and folded by the later f_5 deformation. In specimen T368B from the Casiole/Albiolo mylonite, large muscovite plates are most abundant in the more pelitic bands, reflecting initial compositional variations. These plates show variable optical orientation which is interpreted as reflecting crystallization under a non deviatoric stress field subsequent to the f_3 mylonite event. High water activity is necessary for muscovite growth, and the relatively large grain size compared with that of the mylonite matrix is suggestive of moderate to high P fluid/P total ratios (Gresens, 1967). High fluid pressure was localised in the mylonite zones during the f_3 event, whereas the surrounding gneiss shows only minor mineralogical and textural changes compatible with deformation under lower fluid pressures.

7.30 TEXTURES

7.31 Introduction

Mylonites are typified by fine banding, which in the Tonale Pass area is formed by quartz and pelite rich bands. Characteristic phyllonitic textures are illustrated in Plates 12(b) and 12(c) where the original gneissic compositional banding is now defined by diffuse quartz rich

and mica, clinozoisite and opaque rich bands and lenticular zones. Where quartz veins were initially present in the gneiss, they become much reduced in thickness but still retain their initial cross-cutting relationship as shown in Plate 13(a). The complete recrystallization, (except for rare orthoclase, garnet or clinozoisite porphyroblasts) observed vein/phyllonitic banding relationships, and common occurrence of isoclinal quartz vein folds, show that deformation has occurred largely by ductile flow mechanisms. The small-scale well-defined, lenticular nature of mylonitic banding, which has been reported by several authors (Vernon, 1974; Harker, 1939 p.169) is only found where recrystallization is not dominant. For example, in several f_3 mylonites (Plates 13(b) and 13(c)) quartz grains are deformed into elongate ribbons with well-developed deformation bands, and garnet, clinozoisite and feldspar are fractured and fragmented. Biotite and/or chlorite generally define the new mylonitic foliation. Even in these rocks discordant small folded and sheared quartz veins show continuity <u>across</u> the mylonitic foliation (T136B). Many phyllonitic mylonites show no visible banding and the rocks have the appearance of slates.

The origin of mylonitic banding has been attributed by Vernon (1974) to plastic flow of individual large mineral grains and aggregates in an initially coarse-grained polymineralic rock. Deformation and recrystallization textures similar to those illustrated in Plates 13(b) and 13(c) are reported by Tullis (1968) and Tullis et al (1973) for quartzite experimentally deformed at 15 kb. confining pressure, 700°- 1000°C and $\dot{\varepsilon}$ of 10^{-5} to 10^{-7}/sec. The mylonites described here may be considered by some authors to have deformed by cataclastic flow. The term cataclastic implies brecciation and microfracturing and its use and brittle connotations are best avoided. Bell and Etheridge (1973) have shown that Amphibolite grade mylonitic textures such as polygonisation, sub-grains, serriate grain boundaries and feldspar kink bands, result from ductile deformation, recovery and recrystallization.

Plate 13

(a) Folded quartz vein in a phyllonitic mylonite. Despite very strong deformation the cross-cutting relationships of the vein to the compositional banding are still visible. (T252 - Mt.Tonale/Casiole Mylonite).

(b) Mylonite showing fractured and fragmented feldspar and clinozoisite. The fine banding is defined mainly by biotite, and sericite (M4 - mylonite in uppermost part of Mt.Tonale Sheet).

(c) 'Dry' mylonite consisting of fractured and fragmented grains of oligoclase-andesine, K feldspar, biotite, sillimanite and garnet. Quartz occurs in long strained ribbons. Thin pseudotachylite veins are common in this rock. Minor late kinking has occurred. (T70A - Lowermost part of Vallazza Sheet).

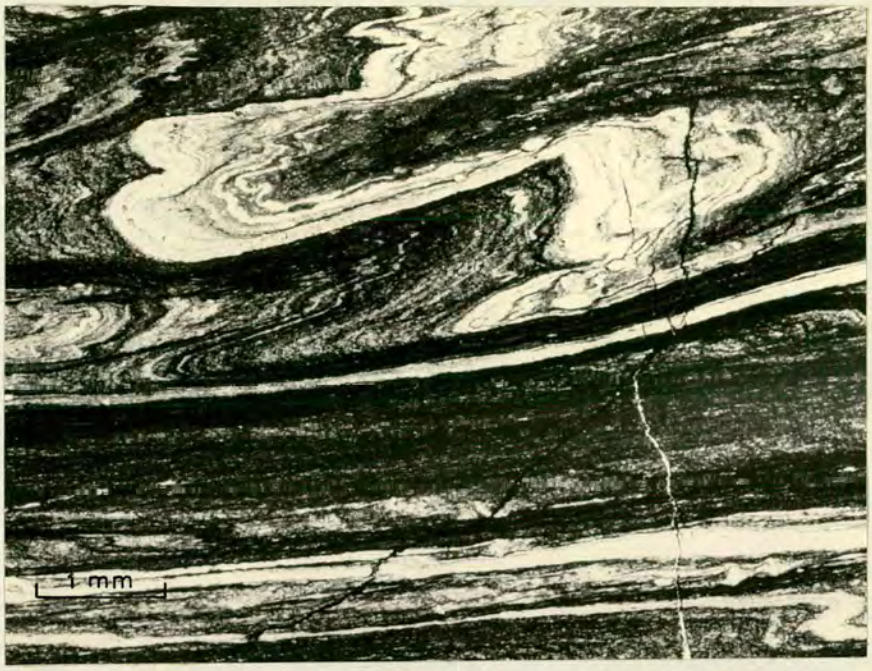
1 mm


2 mm


2 mm

Mylonites in the Tonale Pass area show similar features but recrystallization is generally dominant. The degree of recrystallization is attributed mainly to the availability of water. In f_5 mylonites where muscovite, albite, epidote-clinozoisite and rarely potash feldspar form sparse, small, remnant porphyroclasts, water was probably more readily available than in those f_3 mylonites where only partial garnet retrogression has occurred, and the original gneissic texture has been deformed but not extensively recrystallized.

Several f_3 mylonites contain thin pseudotachylite bands across which dislocation has occurred, showing that very low fluid pressures prevailed (see Sibson, 1973). In general no discrete slip surfaces are seen in the mylonites. Where the mylonitic foliation is strongly developed, lateral displacement is greater and the microscopic textures are best explained by ductile heterogeneous simple shear. The foliation corresponds to the XY plane (Ramsay and Graham, 1970), which at high shear strains lies very close to the shear direction defined by the mylonite zone margins.

7.32 Development of Mylonitic texture

In specimen T262A, from the southernmost part of the Vallazza sheet, a 3.4 cm. long mylonite zone lies in a quartz-feldspar-biotite-garnet-sillimanite gneiss. As shown in Plate 14(a), marked textural, structural and mineralogical changes (see previous section) have occurred in the mylonite zone. Feldspar porphyroblasts with biotite (partly altered to chlorite) pressure shadows are common within the paragneiss. About 4 mm. laterally from the mylonitic zone, a feldspar porphyroblast and adjacent pressure shadow have been rotated 16° ($\gamma = 0.29$). A similar sense of rotation is shown by the orientation of the structures within the 3.4 cm. mylonite zone. The quartz grains in the mylonite zone have a maximum length of 0.1 mm. (cf. gneiss - irregular to rounded grains up to 1 mm. across) and an average aspect ratio of 3.5 : 1. Clinozoisite grains in this zone have an average length of 0.01 mm. whereas in the weak shear zones in the gneiss they are 0.15 mm.

Plate 14

(a) Small mylonite zone developed in pelitic gneiss. Note that the foliation defined by elongate quartz grains lies at a variable angle to the sides of the zone in differing parts. Grain size reduction has occurred and the mineralogy is markedly changed. (T262A - Southern part of Vallazza Sheet).

(b) Quartz recrystallization in a pelitic gneiss caused by the f_3 deformation. The recrystallization has occurred preferentially in small areas of high strain, e.g. between the feldspar grains, and along grain boundaries. Sub-grain development from strained quartz may also be seen. (T85B - Vallazza Sheet).

(c) Quartz recrystallization around an included fragment of white mica. Note the preferential development along grain boundaries and sub-grain growth. (T85B - Vallazza Sheet).

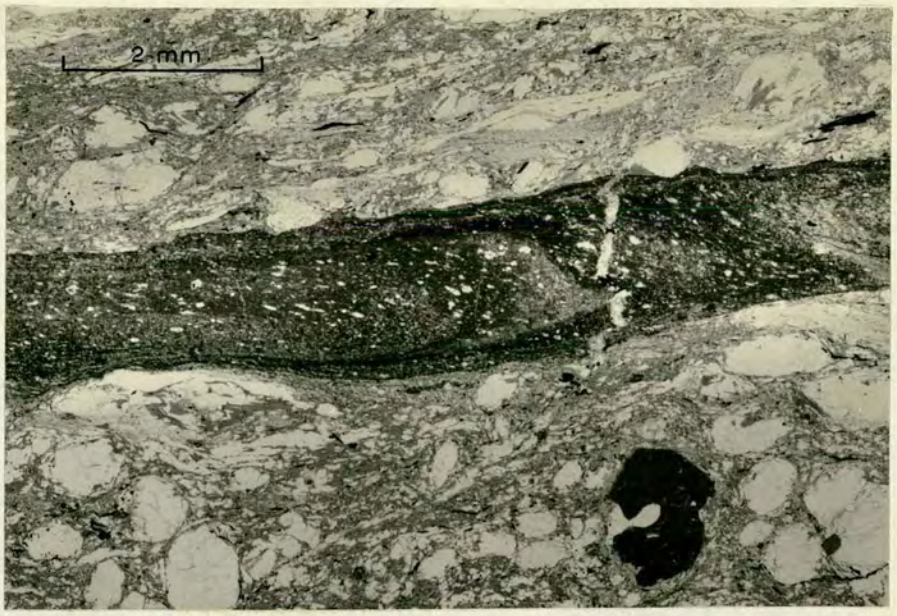
2 mm

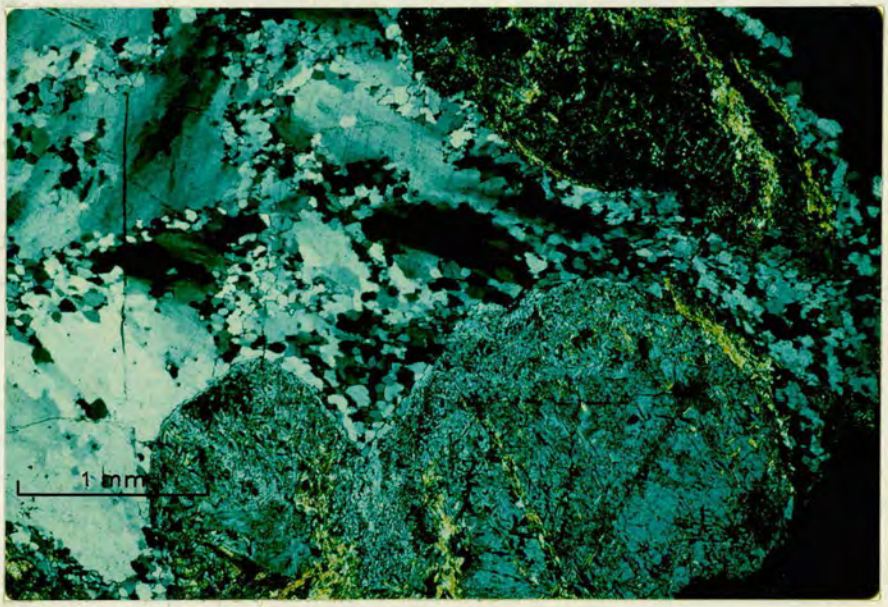
1 mm

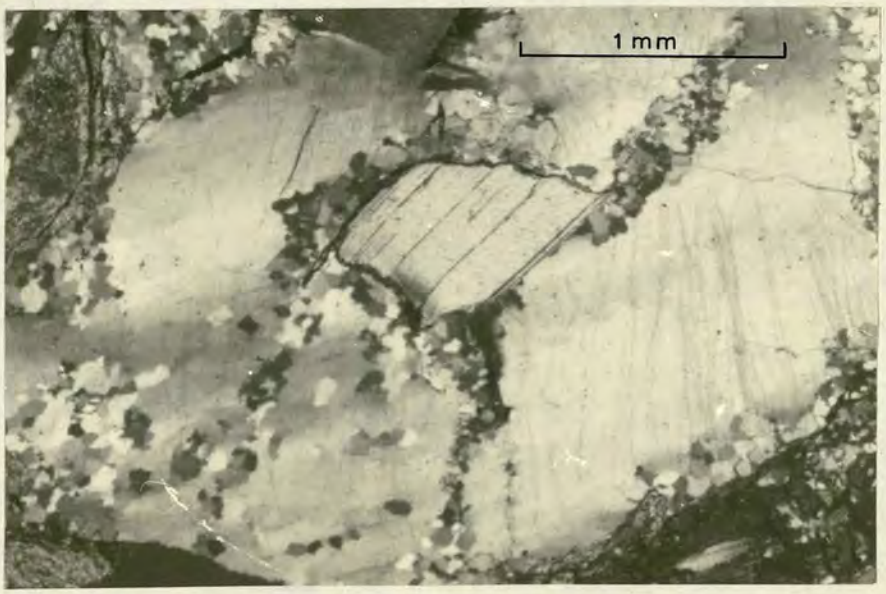
1 mm

long. Chlorite, sericite and clinozoisite are developed in these weak shear zones and suggest that fluid penetration has occurred preferentially along these zones. In the mylonite zone, quartz, clinozoisite, albite, sericite and opaques define a new foliation whose angle to the margins of the mylonite zone varies from 14° in the central part of the zone (foliation strongly developed) to 23° at the extremities (foliation weakly developed). A Z profile fold is defined by compositional banding and the foliation is axial planar to this structure.

These features are consistent with an origin by simple shear. The angle θ, between the foliation and mylonite zone margin, is related to the amount of simple shear (γ) by the formula

$$\gamma . \tan 2\theta = 2$$ (Ramsay and Graham, 1970).

Assuming no pure shear component is involved, maximum values of 3.76 and minimum values of 1.93 are obtained. This evidence suggests that mylonites developed in paragneiss during the f_3 event (Greenschist grade in this area) after a shear strain of about 1.9. Hara et al (1972) have shown that stable C-axis orientations only result after a shear strain of 1.8 suggesting that this amount of strain is required to establish a dominant new fabric.

7.33 Quartz grain size

Grain size reduction has occurred in all mylonite zones in the Tonale Pass area. As shown by Higgins (1971), grain size reduction by cataclasis (fracturing, brecciation) or recrystallization has occurred in all mylonitic rocks. In no specimens from the Tonale Pass area has quartz grain size reduction occurred by cataclasis.

The f_3 and f_5 mylonites can generally be distinguished by their differing textures and mineralogies. The average grain size in f_5 mylonites is 0.006 mm. with quartz veins showing partial recrystallization to grains about 0.017 mm. across. f_3 phyllonitic mylonites have an average grain size of 0.014 mm. with recrystallized grains in quartz veins ranging from 0.02 to 0.15 mm. in diameter. Individual quartz grains are commonly equidimensional except where

large numbers of small mica flakes are present. Average quartz grain size in the pelitic gneiss is 0.8 mm. but large irregular grains up to 6 mm. long are seen.

In specimen T130 quartz grains initially 2 to 4 mm. in diameter become strained (resulting in deformation bands) and then, on further deformation, recrystallise to grains 0.3 mm. across. Further quartz grain size reduction to about 0.02 mm. (0.01 - 0.03 mm.) occurs in the phyllonite zone. Grain size in the mylonites is in part controlled by mica and opaque grain sizes. The figures quoted above refer to pelitic bands, quartz rich bands generally showing slightly larger grains. Moderate fluid pressure and high strain rates which occur during mylonite formation will promote nucleation and development of small grain sizes (high energy configuration). Increased temperature favours growth to larger grain sizes. Bell and Etheridge (1973) report that a quartz-feldspar-mica phyllonitic mylonite which probably formed under Upper Amphibolite conditions (T.H.Bell pers. comm. 1973) shows an average grain size of 0.03 mm. Tullis et al (1973) have produced similar grain sizes (approximately 0.03 mm.) in quartzite experimentally deformed at 900°C and 10^{-7}/sec. These conditions are equivalent to 500°C at 10^{-11}/sec. (see Figure 7 in Tullis et al, 1973). Hobbs (1968) has shown from experimental deformation of single quartz crystals that grain size is inversely proportional to strain rate, all other parameters being constant. Hence we can get a crude qualitative estimate of the maximum strain rate from the size of recrystallized quartz grains in mylonites. Maximum compressive strain rates of about 10^{-11}/sec. are inferred for f_3 and f_5 mylonites in the Tonale Pass area; the smaller grain size in f_5 mylonites results from their lower temperature of formation. It must be emphasized that these estimates are subject to great uncertainty. They do show that strain rates greater than those generally accepted for folding and deep level faulting (approximately 10^{-14}/sec.) occur in mylonite zones. This suggests that mylonites may form in only

3,000 to 4,000 years. Since strain rates probably increase as mylonites develop this is an absolute minimum. Maximum times of 3 to 4 m.y. are obtained if $\dot{e} = 10^{-14}$/sec.

The effects of locally inhomogenous stress patterns on grain size is well seen in specimen T85B, a quartz-feldspar-muscovite-biotite gneiss, deformed by f_4 "crenulation" folds, from the upper part of the Vallazza sheet. The gneiss contains quartz grains up to 4 mm. long although the average size is 0.8 mm. As shown in Plates 14(b) and 14(c) strain shadows are well-developed and quartz recrystallization has occurred along grain boundaries, zones of well-developed strain-shadows, and adjacent to mica inclusions. New grains are approximately equidimensional and have an average diameter of 0.04 mm. The recrystallized quartz grains are small (average 0.017mm.) and elongate where they lie between two large relatively "competent" potash feldspars.

These observations show that recrystallization is partly controlled by the areas of greatest strain, where dislocation densities and hence lattice strain energy are high. The features lower the activation energy of nucleation (Spry, 1969 p.119) and hence promote the formation of large numbers of small grains. Grain boundary diffusion, which Elliot (1973) suggests is aided by the concentration of H_2O, CO_2, HCl, H_2S and HF at grain margins, appears to be important in the development of new grains. This process may be favoured by the development of dense dislocation arrays in quartz adjacent to more rigid feldspars.

Subgrain development is common in T85B, resulting from dislocation climb and migration to form stable wall-like arrays (Spry, 1969 p.66). Dislocation movement is favoured by increased temperature and high intracrystalline shear stresses. Experimental syntectonic recrystallization (confining pressure 10-15kb; T400° - 950°C; $\dot{e}$ 10^{-5} and 10^{-6}/sec) of single quartz crystals (Hobbs,1968) showed that sub-grains form in deformation bands at low strains and increase their relative misorientation as strain

increases. The new grains show partial host orientation control but generally lie with their c-axes at about 50° to σ_1. New grains with c-axes at 20° to 40° to the host c-axis grow at the expense of the orientations. Hobbs rejected the hypothesis of strain assisted nucleation and showed that sub-grain growth as described above, results in a "recrystallized" grain mosaic. In specimen T85B, simple observation with a gypsum plate shows that no particular new grain orientation is dominant. The degree of grain growth is variable, with new grains located at lattice strain discontinuities, except where almost complete recrystallization has occurred and then various stages of the process described by Hobbs are seen. It appears that strain assisted nucleation occurs at sites of locally high strain whereas sub-grain development and recrystallization occurs over more uniformly strained grains.

These recrystallization textures are commonly developed in slightly mylonitic gneiss affected by the f_3 deformation, with new grains having an average diameter of 0.05 mm. In highly micaceous rocks such quartz textures are not developed, probably because mica preferentially absorbs the strain. When chemical reactions become advanced, quartz grains recrystallize to a grain aggregate which becomes progressively deformed with concomitant grain size reduction. In some rocks, for example, phyllonitic mylonite from the Mt.Tonale/Casiole mylonite zone (T362), initially large quartz grains or aggregates become deformed into pods typically 15 mm. long and 0.11 mm. wide.

7.34 Mineralogical textures

Feldspars in mylonites may be partially or even wholly altered to white micas, but generally show fracturing and even brecciation. Deformation twins and kinked albite twin lamellae are rarely seen in plagioclase. Some feldspars retain their coherence and form roughly ellipsoidal porphyroclasts whose size is primarily dependent on the degree of initial alteration. The porphyroclasts may have associated strain shadows infilled with quartz and chlorite. Epidote-clinozoisite and garnet also commonly show

fracturing and brecciation.

Muscovite commonly recrystallizes to fine-grained aggregates which define the mylonitic foliation, lying at between 2^{o} and 5^{o} to the compositional banding. If the shear direction is coincident with the gneissic banding as appears to be the case, then shear strains of 11.5 to 29 are implied. Muscovite rich bands generally show a later fine crenulation cleavage (f_4). Post-mylonite muscovite plates up to 5 mm. across (average 1.5 mm.) are found in and adjacent to f_3 mylonite zones. These muscovites cross-cut isoclinal quartz vein folds and are deformed by f_5 folds. In f_5 mylonites the large muscovites become partially fragmented and recrystallized but may form porphyroclasts.

Biotite recrystallises to smaller less strongly pleochroic (less Fe rich) grains. In some f_5 mylonites, growth of phlogopite from biotite suggests that there is a change in composition of biotite during mylonitisation. Higgins (1971) has suggested that iron may be expelled to form the fine grained magnetite which defines the mylonitic banding. Biotite retrogression to chlorite has occurred in some mylonites.

Garnets in mylonites are reduced in size and become more rounded as mylonitisation proceeds. Some comminution occurs and small fragments are seen along the mylonitic banding. In the "dry" mylonites, and those in which recrystallization is not dominant, garnets are fractured and more rarely fragmented. More generally they are partially retrograded to chlorite and magnetite, and trails of finely comminuted garnet and the retrograde products lie along the mylonitic banding. These features have been used to determine minimum finite shear strains in mylonites. More rarely large fragments of garnet are detached and transported along the foliation. Garnets appear to act as rigid bodies during mylonitisation in the Tonale Pass area.

The textural relationship between porphyroclast or porphyroblast and mylonitic foliation can be used to obtain their relative ages. In the f_3 mylonites, the mylonitic

foliation diverges around garnets and clinozoisite porphyroclasts, although rarely minor truncation occurs. The foliation is generally partially truncated by feldspar porphyroclasts although where the mylonites are highly pelitic, the banding does completely diverge around the feldspar. In rare cases where mica or quartz form small porphyroclasts, the mylonitic banding abuts against them with no deflection. The pattern of porphyroclasts and banding reflects the relative "competence" of both constituents, with maximum foliation deflection occurring where rigid porphyroclasts lie in a ductile matrix.

The variable optical orientation of large muscovites (see previous section) and their abrupt truncation of mylonitic banding and even isoclinal quartz vein folds, shows that they post-date the f_3 mylonitisation. Similar textures are shown by small albites and oligoclase-andesine grains in f_3 mylonites and by epidote-clinozoisite (N.B. act as rigid bodies in f_3 mylonites) and large albites in the f_5 mylonites. These relationships suggest that the minerals grew subsequent to the formation of mylonitic banding. As shown in a previous section, this banding may form at low shear strains ($\gamma = 1.9$) and the presence of deformation twins in albite and partial fragmentation of some epidote-clinozoisite porphyroblasts show that they have been deformed. These features may be explained by synmylonitic growth.

7.35 Occurence and significance of pseudotachylite

Specimen T70A, a pelitic mylonite from the lower Vallazza sheet, consists of quartz, feldspar (mainly K feldspar), biotite, garnet and sillimanite (Plate 13(c). The rock shows a strong planar mineral orientation defined by ribbon quartz and elongate biotite. The quartz shows strong strain shadows which lie parallel to the trace of a later f_4 strain slip cleavage. Biotite laths up to 1 mm. long are commonly fractured, dismembered and strained. They are strongly pleochroic and show no sign of recrystallization. The feldspars are rounded and in places strongly brecciated. Garnet also shows evidence of brecciation and

extension. The sillimanite (fibrolite in part) shows very minor alteration to white mica. Larger crystals are fragmented and rotated, suggesting that they lie at an angle to the principal strain axes (see Ramsay, 1967, Figure 5-72). Small buckle folds of quartz ribbons show well-developed hinge thickening.

Pseudotachylite veins 0.001 to 5 mm. across are abundant in the mylonite. Very minor biotite retrogression to chlorite has occurred adjacent to these veins. Accessory magnetite is brecciated and disseminated along the foliation. A later strain slip cleavage affects all minerals and mylonitic textures; this cleavage lies at 60° (variable 35° to 70°) to the mylonitic foliation. A series of fractures in garnets and feldspars also lie at 55° to 60° to the foliation. These structures can be related to the later f_4 and f_6 events respectively. The textures described above indicate that deformation occurred at very low P H_2O values.

Thin sections of T70A were cut in the plane normal to the pseudotachylite/mylonitic banding intersection, which is taken as approximately the XZ plane. Pseudotachylite veins show a reasonably consistent orientation at an angle of 10°- 16° to the mylonitic banding. The sense of shear in the mylonite is shown by imbrication of garnets, feldspar and sillimanite porphyroclasts, minor quartz vein folds and small-scale folding of some pseudotachylite zones. Pseudotachylite develops by rapid translation across a plane surface in a relatively dry rock (Sibson, 1973; Mackenzie and Brune, 1972; Handin et al, 1973). In T70A, the major pseudotachylite bands are planar and sub-parallel to each other, suggesting that they defined the maximum shear stress direction. Hence, assuming that the foliation developed due to shear strain, the angle θ, between the foliation and the pseudotachylite will define the amount of shear strain, γ. This angle averages 14° and hence γ = 3.76 (γ.tan 2 θ = 2, Ramsay and Graham, 1970). Sub-microscopic mylonitic minor fold axial planes also lie at 14° to the pseudotachylites. Quartz grains in the gneiss are elongated up to 2 to 3 mm. long and 0.2 mm. wide; ratios

in accord with X : Z strain values resulting from simple shear of 3.76 (X:Z = 15.1: 1). Minor pseudotachylite bands show variations in orientation along their length and may be riedel shears, R or R' (Freund, 1974). Alternatively they may result from a heterogeneous shear stress distribution in the banded gneiss. Handin et al (1973) and Logan et al (1973) have shown that glass formed by melting is typical of stick slip movements which take place at temperatures less than 350°C. The glass increases the contact area and raises the frictional resistance of the plane. Hence new pseudotachylite zones are generally formed in the rock for each movement.

Taking the pseudotachylite as a zone of finite width, the temperature rise ($\Delta\theta$) assuming no heat loss is $\Delta\theta = So.d.(\rho.Cp.w)^{-1}$ (Sibson 1973) where So is the shear resistance, d is the displacement, ρ the rock density, Cp, the specific heat, and w, the width of the zone. Taking approximate values for $\Delta\theta$ of 1000°C, Cp of 0.753×10^{7} erg. g^{-1} $^{o}C^{-1}$, and $\rho = 2.75$ gm. cm^{-3}, (Johnson and Wenk, 1974) and measurements of d = 0.5 cm. and w = 2×10^{-3} cm from the thin section;

$$So = \frac{10^{3} \cdot 2.75 \cdot 0.753 \cdot 10^{7} \cdot 2.10^{-3}}{0.5 \cdot 10^{6}} \text{ bars}$$

$$= 83 \text{ bars.}$$

This is rather low compared to experimentally determined shear resistance values (Handin in Clark, 1966).

Mackenzie and Brune (1972) have related the amount of slip along a single plane necessary to cause the formation of pseudotachylite (d) to the shear resistance (So) and total shearing stress - shear resistance (Υ - So) such that

$$d = 2.3 \times 10^{25}/So^{2} (\Upsilon - So)$$

Modifying this equation for the physical parameters above and taking K (conductivity) as 5×10^{-3} cm^{2} s^{-1} gives

$$d = 3.05 \times 10^{24}/So^{2} (\Upsilon - So).$$

$$\text{Hence } \Upsilon - So = \frac{3.05 \times 10^{24}}{0.6856 \times 0.5 \times 10^{16}.10^{6}} \text{ bars.}$$

$$= 890 \text{ bars.}$$

Hence total shearing stress $\Upsilon = 890 + 83 = 973$ bars.
It must be emphasized that these values are minima subject

to large variations dependent on the values of the initial parameters. If we take melting as confined to a series of lenses then (τ - So) is 3.4 times greater. The reduction in frictional stress will be less than for slip along a plane surface and more heat will be transferred to the adjacent rock. From thin sections of T70A, we can see that most small pseudotachylites have a finite length and values for τ are probably in the range 2 to 2.75 kb. 2.5 kb will be taken as a reasonable estimate. Using the law of effective stress $\tau = So + \mu(\sigma_v - p)$ where μ is the coefficient of internal friction, σ_v is the lithostatic pressure (ρgz) and p is the pore fluid pressure, then $\mu(\sigma_v - p) = 2.417$ kb. The lack of alteration of sillimanite, biotite and garnet and presence of pseudotachylite show that p values will be very low (see Sibson, 1973). Taking $\mu = 0.75$ (Jaeger and Cook, 1969, p.402; Handin in Clark, 1966) and $\lambda = 0.1$ where $\lambda = p/\sigma_v$

Then $\sigma_v = 2.417/0.6475$ kb. = 3.58 kb.

It is probable that σ_v lies between this value and 3.22 kb (when $\lambda = 0$). 3.3kb is taken as an average value, and this is equivalent to a depth of formation of 12.2 km.

The shear stress (τ) in a rock system approximates to $\sigma_1 - \sigma_3(\sin 2\phi)/2$ (Price 1966 p.60) where ϕ is the angle between the plane of maximum shear and σ_1. The angle ϕ will probably be about 20° - 27°, dependent on the angle of internal friction and the effects of gneissic anistropy (Jaeger and Cook, 1969, p.402; Price, 1966 p.64; Sibson, 1974).

Taking $\phi = 27^\circ$, $\sigma_1 - \sigma_3 = 6.18$ kb.

Since $\sigma_3 = \sigma_v$ then $\sigma_1 \geqslant 6.18 + 3.3 = 9.48$ kb.

Even taking $\phi = 45^\circ$ we get a minimum value of $\sigma_1 \geqslant 8.3$kb.

Hence we must postulate high tectonic overpressures in order to account for the observed pseudotachylites, provided that the above approximations and assumptions are correct.

Brace, Ernst and Kellberg (1970) showed that massive greywacké will support overpressures of 9.9 kb (confining pressure 4.08 kb, T = 214°C, $\dot{e} = 10^{-4}$/sec. p fluid = 0)

provided that no weak beds (e.g. shale, limestone) were present. Rutter (1974) showed that Carrara marble can support differential stresses of about 3 kb. at 200°C (confining pressure 1.5 kb.) almost independent of strain rate. The strength becomes significantly lower at higher temperatures as slip and polygonisation take place. Donath and Fruth (1971) showed that Solnhofen limestone and sandstone both maintained differential stresses greater than twice the confining pressure at 25°C. Provided that "cataclastic" flow is the dominant deformation mechanism, differential pressure is independent of strain rate. Stesky et al (1974) have shown that differential stresses of about 11 kb (3 kb confining pressure) are needed at 300°C to cause fracturing in most rock types but that quartz rich rocks are generally stronger than mica and amphibole rich rocks.

The large quartz grains in T70A have sharply defined thin deformation bands (Carter et al, 1964) and show very slight quartz recrystallization (new grains 0.005 to 0.01 mm.) and textures compatible with sub-basal slip and recovery (vacancy migration and dislocation rearrangement). Elongate ribbon grains have formed by this recovery process along deformation bands, and once formed, the newly orientated grains acted as a sink for nearby highly strained areas. The new grains grow to absorb neighbouring bands except in grains whose orientation is unfavourable (c axis perpendicular or parallel to σ_1). Dentate grain boundaries show that grain growth occurred under a directed stress field. Tullis et al (1973) experimentally produced similar textures in quartzite (confining pressure 10 - 15 kb) at 700°C, $\dot{e} = 10^{-7}$/sec. (equivalent to 300°C, 10^{-11}/sec) under a differential stress of 6 kb. Hence the above stress estimates suggest that high differential stresses prevailed in the almost dry gneiss-marble-amphibole sequence prior to the diffusion of water along zones of contact strain, which in turn promoted mylonite formation. This initial deformation must have occurred at temperatures below 350°C to maintain the necessary differential stresses and lie within the

stick slip fracture field (Stesky et al, 1974). The presence of pseudotachylite implies that brittle fracturing created a zone of high fluid diffusion which was then followed by recrystallization and increased deformation. Point T70A at present lies 1.13 km. below the uppermost exposed level of the Austro-Alpine Nappes. The mineralogical changes in the f_3 mylonites show that metamorphic grade increased (T. approximately 550°C) as mylonitisation occurred; in the southernmost part of the Central Alps where assemblages are typical of the Upper Greenschist facies this temperature rise was less marked.

7.36 Amphibolite mylonite

In contrast to the majority of amphibolites in mylonite zones where recrystallization is dominant over brittle deformation mechanisms, at M197 an amphibolite mylonite occurs. Under the microscope, this grey finely banded rock comprises tremolite laths and rounded albite porphyroblasts in a matrix of clinozoisite, white mica (some phlogopite,) minor quartz, magnetite, tremolite and albite. Tremolites are commonly fractured, kinked and recrystallized to aggregates of smaller grains. Their lack of pleochroism and moderately high 2V suggests a low Fe content. Late stage muscovite plates up to 1.5 mm. across are present.

The fine colour banding reflects the amount of disseminated magnetite and hence degree of mylonitisation, but is primarily a consequence of compositional banding (Amphibole and plagioclase rich bands). The mylonitic banding is folded into open to very tight, asymmetrical, minor folds which show a northerly vergence. Small dislocations are common and displacements of 1 to 2 mm. are seen. These small thrusts are seen to be folded in some parts of the thin section and hence pre-date at least part of the mylonitic deformation.

The texture and mineralogy imply that temperatures lay below 475° (Liou et al 1974) and that high fluid pressures and probably high strain rates prevailed during mylonitisation. High fluid pressure and temperatures above 250°C (for the recrystallization of tremolite) would preclude

the development of pseudotachylite. The textures suggest that deformation generally occurred in the stable sliding region with regard to frictional behaviour above 250°C for amphibole rich rocks at 3 to 4 kb. (Stesky et al, 1974).

7.40 STRAIN ESTIMATES

In the mylonites and phyllonites, deformed quartz aggregates have been measured to determine approximate axial ratios for the strain ellipsoid. Estimates of the amount of simple shear strain have been deduced from the examination of small shear displacements and of garnet trails.

7.41 Deformed quartz aggregates

In thin sections (T362) of the phyllonite which lies between the Mt.Tonale and Casiole sheets (mylonite 5), elongate aggregates of recrystallized quartz are present. These aggregates form small discrete bodies in the mylonite and are easily distinguished from the finer-grained quartz, feldspar, muscovite, and clinozoisite matrix. The quartz grains in these aggregates show dentate boundaries and only rare strain shadows; deformation lamellae are absent. The features are indicative of recrystallization under stress (Spry, 1967; Bell and Etheridge, 1973). The quartz aggregate shape is assumed to be representative of the bulk strain in the mylonite.

The specimen was cut in three planes orthogonally related to the mylonitic foliation (069/86° S), with the two near vertical sections intersecting in the weak lineation pitching 86° to 249°. This lineation corresponds to the axis of very tight quartz vein folds which show extreme hinge thickening and apparent elongation along the axes. Measurements of the major and minor semi-axes of the elliptical quartz aggregates in three planes are given in Appendix 4(c). These planes are designated XY, YZ and XZ, assuming X corresponds to the above lineation and X and Y lie in the plane of the mylonitic foliation. The readings are graphically plotted on Figure 45(a) such that the results are consistent in the three planes, taking into

Figure 45(a) - a - b diagram showing measurements taken from deformed quartz aggregates in phyllonitic mylonite (T362). Initial aspect ratios are derived from measurements of quartz grains in pelitic gneiss not affected by the f_3 deformation.

Figure 45(b) - Trails of fragmented garnet and related partially retrograde porphyroblast in pelitic gneiss (T140A). The trail can be measured to give an estimate of minimum simple shear assuming rotation of the porphyroblasts. Mineral abbreviations are given in section 1:50 with the exception of Mt - Magnetite.

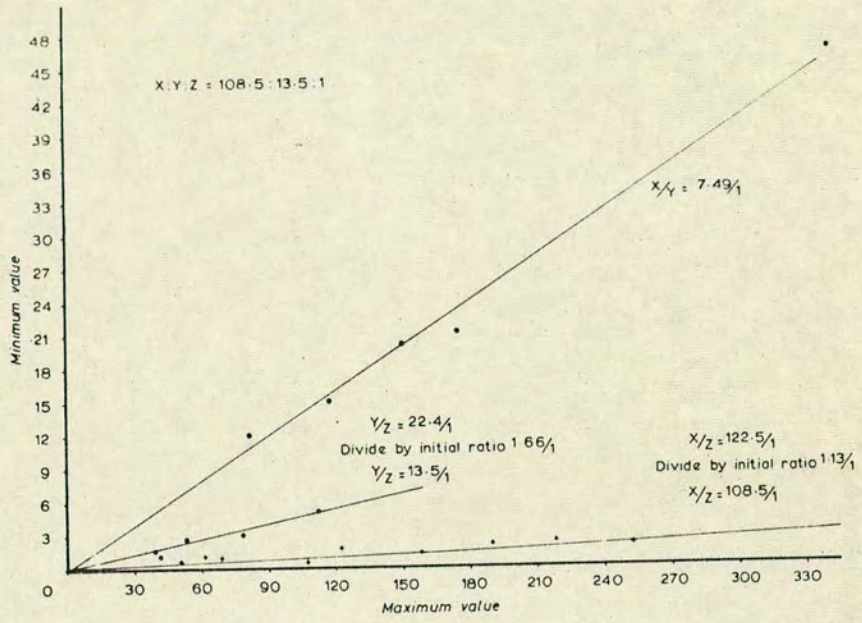
X:Y:Z = 108·5 : 13·5 : 1
X/Y = 7·49/1
Y/Z = 22·4/1
Divide by initial ratio 1·66/1
Y/Z = 13·5/1
X/Z = 122·5/1
Divide by initial ratio 1·13/1
X/Z = 108·5/1
Minimum value
Maximum value
0
3
6
9
12
15
18
21
24
27
30
33
36
39
42
45
48
30
60
90
120
150
180
210
240
270
300
330

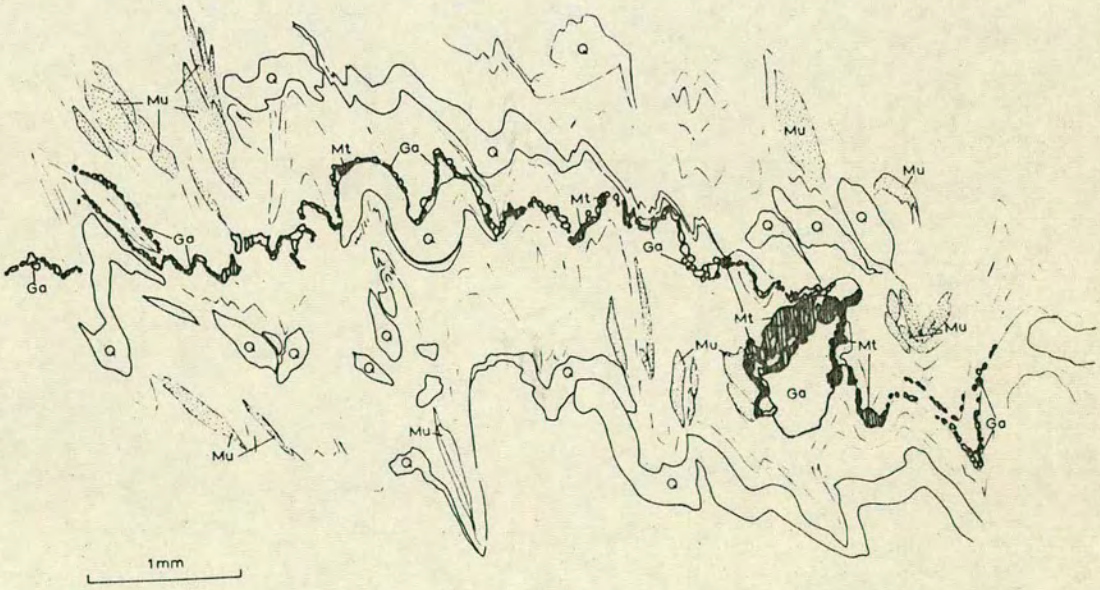
Mu
Mt
Ga
Q
1mm

account the initial shape factor. These elongate quartz aggregates are taken to represent the deformed equivalents of 0.5 to 5 mm. wide prolate ellipsoidal quartz grains and aggregates, which are abundant in the non-mylonitic gneiss. Readings from typical quartz grains and aggregates in this gneiss (see Appendix 4(d)) are assumed to be a reasonable approximation to the shape of grains prior to the f_3 event.

The finite strain ellipsoid which results from these measurements gives X : Y : Z ratios of 108.5 : 13.5 : 1. This ellipsoid has a k value of 0.563, and we may separate the flattening and plane strain components. Assuming a k value of 0.1 (average value in mylonitic gneiss) for the flattening strain, X : Y : Z ratios of 1.925: 1.79 : 1 (or 1.273 : 1.18 : 0.66 for unit volume ellipsoid) can be deduced. The remaining plane strain component of 56.4 : 7.54 : 1 would indicate a simple shear of $\gamma = 7.4$. This rather simple model serves to illustrate that the strain is compatible with high shear strain values.

In this calculation (as in those for mylonitic gneiss) no dilation is assumed to have occurred. This is a reasonable assumption since the pre-existing rock was a high grade gneiss and there is as yet no mineralogical evidence of any bulk chemical change in the mylonitic gneiss or mylonite.

7.42 Evidence for rotational strain in mylonites

In thin sections of several mylonites, trails of fragmented mineral along the mylonitic foliation can be related to larger porphyroblasts. The minerals most commonly exhibiting this feature are garnet, clinozoisite and epidote. Small garnets generally form rounded grains in the mylonite and in such cases act as rigid bodies with no fragmentation. Sub-angular larger garnets are commonly retrograded to chlorite and magnetite prior to mylonitisation and these porphyroclasts show extensive fragmentation along the mylonitic lamination. Figure 45(b) and Plate 15(a) show two examples of such fragmentation. In Figure 45(b) the mylonitic lamination has been folded by the f_4 event, but this is assumed to have altered the length of the garnet trail

Plate 15

(a) Fragmentation of a partly retrograded garnet showing the formation of a garnet trail along the mylonite foliation. (T140A - Mt.Tonale/Cadi[illegible] mylonite)

(b) Complex interference folding of a pegmatitic vein in a phyllonitic mylonite. Highly thickened hinges are seen in this specimen. (T362 - Mt.Tonale/Casiole mylonite).

(c) Asymmetrical 'internal' folding of amphibolite banding. (T260 - Casiole Sheet)

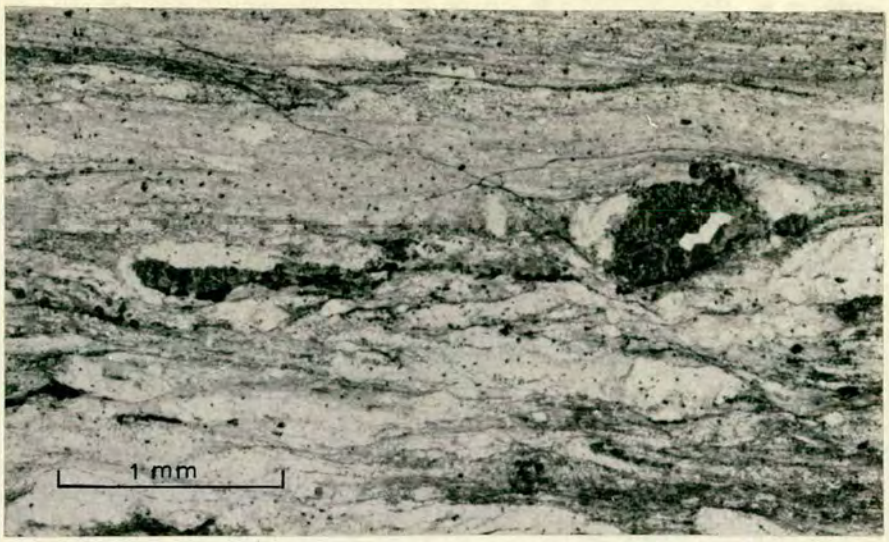
1 mm


5cm

only slightly. In Plate 15(a) the garnet which is fragmented, reflects three distinct metamorphic events ;-
1) primary development of garnet in the pelitic gneiss, 2) retrogression to chlorite and magnetite, 3) further growth of new garnet. These last two events precede the fragmentation and it is suggested that they represent a Greenschist facies metamorphic event just prior to mylonitisation. This event is localised along planar zones in the gneiss, along which translation subsequently occurred. In these zones the high shear strain, confining pressure, and moderate water pressure favour the growth of clinozoisite and epidote, as shown in the section on mylonite mineralogy. These minerals are not typical of the earlier Hercynian metamorphism, and their growth is assigned to a metamorphic event preceding mylonitisation.

Rotated inclusion trails in metamorphic porphyroblasts (e.g. quartz inclusion trails in "snowball" garnets) have been variously interpreted by different authors (Ramsay, 1962; Spry, 1963). Recent ~~conclusive~~ interpretations (Cox, 1969; Elliot, 1972) show that such patterns result from rotation of the porphyroblast during metamorphism. Thus the inclusion trails in garnet, such as described by Flett (1912) show that the porphyroblast rotated 540° during its growth.

In order to explain the long trails leading from the porphyroclasts along the mylonitic foliation in the mylonites of the Tonale Pass area, it is proposed that rotation during mylonitisation has occurred. This has resulted in brittle fragmentation of marginal zones of the porphyroclasts and subsequent transport along the foliation. Although the mylonitisation is interpreted as a dominantly "ductile" event, garnet and clinozoisite have acted as dominantly brittle material.

The shear direction and mylonitic foliation (representing the XY plane of the mylonitic strain ellipsoid) are approximately coincident at high simple shear values, especially if some flattening strain has occurred. For example at a simple shear of $\gamma = 7.4$ and a flattening strain

(k = 0.1) of 1.273 : 1.18 : 0.66 (values taken from strain ellipsoid based on quartz aggregate measurements in mylonite), the angle between the shear direction and XY plane would be 4°.

In thin sections from specimen T363, (phyllonitic mylonite), the micaceous bands (muscovite) contain a strong foliation lying at 4.5° to the mylonitic banding. In these bands there is likely to be a concentration of shear strain effects since mica slips very readily along its basal cleavage. Hence the shear direction may be assumed to be parallel to the bounding margin of the micaceous band and the foliation angle is then dependent on the amount of simple shear. Taking an angle of 4.5°, then a shear strain of $\gamma = 13$ can be inferred. Etheridge (1973) has shown that experimentally deformed phlogopite shows a constant sense of orientation in relation to the direction of simple shear. Note that if flattening strain of say 2/1 is postulated, then this shear strain value would be reduced to $\gamma = 5.3$. Early muscovites up to 0.8 mm. long are partially recrystallized and fractured in these micaceous zones. These porphyroclasts show dextral rotation, implying north directed translation during mylonitisation.

Rotational features are also observed in the field, where garnets are present in mylonite zones. At M17, a mylonite which lies adjacent to a 15 to 20 m. phyllonite contains ovoid garnets whose long axes consistently plunge 5° to 10° south relative to the mylonitic foliation. This implies that they behave as more viscous bodies than the bulk of the mylonite, and do not fully rotate into the XY plane (the mylonitic foliation). A similar feature has been observed in strained belemnites and boudins developed in a layer inclined to the principal strain axes, (Ramsay, 1967 p.248; p.109; Badoux, 1963). In contrast, at T244, mylonitic gneiss adjoining 15 m. of phyllonitic mylonite contains rounded garnets about 1 cm. in diameter, with linear inclusion trails which retain their initial orientation (as measured in the surrounding gneiss), and have not rotated the 16° into the plane of the mylonitic

foliation. This shows that there is a sharp change from a dominantly pure shear deformation in mylonitic gneiss to dominantly simple shear deformation in the mylonite.

Thin mylonite zones (< 2 cm.) are common within the pelitic gneisses of the Casiole sheet. In two good outcrops (T367 and M273), the gneissic banding may be traced across these mylonite zones and an estimate of the amount of simple shear made.

In M273, taking the dip of the gneiss outside the 8 mm. mylonite zone, and then calculating the relative displacement across the mylonite zone, a simple shear value of $\gamma = 10.3$ is obtained. Assuming that some flattening strain has reduced the zone thickness and extended the layer along the X direction, this may represent a maximum value. Using previous flattening values of 1.273 : 1.18 : 0.66 ($k = 0.1$), which are probably over-estimates for non phyllonitic mylonites, we obtain a γ of 5.45. The higher value is considered a better approximation of shear strain in this particular mylonite zone.

In T367, 31 cm. of translation occurs across a 1.2 cm. phyllonite zone. This phyllonite is associated with a north facing f_3 fold with an axis plunging 12° to 256°. Shear strain values of $\gamma = 25.8$ are calculated from these measurements, assuming simple shear in the plane normal to the fold axis. Taking the above flattening values, which are probably more applicable to this phyllonite zone, we obtain $\gamma = 13.5$.

7.43 Discussion

The textures and strain measurements in the mylonites are compatable with dominantly high shear strain and minor flattening strain. The resulting X direction of the f_3 finite strain ellipsoid plunges south in the plane of the mylonitic foliation. Northward directed translation has occurred across these mylonites. An approximate estimate of the total translation may be obtained by multiplying the total thickness of mylonite by a representative unit shear value (γ) of 14. A minimum estimate of total

mylonite thickness is 300 m, which gives a total translation over the area mapped of 4.2 km. The Austro-Alpine Nappes however, must have been thrust at least 20 to 30 km. and possibly up to 120 km. to the north. Hence a considerably greater thickness of mylonite is necessary for their total translation, or shear strain values must be greater by a factor of 5 to 30. Shear strain values (γ) of about 20 have been calculated from deformed pipes in mylonitic Cambrian quartzite along the Moine Thrust (J.Soper pers. comm. 1973). Hence γ values in the order of 10 to 20 appear to be reasonable and it is probable that the mylonites in this area reflect only a small part of the movement of the Austro-Alpine Nappes.

7.50 MYLONITIC FOLDS

Close to isoclinal, upright, gently plunging to reclined folds (Fleuty, 1964) are ubiquitous on all scales within mylonite and strongly mylonitic pelitic gneiss in the Tonale Pass area. The folds are generally defined by quartz veins and commonly have one short limb, giving the folds a pronounced S or Z profile when viewed down their axes. In some mylonites, quartz and pelite rich "cataclastic" bands exhibit mylonitic folds. All folds have straight limbs, generally angular hinges, short wavelengths and large amplitudes. A few thick quartz and pegmatite veins are folded across thin mylonite zones. Quartz veins which define the mylonitic folds range in thickness from 0.5 mm. to 20 cm. with most veins 1 to 5 mm. thick. The tightness of folds increases with the degree of mylonitisation of the gneiss, isoclinal folds being present in phyllonite.

In several mylonite zones, particularly those in the northern part of the area mapped, the mylonitic foliation and mylonitic folds are refolded by f_5 southward facing asymmetrical folds, and symmetrical open to close folds. In the mylonitic matrix, the strain variations caused by this f_5 event are taken up by dislocations along many small fractures. Quartz vein folds formed during the mylonite event are refolded by the f_5 event, when they were

apparently more ductile than the surrounding matrix. Minor sericite growth is associated with the f_5 event. No quartz recrystallization has occurred. In some mylonites, a later crenulation cleavage is superimposed on the f_3 structures which are related to the mylonitisation.

7.51 Orientation and Geometry

The axial planes of mylonitic folds lie coincident with the mylonitic foliation or within a few degrees of it, depending on when mylonitisation occurred. The orientation of planar and linear elements in the Tonale/Casiole mylonite (mylonite 5) and in a restricted area of a mylonite zone (mylonite 6(b)) within the Albiolo sheet is shown in Figure 46. In both stereograms, the scatter of foliation poles and, to a lesser extent, of fold axes and intersection lineations, is due partly to the post-mylonitisation folding. The plunge variation of minor quartz vein fold axes depends on the initial attitude of the quartz vein or pod relative to the mylonitic strain ellipsoid and the effects of fold axis rotation towards the X axis during progressive deformation. In mylonite 5 the major fold axis concentration lies in a vertical plane varying in strike from 066° to 077°. This plane is approximately coincident with the average mylonitic foliation as defined by the maximum density of poles to foliation. The great circle corresponding to the pole maximum defines a plane striking 068° and dipping 86° S. Ramsay and Graham (1970) have shown that the schistosity within a shear zone lies perpendicular to the principal finite shortening direction and does not accord with the shear direction. Hence the mylonitic foliation in the Tonale Pass area may be taken to define the XY plane of the finite strain ellipsoid whether we assume that the mylonites are zones of dominantly simple or pure shear.

Sanderson (1973) has shown that considerable rotation of fold axes may occur if X/Y ratios for the deformation ellipsoid exceed 3, given a high initial variability in the attitude of fold axes. For example, folds initiated with axes at 30° to the Y direction would be rotated by a strain

Figure 46(a) - Stereogram showing the orientation of planar and linear elements in the mylonite between the Mt.Tonale and Casiole Sheets.

Figure 46(b) - Stereogram showing the orientation of planar and linear elements for mylonite and mylonitic gneiss in the Passo di Contrabandieri - Vetta d'Albiolo area.

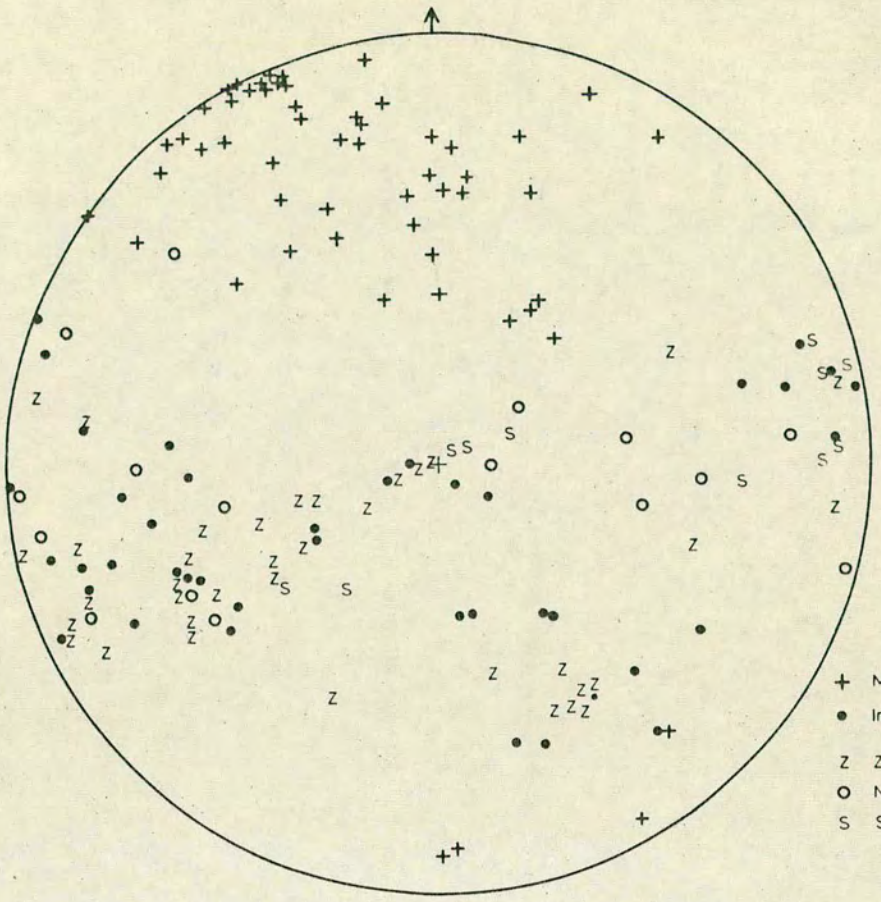
Mylonitic foliation
Intersection lineation
Z Z profile
O Neutral
S S profile
Minor folds

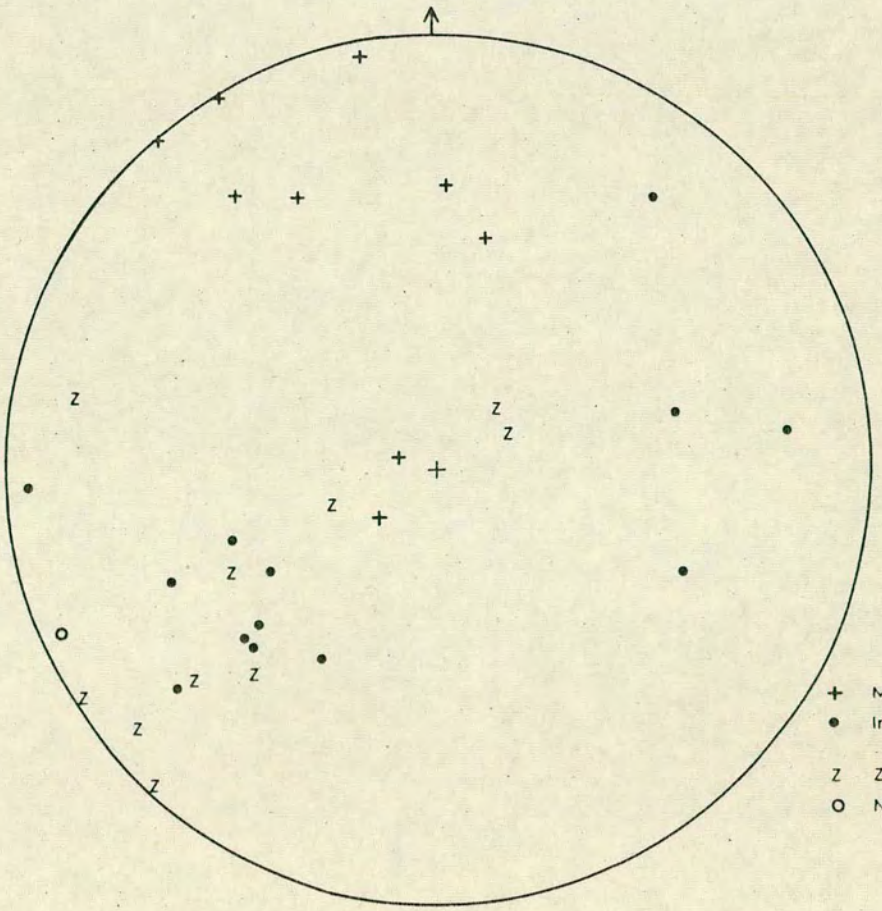
Mylonitic foliation
Intersection lineation
Z Z profile
O Neutral
Minor folds

with an X/Y ratio of 5, approximately 45° towards the X direction. In contrast, for folds initiated with axes at 5° to the Y direction, the rotation towards the X direction caused by an X/Y ratio of 3 is not significant. Although this mechanism may account for several axial orientations at angles of up to 50°or 60° to the Y direction, the fold axes close to the vertical are thought to be generally due to the initial attitude of the quartz pegmatite vein or pod. The veins and pods are folded early in the mylonitic deformation to give buckle folds with near vertical axes, which are then flattened on progressive deformation to give isoclinal folds with highly thickened hinges. Such a fold is illustrated in Plate 15(b). The near vertical X direction is deduced from the geometry of the large scale f_3 structures and deformed quartz aggregates and sillimanite porphyroblasts. Since the pre-existing f_1 folded quartz vein axes lie close to the Y direction of the mylonitic strain ellipsoid, they probably undergo only slight rotation by the mechanism proposed by Sanderson (1973).

The neutral fold axes may be in part the tightened and rotated f_1 quartz vein folds which originally plunged at low angles to the west and east.

Three types of mylonitic folds may be generally distinguished by their differing styles in mylonites and strongly mylonitic gneisses derived from pelitic gneiss. All types of fold are defined by quartz veins but type 2 folds are also rarely found in the "cataclastic" banding. The rarity of mylonitic folds in many mylonites in other orogenic regions is a reflection of the initial rock type from which they are formed. The mylonites in the Tonale Pass area are unusual in that the pelitic gneiss contained very abundant quartz and pegmatite pods and veins prior to mylonitisation.

Type 1) mylonitic folds are tight to isoclinal quartz vein folds with rounded thickened hinges, very short wavelengths and large amplitudes. Their axial planes lie in the mylonitic foliation. The folds are generally only half wavelength and are represented in the gneiss outside

the mylonite zones as pre-existing tight to isoclinal f_1 quartz vein folds. The effect of mylonitization is to increase their amplitude, decrease the interlimb angle and shorten their wavelength. The limbs are thinned and extended and the hinges markedly thickened. Mylonitic and f_1 foliations (the latter corresponding almost everywhere to the prominent gneissic banding) are approximately coincident in many areas and f_1 folds are co-axial with mylonitic folds and related f_3 asymmetrical folds. Hence there has generally been little rotation of f_1 fold axes into the mylonitic XY plane, since most f_1 folds initially had axial planes roughly corresponding to this plane. The variations in type 1) fold axis plunge in the XY plane are attributed to initial variations in f_1 fold axis plunges and minor rotation by the mylonitic strain, (Sanderson,1973). In rare cases where the f_1 fold axial plane has a strike which lies at a high angle to that of the superimposed mylonitic foliation, the fold is tightly to isoclinally refolded.

Type 2) mylonitic folds are defined by short quartz veins and more rarely by the "cataclastic" banding. The folds have sharp hinges showing only slight thickening, generally one short limb and irregular amplitudes and wavelengths. The amplitude is commonly greater than the wavelength, which rarely exceeds 5 cm. These folds are the most abundant type in the mylonites and generally show an S or Z profile. The fold axial planes are coincident with the mylonitic foliation and the folds are commonly flattened in this plane. The folded veins are the deformed equivalents of quartz segregations which are abundant in the pelitic gneiss. These veins or pods generally lie subparallel to the gneissic banding. Type 2) folds may also affect longer roughly concordant Hercynian quartz or pegmatite veins.

Type 3) mylonitic folds are trains of tight to isoclinal folds, which have a fairly consistent short wavelength and large amplitude, and may exhibit multiple S or Z profiles (commonly S profile) when viewed down the plunge of their axes. The axial planes of the folds are

coincident with the mylonitic foliation. The quartz or pegmatite veins which define the folds show a modified cross-cutting relationship with the "cataclastic" banding. The folds result from deformation of cross-cutting planar Hercynian pegmatite or quartz veins during the mylonitic event. The type 3) folds are not abundant in mylonites.

7.52 Fold formation

The origin of mylonitic folds can best be understood if we consider the effects of large flattening and rotational strains in the pre-existing pelitic gneiss with its quartz pods, discordant pegmatite veins and tightly folded quartz veins (f_1). Strain measurements and evidence from mylonitic textures suggest that both high flattening and rotational strain values are present in mylonites. Approximate finite strain values are estimated from measurements of deformed quartz aggregates in phyllonite to be X : Y : Z = 100 : 17 : 1.

Type 1) mylonitic folds were formed when pre-existing f_1 quartz vein folds were affected by the mylonitic deformation. Since the majority of f_1 folds have axial planes within a few degrees of the XY plane of the superimposed mylonitic finite strain ellipsoid, their profiles lie entirely within a zone of extension. Fold amplitude is thus increased and wavelength decreased as mylonitic deformation progresses. Limbs become thinned and hinges thickened. The effects of the rotational component of simple shear are minimal since the f_1 folded veins have limbs lying at very low angles to the shear direction. Subsequent deformation would tend to amplify the pre-existing structure and not initiate new folds similar to the one already present. Ramsay (1967, p. 548) has stated that rocks containing folded structures are much more difficult to buckle than those where the layers are all unfolded.

In rare cases where the f_1 axial plane lay at a high angle to the XY plane of the mylonitic strain ellipsoid, buckle folding of the f_1 tight quartz vein fold has occurred.

The type 2) mylonitic folds are commonly single Z

profile folds (looking down the west to southwest axial plunge). Each vein shows only slight changes in thickness, with the tighter folds showing some vein thickening at the hinges. The relative abundance of both quartz pods in the unmylonitised gneiss, and elongate pods and Z folds in the mylonite, are comparable. This strongly suggests that the folds were derived from the quartz segregations and small veins which lie approximately within the gneissic foliation. Since the mylonitic and gneissic foliations have similar orientations, we cannot derive this type of mylonitic fold by buckling normal to the XY plane of mylonitic strain ellipsoid (i.e. by the flattening component of strain). Evidence from garnet trails and shear displacements in different mylonites give simple shear strain values (γ) of 7 to 14. Assuming that these values are representative of the true shear strains, and taking into account the effects of late f_3 and f_5 flattening, we may consider the effect of shear strain in the order of $\gamma = 5$ to 10 on initially discoid quartz pods and thin quartz veins. There are then two feasible models for the formation of type 2) mylonitic folds.

a) Observed small scale changes in the mylonitic texture and hence degree of mylonitisation may be attributed to heterogeneous simple shear. Such changes would cause differential rotation and flattening of planar quartz veins or pods across a mylonite zone, provided that they lay at some angle to the shear direction. Unless this variation in simple shear has a common periodicity, it is difficult to explain how recurring Z fold profiles would be formed. There is no evidence for such periodic variation and this mechanism is considered to be relatively unimportant. Heterogeneous shear may modify the general shape of the type 3) folds during the deformation of long discordant veins.

b) Since most Z folds have short wavelengths, it is more satisfactory to consider the effects of uniformly high simple shear strain on a quartz vein or pod with variations in attitude along its length. Figure 47 shows

Figure 47 - Graph showing the relationship between the angle between a line and the shear direction and amount of simple shear. The graph illustrates that at high shear strains ($\gamma > 7$) almost all lines will have rotated into near parallelism.

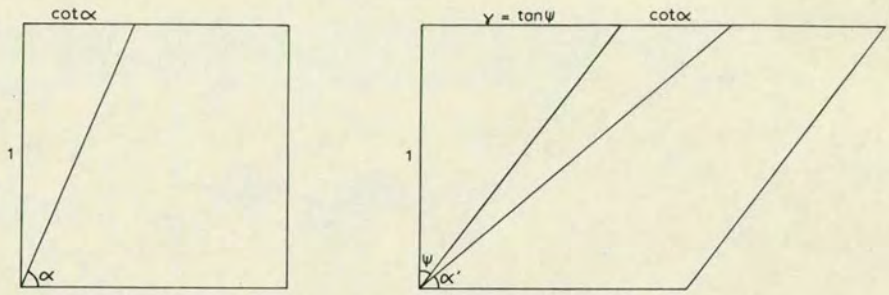

$$\cot\alpha' = \cot\alpha + \gamma$$

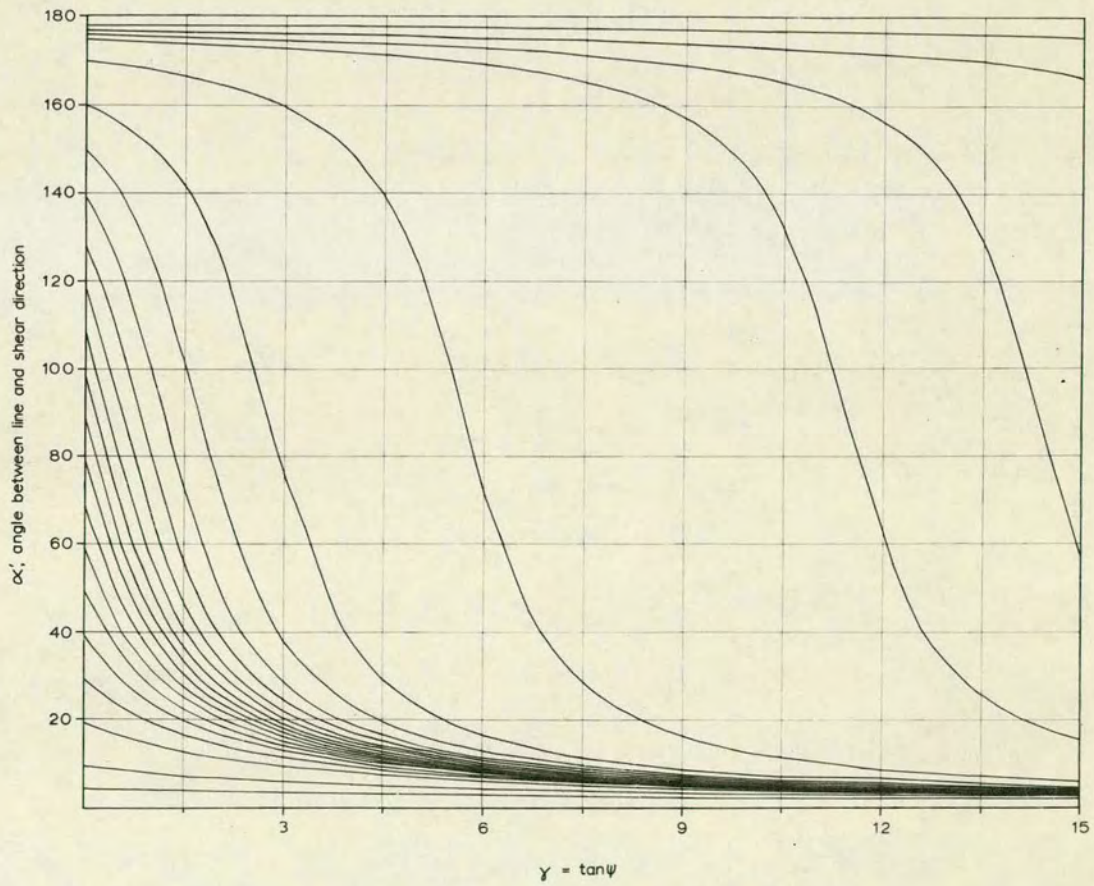

the effect of increasing simple shear on the orientation of lines lying initially at varying angles to the shear direction (after Ramsay, 1967, p.87). It is important to note that after a high shear strain (e.g. $\gamma = 7$), lines orientated even at a high initial angle to the shear direction are rotated to within about 10° of the shear direction. Figure 48 shows the results of the combination of possible initial variations in attitude in the plane of maximum simple shear (XZ plane), and varying amounts of simple shear. These shapes represent various initial quartz vein or pod orientations in the XZ section of the simple shear ellipsoid (in simple shear Y = 1 so that all strain is confined to the XZ plane). The effects of buckling are ignored, as most veins rotate towards the extension direction and early formed buckle folds may be either unfolded or boudinaged. The effect of buckling in some cases is to emphasize the fold shape formed by differential rotation. Figure 48 shows that, in two possible vein orientations, sharp hinged Z profile folds may be formed. In the non-mylonitic pelitic gneiss, variations in attitude of 1° to 20° in north-south section, are common in small quartz veins and discoid quartz pods. These variations may be strongly amplified by differential rotation as shown above, and hence tight Z profile folds produced. Although such a model is rather simplified in that it ignores the effects of ductility contrast and hence local strain fields, these effects should be small and the veins and pods should merely act as "passive" markers during mylonitisation. The mechanism is considered to be the primary mode of formation of the majority of observed mylonitic folds as it would be effective even with simple shear values (γ) as low as 2 ot 3. The folds develop as simple shear deformation, and hence translation, increases. Their rate of amplification is dependent primarily on the initial angular variations in the quartz vein or pod. Folds formed by small amounts of rotation during the early stages of mylonitisation would show marked hinge thickening, high amplitude/wavelength ratios (1.5 to 5) and tight to isoclinal styles on progressive deformation, since flattening would become dominant

Figure 48 - Diagram showing the resultant shapes after differing amounts of shear strain on various initial patterns. The shapes represent small deformed quartz veins commonly found in mylonites in the Tonale Pass area.

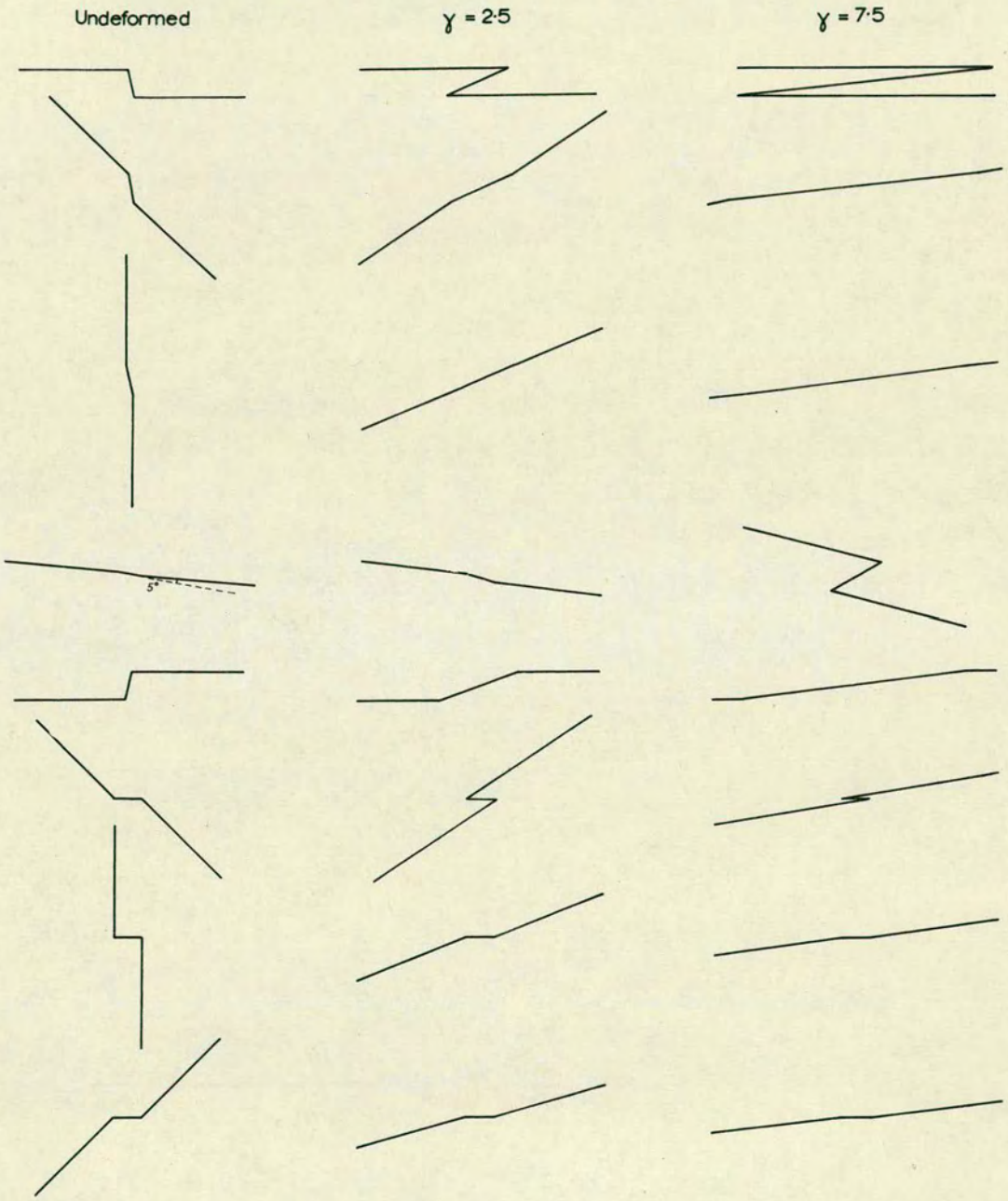
Undeformed
γ = 2·5
γ = 7·5
5°

in the later stages of mylonitisation. Conversely, folds formed late in the mylonitic event would have more constant layer thicknesses, open to tight styles and moderate to low amplitude/wavelength ratios (0.5 to 2). The "cataclastic" banding (mylonitic lamination) may be folded late in the mylonitisation if small variations in its orientation develop during mylonitisation. These fold types may all be recognized on a microscopic and macroscopic scale in the mylonites of the Tonale Pass area.

Type 3) folds are formed when long discordant Variscan quartz or pegmatite veins are buckled by the flattening component of strain, and the fold train is rotated by the simple shear component. Hudleston (1973a, b) has shown that in rocks deformed under ductile conditions, most of the similar style folds are best described as buckle folds subsequently tightened by homogeneous flattening. Although high rotational strains have been deduced for mylonite zones, the relative importance of the flattening and rotational components of strain will depend on the initial orientation of the discordant veins, as shown quantitatively in Figure 49. The theoretical basis for the origin of these folds is presented and discussed in Appendix 5.

Buckling is the most important mechanism of fold initiation for discordant pegmatite and quartz veins. Cobbold et al (1972) have shown by the comparison of theory, model experiments and field examples, that banded gneiss may be regarded as a homogeneous medium when considering buckling of quartz or pegmatite veins within it. This assertion is confirmed by the relatively consistent style, wavelength and amplitude of type 3) folds in mylonite zones in the Tonale Pass area. The amount of asymmetry of the type 3) folds is shown in Figure 49 to be dependent on the amount of rotation which is in turn consequent on initial orientation. The differing limb thicknesses observed in type 3) folds are a natural product of this mode of formation. There is a particular initial quartz or pegmatite vein attitude where the flattening due to simple shear strain and the pure shear component, combine to give the

Figure 49 - Diagram showing the theoretical effects of combined simple shear and flattening for vein orientations lying initially at 170°, 160° and 120° to the shear direction. The amplitudes and wavelengths of the folds are only qualitative.

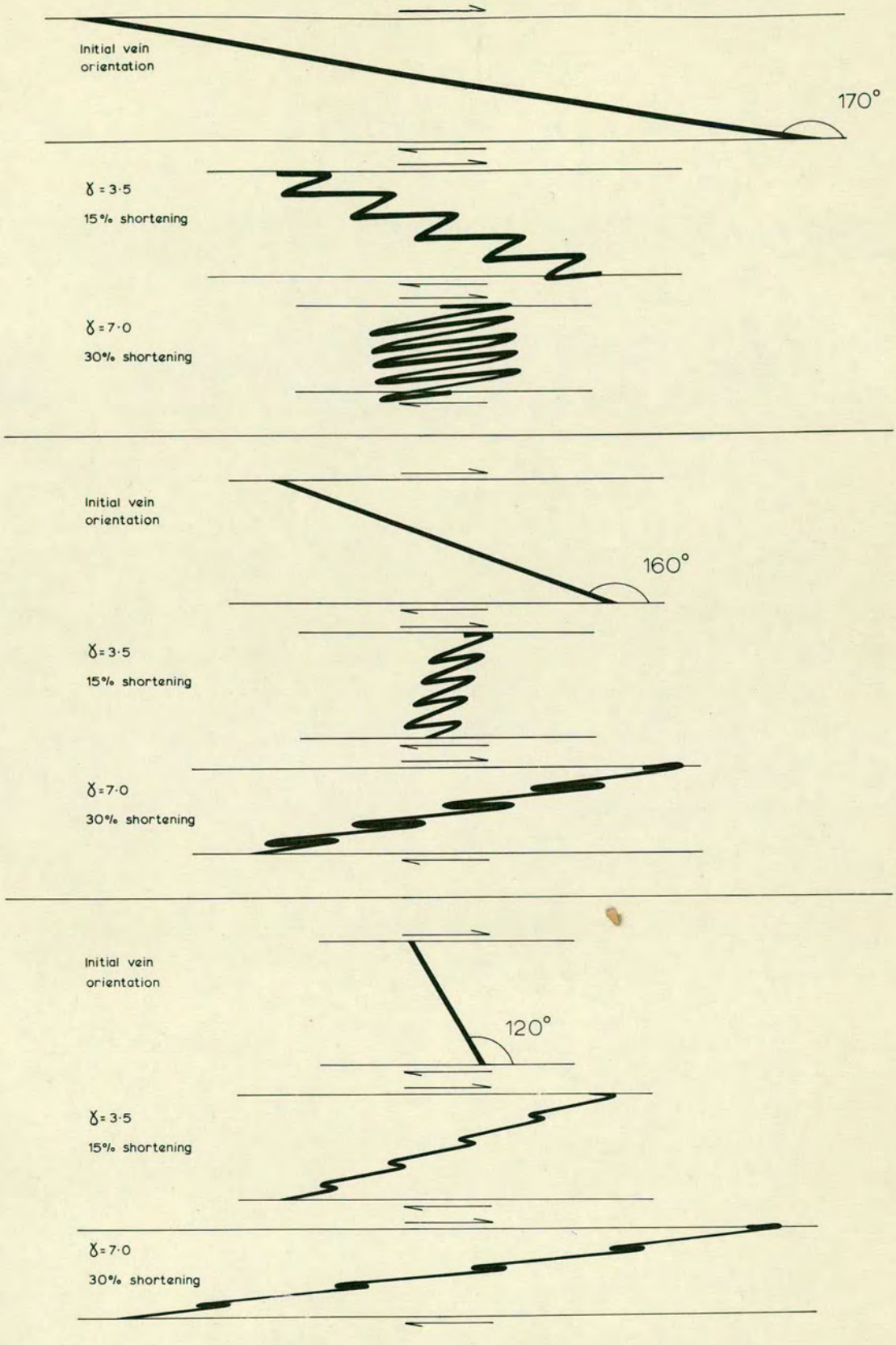
Initial vein orientation
170°
γ = 3·5
15% shortening
γ = 7·0
30% shortening
Initial vein orientation
160°
γ = 3·5
15% shortening
γ = 7·0
30% shortening
Initial vein orientation
120°
γ = 3·5
15% shortening
γ = 7·0
30% shortening

maximum shortening for a given amount of deformation. Examples of the resultant folds, which are generally very tight is isoclinal in phyllonite zones, have an S profile when viewed down their south-westerly plunge (e.g. T368A, M60, M387). Where these folds are present in the phyllonite, they provide spectacular evidence of the amount of shortening which has occurred across mylonite zones.

We may conclude that all folds in mylonites derived from pelitic gneiss in the Tonale Pass area, result from the interaction of two main factors and their relationship in time. These factors are :-

a) the initial size, shape, orientation and composition of the quartz or pegmatite vein or pod in relation to the superimposed mylonitic deformation.

b) the amounts of effective pure and simple shear.

It is important to realise that although several modes of origin have been proposed for mylonitic folds, these are not mutually exclusive. All the factors mentioned above play some part in fold initiation and amplification, but generally for each type of fold one mode of formation is dominant.

7.60 FOLDS IN AMPHIBOLITE

Folds are only present within amphibolite bands where these bands lie adjacent to mylonitic zones and close to marble bands. Although f_3 large to medium scale, open to tight folds affect the amphibolite bands in many parts of the area, these folds do not occur on a small scale and are unrelated in style, asymmetry and, in places, orientation, to the internal folds discussed here. The latter folds are present within planar bands of amphibolite.

7.61 Geometry and Field relationships

These mylonitic amphibolite folds show a strong asymmetry and have long limbs and relatively small hinge areas as shown in Plate 15(c). They range in amplitude from 1 cm. to 1 m. and in wavelength from 0.5 cm. to 1 m. Typical amplitude/wavelength ratios would be in the range 0.75 to 7.5 (average about 2). The folds range in style from open to tight and rarely isoclinal, and are more abundant and

tighter as the adjacent mylonite or marble is approached. In some areas (e.g. T38, T70, M197), where the folds are tight the fold limbs are sheared and a fine-grained green alteration zone is present. Chlorite, clinozoisite-epidote, sericite and minor quartz have replaced the hornblende-plagioclase assemblage.

Amphibolite folds only occur in amphibolite bands < 5 m. thick and where marble and mylonites are the lithologies adjacent, or close to the amphibolite band. In the general case, marble overlies the amphibolite. Structures in the marble usually indicate that southward directed ductile flow has occurred during the f_3 deformation event. Since the underlying mylonite and strongly mylonitic gneiss have structures and textures showing northward directed ductile flow, a shear couple is created in the amphibolite. This couple gives rise to the southward facing folds generally seen. Less commonly (e.g. in the Albiolo sheet) the marble has apparently been "squeezed" upwards and northwards, and there is an overall northward directed shear couple which is amplified across the amphibolite by large relative movements in the marble overlying it. In such a situation, northward facing folds are produced. Structural and textural observations show that there is a large strain variation across the amphibolite/marble and amphibolite/mylonite contacts. Few shear zones are developed at these boundaries, the majority lying within the amphibolite band, and these may be present without folding.

7.62 Orientation and strain estimates

The amphibolite folds have axial planes whose strikes accord with those of the amphibolite and gneissic banding, and whose dips range subparallel to up to 25° to the banding. Poles to banding for the observed folds are shown in Figure 50(a). It was rarely possible to accurately measure the true axial planes in the field. Fold axes are variable in orientation but generally lie close to a broad girdle with the orientation 070/45°S, as shown in Figure 50(b). The effects of superimposition of amphibolite folds on earlier f_2 structures which commonly control the initial

Figure 50(a) - Stereogram showing the orientation of amphibolite banding and shear planes. Amphibolite banding with internal folding is separated from that with no internal folding but a strong lineation. The lack of internal folding in northwesterly dipping amphibolite bands suggests that this orientation did not favour its formation.

Figure 50(b) - Stereogram showing the orientation of minor folds and lineations within amphibolites. The dashed line is the probable plane of maximum shear strain.

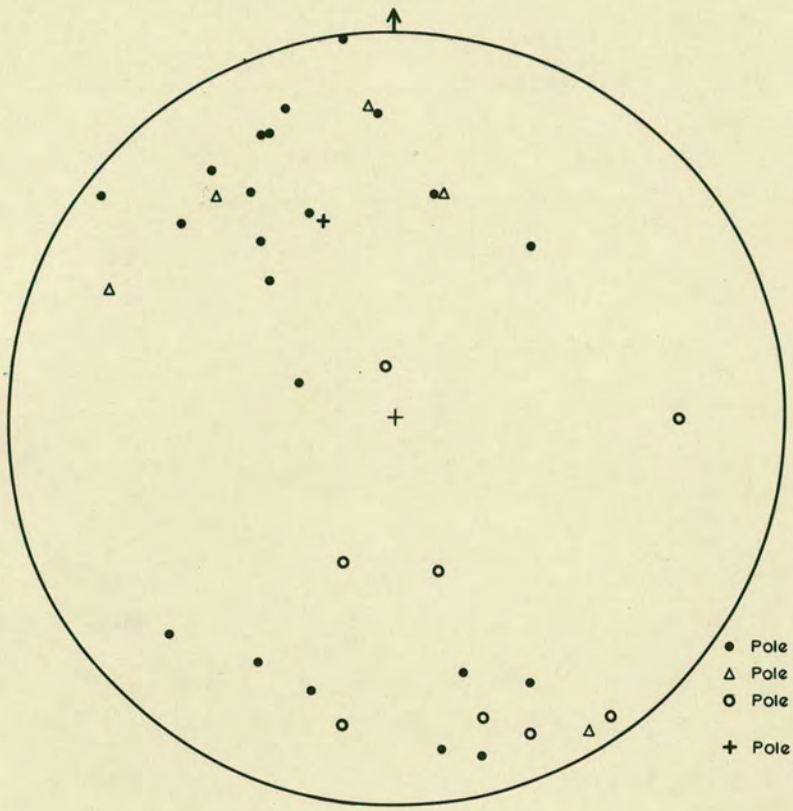

● Pole to banding with internal folding
△ Pole to shear plane
O Pole to banding with no internal folding, and strong lineation
+ Pole to broad circle of fold axes

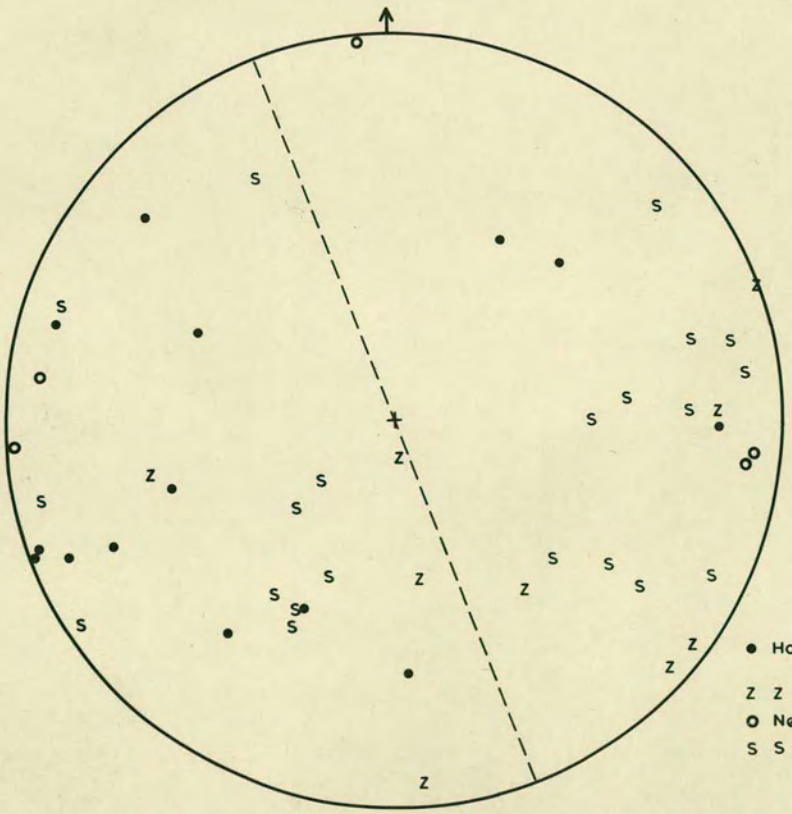

● Hornblende lineation

Z Z profile
O Neutral
S S profile
} Minor folds

banding orientation, is shown by the spread of poles to banding. Later f_5 structures cause a wide scatter of poles to banding and fold axes on the stereograms; these effects are limited to small areas however. There is a secondary pole concentration in Figure 50(a) in the south south-east of the stereogram (banding dipping steeply north) but this has a large proportion of poles to banding in which lineations only are developed. These measurements show that amphibolite folds developed preferentially in amphibolite bands dipping 60° to 70° SE.

Simple shear must be a dominantly strain component in the formation of amphibolite folds. If we consider a shear couple acting along the planar boundaries of the amphibolite band, then S profile folds (looking W) would have an associated X axis of the strain ellipsoid dipping at lower angles to the south southeast than the banding. Conversly for Z profile folds, the X axis would dip at steeper angles than the banding, since the sense of shear is reversed. It is reasonable to assume that the fold axial planes will accord with the XY plane of the finite strain ellipsoid, since shear strain is a maximum across this plane. Assuming that the Y axis of the strain ellipsoid is horizontal or plunges gently to about 250° (c.f. Boudinage axis) then the X axis for S profile folds would plunge moderately south southeast. Hence since fold axes are constrained to lie in the XY plane, and provided that the effects of later folding are slight, the south facing fold axes should trace out a more gently dipping plane than those for N facing folds. This broad effect can be seen in Figure 50(b). By getting some estimate of the overall XY plane for S facing folds and comparing this to the average banding orientation, we can obtain an angle between the X direction and the planar boundaries of the layer (angle between dip of axial plane and banding). This angle is related to the amount of simple shear and ranges from about 5° to 25° ($\gamma = 11.34$ to $\gamma = 2.38$) in the field. An average value would be 15° giving $\gamma = 3.6$. The resultant plane strain would have axial ratios X : Y : Z = 12.95 : 3.6 : 1. The regional

stress field may have contributed to this result, since an overall N-S compression would tend to reduce the angle between the XY plane of the strain ellipsoid and the dip of the banding. Amphibolite appears to act as a relatively competent material under Lower Amphibolite facies conditions when undergoing flattening strain. Thus it is reasonable to assume that angular modifications are small. The shear strain estimate must be taken as a maximum value however.

These strain estimates for the amphibolite in mylonitic zones should be contrasted with those from mylonites derived from pelitic gneiss, where more typical values of shear strain are γ = 7 to 14 and average strain ellipses are of the order of X : Y : Z = 110 : 14 : 1. The results show that amphibolite has acted in a more competent manner than the pelitic gneiss (c.f. 6.50).

7.63 Petrography and genesis

In thin section, the hornblende in the amphibolite fold hinges shows no evidence of bending, fracturing or alteration. The polygonal hornblendes are aligned with their Z crystallographic axes sub-parallel to the fold axis in the hinge area and perpendicular to the axis on the limbs. The rock also contains fresh anhedral andesine/labradorite (An 45-50) and apatite ($CaFPO_4$). This texture and mineralogy show that fold formation was synchronous with amphibolite recrystallization. This recrystallization is assumed to have occurred under Lower Amphibolite facies conditions, as shown by the mineralogy of the adjacent mylonite zones. The growth of abundant apatite and presence of amphibolite folds only in close proximity to mylonite zones, where other criteria indicate high water activity, shows that a fluid phase is required for the deformation of amphibolite. Orville (1969) has shown that feldspar solution and redeposition may occur very rapidly: e.g. reaction time 1 day for $2NaAlSi_3O_8 + CaCl_2 \rightleftharpoons CaAl_2Si_2O_8 + 2NaCl + 4SiO_2$ at 700°C and 2 kb in the presence of alkali chloride solutions. Such solutions are commonly found in igneous and metamorphic rocks as fluid inclusions

(Newhouse, 1932; Tuttle, 1949; Roedder and Coombs, 1967) and we can qualitatively extrapolate Orville's results to Lower Amphibolite facies conditions, to show that we would expect recrystallization of plagioclase if the necessary fluid was present. We may conclude that fold formation in amphibolites is dependent on both the type and degree of deformation, and suitable chemical conditions during deformation. The folds described here are assumed to initiate at small changes in banding orientation and to amplify by the mechanism shown to occur in type 2) mylonitic folds.

Thin section observations on folded amphibolite show that there is a preferred growth of hornblendes with their long axes parallel to the fold axis. Since amphibolite is a relatively competent material, the resultant stress field in any fold structure would show stress minima in the hinge areas. Results obtained by Stephansson (1974) show that all types of buckle fold have a mean stress gradient with minima on the hinge areas. These conclusions can be used for "shear" folds in amphibolites since similar properties are found in both types of fold. Hornblende has grown in a crystallographic orientation related to the internal stress field. The crystals have aligned themselves parallel to the local Y axis of the finite strain ellipsoid in cases where no folding is seen. The hornblende lineations shown in Figure 50(b) generally plunge at moderate to shallow angles to the south or southeast but there is a scatter of readings. The banding orientations in which lineations, and not folds are present generally dip steeply to moderately north to north north west. The shear stress has apparently not been great enough to generate folds in these bands and yet a direction of minimum stress is given by the hornblende lineation. The direction of this lineation may be related to the regional stress field associated with the main f_3 event, and not controlled by local shearing.

The presence of shear zones in amphibolite is attributed to high strain rates associated with zones of fluid movement. Amphibolite appears to be very susceptible to deformation under high shear stress (but not under normal

trixial stress) in the presence of a fluid phase. The amphibolite shear zones south of Scourie in N.W. Scotland are good examples of this tendency to deform under shear stress. Beach and Fyfe (1972) have shown that major chemical changes have accompanied this deformation, involving large amounts of fluid movement.

8.00 CONCLUSIONS and DISCUSSION

The present work must be placed in a broader context for its significance to be appreciated. Information obtained from parts of the Central and Eastern Alps, including the area mapped, are used to define a genetic model with particular emphasis on the Alpine event. Problems associated with this and other models are discussed.

8.10 CONCLUSIONS FROM THE TONALE PASS AREA

8.11 Adamello Massif

A number of ovoid intrusive bodies of calc-alkaline affinity form a composite intrusion, which in the area mapped intrudes the Edolo Schists. By measuring the inclination of the individual pluton contacts and assuming an initial spherical shape, we can estimate the depth of cover at the time of intrusion, taking $P.H_2O$ = P total = 3kb. This figure is obtained from a study of the contact metamorphic assemblages. The biotite-quartz-diorite pluton lay 7.8 km. below the surface and the tonalite 2.85 km. below. The maximum temperature at the intrusive contact was about 715°C.

The contact aureole is 0.8 km. wide with biotite, sillimanite, cordierite, and more rarely garnet developed in its inner part. Andalusite and biotite are characteristic minerals up to 0.3 km. from the intrusion. Quartz grains in the tonalite aureole show markedly serrate boundaries. Minor anatexis has occurred adjacent to the tonalite, and no dykes were noted. In contrast the biotite-quartz-diorite pluton has no associated anatexis and dykes are abundant in the inner 375 m. of the aureole. Dyke distribution is in accord with shear stress trajectories associated with intrusion of spherical bodies into semi-brittle rock.

Experimental data suggest that the temperature of intrusion of the magma was about 960°C. The biotite-quartz-diorite and tonalite both contain plagioclase with oscillatory normal and patchy zoning; features best explained by intrusion of a relatively dry magma (approx.

2% H_2O). Diffusion rates during solidification were slow, as shown by the depletion of biotite around a xenolith margin. A rise in f O_2 occurred during solidification and subsequent foliation development.

Deformation has occurred at the northern margin of the Adamello massif and in the inner part of the aureole. Xenolith measurements show a maximum shortening of 74% (X : Y : Z = 8.8 : 6.2 ; 1, k = 0.08) at the margin of the tonalite where large new biotites are developed. In the biotite-quartz-diorite, maximum shortening values of 65% (k = 0.08) occur over a wider zone around the intrusive contact. A deformation sequence for biotite shows initial kinking followed by recovery and subsidiary kinking. The result is a number of small biotite flakes of slightly differing optical orientation which form an aggregate. This deformation is termed f_5, and correlated with deformation events north of the Tonale Line. f_6 shear zones post-date the foliation and joints are well-developed. Pseudotachylite has formed by later uplift along chloritic joints.

Deformation and uplift probably followed rapidly on intrusion. Textural and mineralogical features in the deformed tonalite and biotite-quartz-diorite suggest that the latter body was still at about 300°C when the f_5 deformation and synchronous tonalite intrusion occurred. A minimum time lag of 3.6×10^5 yrs is suggested by time-temperature data. Taking 400,000 years as a reasonable estimate of total cooling time for the tonalite, a strain rate of 5.8×10^{-14}/sec. is obtained for the f_5 deformation.

8.12 Tonale Line

This sub-vertical, east-west trending regional lineament is marked by 40 to 70 m. of brecciated gneiss. The dark-grey sheared rock consists of fragments of pseudotachylite and altered K feldspar and albite in a cataclasite matrix. Thin mylonite zones are present. These features suggest that early movements occurred when low P H_2O conditions prevailed but later movements (Alpine ?) were accompanied by a high P H_2O. The Tonale Line is a

zone of repeated movement with the more northerly block being relatively uplifted throughout the Alpine Event.

8.13 Stavel Gneiss

This foliated quartz-feldspar-phengite-muscovite gneiss forms a 0.7 to 1 km. wide zone immediately north of the Tonale Line. Remnant gneissic banding was seen west of the Tonale Pass. A strong lineation occurs in the northern part of the zone where dislocated feldspars show that $\sqrt{\lambda}$ has a minimum value of 1.87 parallel to the lineation plunging 5^{o} WSW. Perpendicular to the lineation $\sqrt{\lambda}$ equals 1.5. The flattening ellipsoid implied by these measurements ($0<k<0.1$) is confirmed by a tightly folded vein which indicates shortening of about 75%.

Microcline-orthoclase augen measurements taken further south in non-lineated gneiss show consistent values of X : Y : Z = 7 : 2.56 : 1 (k = 1.11), assuming an initially spherical shape. The values are improbably high for deformed feldspars and textural evidences suggest that only slight deformation of the feldspars has occurred. The values are best related to the stress field at a time of feldspar augen growth which post-dates the main foliation formation.

The phengite forms sheaths around plagioclase and K feldspar and also infills cracks in feldspar. Velde (1965, 1967) has shown that high P H_2O/P total ratios favour phengite development, in agreement with the observed feldspar fracturing. Electron probe analyses show that plagioclase feldspars are generally strongly albitic (Ab_{98}) and potash feldspars approximate to $Or_{96}Ab_4$. The phengites show a range of composition with the green pleochroic plates resulting from high values of $R^{2+}, Si \rightleftharpoons Al^{iv}, Al^{vi}$ substitution and the colourless discordant "muscovites" showing lower values. The points fit the following equations

$$\% Al_2O_3 = 38.4 - 2.136 (\% FeO + \% Fe_2O_3)$$
$$\% Al_2O_3 = 38.4 - 2.206 (\% FeO + \% MgO + \% MnO)$$

The compositional change is thought to reflect a decrease in available biotite since petrography suggests that

phengite forms primarily by the reaction:

$$3\ NaAlSi_3O_8(Ca\ Al_2Si_3O_8)_{0.5} + K(Mg,Fe)_3AlSi_3O_{10}(OH)_2 +$$
Andesine (An_{33}) Biotite

$$5\ KAlSi_3O_8 + 5H_2O \rightleftharpoons 3K_2(Mg,Fe)Al_3Si_7AlO_{20}(OH)_4 +$$
K feldspar Phengite

$$9\ SiO_2 + 3Na^+ + 1.5Ca^{++} + 3[O]^{--}$$
Quartz

Phengite d spacing shows a complex relationship to composition and the main factors affecting these two features are pressure, temperature, ionic activity, pH, bulk rock chemistry and f O_2. Güven (1967) has shown that tetrahedral tilt decreases as phengite substitution increases and this basic trend is confirmed by data from other sources. Phengite compositions show a relationship to particular co-existing mineral assemblages. This relationship is again complex but d spacing may in some instances be used as a guide to P, T conditions or bulk chemical composition.

A sequence of solution changes resulting from pressure changes and minor temperature changes accompanying uplift can best explain the observed textures and mineral compositions. The initial fluid concentration may result from subduction of sediments beneath the embryo Austro-Alpine Nappes, and their subsequent dehydration and upward movement along zones of movement (e.g. Tonale Line).

8.14 Central Alps

This unit consists of a series of paragneiss and schist-psammite sheets separated by mylonite zones. The Peio Line, a Late Alpine mylonite zone which runs from the north of Mt.Tonale through the Passo di Montozzo, separates the Caledonian paragneiss to the south from the Hercynian schists, psammites and quartzites to the north. The latter meta-sediments are probably of Lower to Upper Palaeozoic age.

The paragneiss sequence consists of pelitic gneiss, marble and amphibolite with minor quartzite, pegmatites and feldspar porphyry. The Caledonian metamorphism (m_1) has resulted in the development of Upper Amphibolite

assemblages in these rocks. Sillimanite and andesine formed extensively in pelitic gneisses, and diopside, grossular and forsterite in marble. Using experimental data, the conditions of metamorphism are fixed between 4 to 5 kb. P fluid, 600° - 660°C and X CO_2 about 0.4. Diffusion is rapid at these temperatures and element partition coefficients approach unity.

The subsequent Hercynian metamorphism (m_2) was typified by chloritoid, garnet, biotite and oligoclase to albite in pelitic rocks. Tremolite, chondrodite and related clinohumite minerals, clinozoisite and phlogopite were commonly developed in marbles. These assemblages are not formed in some parts of the paragneiss, where the original m_1 assemblage is still found. The m_2 metamorphism probably occurred under the following conditions; X CO_2 0.2, P fluid = 2 to 4 kb., T = 450° - 500°C.

The Early Alpine metamorphism (m_2) was restricted to mylonite zones and areas of strong Alpine deformation. In the marble, chondrodite was retrograded to serpentine and some tremolite growth occurred. Almandine porphyroblasts have grown in mylonite and the metasediments north of the Peio Line. Experimental data are used to infer conditions of metamorphism as P fluid = 3 kb, T = 500°C, X CO_2 - low.

The Late Alpine event (m_4) was of lower grade and f O_2 values were probably greater than in preceding events. It was restricted to areas where late movements and folding occurred. Minor biotite in association with albite, chlorite and epidote suggest that conditions may be approximated to T = 400°C, and P fluid = 2 kb.

Six fold sets are recognised in parts of the Central Alps. A possible seventh set may also be present. These are as follows:-

f_0 - possible minor isoclinal folds. Axes plunge steeply SW. Strong foliation and mineralogical banding.

f_1 - small-scale, tight to isoclinal folds of quartz veins and banding commonly with a southerly vergence. Biotite foliation generally parallel

to S_0. Axes plunge gently E or W but orientation may be modified by later folding. Class 1C folds.

f_2 - large and small-scale, open to tight folds restricted to marble bands. No related foliation. Flattened buckle folds with axes plunging moderately SE. Similarly orientated cuspate structures with associated local slaty cleavage.

f_3 - regional to small-scale, open to very tight, asymmetrical folds commonly with a northward vergence. Classes 1C and 3 folds. Axes plunge gently E or W but show a spread within the axial surface which dips steeply SSE to S. New foliation (S_3) in mylonitic zones. Rotational deformation with tectonic transport to 355°. f_3 marble folds tightly appressed with rounded hinges. Some highly disharmonic marble structures. Strongly associated lineation.

f_4 - large to small-scale, open to close chevron folds, rarely similar in style. Fracturing occurs at limbs of f_4 pegmatite folds. Consistent axial direction 070° - 250°. Crenulation cleavage lineation. Folds developed in Val di Strino area, and in and adjacent to mylonites and marble bands.

f_5 - medium to small-scale, open to tight southward verging folds with almost perfect class 1B symmetry. Found in and adjacent to late mylonite zones and thick marble bands. Axes plunge gently E to NE and W to SW.

f_6 - small-scale conjugate kink sets with axes plunging to 080° - 260° or about 180°. Also large scale, very open, regional folds with steeply dipping axes to the S.

Interference structures are common in the gneiss (f_1/f_3) but are particularly well seen in the banded marble where up to four sets of folds may be seen in a single outcrop ($f_1/f_2/f_3/f_4$).

Lineations in the paragneisses are generally defined

by quartz rodding which in many places results from quartz growth, preferentially along the $S_3/S_{0,1}$ intersection. No relationship could be established between quartz rodding and the finite extension direction (X), although in some cases the rodding does appear to reflect the direction of minimum stress in the plane of the banding (Y?) during a particular deformation event. Amphibole and epidote minerals may show a consistent crystallographic orientation if growth occurred during deformation.

Boudinage (f_3 structure) is widely developed in pegmatite and quartz veins in the Central Alps. The spread of boudin neck axes in the mylonitic foliation plane shows that this is a plane of flattening. Pegmatite boudins are generally larger than quartz boudins, reflecting their greater viscosity (? feldspar content). There is a negative logarithmic relationship between boudin size and ratios. In the Mt.Tonale and Albiolo Sheets, X, Y and Z strain axes for the f_3 event can be defined, assuming that principal stresses were orthogonally related to the gneissic banding. Y lies close to the horizontal trending 065° in the more northerly thrust sheets, but plunges sub-vertically in the more southerly ones.

Boudinage is considered as a way in which a deforming vein tries to minimise the energy of the system. Under high P fluid, moderate temperature conditions, quartz appears to act as a moderately ductile material. Similar conclusions were obtained from measurements on buckle folded quartz and pegmatite veins. The values of % shortening normal to the foliation are related to rock type and degree of foliation development. Buckle folding occurs in three phases - an initial buckling, a subsequent period of synchronous buckling and flattening, and a final stage of flattening.

In mylonitic gneiss (N.B. not mylonite) measurements on deformed sillimanite porphyroblasts and feldspar crystals show that strain during the f_3 event had k values of 0.07 to 0.19 (flattening). Strain intensity increases as we approach the mylonite zones.

The mineralogy and texture of mylonites, and geometry of associated deformed veins and quartz aggregates, are compatible with high values of shear strain along narrow zones of moderate P H_2O.

Mylonite development is a natural consequence of large-scale shear movements in a heterogeneous paragneiss sequence. Both overthrusting and underthrusting have occurred and mylonite development is related to the f_3 folding and regional northward thrusting in the Early Alpine orogeny. Some mylonite formation also occurred at the time of the f_5 event (Late Alpine). Where shear strain becomes localised, e.g. around a pegmatite or adjacent to a gneiss/marble contact, differential movement preferentially takes place. As a result of stress refraction the maximum shear stress builds up in the more viscous material beneath the pegmatite. Where fluid pressure was initially low, pseudotachylite may develop. An estimate of conditions under which such development may occur gives P load = 3.3kb., σ_1 = about 9 kb. and T = about 300°C. Subsequent water diffusion which occurred along the high shear stress zones caused a rise in temperature to give the observed metamorphic reactions (m_3 and m_4), and a reduction in shear strength.

Strain values from measurements on folded quartz veins, deformed quartz aggregates, thinned pegmatites, and displacements across small mylonite zones, show that +95% shortening has occurred. Textural studies are used to infer that this deformation is ductile and that original geometrical relationships (e.g. discordant quartz veins) are strongly modified but not generally disrupted. The rare mylonitisation of amphibolite occurs only in an area where fluid penetration and resultant retrograde reactions were well-advanced. Thin pseudotachylites developed in the amphibolite and then folded, suggest that brittle movement preceeded the main mylonitisation.

Estimating the temperature of deformation to the nearest 100°C, quartz grain size measurements can be extrapolated from experimental work to show that both f_3

and f_5 mylonites formed at a maximum strain rate of 10^{-11}/ sec. Features controlling quartz recrystallization are examined in the light of mylonite textures. Strain assisted nucleation and grain boundary diffusion apparently occur at the margins of large quartz aggregates, in zones of high lattice strain, and adjacent to micas. More generally a process of progressive sub-grain disorientation in response to applied stress and initial lattice orientation has occurred.

Feldspar, clinozoisite, garnet and sillimanite all deformed by fracturing and fragmentation in mylonites. Garnet fragmentation is used to estimate minimum shear strain (γ) values of $\gamma = 14$ assuming plane strain. Mica orientation in pelitic zones and displacements on minor zones suggest similar values. Deformed quartz aggregates give minimum X : Y : Z values of 108.5 : 13.5 : 1 ($k = 0.563$) suggesting that γ has a minimum value of 7.4.

Mylonitic fold geometry results from high shear strain on quartz veins of differing initial orientation and configuration. The relative importance of buckling and differential rotation is dependent on these initial factors. Internal amphibolite folds only developed where a strong shear couple acted across an amphibolite band. These bands have undergone less deformation than the adjacent marble or mylonite and average γ values of 3.6 are obtained from the orientation of fold axial planes relative to the amphibolite band.

Quartz preferred orientation measurements taken on a universal stage are best interpreted in the light of the results of Hara et al (1972), who showed that a stable quartz c-axis pattern developed after γ of 1.8. All patterns are interpreted to give X, Y and Z axes although the fabrics only reflect the stress field during the period of quartz recrystallization. The inferred axes generally agree with those determined by other methods. Differences in several patterns are attributed to grain boundary effects of micas and accessory minerals. The patterns may be explained by quartz c-axis migration until they lie perpendicular to the zone of extension. Hence mylonites

give a single diffuse girdle and banded gneiss distinct crossed girdles. The maximum angle between the girdles reflect differential stress (and hence partial strain).

Magnetic anisotropy measurements show the importance of lineation as a principal fabric feature although this does not necessarily relate to the finite extension direction. The m value ($m = k_{max} - k_{int}/k_{int} - k_{min}$ where k = magnetic susceptibility difference) specifies the magnetic ellipsoid shape, and varies from 0.14 in the strongly mylonitic gneiss and 0.19 in the non-mylonitic gneiss, to 0.60 in the moderately mylonitic gneiss. Where both initial banding and mylonitic foliation are equally developed and m value is large, and where a strong planar anisotropy exists, it is small. This reflects the strength and relative orientation of $f_o(f_1)$ and f_3 fabrics. Anisotropy strength, defined by H ($k_{max} - k_{min}/K$, where K is the specific bulk susceptibility), is greater in the mylonitic gneiss than in the non-mylonitic gneiss although all H values are not particularly high. In general foliation and lineation show a close relationship in magnetic fabric axes.

Thin andesite to trachyte dykes are common in many parts of the Central Alps. They post-date f_3 structures but are deformed and metamorphosed by the f_5 and related m_4 events. Most dykes strike NE and dip gently SE. Their intrusion was approximately coeval with that of the Adamello massif and the hornblende porphyry dykes of the Bergamasque and Ortles Alps.

A small ultramafic (dunite) intrusion cross-cuts mylonitic fabrics and forms a small pod in the paragneiss. The dunite shows no internal deformation and mineralogical changes at the intrusion margins result from dunite-water reactions at differing temperatures. Initial Mg-chlorite formation probably acted as a barrier to further inward fluid diffusion during the uprise of the ultramafic body. The minor serpentinization which occurred probably formed by the reaction

$$5(Mg_{0.9}Fe_{0.1})_2SiO_4 + 6.83H_2O \rightleftharpoons 2.5Mg_3Si_2O_5(OH)_4$$
Forsteritic Olivine — Serpentine
$$+ 0.33Fe_3O_4 + 1.5Mg(OH)_2 + 0.33H_2$$
Magnetite — Brucite

This study has shown that the area has been deformed during three separate orogenies. The results are not compatible with subduction along the Tonale Line during the Alpine event.

8.15 Correlation of f_1 and f_3 structures across the Tonale Line

The similar geometry and orientation of the f_1 and f_3 structures in the Central and Southern Alps suggests that they may be correlated across the Tonale Line. The m_2 Lower Amphibolite metamorphism post-dates the f_1 event, and precedes the f_3 event in the Central Alps. Pegmatites are widely associated with this metamorphism which increases in grade towards the northwest in the gneisses of the Austro-Alpine Nappes (Hoernes, 1971; Purtscheller, 1969). These pegmatites give Rb-Sr muscovite ages of 252±25 m.y. (Hanson et al, 1966). Muscovites and biotites in paragneiss and orthogneiss from the Ötztal sheet and Altkristallin sheet of the Zillertaler Alps give K-Ar and Rb-Sr ages of 280 - 300 m.y. (Harre et al, 1968; Borsi et al, 1973). Similar structural - metamorphic relations are seen in the Southern Alps, although the metamorphism is of Lower Greenschist (biotite) grade. When these metamorphics are traced westward there is a marked increase in grade and around Lake Como, sillimanite grade schist and paragneiss (Gansser, 1968) are found. Pegmatites associated with this metamorphism give Rb-Sr muscovite ages of 250±25 m.y. (Hanson et al, 1966). Hence the two Hercynian metamorphic events may be correlated in the Central and Southern Alps.

Although there is no prima facie case for the correlation of both f_1 and f_3 events across the Tonale Line, this would result in a simplification of the regional tectonics compatible with the geochronological evidence. This correlation is accepted by the author. The differing magnitude and direction of the tectonic transport directions for the

f_3 event in the Central and Southern Alps would then show that the Tonale Line is a very significant regional structure.

8.20 SYNTHESIS OF FACTS FROM OTHER WORK IN THE CENTRAL AND EASTERN ALPS

There is not space to describe the detailed stratigraphy, structure and metamorphism of this part of the Alps, and an attempt will be made to limit the following description to areas and rock types which are directly relevant to the Tonale Pass area and the discussion of the origin of the observed features. Excellent summaries are given by Oxburgh (1968), Oberhauser (1968) and Trumpy (1973).

8.21 Caledonian event

The Caledonian metamorphism has been studied in detail in the Silvretta and Ötztal sheets. Hoernes (1971) has shown that disequilibrium mineral assemblages (ky - sill - st - ga - bi - mu) are present and suggested that two metamorphic phases can be distinguished. Fritsch (1964) has recorded several phases of deformation and complex mineral growth sequences in the E. Kärnten (S.Austria).

Granite from the Silvretta sheet gives an Rb-Sr isochron age of 428±17 m.y. (Grauert, 1966) and Rb-Sr total rock analyses from the Ötztal sheet indicate a major event at 410 m.y. (Harre et al, 1968). $Pb_{207/206}$ ages of 540±25 m.y. from granodioritic gneiss and U-Pb ages of 480±20 m.y. on zircons from the Ötztal sheet (Schmidt et al, 1967) show that the original sediments were probably Cambrian or Pre-Cambrian. The presence of eclogite, peridotite and several phases of deformation suggest that the "Altkristallin" has a complex Caledonian orogenic history. In the area between Mules and the Iseltal, north of the Pusteria Line (N.Italy) detailed geochronological and petrographic work has recently been carried out (Borsi et al, 1973; Sassi et al, 1974). Rb-Sr whole rock analyses on paragneiss give an isochron of 497±38 m.y. whereas orthogneiss yields on Rb-Sr isochron of 434±4 m.y. The staurolite + kyanite ± sillimanite

assemblage from the paragneiss pre-dates the orthogneiss and is related to the widespread 500 m.y. metamorphic event. The slight differences between the $Pb_{207/206}$ and U-Pb ages in the Ötztal sheet and the Rb-Sr ages in the S.Austro Alpine sheet may be attributed to the temperatures at which the various isotopic systems became closed.

8.22 Upper Palaeozoic

The Upper Greenschist, Palaeozoic, quartzite and phyllites (Turntaler Phyllites) lying unconformably on the highly deformed para- and orthogneiss (Sassi and Zanferrari, 1972) in the area south of the Tauern Window, shows that uplift and erosion occurred between the Caledonian and Hercynian events. Similar metasedimentary sequences are recognised in the Brenner Pass area (Steinach quartz phyllites), the Ötztal sheet (Förster and Leonhardt, 1972), the Ortler area, and in the Tauern Window (Oxburgh, 1967). In the Tauern Window the Habach Series (Frasl, 1958) a sequence of Upper Greenschist black phyllites, amphibolites and minor metasediments and basic and ultra-basic intrusives shows lithological similarities to the Grauwackenzone, which ranges in age from Silurian to Carboniferous (Oxburgh, 1967).

8.23 Hercynian event

Hercynian metamorphism has overprinted the Caledonian Upper Amphibolite gneisses of the "Altkristallin" sheet, and affected parts of the overlying sedimentary cover. Rb-Sr isotopic age dates on muscovites and biotites from the Ötztal and Silvretta sheets (Harre et al, 1968; Grauert 1966) show that overprinting occurred around 295 m.y. Borsi et al (1973) obtained identical Rb-Sr mica ages from ortho- and paragneiss of the Italian Zillertaler Alps. These cooling ages give a minimum age for the Hercynian metamorphism. Some augen gneiss formation occurred during this event. Cliff et al (1971) showed that hornblendes gave K-Ar ages ranging from 597 m.y. to 33 m.y. in the Tauern Window. They concluded that the majority of hornblendes were formed during the Hercynian event, because they are generally aligned parallel to Hercynian fold axes.

Outgassing occurred subsequently. Sassi and Scolari (1974) have shown that phengites with low b_o values, which imply temperatures of around 500°C and low pressures, are developed in the Turntaler Phyllites. There is a general increase in metamorphic grade to the northwest and Upper Amphibolite grade assemblages have been reported in the Silvretta sheet (Purtscheller, 1969).

In the Tonale Pass area and over much of the Austro-Alpine Nappes, Hercynian metamorphism of Upper Greenschist - Lower Amphibolite grade has resulted in equilibration of biotite, muscovite and hornblende and some garnet growth. It is difficult to envisage high grade metamorphism occurring in a pre-existing gneiss with a low water content.

Associated with, and subsequent to the Hercynian metamorphism are a series of granodiorite, tonalite and granite intrusions and related pegmatites. These are particularly well developed in the Zentralgneiss of the Tauern Window where Rb-Sr isochron ages of 244±6 m.y. (Cliff et al, 1971) and 243±11 m.y. (Lambert, 1964) have been obtained. Ages of 225 to 250 m.y. were obtained by Borsi et al (1973) from pegmatitic gneiss in the Italian Zillertaler Alps. A thermal event also occurred in the Ötztal and Silvretta sheets at around 350 m.y. (Harre et al, 1968, K-Ar model age; Grauert, 1966, Rb-Sr isochron).

Zwart (1969) has suggested that the Hercynian orogeny was characterised throughout Europe by low pressure metamorphism, high geothermal gradients, wide lateral extent, and abundant granitic intrusives.

8.24 Alpine event

The Alpine metamorphism and deformation has been shown by recent isotopic age dating (Dal Piaz et al, 1973) and detailed stratigraphical studies (Trumpy, 1973; Woletz, 1967; Oberhauser, 1968) to have occurred between the Lower Cretaceous (Albian) and Upper Miocene, a period of about 100 m.y. Detailed correlation of tectonic and metamorphic events throughout the Alps has not been attempted and Trumpy (1973) has shown that most areas possess a unique sequence of events.

Mesozoic stratigraphy - In the northern part of the Eastern Alps a phase of tensional faulting occurred in the Triassic and Jurassic with deposition of platform carbonates and deep sea sediments. These latter pelagic linestones, or red or black shales with manganiferous horizons (Halstatt facies) are more common south of the main area of carbonate deposition (Oxburgh, 1968). Rapid facies variations, breccias and local non-sequences are common in the Middle and Upper Jurassic in what is now the southern part of the Northern Calcareous Alps. In the Pennine zone the Triassic is represented by 100 m. of phengitic quartzite, quartz conglomerates and feldspathic schists (Wüstkogel Series) and about 200 m. of marble, dolomite (schistose and gypsiferous) and chloritoid phyllites (Seidlwinkl Trias). This is conformably overlain by the Jurassic and Lower Cretaceous Bundnerschiefer (equivalent to the unit of the same name in the Western Alps). This comprises phyllite, calc-mica schist, calc phyllite, minor lenses of quartzite and large ophiolite bodies. Radiolaria, aptychus limestone and manganese nodules are present within the sequence. Trumpy (1971, 1973) has shown that the Platta serpentinite and associated Albian pillow lavas were emplaced in the Lower to Middle Cretaceous (105 - 90 m.y.) Bucher and Pfeifer (1973) concluded from petrographic studies of the Malenco serpentinite that serpentinisation occurred prior to Early Alpine Greenschist grade metamorphism and deformation.

The presence of chromite as a heavy mineral in the Albian and Aptian Flysch of the Salzburg area (Trumpy, 1973) and in the Cenomanian to Lower Campanian (100 - 75 m.y.) Gosau Beds (Woletz, 1967) shows that ultrabasics were uplifted south of the depositional trough. In Cretaceous Flysch and Helveticum, detrital garnet is abundant; it is also common in post Campanian ($\sim$75 m.y.) Gosau Beds.

Folding of the Austro-Alpine gneisses on NE - SW axis and metamorphism to epidote amphibolite facies probably occurred prior to the Coniacian (85 m.y.) according to Trumpy. It is interesting that local basaltic volcanism

of Upper Maastrichtian to Palaeocene (75 to 65 m.y.) age occurred in the Southern Alps in a zone 10 to 25 km. east of the Judicaria Line (Piccoli et al, 1971).

Early Alpine event - The Eastern Alps do not show such spectacular Early Alpine metamorphic parageneses as the Western Alps (see Dal Piaz et al, 1973; Chinner and Dixon, 1973), but Cliff et al (1971) have reported oligoclase to albite, garnet, phengite, biotite and epidote in the Bundnerschiefer. More rarely near the southern margin of outcrops, staurolite is present. Höck (1974) has reported paragonite, phengite and margarite from kyanite - chloritoid schists, chlorite-chloritoid schists and zoisite calc-schists in the Central Tauern Window. More rarely glaucophane is present (Oxburgh, 1968). The highest An contents of plagioclase (An_{29}) occur in the western Tauern Window (Morteani and Raase, 1974) but these are probably a product of the Late Alpine metamorphism. The occurrence of widespread glaucophane in the Cenomanian (100 - 90 m.y.) Walserberg Sandstone of the Salzburg area (Oberhauser, 1968) shows that high P, low T, Early Alpine metamorphic assemblages were at one time more widespread than at present. It is significant that Sassi et al (1974) have reported phengitic muscovite (bo 9.025 - 9.045 Å) and a "lavender blue amphibole resembling glaucophane" (K-Ar appr. age of 90 m.y.) in the 'Altkristallin' gneisses south of the Tauern Window. In the Schneeberger Zug (S.W. Ötztal sheet) Alpine kyanite, biotite, paragonite and muscovite occur (Justin-Visentin and Zanettin, 1973). The age of this assemblage has been debated (see Purtscheller et al, 1972), but I would suggest that the above minerals are typically Alpine.

In the Southern Glockner area of the Tauern Window, N-S trending folds affect the Bundnerschiefer (Frasl and Frank, 1964). The Early Alpine metamorphism is syntectonic with respect to these folds (Oxburgh, 1968) but predates the major WNW-ESE trending large scale recumbent folds which are common in the northern part of the Glockner Depression. These latter folds are associated with the

northward thrusting of the Austro-Alpines, and locally refold the earlier N-S trending structures. This structural sequence is compatible with the f_2 and f_3 deformations in the Tonale Pass area.

Thrusting - A thick zone of phyllonite (Cima Dura Phyllites) separates the "Altkristallin" from the underlying Bundnerschiefer (Sassi et al, 1974) at the southern margin of the Tauern Window. More generally a highly sheared sequence of Mesozoic sediments (the Matrei, Gerlos and Katschberg Zone) belonging to the Lower East Alpine sheet is present. It is notable that these highly deformed quartz phyllites, chlorite schists, dolomites and diaphthoritic mica schists exhibit Lower Greenschist parageneses (Prey in Exner, 1964). In contrast, the underlying Schieferhulle (Palaeozoic and Mesozoic sediments and volcanics including the Bundnerschiefer) contains staurolite and kyanite. Phengites in phyllonite from the thrust zone contain excess radiogenic argon (Lambert, 1970) which may be attributed to a high partial pressure of Ar_{40} (Harper, 1970) and a high fluid content (Hofmann and Giletti, 1970) during metamorphism. The formation of low K phengite would then favour retention of Ar_{40} in the interlayer site.

Oberhauser (1968) has shown from stratigraphic evidence that the major northward thrusting of the "Altkristallin" sheet occurred progressively later both northwards and westwards. Thrusting in the western part of the Austro-Alpine Nappes (Engadine) continued until at least the Eocene. Associated with and subsequent to thrusting, northward verging folds were formed extensively in the "Altkristallin" sheet and underlying sediments.

The "Altkristallin" sheet is cut by numerous major mylonite zones (e.g. see Andreatta, 1948; Borsi et al, 1973; Schmid, 1973; Clar, 1973) and the detailed metamorphic and tectonic history of the resultant segments cannot always be correlated. The presence of Palaeozoic and Mesozoic sediments in many of these segments is shown diagrammatically in Figure 16 (see 4.10). R.F.Cheeney (pers.comm. 1974) has noted the presence of fractured and

sheared dolomite at the base of the Ortler Mesozoic sequence. Cadisch et al (1919) have shown that in the Silvretta sheet major thrusting generally followed SW - NE folding and was in turn succeeded by further thrusting and WSW - ENE folding.

The minimum age of thrusting which has occurred across mylonite zones is given by Rb-Sr and K-Ar biotite and muscovite cooling ages of 65 to 90 m.y. (Harre et al, 1968; Brewer, 1970; Lambert, 1970). These results imply that temperatures of over 300°C and possibly near to 500°C (biotite and muscovite, Sr and Ar equilibration temperatures respectively - Cliff et al, 1971) were attained in the Cretaceous and that the thrusting caused a significant temperature drop. Average values for biotites are 80 m.y. and for muscovites 86 m.y. These ages were not obtained from the Silvretta sheet and northern part of the Ötztal sheet where only partial Sr and Ar loss from biotite has occurred (Harre et al, 1968; Schmidt et al, 1967; Grauert, 1966).

Late Alpine event - A period of Greenschist grade metamorphism (appr. 38 to 46 m.y. - Hunziker, 1970; Steiger 1964) succeeded thrusting and deformation in the southern part of the Western Alps. In the Ticino Dome and its eastern extension to the Bergell Massif (Wenk and Keller, 1969) metamorphism attained Upper Amphibolite grade. In the Tauern Window (Cliff et al, 1971, Morteani and Raase, 1974) metamorphism reached Lower Amphibolite grade. It is difficult in the Eastern Alps to distinguish between Early and Late Alpine metamorphic assemblages but Cliff et al (1971) have shown that in the Bundnerschiefer (Peripheral Schieferhulle) staurolite and chloritoid are commonly in disequilibrium with the associated parageneses. Kyanite alteration to oligoclase has also occurred (possibly by metasomatism) and zoned garnets indicate two phases of growth; an earlier Upper Greenschist facies growth with rotational textures; and a later Amphibolite facies growth with no rotational textures. Biotite shows mimetic crystallization around early folds but is overgrown by further

biotites.

K-Ar and Rb-Sr cooling ages from biotites and muscovites in and around the Tauern Window range from 34 to 16 m.y. (Cliff et al, 1971, Lambert, 1970). It is interesting that similar ages are obtained from the adjacent "Altkristallin" sheet (Borsi et al, 1973). The intrusion of several tonalite and granodiorite bodies (e.g. Bergell, Adamello, Reiseferner and Wollanerkopf) is associated with this thermal event. Rb-Sr and K-Ar biotite ages of 31 to 45 m.y. were obtained by Borsi et al (1966) from the Adamello massif and Gulson (1973) obtained a true age of intrusion of 30 m.y. for the Bergell massif (U-Pb on sphene, monazite, zircon).

The presence of Bergell granite boulders in conglomerate in Middle to Upper Oligocene, Como Molasse (Gulson 1973, Longo 1968) suggests that rapid uplift and erosion occurred. Trumpy (1973) draws attention to the coincidence of isotopic uplift ages (30 - 11 m.y.) and the period of major Molasse sedimentation. Gravitational emplacement of the Pre-Alpine, Helvetic and Penninic Flysch Nappes also occurred at around 30 m.y. These features are a product of uplift which has a minimum value of 15 km. near the Insubric Line. Uplift and erosion rates of 0.5 to 1 mm/yr. are obtained from heat flow data (Clark and Jäger, 1969), Molasse sedimentation and present day measurements (Trumpy, 1973).

Late Tertiary to Recent - Minor thrusting and folding on WSW-ENE axes occurred in the Austro-Alpine Nappes subsequent to the Oligocene/Eocene metamorphism (Clar, 1973; Cliff et al, 1971) probably associated with the well-documented uplift. Clar (1973) has suggested that sisistral movement has occurred in the Eastern Alps, which is supported by evidence of 15 km. of lateral movement on the Engadine Fault (Trumpy, 1971) which displaces Alpine metamorphic zones. This fault passes eastwards in a steep thrust of the Ötztal sheet over the Silvretta sheet. Minor dextral movement has occurred along the E-W trending Insubric-Tonale-Pusteria-Gailtal lineament (Gansser, 1968;

Van Bemmelen, 1966; Sassi et al, 1974).

Minor E-W trending faults with relative northerly uplift have occurred in the Central Alps in recent time and faulting is still continuing as shown by minor seismicity and Holocene faulting of local moraines (Jackli,1951). These faults determine the trend of the Rhine and Rhone Valleys lying between Martigny and Chur.

8.25 Geophysical data

Ahorner and Murawski (1972) analysed seismic activity along a profile from the North Sea to the North Appenines. Almost all earthquake foci in the Alpine area lie in the upper crust, and seismograph records give a uniform stress distribution picture with σ_1 lying in a horizontal plane and trending NNW - SSE. A section across the Alps shows a thickening of the lower crust from the normal depth of about 30 km. in the Black Forest and near Lake Garda up to a maximum depth of 60 km. beneath the Silvretta sheet.

Gravity and seismic reflection data were used by Mueller and Talwani (1971) to construct a crustal profile between Munich and Florence. Seismic discontinuities exist at 10 and 20 km. depth beneath the Central Alpine area. A bulge of lower crust is interpreted beneath this area extending down to 55 km. Gravity data was used to infer the presence of a high density (possibly basic) body which extends from near Verona (at depth of 12 - 15 km.) to link with the Ivrea Zone to the west. Giese (1968) showed that this latter zone is a slab of lower crust/mantle material beneath which a low velocity wedge of sialic rocks is present.

8.26 Heat Flow data

Giese (1970) has experimentally determined velocity measurements on samples of igneous rocks under pressures up to 6 kb. and temperatures of 300°C, combined with deep seismic data to predict crustal temperatures across the Eastern and Western Alps. In the Eastern Alps a low velocity layer is developed at about 15 km. depth under a central axial zone, and temperatures over 700°C are attained between 20 and 25 km. depth. In the Western Alps

a more marked velocity inversion is present. Hence the geothermal gradient will vary from 8°C/km. (S.Germany) to 37°C/km.(W.Alps).

Measurements of the geothermal gradient in the Alpine rail tunnels are given below (from Clark, 1966);

Gotthard Tunnel	20.9°C/km.
Simplon Tunnel	32.8°C/km.
Loetschberg Tunnel	24.4°C/km.
Tauern Tunnel	23.0°C/km.
Arlberg Tunnel	17.3°C/km.

An average value for the present heat flow is thus about 20°C/km.

8.30 THEORIES OF ALPINE OROGENESIS

The structures of the Alps have stimulated theories of orogenesis since the time of Escher von der Linth and his pupil Albert Heim (Heim, 1878). The movement of the "African" block northwards as a "traineau ecraseur" was proposed as long ago as 1916 by Argand. The Deckentheorie of Termier (1903), which interpreted the Eastern Alps as a pile of allochthonous thrust sheets, has been subsequently confirmed beyond reasonable doubt (see Oxburgh, 1968, p.41).

Van Bemmelen (1960, 1966) has rejected the classic theory of crustal shortening and proposed that differential uplift and resultant gravitational sliding can account for the observed structures. Although this mechanism is generally accepted as being primarily responsible for some Alpine structures (e.g. Pre-Alpine and Penninic Flysch Nappes - Trumpy, 1973; Southern Alps asymmetrical folds - Van Hilten 1960) it cannot explain many of the observed structures, particularly those with a regular style and orientation. Since there is a greater amount of Mesozoic rocks in the East Alpine thrust sheets than can be accommodated between the autochthonous beds of the Southern Alps and the Molasse of the Bohemian massif, crustal shortening must be inferred even allowing for bulk deformation and strike slip faulting. Trumpy (1973) has suggested that in the Western Alps total shortening has a minimum value of 360 km. The presence of thick mylonite zones

at the margin of the Tauern Window and in the western Alps (see Johnson, 1973) are not compatible with gravitational movements if the arguments for rotational strain as proposed in this thesis are correct.

The theory of plate tectonics as proposed by Mackenzie and Parker (1967), Le Pichon (1968) and Isacks et al (1968) states that movements of a small number of large semi-rigid plates on a low velocity layer may be defined by rotation about a specific pole. The seismic belts of the world are zones where differential movements between rigid plates occur. Hence each plate which is generated at an ocean ridge spreads out across the ocean floor and is eventually subducted beneath an adjacent plate which may contain a continental mass. Continents are less dense than oceanic plates and accretion commonly occurs at their margins through time. A more detailed exposition of the theory and its ramifications is given in the book by Le Pichon et al (1973).

Plate tectonics provides a framework in the light of which orogenic events may be interpreted (see Dewey and Bird, 1970; Roedder, 1973). Detailed plate tectonic models for the Alpine area have been proposed by Smith (1971) and Dewey et al (1973). Smith has proposed that two main plates, Africa and Eurasia, have moved relative to one another in differing ways in the periods 180 - 81 m.y. 81 - 42 m.y. and 42 m.y. - present. Local rotations of Italy, Greece - Yugoslavia - Turkey, and Spain are suggested to account for palaeomagnetic and fitting discrepancies.

The model of Dewey et al (1973) is more complex and based on a series of microplates using step-wise rotation based on Atlantic opening rates. The major problem of this reconstruction is that features used for recognising continental margins, accreting ridges, arcs and trenches are open to criticism. Their documentation (e.g.ultramafic rock sequences, platform carbonates) is generally not well known; for example Jenkyns (1971) has shown that in the Lower Jurassic the downfaulted continental margin in North Tethys contained suites of pelagic sediments indistinguishable from true oceanic facies except where

ophiolitic basement is present. The motions used by Dewey et al (1973) are; 180 - 148 m.y., S.E. directed tension; 148 - 80 m.y., rotation of Africa counter clockwise with strike slip in the west and compression in the east; 80 - 63 m.y., N-S compression; 63 - 53 my., E - W strike slip; 53 - 9 m.y., counterclockwise movement of Africa about a pole at Tangier; 9 m.y. - present, N-S compression.

Laubscher (1971 a,b) has used palaeogeographic and large scale tectonic evidence to postulate N-S compression in the Eastern Alps before the Oligocene, and 300 km. of dextral strike slip along the Insubric fault zone in Oligocene - Neogene times. Palaeomagnetic data (Zijderveld et al, 1970) and microtectonic studies suggest that small scale counterclockwise rotational movements (N.B. sinistral) may have occurred in post - Oligocene times. The major Alpine event involved large scale north northwestward translation.

Zijderveld (1973 - Alpine Conference, London) showed that the major relative counterclockwise movement of 35° to 50°, which has been recorded in the Southern Alps, occurred in the Upper Cretaceous. The Carnic Alps show palaeomagnetic directions in agreement with those from Northern Europe. These apparently conflicting results may be explained by local differential rotation of crustal blocks in the plate tectonic model.

Dal Piaz et al (1973) have put forward a model for the origin of the Penninic Nappes and Sesia Zone in the Western Alps. The sequence of events proposed is ;-

1) Pre-Jurassic - continental basement from Penninic Zone to the Southern Alps.

2) Jurassic - some crust-plate consumption to the south causing the formation of the Piedmontese trough and separating the Sesia-Lanzo zone.

3) Cretaceous - slab moves down to the south, producing deformation and high pressure parageneses in the Penninic realm. Metamorphism was first static and then synkinematic (83 m.y.)

4) Late Cretaceous to Eocene - oblique uprise of lithospheric material. Development of schistosity.

5) Oligocene - transverse shortening and post kinematic metamorphism.

This model explains the isotopic age dates and metamorphic assemblages in the Western Alps.

Ernst (1971) has shown that subducted plates will show a metamorphic zonation with high pressure parageneses formed at depths of 25 - 35 kms. and zeolite facies assemblages at shallower levels. In a metamorphic model for the Alps (Ernst, 1973) he suggested that plate subduction occurred beneath the Austro-Alpine Nappes. Although this basic idea was accepted by Oxburgh (1973), he has suggested that the Southern Alps were split and the Austro-Alpine Nappes were flakes pushed northwards during plate collision. The northward subduction of the lower part of the Italian plate is at variance with metamorphic zonations in the Western Alps (Chatterjee, 1971; Ernst, 1971).

8.40 THE MODEL

The proposed model for the origin of the Austro-Alpine Nappes is illustrated in Figure 51.

Little can be said about the geological history of the area prior to the Hercynian event. A deep seated Upper Amphibolite grade event affected the pelites, limestones and marls in the Early Ordovician. Minor granitic intrusions were emplaced subsequently.

The Insubric Line is interpreted as a Hercynian subduction site in the Western Alps. The geophysical evidence (Giese, 1968) suggests that this dipped to the south. In the Eastern Alps this line of subduction now probably lies to the south of the Tonale Line, beneath the basement of the Southern Alps. Geophysical data suggests a correlation between a linear gravity high near Verona and the Ivrea body to the west.

The Tonale Line formed a basic weakness in the Southern Alpine basement during the Alpine event. It has probably acted as a major fault since the late Palaeozoic.

Figure 51 - Model for the hypothetical development of the Austro-Alpine Nappes since the Late Jurassic. The position of the area mapped is shown in relation to the regional structure. There is no vertical exaggeration in the sections. Parts of the present section are hypothetical, particularly at depth.

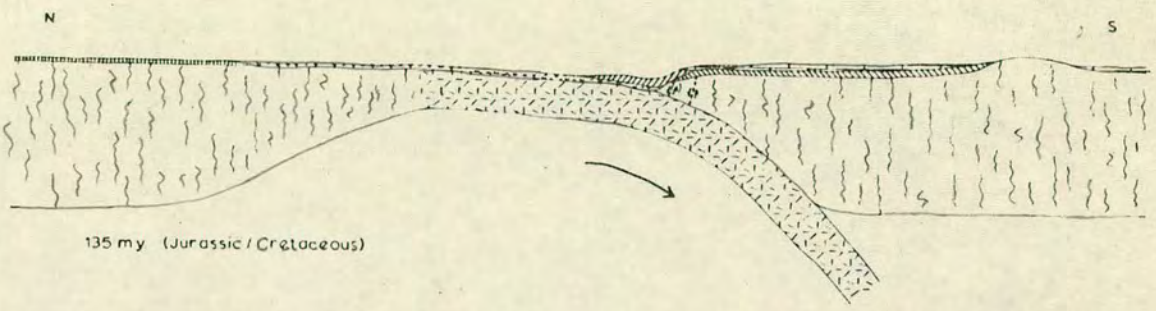

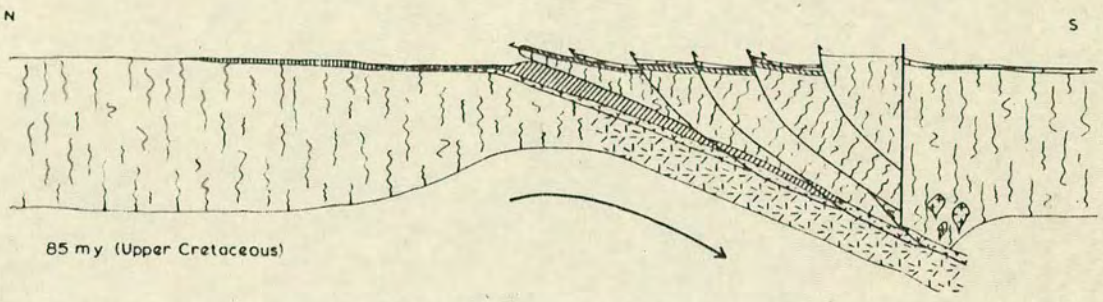

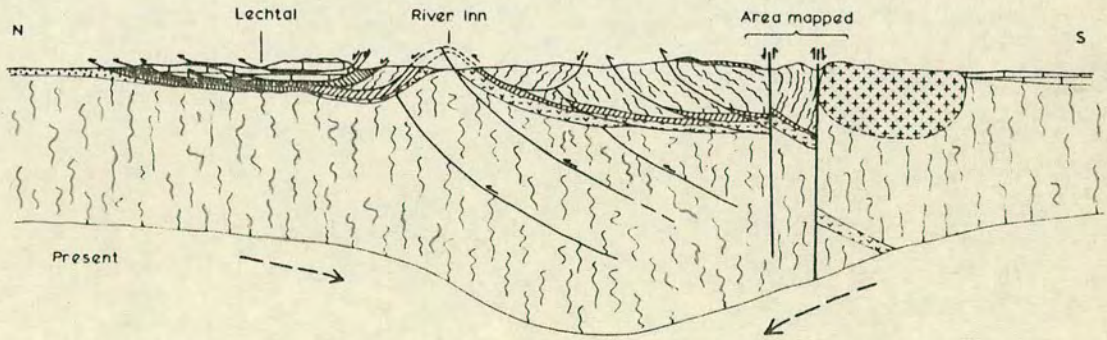

Molasse

Helveticum

Flysch

Northern Calcareous Alps and Mesozoic sediments

Bündnschiefer

Lower Austro - Alpine sheet (includes trench side sediments, basement)

Grauwackenzone

Basement Gneiss

Oceanic Crust

Calc - alkaline magma bodies

Thrust

Faults (arrows indicate downthrow side)

In the Jurassic, the basement gneiss, which constitutes a large part of the Austro-Alpine Nappes, was probably the northerly part of the Southern Alps but it is possible that a small ocean basin existed between the two units. North of these basement gneisses was a trench zone in which the Bundnerschiefer and associated ophiolites accumulated.

In the Lower Cretaceous, the rate of subduction increased, the angle of subduction lessened (Luyendyk, 1970), and the trench sediments, volcanics and intrusives were pulled down to a minimum depth of 25 km. The parts of the northward projecting South Alpine basement which later formed the Austro-Alpine Nappes were also involved in this event. The basement probably fractured in parts, causing the more northerly blocks to be subducted to greater depths.

In the Upper Cretaceous - Eocene, isostatic readjustment and strong NNW-SSE directed compressive forces caused the extensive northward thrusting of the Austro Alpine Nappes, with associated asymmetrical folding. Extensive metasomatic reactions (feldspar - mica) occur in the most southerly part of the thrust sheets, resulting from dehydration of the subducted sediments and upward fluid flow along shear and fault zones (Stavel Gneiss). Flysch deposition occurred extensively to the north of the main Alpine chain. Southward verging gravity controlled overfolds formed in the Mesozoic cover of the Southern Alps.

Subsequent to thrusting, uplift occurred and the Adamello massif, andesite dykes and small ultrabasic intrusions were emplaced along weak zones in the crust (Lower Oligocene). Later compression in a NW - SE plane caused the development of a marginal foliation in the Adamello massif and some localised thrusting and folding ocurred. Rapid uplift accompanied and followed this event (probably Upper Oligocene - Miocene). Since the greatest mass of continental material lay beneath the "root zone" region, uplift was maximum along the pre-existing Tonale - Insubric Line.

The present day geophysical and topographic information

is compatible with northward directed subduction; the Po valley forming the zone of downbuckling due to flexing of the main Italian plate. Hence a flip in the subduction direction must be postulated, probably in the Miocene.

8.50 MECHANISM OF MYLONITE INITIATION AND DEVELOPMENT

It is important to determine whether any differential upward thrusting can be related to density differences in the paragneiss sequence of the Central Alps in the area mapped (c.f. Ramberg, 1972). The following density values were obtained from hand specimens using simple experimental methods:-

Pelitic Gneiss		Amphibolite		Marble	
M156(2)	2.72 gm/cc.	M56	2.80 gm/cc.	M367	2.73 gm/cc.
T179C	2.87 gm/cc.	T26	2.80 gm/cc.	T227	2.76 gm/cc(+phl)
T131C	2.90 gm/cc.	T68A	3.05 gm/cc(+ga)	T41	2.81 gm/cc(+fo)

Mylonite		Phengite gneiss	
M156(4)	2.72 gm/cc(Casiole sheet)	T438	2.69 gm/cc.
M298	2.88 gm/cc(Peio Line)	T8	2.71 gm/cc.

All values are accurate to $\pm$ 0.05 gm/cc. Although the phengite gneiss (Stavel Gneiss) shows consistently lower values than the other lithologies, the rocks of the Central Alps all have values close to 2.8 gm/cc. The generation and emplacement of individual thrust sheets must thus only reflect contact strain effects and differing stress-strain responses of the various lithologies. Local lithological variations and structural geometry are of prime importance in determining the site of mylonite initiation.

It is probable that subduction of continental crust (average density = 2.8 gm/cc) into mantle material (average density = 3.3 gm/cc) is partly responsible for the differential stress system which results in thrusting. Lithostatic stress (σ_L) is given by $\rho . g . z./10^9$kb. where ρ = density, g = acceleration due to gravity, and z is the depth in cm. Mylonite textures suggest that overpressures of about 2 σ_L build up in dry paragneiss sheets.

Heat conduction considerations show that the complete 180 km. of Austro-Alpine thrust sheets cannot be subducted. Taking a minimum temperature of 1200°C for the mantle and

500°C for the maximum slab temperature, and using the graph for heat conduction in a slab (Carslaw and Jaeger, 1959 - p.101)

$$kt/l^2 = 0.3$$

where k = diffusivity of the slab, t = time in secs. and l = half the plate width. Using the diffusivity values of Johnson and Wenk (1974)

$$8.10^{-3}.\ t = 0.3\ (25.10^5)^2$$

$$t = \frac{62.5.\ 3.\ 10^{12}}{8.\ 10^{-3}.\ 3.10^9}\ \text{yrs}$$

$$= 7.8 \times 10^4\ \text{yrs.}$$

This value implies a subduction and uprise rate of 46 cm/yr. Mackenzie (1972) has shown that along the North Anatolian Fault a maximum movement of 4 cm/yr. occurs.

For subduction to about 25 km. depth, taking a minimum temperature of 700°C for the mantle and 500°C for the maximum slab temperature $t = 1.82 \times 10^5$ yrs. Taking 4 cm/yr. as a feasible subduction and uprise rate then 1.25×10^6 yr. are needed, assuming constant movement (itself an unlikely circumstance). The low observed temperature rise in the subducted paragneiss compared to theoretical heat considerations may be explained in part by fluid flow along mylonite zones, metamorphic reaction and possibly calc-alkaline magma generation, all of which absorb heat.

Le Pichon et al (1973) have shown that continental underthrusting is presently occurring in the Himalayan and Iranian mountain chains. Rastogi (1964) has calculated 7 focal mechanism solutions for earthquakes in the Himalayas and shown that σ_1 acted subhorizontally at right angles to the structural trend of the mountain chain. Several authors (e.g. Hast, 1958; Merrill, 1964) have shown that horizontal stress may exceed lithostatic pressure particularly at shallow crustal levels.

The differential stress $(\sigma_1 - \sigma_L)$ resulting from subduction of continental crust to a depth of 25 km. and resultant buoyant uprise is $g.z.(\rho_1-\rho_2)$ where ρ_1= density of mantle and ρ_2= density of crust.

$$\therefore \quad \sigma_1 - \sigma_L = 981.25.10^5.(0.5)/10^9 \text{ kb.}$$
$$= 1.23 \text{ kb.}$$

Using the equation given by Mackenzie (1969) we can show that downward forces resulting from temperature differences would reduce this value by about 1 kb.(assuming subducted lithosphere 75 km. thick, T at base 1200°C, other parameters as Mackenzie). Buoyancy and temperature effects may determine the depth to which "wet" sediments may be subducted. Taking the parameters given by Sclater and Francheteau (1970) we find that continental crust of 18 km. thickness may be subducted to a considerable depth. Pressure estimates from Alpine mineral assemblages around the Tauern Window (Sassi et al, 1974; Abraham et al,1974) suggest that this depth is in the range 25 - 30 km.

In order to explain the observed textures in the paragneiss of the Central Alps, we must postulate the presence of tectonic forces in addition to any gravitational uprise.

When brittle movement occurs in the "dry" paragneiss and zones of high contact strain are built up, fluid diffusion will take place preferentially along these zones. The resultant drop in shear stress which will accompany fluid diffusion (since rocks under high P fluid cannot support overpressures over about 1 kb - Brace et al, 1970) will promote differential movement and a mylonite zone will be produced. Fluid diffusion rates along the mylonite zone will be several times greater than those normal to the zones. At shallow crustal levels mylonites may change into a series of discrete thrusts and form a complex mélange - imbricate zone (e.g. Gerlos Zone).

REFERENCES

ABRAHAM, K., HÖRMANN, P.K., & RAITH, M.,1974. Progressive metamorphism of basic rocks from the Southern Hohe Tauern area, Tyrol (Austria). Neues Jahrb. Mineralogie, Abh. 122 1-35.

ACKERHAND, D., & KARL, F.,1972. Experimental studies on the formation of inclusions in plagioclases from metatonalites, Hohe Tauern, Austria (Low Temperature stability limit of the paragenesis Anorthite and Potash Feldspar). Contrib. Mineral, Petrol. 35, 11-21.

AHORNER, L., & MURAWSKI, H.,1972. Seismotektonische. Traverse von der Nordsee bis zum Appennin. Geol.Rundsch 61, 915-942.

ALBUQUERQUE, C.A.R.De.,1973. Geochemistry of biotite from granitic rocks, Northern Portugal. Geochim. Cosmochim. Acta 37, 1779-1802.

ALTHAUS, E., KAROTKE, E.,& NITSCH, K.H.,1970. An experimental re-examination of the upper stability limit of muscovite plus quartz. Neues Jahrb. Mineralogie, Monatsh. 7, 325-336.

ANDERSON, E.M.,1951. The Dynamics of faulting. Oliver & Boyd, Edinburgh.

ANDREATTA, C.,1948. La 'Linea di Peio' nel massiccio dell' Ortler e le sue miloniti. Acta Geol. Alpina (Univ. Bologna) 1, 1-63.

ANDREATTA, C., 1953. Syntektonische und post tektonische magmatische Erscheinungen der Ortlergruppe in Bezichung zum Alpinen Magmatismus. Tschermaks. Mineral. Petrogr. Mitt. 3, 93-114.

ARGAND, E., 1911. Les nappes de recouvrement des Alpes Pennines et leurs prolongements structuraux. Mater. Carte Geol. Suisse 31(6), 1-26.

ARGAND, E.,1916. Sur l'arc des Alpes Occidentales. Eclogae Geol. Helv. 14, 145-191.

ARMSTRONG, R.L., JÄGER, E., & EBERHARDT, P.,1966. A comparison of K-Ar and Rb-Sr ages on Alpine biotites.

Earth Planet. Sci. Lett. 1, 13-19.

BADOUX, H., 1963. Les belemnites tronconnees de Leytron (Valais). Bull.Lab.Geol., Mineral. Geophys. Musee Geol. Univ. Lausanne, 138, 1-7.

BARNES, H.L. & KULLERUD, G., 1961. Equilibria in sulfur-containing aqueous solutions in the system Fe-S-O and their correlation during ore deposition. Econ.Geol. 56, 648-688.

BARNES, H.L. & CZAMANSKE, G.K., 1967. Solubilities and transport of ore minerals. Geochemistry of Hydrothermal Ore Deposits. H.L.Barnes (Ed.) Holt, Rinehart and Winston U.S. 334-381.

BARNES, I., RAPP, J.B., O'NEILL, J.R., SHEPPARD, R.A. & GUDE III, A.J.,1972. Metamorphic assemblages and the direction of flow of metamorphic fluids in four instances of serpentinization. Contrib.Mineral.Petrol. 35, 263-276.

BARTH, T.F.W., 1962. The feldspar geological thermometers. Norsk. Geol. Tidssk. 42, 330.

BARTH, T.F.W.,1968. Additional data for the two-feldspar geothermometer. Lithos. 1, 305-306.

BARTH, T.F.W.,1969. Feldspars. Wiley, Bath (England) 261 pp.

BARTON, P.B.Jnr. & SKINNER, B.J.,1967. Sulfide mineral stabilities. In: Geochemistry of Hydrothermal Ore Deposits. H.L.Barnes (Ed.) Holt, Rinehart and Winston, U.S. 236-333.

BASKIN, Y., 1956. A study of authigenic feldspars. J. Geol. 64, 132-155.

BATEMAN, P.C. & DODGE, F.C.W., 1970. Variations of major chemical constituents across the Central Sierra Nevada batholith. Geol.Soc.Am., Bull. 81, 400-420.

BEACH, A. & FYFE, W.S., 1972. Fluid transport and shear zones at Scourie, Sutherland: Evidence of overthrusting. Contrib. Mineral. Petrol. 36, 175-180.

BELL, T.H. & ETHERIDGE, M.A.,1973. Microstructure of mylonites and their descriptive terminology. Lithos 6, 337-348.

BEMMELEN, R.W. VAN, 1960. New views on East Alpine Orogenesis. Int. Geol. Congr. Copenhagen 18, 99-116.

BEMMELEN, R.W. VAN, 1966. The structural evolution of the Southern Alps. Geol.Mijnbouw 45, 405-444.

BERAN, A., 1969. Beiträge zur verbreitung und genesis Phengit-führender gesteine in den Ostalpen. Tschermaks Mineral, Petrogr. Mitt. 13, 115-130.

BIANCHI, A. DAL PIAZ, G. et al. 1940. Il settore nord-occidentale del massiccio dell'Adamello. Soc.Geol. Ital., Boll. 65, 1-20.

BIANCHI, A., DAL PIAZ, G., TRENER, G.B. et al, 1953. Monte Adamello. Foglio 20 della Carta d'Italia al 100,000 dell'Instituto Geografica Militare. Firenze.

BIANCHI, A., CALLEGARI, E. & JOBSTRAIBIZER, P.G., 1970. I tipi petrografici fondamentali del plutono dell'Adamello. Consig. Naz. delle richerche, Univ. Padova.

BIOT, M.A., 1961. Theory of folding of stratified visco-elastic media and its implications in Tectonics and Orogenesis. Geol. Soc. Am., Bull. 72, 1595-1620.

BOETTCHER, A.L., 1973. Volcanism and Orogenic belts - the origin of andesites. Tectonophysics. 17, 223-240.

BORSI, S., FERRARA, G., & TONGIORGI, E., 1966. Rb-Sr and K-Ar ages of intrusive rocks of Adamello and Mt.Sabion (Trentino, Italy). Earth Planet. Sci.Lett. 1, 55-57.

BORSI, S., DEL MORO, A. & FERRARA, G., 1972. Eta' radiometriche delle rocce intrusive del Massiccio di Bressanone - Ivigna - Monte Croce (Alto Adige). Soc. Geol. Ital. Boll. 91, 387-406.

BORSI, S., DEL MORO, A., SASSI, F.P. & ZIRPOLI, G.,1973. Metamorphic evolution of the Austridic rocks to the south of the Tauern Window (Eastern Alps). Radiometric and Geo-petrologic data. Soc.Geol.Ital., Mem. 12, 549-571.

BOTTINGA, Y., KUDO, A. & WEILL, D., 1966. Some observations on Oscillatory Zoning and crystallization of magmatic plagioclase. Am. Mineral. 51, 792-806.

BOWEN, N.L., 1913. Melting phenomena in plagioclase feldspars. Am. J. Sci. 35, 590

BOWEN, N.L.,1928. The evolution of igneous rocks. Princeton Univ. Press. Princeton, N.J. 1928.

BOWEN N.L., & SCHAIRER, J.F.,1936. The problem of the intrusion of dunite in the light of the olivine diagram. 16th Int. Geol. Cong. Rpts. (1933). 391-396.

BOWEN, N.L. & TUTTLE, O.F. 1949. The system $MgO-SiO_2-H_2O$ Geol. Soc. Am., Bull. 60, 439-460.

BOYD, F.R.,1961. Welded tuffs and flows in the Rhyolite plateau of Yellowstone Park. Geol.Soc.Am.,Bull. 72,387-426.

BRACE, W.F., ERNST, W.G., & KALLBERG, R.W. 1970. An experimental study of tectonic overpressures in Franciscan rocks. Geol.Soc. Am. Bull. 81, 1325-1338.

BREWER, M.S.,1970. K-Ar age studies in the Eastern Alps - the Oberostalpindecke of Kärnten - D.Phil. thesis (unpubl.), Oxford, 1970.

BROWN, E.H., 1967. The Greenschist Facies in part of Eastern Otago, New Zealand. Contrib. Mineral Petrol. 14, 259-292.

BROWN, G.C., 1971. Granitic liquids: their generation and intrusion. Geol. Mag. 108, 343-345.

BROWN, G.C.,1973. Evolution of Granite Magmas at Destructive Plate Margins. Nature; Phys. Sci. 241, 26-28.

BUCHER, K., & PFEIFER, H.R., 1973. Über Metamorphose und Deformation der östlichen Malenco - Ultramafitite und deren Rahmengesteine (Prov. Sondrio, N.Italien). Schweiz. Mineral. Petrogr. Mitt. 53, 231-242.

BUDDINGTON, A.F. 1959. Granite emplacement with special reference to North America. Geol.Soc.Am., Bull.70, 671-747.

CADISCH, J., LEUPOLD, W.,EUGSTER, H. & BRAUCHLI, R., 1919. Geologische Untersuchungen in Mittelbünden. Vierteljschr. Natf. Ges. Zürich. 64, 359-417.

CADY, W.M., ALBEE, A.L. & CHIDESTER, A.H.,1963. Petrology

and geochemistry of selected talc-bearing ultramafic rocks and adjacent rocks in North-central Vermont. U.S.Geol.Surv. Bull. 1122-B, 1-78.

CANN, J.R., 1970. Upward movement of granitic magma. Geol. Mag. 107, 335-340.

CARR, J.M.,1954. Zoned plagioclases in layered gabbros of the Skaergaard intrusion, East Greenland. Mineral, Mag. 30, 367-375.

CARRARO, F. & FERRARA, G. 1968. Alpine 'tonalite' at Miagliano, Biella (Zona Diorito - Kinzigitica): a preliminary note. Schweiz Mineral Petrogr. Mitt.48, 75-80.

CARRARO, F., DAL PIAZ, G.V. & SACCHI, R.,1970. Series di Valpelline e Il Zona Diorito-Kinzigitica sono i relitti di un reciprimento proveniente della Zona Ivrea-Verbano. Soc. Geol. Ital., Mem. 9, 197-224.

CARSLAW, H.S. & JAEGER, J.C., 1959. Conduction of Heat in Solids. Oxford University Press (Clarendon), Oxford.

CARTER, N.L., CHRISTIE, J.M. & GRIGGS, D.T.,1964. Experimental deformation and recrystallization of quartz. J.Geol. 72, 687-733.

CHATTERJEE, N.D., 1971. Phase equilibria in the Alpine Metamorphic Rocks of the Environs of the Dora-Maira Massif, Western Italian Alps. Neues Jahrb Mineralogie, Abh. 114, 181-210, 211-245.

CHESSEX, R.,1962. Determination d'age des quelques roches des Alpes du Sud et des Apenins par le methode des "dommages due a la radioactivite". Bull.Suisse Mineral.Petrogr. 42, 653-655.

CHIESA, S., LIBORIO, G., MOTTANA, A. & PASQUARE, G., 1972. La Paragonite nel Calcescisti delle Alpi: Distribuzione e interpretazione geo-petrologica. Soc. Geol. Ital., Mem. 11, 1-30.

CHINNER, G.A., & DIXON, J.E.,1973. Some High-pressure parageneses of the Allalin Gabbro, Valais, Switzerland. J. Petrol. 14.

CHRISTIE, J.M., 1963. Moine Thrust Zone in the Assynt region, North-West Scotland. Calif. Univ., Publ. Geol. Sci. 40, 345-440.

CIPRIANI, C., SASSI, F.P., & SCOLARI, A., 1971. Metamorphic White Micas: Definition of paragenetic fields. Schweiz. Mineral. Petrogr. Mitt. 51, 259-302.

CLAR, E., 1973. Review of the structure of the Eastern Alps. In Gravity and Tectonics, ed. De Jong & Scholten. J. Wiley & Sons., N.Y., 253-270.

CLARK, S.P.Jnr., 1966. Handbook of Physical Constants. Geol. Soc. Am., Mem. 97, 1-587.

CLARK, S.P. & JÄGER, E., 1969. Denudation Rate in the Alps from geochronologic and heat flow data. Am. J. Sci. 10, 1143-1160.

CLIFF, R.A., NORRIS, R.J., OXBURGH, E.R. & WRIGHT, R.C., 1971. Structural, metamorphic and geochronological studies in the Reisseck and Southern Ankogel Groups, the Eastern Alps. Geol. Bundesant. Wein. Jahrb. 114, 121-272.

CLOOS, E.,1947. Oolite deformation in South Mountain fold, Maryland. Geol. Soc. Am. Bull. 58, 843-918.

CLOOS, E., 1971. Microtectonics along the western edge of the Blue Ridge, Maryland and Virginia. Studies in Geology. Univ. Johns Hopkins 20. Johns Hopkins Press, Baltimore, Maryland. 234pp.

COBBOLD, P.R., COSGROVE, J.W. & SUMMERS, J.M.,1972. Development of internal structures in deformed anisotropic rocks. Tectonophysics. 12, 23-53.

COLEMAN, R.G.,1967. Low-temperature reaction zones and alpine ultramafic rocks of California, Oregon and Washington. U.S. Geol. Surv. Bull. 1247 49pp.

COX, R.C., 1969. Inclusions in garnet: discussion and suggested mechanism of growth for syntectonic garnets. Geol. Mag. 106, 57-62.

CZAMANSKE, G.K. & WONES, D.R.,1973. Oxidation during magmatic differentiation; Finnmarke Complex, Oslo area,

Norway: Part 2, the mafic silicates. J.Petrol.14, 349-380.

DALLMEYER, R.D., & DODD, R.T., 1971. Distribution and significance of Cordierite in Paragneisses of the Hudson Highlands, Southeastern New York. Contrib.Mineral.Petrol. 33, 289-308.

DAL PIAZ, G.V., GROSSO, G. & MARTINOTTI, G.,1971. La Il Zona Dioritico - Kinzigitica tra la Valsesia e la Valle d'Ayas (Alpi occidentali). Soc. Geol.Ital.,Mem.10, 257-276.

DAL PIAZ, G.V. HUNZIKER, J.C. & MARTINOTTI, G.,1972. La Zona Sesia - Lanzo e L'evoluzione tettonico-metamorfica delle Alpi Nordoccidentali interne. Soc. Geol. Ital., Mem. 11, 433-460.

DAL PIAZ, G.V. HUNZIKER, J.C. & MARTINOTTI, G.,1973. Excursion to the Sesia Zone of the Schweiz. Mineralogische und Petrographische Gesellschaft. Schweiz. Mineral. Petrogr. Mitt. 53, 477-490.

DALZIEL, I.W.D., & BAILEY, S.W.,1968. Deformed garnets in a mylonitic rock from the Grenville Front and their tectonic significance. Am. J. Sci. 266, 542-562.

DAY, H.W.,1973. The high temperature stability of muscovite plus quartz. Am. Mineral. 58, 255-262.

DE CAPRARIIS, P., 1974. Stress-induced viscosity changes and the existence of dominant wavelengths in folds. Tectonophysics 23, 139-148.

DEER, W.A., HOWIE, R.A. & ZUSSMAN, J.,1962. Rock-forming minerals, 5 Vols. Longmans, London.

DEER, W.A., HOWIE, R.A. & ZUSSMAN, J. 1966. An introduction to the rock-forming minerals. Longmans, London.

DEWEY, J.F., 1965. Nature and origin of kink bands. Tectonophysics, 1, 459-494.

DEWEY, J.F. & BIRD, J.M.,1970. Mountain belts and the new global tectonics. J.Geophys. Res. 75, 2625-2647.

DEWEY, J.F., PITMAN, W.C., RYAN, W.B. & BONNIN, J.,1973. Plate tectonics and the Evolution of the Alpine System. Geol. Soc. Am., Bull. 84, 3137-3180.

DICKINSON, W.R., 1970. Relation of andesites, granites and derivative sandstones to arc-trench tectonics. Rev. Geophys. Space Phys. 8, 813-860.

DONATH, F.A. & FRUTH, L.S. Jnr. 1971. Dependence of strain-rate effects on deformation mechanism and rock type. J.Geol. 79, 347-371.

EGGLER, D.H., 1972. Water-saturated and undersaturated melting relations in a Paricutin andesite and an estimate of water content in the natural magma. Contrib. Mineral. Petrol. 34, 261-271.

EISBACHER, G.H., 1970. Deformation mechanics of mylonitic rocks and fractured granites in the Cobequid Mountains, Nova Scotia, Canada. Geol. Soc. Am., Bull. 81, 2009-2020.

ELLIOT, D., 1972. Deformation Paths in Structural Geology. Geol. Soc. Am., Bull. 83, 2621-2638.

ELLIOT, D., 1973. Diffusion flow laws in Metamorphic Rocks. Geol. Soc. Am., Bull. 84, 2645-2664.

ERNST, W.G., 1963. Significance of Phengitic Micas from low-grade schists. Am. Mineral. 48, 1357-1371.

ERNST, W.G., 1965. Mineral paragnesis in Franciscan metamorphic-rocks, Panoche Pass, California. Geol. Soc. Am., Bull. 76, 879-914.

ERNST, W.G., 1971. Metamorphic zonations on presumably subducted Lithospheric plates from Japan, California, and the Alps. Contrib. Mineral. Petrol. 34, 43-59.

ERNST, W.G., 1973. Interpretive Synthesis of metamorphism in the Alps. Geol. Soc. Am. Bull. 84, 2053-2078.

ERNST, W.G., SEKI, Y., OWUKI, H. & GILBERT, M.C., 1970. Comparative study of Low-grade metamorphism in the California Coast Ranges and the Outer Metamorphic belt of Japan. Geol. Soc. Am. Mem. 124, 276pp.

ETHERIDGE, M.A., 1973. Experimentally produced slaty and crenulation cleavages during a single deformation. J. Geol. Soc. Aust. 20, 223-227.

ETHERIDGE, M.A. & HOBBS, B.E., 1973. Chemical and

deformational controls on recrystallization of mica. Contrib. Mineral. Petrol. 43, 111

EUGSTER, H.P. & YODER, H.S., 1955. Micas. Carnegie Inst. Washington Yearb. 54, 124-129.

EVANS, B.W., 1965. Application of a reaction rate method to the breakdown equilibria of muscovite plus quartz. Am. J. Sci. 263, 647-667.

EVANS, B.W. & TROMMSDORFF, V., 1970. Regional metamorphism of ultramafic rocks in the Central Alps: Parageneses in the system CaO-MgO-SiO_2-H_2O. Schweiz Mineral. Petrogr. Mitt. 50, 481-492.

EXNER, Ch., 1965. Phengit in gesteinen der östlichen Hohen Tauern. Carinthia II, 80-89.

FAWCETT, J.J., & YODER, H.S., 1966. Phase relationship of Chlorites. Am. Mineral. 51, 353-380.

FLETT, J.S., 1912. The Geology of Ben Wyvis. Mem. Geol. Surv. Scot. 109.

FLEUTY, M.J., 1964. The Description of folds. Geol.Assoc. (London), Proc. 75, 461-492.

FLINN, D., 1962. On folding during three-dimensional progressive deformation. Geol.Soc. Lond., Q.J. 118, 385-428.

FLINN, D.,1965. Deformation in Metamorphism. In: Controls of Metamorphism. W.S. Pitcher & G.W. Flinn (Eds.) Oliver & Boyd, Edinburgh. 46-72.

FÖRSTER, H., & LEONHARDT, J., 1972. Die Ötztaler Masse - ein präkambrisches element in den Ostalpen ? Geol. Rundsch 61, 69-87.

FRASL, G., 1958. Zur Seriengliederung der Schiefierhülle in den mittleren Hohen Tauern. Jb. Geol. Bundesanst, Wien 101, 323-472.

FRASL, G., & FRANK, W., 1964. Mittlere Hohe Tauern. In : Geologischer Führer zur Exkursionen durch die Ostalpen. Mitt. Geol. Ges., Wein. 57, 17-32.

FREUND, R., 1974. Kinematics of Transform and Transcurrent Faults. Tectonophysics 21, 93-134.

FRITSCH, W., 1964. Mittel kärnten. In: Geologischer Führer eu Exkursionen durch die Ostalpen. Mitt. Geol. Ges. Wien. 57, 331-352.

FYFE, W.S., 1971. Some thoughts on granitic magmas. In: Mechanism of Igneous Intrusion. G.Newall and N.Rast (Eds.) Gallery, Liverpool. 201-216.

FYFE, W.S., 1973. The generation of batholiths. Tectonophysics 17, 273-284.

GANSSER, A., 1968. The Insubric Line, a major geotectonic problem. Schweiz. Mineral. Petrogr. Mitt. 48, 123-143.

GAY, N.C.,1968. Pure shear and simple shear deformation of inhomogeneous viscous fluids. 1. Theory. Tectonophysics 5, 211-234.

GEZE, B., 1962. Relations entre volcans et plutons dans la Montagne Noir, les Causses et le Bas-Languedoc (Sud de la France). Bull. Volcanol. Ser. 2, 24, 87-91.

GIESE, P., 1968. Die Struktur der Erdkruste im bereich der Ivrea-Zone. Schweiz. Mineral. Petrogr. Mitt. 48, 261-284.

GIESE, P., 1970. Die Temperaturverteilung in der Erdkruste des Alpenvorlandes und der Alpen, abgeschätzt aus tiefenseismischen Beobachtungen. Schweiz. Mineral. Petrogr. Mitt. 50, 597-610.

GRAESER, S & NIGGLI, E., 1967. Zur Verbreitung der Phengite in den Schweizer Alpen; ein Beitrag zur Zoneographie der Alpinen Metamorphose. In: Etages Tectoniques, Colloque de Neuchatel. Neuchatel, Suisse. pp. 89-104.

GRAESER, S. & HUNZIKER, J.C., 1968. Rb-Sr and Pb-Isotopen-Bestimmungen an Gesteinen und Mineralien der Ivrea-Zone. Schweiz. Mineral. Petrogr. Mitt. 48, 189-204.

GRAUERT, B., 1966. Rb-Sr Age Determination on Orthogneiss of the Silvretta (Switzerland). Earth Planet Sci. Lett.1, 139-147.

GREEN, D.H., 1967. High-temperature peridotite intrusions. In: Ultramafic and Related Rocks. P.J.Wyllie, (Ed.) John Wiley & Sons, New York. 212-221.

GREEN, T.H. & RINGWOOD, A.E., 1968. Genesis of the calc-alkaline igneous rock suite. Contrib. Mineral. Petrol. 18, 105-162.

GREEN, H.W., GRIGGS, D.T. & CHRISTIE, J.M., 1970. Syntectonic and annealing recrystallization of fine-grained quartz aggregates. In: Experimental and Natural Deformation, P. Paulitsch, (Ed.). Springer-Verlag, Berlin/Heidelberg. 272-335.

GRESENS, R.L., 1967. Tectonic-hydrothermal pegmatites 1. The Model. Contrib. Mineral. Petrol. 15, 345-355.

GRIEVE, R.A.F. & FAWCETT, J.J., 1974. The Stability of chloritoid below 10kb. P H_2O. J.Petrol. 15, 113-139.

GRIGGS, D.T., 1967. Hydrolytic weakening of quartz and other silicates. R. Astron. Soc., Geophys.J. 14, 19-31.

GRIGGS, D.T., TURNER, F.J. & HEARD, H.C., 1960. Deformation of rocks at 500°C - 800°C. In: Rock Deformation: a symposium. D.T.Griggs & J.W. Handin (Eds.). Geol.Soc. Am., Mem. 79, 39-104.

GRIGGS, D.T., & BLACIC, J.D., 1965. Quartz; Anomalous weakness of synthetic crystals. Science 147, 292.

GULSON, B.L., 1973. Age relations in the Bergell region of the southeast Swiss Alps: with some geochemical comparisons. Eclogae Geol. Helv. 66, 293-313.

GÜVEN, N., 1967. The crystal structures of 2M Phengite and 2M Muscovite, Carnegie Inst. Washington, Yr.Book 66, 487-492.

GWINNER, M.P., 1971. Geologie der Alpen. Nagele und Obermiller, Stuttgart.

HAFNER, W., 1951. Stress distributions and faulting. Geol. Soc. Am., Bull. 62, 373-398.

HALL, A., 1967. The distribution of some major and trace elements in feldspars from the Rosses and Ardara granite complexes, Donegal. Ireland. Geochim. Cosmochim. Acta. 31, 835-847.

HAMMER, W. & TRENER, G.B., 1908. Geologische spezialkarte, Blatt Bormio und Passo del Tonale e relative Erläuteringen, k.k. geol. Reichsanstalt. Wien.

HANDIN, J., 1966. in CLARK, S.P. Jnr: Handbook of Physical Constants. Geol. Soc. Am., Mem. 97.

HANDIN, J., FRIEDMAN, M.,LOGAN, J., SOWERS, G.M. & STEARNS D.W., 1973. Mechanical properties of rocks affecting earthquake generation: Semi-annual Progr. Rep. No.2. A.R.P.A. Contract No.14-08-0001-12723. Office of Earthquake Research. U.S. Geol.Survey, Menlo Park, Calif. 1-72.

HANSEN, E., 1966. Structural geology - in particular the determination of slip plane orientations from the geometry of folds. Ann.Rep. Director, Geophys. Lab., 386-410, Washington, D.C.

HANSON, G.N., EL TAHLAWI, M.R. & WEBER, W., 1966. K-Ar and Rb-Sr ages of Pegmatites in the South Central Alps. Earth Planet Sci. Lett. 1, 407-413.

HARA, I. & PAULITSCH, P., 1971. c-axis fabrics of quartz in buckled quartz veins. Neues Jahrb. Mineralogie Abh. 115, 31-53.

HARA, I., TAKEDA, K., & KIMURA, T., 1972. Preferred lattice orientation of quartz in shear deformation. J.Sci. Hiroshima Univ. 7, 1-10.

HARKER, A., 1939. Metamorphism. 2nd Edition. Methuen & Co. London.

HARLOFF, C., 1927. Zonal structure in plagioclases. Leidsche Geol. Mededeel. 2, 99-114.

HARPER, C.T., 1970. Graphical solutions to the problem of radiogenic Argon-40 loss from metamorphic minerals. Eclog. Geol. Helvetiae. 63, 119-140.

HARRE, W., KREUZER, H., LENZ, H., MÜLLER, P., WENDT, I. & SCHMIDT, K., 1968. Rb/Sr and K/Ar - Altersbestimmungen am Gesteinen der Ötztalkristallins (Ostalpen). Geol. Jahrb. 86, 797-825.

HARRIS, P.G., KENNEDY, W.Q. & SCARFE, C.M. 1971. Volcanism versus plutonism - the effect of chemical composition. In: Mechanism of Igneous Intrusion. G. Newall and N.Rast (Eds.) Gallery Press. Liverpool. 187-200.

HAST, N., 1958. The measurement of rock pressure in mines. Sver. Geol. Undersokn. 52, Stockholm. 1-183.

HATHERTON, T. & DICKINSON, W.R., 1969. The relationship between andesitic volcanism and seismicity in Indonesia, the Lesser Antilles, and other island arcs. J.Geophys. Res. 74, 5301-5310.

HEIM, A., 1878. Untersuchungen über den Mechanismus der Gebirgsbilding. Schwabe, Basel.

HEIM, A., 1922. Geologie der Schweiz. Tauchnitz, Leipzig.

HEINRICKSEN, Th., & SCHURMANN, K.,1971. Synthese und stabilität von glimmern im system $CaO-Na_2O-Al_2O_3-SiO_2-H_2O$. Fortschr. Mineral. 49, 21-22.

HELGESON, H.C., 1974. Chemical interaction of feldspars and aqueous solutions. In: The Feldspars. W.S.Mackenzie & J.Zussman. (Eds.) Manchester University Press.

HEMLEY, J.J. & JONES, W.R., 1964. Chemical aspects of hydrothermal alteration with emphasis on hydrogen metasomatism. Econ.Geol. 59, 538-569.

HENRY, B., 1973. Studies of Microtectonics, anisotropy of magnetic susceptibility and palaeomagnetism of the Permian Dome de Barrot (France): Palaeotectonic and palaeosedimentological implications. Tectonophysics. 17, 61-72.

HESS, P.C., 1969. The metamorphic paragenesis of cordierite in pelitic rocks. Contrib. Mineral. Petrol. 24, 191-207.

HESS, H.H. & OTALORA, G., 1964. Mineralogical and chemical composition of the Mayaguez serpentinite cores. In: A study of serpentinite. C.A.Burk, (Ed.) Nat.Acad. Sci - Nat. Res. Coun. Publ. 1188, 152-168.

HIETANEN, A., 1974. Amphibole pairs, epidote minerals, chlorite and plagioclase in metamorphic rocks, Northern Sierra Nevada, California. Am. Mineral. 59, 22-40.

HIGGINS, M.W., 1971. Cataclastic Rocks. U.S.G.S. Prof. Paper 687, Washington. 1-97.

HILLS, E.S., 1936. Reverse and oscillatory zoning in plagioclase feldspars. Geol. Mag. 73, 49-56.

HILTEN, D.VAN. 1960. Geology and Permian palaeomagnetism of the Val di Non area, W. Dolomites. Geologica Ultraiectina 5, 1-95.

HILTEN D VAN, 1964. Evaluation of some geotectonic hypotheses by palaeomagnetism. Tectonophysics. 1, 3-71.

HOBBS, B.E., 1966. Microfabrics of tectonites from the Wyangala Dam, New South Wales, Australia. Geol. Soc. Am., Bull. 77, 685-706.

HOBBS, B.E., 1968. Recrystallization of single crystals of quartz. Tectonophysics 6, 353-401.

HÖCK, V., 1974. Co-existing phengite, paragonite and margarite in metasediments of the Mittlere Hohe Tauern, Austria. Contrib. Mineral.Petrol. 43, 261-273.

HOERNES, S., 1971. Petrographische Untersuchungen an Paragneisen des polymetamorphen Silvrettakristallins. Tschermaks Mineral. Petrogr. Mitt. 15, 56-70.

HOFMANN, A.W., & GILETTI, B.J., 1970. Diffusion of geochronologically important nuclides in minerals under hydrothermal conditions. Eclog. Geol. Helvetiae 63, 141-150.

HOLDAWAY, M.J., 1966. Hydrothermal stability of clinozoisite plus quartz. Am. J. Sci. 264, 643-667.

HOLDAWAY, M.J., 1971. Stability of andalusite and the aluminium silicate phase diagram. Am. J. Sci. 271, 97-131.

HOLM, J.L. & KLEPPA, O.J., 1966. The thermodynamic properties of the aluminium silicates. Am. Mineralogist 51, 1608-1622.

HÖRMANN, P.K. & RAITH, M., 1973. Bildungsbedingungen von Al-Fe(III) - Epidoten. Contrib.Mineral.Petrol.38, 307-320.

HOSCHEK, G., 1969. The stability of staurolite and chloritoid and their significance in metamorphism of pelitic rocks. Contrib. Mineral. Petrol. 22, 208-232.

HOSCHEK, G., 1973. Die Reaktion Phlogopit+Calcit+Quartz = Tremolit+Kalifeldspar + H_2O + CO_2. Contrib. Mineral. Petrol. 39, 231-237.

HOSSACK, J.R., 1968. Pebble deformation and thrusting in the Bygdin Area (South Norway). Tectonophysics 5, 315-339.

HOSTETLER, P.B., COLEMAN, R.G., MUMPTON, F.A. & EVANS, B.W., 1966. Brucite in Alpine Serpentinites. Am.Mineral 51, 75-98.

HOWARD, K.A. 1968. Flow direction in triclinic folded rocks. Am. J. Sci. 266, 758-765.

HSU, L.C., 1968. Selected phase relationships in the system Al-Mn-Fe-Si-O-H - A model for garnet equilibria. J. Petrol. 9, 40-83.

HU, H.,1969. Reorientation in recrystallization. In: Textures in Research and Practice. J.Grewen & G.Wassermann (Eds.) Springer-Verlag, Berlin, 200-226.

HUDLESTON, P.J., 1973. Fold Morphology and some geometrical implications of theories of fold development. Tectonophysics 16, 1-46.

HUDLESTON, P.J., 1973. The analysis and interpretation of minor folds in the Moine rocks of Monar, Scotland. Tectonophysics 17, 89-132.

HUDLESTON, P.J. & STEPHANSSON, O., 1973. Layer shortening and fold-shape development in the buckling of single layers. Tectonophysics 17, 299-321.

HUNZIKER, J.C.,1966. Zur Geologie und Geochemie der Gebiete zwischen Valle Antigorio (Prov. di Novara) und Valle di Campo (Kt. Tessin). Schweiz Mineral. Petrogr. Mitt. 46, 473-552.

HUNZIKER, J.C.,1970. Polymetamorphism in the Monte Rosa, Western Alps. Eclogae Geol. Helv. 63, 151-161.

HUNZIKER, J.C., 1974. Rb-Sr and K-Ar age determinations and the Alpine tectonic history of the Western Alps. Mem. Inst. Geol. Mineral. Univ. Padova. XXXI.

HYNDMAN, D.W.,1972. Petrology of Igneous and Metamorphic rocks. McGraw Hill. N.Y.

ISACKS, B., OLIVER, J. & SYKES, L.R.,1968. Seismology and the new global tectonics. J.Geophys. Res. 73, 5855-5899.

JÄCKLI, H., 1951. Verwerfungen jungquartären Alters im südlichen Aarmassiv bei Somnix - Rabius (Graubünden). Eclog. Geol. Helv. 44, 332-337.

JAEGER, J.C.,1957. The temperature in the neighbourhood of a cooling intrusive sheet. Am. J. Sci. 255, 306-318.

JAEGER, J.C.,1959. Temperatures outside a cooling intrusive sheet. Am. J. Sci. 257, 44-54.

JAEGER, J.C. & COOK, N.G.W.,1969. Fundamentals of Rock Mechanics. Methuen.

JÄGER, E., 1970. Rb-Sr systems in different degrees of metamorphism. Eclogae Geol. Helvetiae. 63, 163-172.

JÄGER, E., NIGGLI, E. & WENK, E.,1967. Rb-Sr Altersbestimmungen an Glimmern der Zentralalpen. Beitr. Geol.Karte Schweiz., N.F. 134, 1-67.

JAKES, P. & WHITE, A.J.R.,1970. K/Rb ratios of rocks from island arcs. Geochim. Cosmochim. Acta. 34, 849-856.

JAMES, D.E.,1971. Plate tectonic model for the evolution of the central Andes. Geol. Soc. Am., Bull. 82, 3325-3346.

JENKYNS, H.C., 1971. The genesis of condensed sequences in the Tethyan Jurassic. Lethaia 4, 327-352.

JOHANNES, W., 1968. Experimental investigation of the reaction forsterite + H_2O = serpentine + brucite. Contrib. Mineral. Petrol. 19, 309-315.

JOHNSON, L.R. & WENK, H.R.,1974. Anistropy of physical properties in metamorphic rocks. Tectonophysics 23, 79-98.

JOHNSON M.R.W.,1961. Polymetamorphism in movement zones in the Caledonian thrust belt of N.W. Scotland. J.Geol. 69, 417-432.

JOHNSON, M.R.W.,1963. Some time relations of movement and metamorphism in the Scottish Highlands. Geol. Mijnbouw. 42., 121-142.

JOHNSON, M.R.W.,1973. Displacement on the Insubric Line. Nature: Phys. Sci. 241, 116-117.

JUSTIN-VISENTIN, E. & ZANETTIN, B.,1968. Genesi di

cornu-bianiti a staurolite-granato-andalusite-cordierite nell' aureola di contatto dell'Adamello: Studi Trentini Scienze Nat., 45, 224-245.

JUSTIN-VISENTIN, E. & ZANETTIN, B., 1973. On the age of white mica porphyroblasts in the Schneeberger Schists. Contrib. Mineral. Petrol. 39, 341-342.

KAHLER, F. & PREY. S.,1963. Erlauteringen zur Geologischen Karte des Nassfeld-Gartnerkofel-Gebietes in den Karnischen Alpen. Geol. Bundesanst. Wien.

KAMB, W.B., 1959. Theory of preferred crystal orientation developed by crystallization under stress. J.Geol.67,153-171.

KARL, F.,1959. Vergleichende petrographische Studien an den Tonalitgraniten der Hohen Tauern und den Tonalit-Graniten einiger periadriatisher Intrusive-massive. Jb. Geol. Bundesanst., Wien, 102, 1-192.

KERRICK, D.M.,1968. Experiments on the upper stability limit of pyrophyllite at 1.8 kilobars and 3.9 kilobars water pressure. Am. J. Sci. 266, 204-214.

KERRICK, D.M.,1972. Experimental determination of muscovite + quartz stability with P H_2O < P Total. Am.J.Sci.272, 946-958.

KERRICK, D.M.,CRAWFORD, K.E. & RANDAZZO, A.F.,1973. Metamorphism of calcareous rocks in three roof pendants in the Sierra Nevada, California. J.Petrol. 14, 303-325.

KOBER, L.,1955. Bau und Enstehung der Alpen. Deuticke, Wien. 2nd ed.

KÖPPEL, V., 1973. Isotopic U-Pb ages of monazites and zircons from the crust-mantle transition and adjacent units of the Ivrea and Ceneri Zones. (S.Alps. Italy). Contrib. Mineral. Petrol. 43, 55-70.

KRAUSKOPF. K.B.,1967. Introduction of Geochemistry. Mc.Graw-Hill, N.Y. 721 pp.

KUNO, H., 1960. High-alumina basalt. J.Petrol.1, 121-145.

KUNO, H.,1968. Differentiation of basalt magmas. In: H.H. Hess and A. Poldervaart (Eds.), Basalts, 2. Interscience N.Y. 623-688.

KUSHIRO, I., 1973. Origin of some magmas in oceanic and circum-oceanic regions. Tectonophysics. 17, 211-222.

LAMBERT, I.B. & WYLLIE, P.J.1970. Melting in the deep crust and upper mantle and the nature of the low velocity layer. Phys. Earth. Plan. Int. 3, 316-322.

LAMBERT, R.St.J. 1959. The mineralogy and metamorphism of the Moine Schists of the Morar and Knoydart districts of Inverness-shire. Trans. Roy. Soc. Edin. 63, 553.

LAMBERT, R. St.J. 1964. Isotopic age determinations on gneisses from the Tauernfenster. Vh. Geol. B.-A, 1964, 16-27. Wien.

LAMBERT, R.St.J. 1970. A potassium-argon study of the margin of the Tauernfenster at Döllach, Austria. Eclogae Geol. Helv. 63, 197-205.

LAPWORTH, C.,1885. The Highland Controversy in British Geology. Nature 32, 558-559.

LARSEN, E.S.,IRVING, J., GONYER, F.A. & LARSEN, E.S.III, 1938. Petrologic results of a study of minerals from the Tertiary volcanic rocks of the San Juan region, Colorado. 7. The Plagioclase feldspars. Am.Mineralogist 23,227-257.

LAUBSCHER, H.P., 1971(a). The large-scale kinematics of the Western Alps and the Northern Apennines and its palinspastic implications. Am.J. Sci. 271, 193-226.

LAUBSCHER, H.P.,1971 (b). Des Alpen-Dinariden-Problem und die palinspastik der Südlichen Tethys. Geol.Rundsch. 60, 813-833.

LEAKE, B.E.,1964. The chemical distinction between Ortho- and Para-amphibolites. J.Petrol. 5, 238-254.

LEAKE, B.E.,1972. The Mineralogical modification of the chemistry of metamorphic rocks. Geol. Mag. 109, 331-337.

LEAKE, B.E.,1974. The crystallization history and mechanism of emplacement of the western part of the Galway Granite, Connemara, Western Ireland. Mineral.Mag. 39, 498-513.

LE PICHON, X., 1968. Sea-floor spreading and continental drift. J.Geophys. Res. 73, 3661-97.

LE PICHON, X., FRANCHETEAU, J. & BONNIN, J.,1973. Plate Tectonics. (Developments in geotectonics, 6). Elsevier, Amsterdam, 300 pp.

LIOU, J.G.,1973. Synthesis and stability relations of epidote. $Ca_2Al_2FeSi_3O_{12}(OH)$. J.Petrol. 14, 381-413.

LIOU, J.G., KUNIYOSHI, S. & ITO, K.,1974. Experimental studies of the phase relations between Greenschist and Amphibolite in a basaltic system. Am.J.Sci. 274, 613-632.

LOFGREN, G.,1974. Temperature induced zoning in synthetic plagioclase feldspar. In: The Feldspars, W.S. Mackenzie and J.Zussman (Eds.) Man.Univ.Press, New York, Manchester 717pp.

LOGAN, J.M. FRIEDMAN, M. & RIGERT, J.A.,1973. Partial melting of sandstone during frictional sliding in triaxial experiments. EOS (Am. Geophys. Union, Trans.) 54(4), 465 (abstract).

LONGO, V.,1968. Geologie und stratigraphie des gebietes zwischen Chiasso und Varese, Italy. Zurich Univ. Geol. Inst. Eidgenoss. Tech. Hochsch. Geol.Inst.,Mitt.86, 1-180.

LORENZONI, S., & ZANETTIN-LORENZONI, E.,1969. Contributo alla conoscenza della petrografia e della geologia di Monte San Vigilio (Merano-Alto Adige). Soc.Geol.Ital. Mem. VIII, 93-120.

LOVERING, J.S.,1935. Theory of heat conduction applied to geological problems. Geol.Soc. Am., Bull.46, 69-94.

LUTH, W.C.,1967. $KAlSiO_4$-Mg_2SiO_4-SiO_2-H_2O - Part 1 : Inferred phase relations and petrologic applications. J.Petrol. 8, 372-416.

LUYENDYK, B.P.,1970. Dips of downgoing lithospheric plates beneath Island Arcs. Geol.Soc. Am., Bull.81, 3411-3416.

MACKENZIE, D.B.,1960. High temperature alpine-type peridotite from Venezuela. Geol. Soc. Am., Bull.71, 303-318.

MACKENZIE, D.P.,1969. Speculations on the consequences and causes of plate motions. R.Astron.Soc., Geophys. J.18,1-32.

MACKENZIE D.P.,1972. Active Tectonics of the Mediterranean Region. R.Astron. Soc., Geophys. J. 30, 109-185.

MACKENZIE, D.P. & PARKER, D.L.,1967. The North Pacific: An example of tectonics on a sphere. Nature 216, 1267-1276.

MACKENZIE D.P. & BRUNE, J.N.,1972. Melting on fault planes during large earthquakes. R.Astron.Soc., Geophys. J. 29, 65-78.

MAKANJUOLA, A.A. & HOWIE, R.A.,1972. Mineralogy of the glaucophane schists and associated rocks from Ile de Groix, Brittany, France. Contrib. Mineral.Petrol. 35, 83-118.

MARTIN, R.F.,1974. Controls of ordering and subsolidus phase relations in the alkali feldspars. In: The Feldspars. W.S.Mackenzie & J.Zussman (Eds.) Man.Univ. Press. New York, Manchester. 717pp.

MASCH, L.,1973. Untersuchung der Aufschmelzung und Deformation der Pseudotachylite der Silvretta (Österreich, Schweiz.) Neues Jahrb. Mineralogie, Monatsh. 11, 487-509.

MAUCHER, A.,1960. Der Permische vulkanismus im Raum von Trient. Geol. Rundschau. 49, 487-498.

MAXWELL, J.C.,1962. Origin of slaty and fracture cleavage in the Delaware Water Gap Area, New Jersey & Pennsylvania. In: Petrologie Studies - a volume in honor of A.F.Buddington, New York, Geol. Soc. Am., 281-311.

McCALLUM, M.E.,1974. Dedolomitised marble lenses in shear zone tectonites, Medicine Bow Mountains, Wyoming. J. Geol. 82, 473-488.

McDOWELL, F.W.,1968. Potassium-argon ages from the Ceneri zone of southern Switzerland. Schweiz. Mineral. Petrog. Mitt. 48, 211-212.

MENDUM, J.R.,1972. Experimental study of conglomerate deformation using plasticine model analogues. MSc.thesis. (Unpubl.)

MERRILL, R.H.,1964. In situ determination of stress by relief techniques. In: State of Stress in the Earth's Crust. W.R. Judd (Ed.) Elsevier, N.Y., 343-378.

METZ, P., 1970. Experimentelle untersuchung der metamorphose von kieselig dolomitischen sedimenten: II, Die bildungsbedingungen des Diopsids. Contrib. Mineral. Petrol. 28, 221-250.

METZ, P.W. & WINKLER, H.G.F., 1964. Experimentelle untersuchung der diopsidbildung aus tremolit, calcit und quarz. Naturwiss. 51, 460.

MEYER, C. & HEMLEY, J.J., 1967. Wall rock alteration. In: Geochemistry of Hydrothermal Ore Deposits. H.L.Barnes (Ed.) Holt, Rinehart and Winston, U.S., 166-235.

MILLER, D.S., JÄGER, E. & SCHMIDT, K., 1967. Rb-Sr Alterbestimmungen an Biotiten der Raibler Schichten des Brenner Mesozoikums und am Muskovitgranitgneis von Vent (Ötztaler Alpen). Eclogae. Geol. Helv. 60, 537-541.

MIYASHIRO, A., 1972. Metamorphism and related magmatism in plate tectonics. Am. J. Sci. 272, 629-656.

MIYASHIRO, A., 1973. Metamorphism and Metamorphic belts. George Allen and Unwin. London. 492 pp.

MOORE, J.G., GRANTZ, A. & BLAKE, M.C.Jr. 1963. The quartz-diorite line in north-western North America. U.S. Geol. Surv. Prof. Pap. 450-E, 89-93.

MOORES, E.M. & MACGREGOR, I.D., 1968. Depth Classification of Alpine Peridotites (abstract). Geol. Soc.Am.Spec.Pap. 115, 1-155.

MORTEANI, G. & RAASE, P., 1974. Metamorphic plagioclase crystallization and zones of equal anorthite content in epidote-bearing, amphibole-free rocks of the western Tauernfenster, Eastern Alps. Lithos 7, 101-111.

MUELLER, I.I., 1973. Vertical crustal motions and their causes. EOS (Am.Geophys.Union, Trans.) 54, 1257-1260.

MUELLER, S. & TALWANI, M., 1971. A crustal section across the Eastern Alps based on gravity and seismic reflection data. Pure & Appl. Geophys. 85, 226-239.

NADAI, A., 1950. Theory of flow and fracture of solids. Vol. 1. 2nd ed. McGraw Hill. New York. 705 pp.

NEWHOUSE, W.H., 1932. The composition of vein solutions as shown by liquid inclusions in minerals. Econ. Geol. 27, 419-436.

NUR, A. & MAVKO, G., 1974. Postseismic viscoelastic rebound. Science, 183, 204-206.

OBERHAUSER, R., 1968. Beiträge zur Kenntnis der Tektonik und der Paläogeographie während der Oberkreide und dem Paläogen im Ostalpenraum. Jahrb.Geol.Bundesanstalt Wein. III, 115-145.

O'HARA, M.J.,1965. Primary magmas and the origin of basalts. Scott. J. Geol. 1, 19-40.

OHMOTO, H.,1972. Systematics of sulphur and carbon isotopes in hydrothermal ore deposits. Econ.Geol.67, 551-578.

ORVILLE P.M.,1963. Alkali ion exchange between vapor and feldspar phases. Am. J.Sci. 261, 201-237.

ORVILLE, P.M.,1967. Unit cell parameters of the microcline-low albite and the sanidine-high albite solid solution series. Am.Mineral. 52, 55-86.

ORVILLE, P.M.,1969. A model for metamorphic differentiation origin of thin layered amphibolites. Am.J.Sci.267,64-86.

ORVILLE, P.M., 1972. Plagioclase cation exchange equilibria with aqueous chloride solution: results at 700°C and 2000 bars in the presence of quartz. Am.J.Sci. 272, 234-272.

OSBORN, E.F.,1962. Reaction series for subalkaline igneous rocks based on different oxygen pressure conditions. Am. Mineral. 47, 211-226.

OXBURGH, E.R.,1967. Mantle convection and the thermal requirements of various crustal phenomena. R.Astron.Soc., Geophys. J. 14, 403-411.

OXBURGH, E.R.,1968. 1. An outline of the geology of the Central Eastern Alps. 2. The Eastern Alps - A geological guide. Geol. Assoc. (Lond). Proc. 79, 1-127.

OXBURGH, E.R.,1972. Flake tectonics and continental collision. Nature 239, 202-204.

OXBURGH, E.R., 1973. Plate tectonics and continental collision (Abstr.) Geol.Assoc.(Lond),(Circ.)No.749, 1-2.

PEACH, B.N. & HORNE, J. et al, 1907. The geological structure of the North-West Highlands of Scotland. Mem. Geol. Surv. Scotland.

PHEMISTER, J., 1934. Zoning in plagioclase feldspar. Mineralog. Mag. 23, 541-555.

PHILPOTTS, A.R.,1964. Origin of Pseudotachylites. Am.J. Sci. 262, 1008-1035.

PICCOLI, G., CETTO, G. & BROSEGHINI, E.,1971. Le formazione vulcaniche terziarie del Trentino centrale e occidentale. Studi Trentini di Scienze Naturali. XLVIII, 166-182.

PIWINSKII, A.J.,1968. Experimental studies of Igneous rock series: Central Sierra Nevada Batholith, California. J.Geol. 76, 548-570.

PIWINSKII, A.J. & WYLLIE, P.J.,1968. Experimental Studies of Igneous rock series: A zoned Pluton in the Wallowa Batholith, Oregon. J.Geol. 76, 205-234.

POWELL, D. & TREAGUS, J.E.,1967. On the geometry of S-shaped inclusion trails in garnet porphyroblasts. Mineralog. Mag. 36, 453-456.

PREY, S., in EXNER, Ch., 1964. Erläuterungun zur geologischen Karte der Sonnblickgruppe. Geol. Bundesanst. Wien.

PRICE, N.J.,1966. Fault and joint development in brittle and semi-brittle rock. Pergamon. London.

PRINZ, M. & POLDERVAART, A.,1964. Layered mylonite from Beartooth Mountains, Montana. Geol. Soc. Am., Bull.75, 741-744.

PURTSCHELLER, F.,1969. Petrographische untersuchungen an aluminosilikatgneisen des Ötztaler-Stubaier Altkristallins. Tschermaks Mineral.Petrogr. Mitt. 13, 35-54.

PURTSCHELLER, F., HOERNES, S. & BROWN, G.C.,1972. An example of occurrence and breakdown of paragonite. Contrib. Mineral.Petrol. 35, 34-42.

RADOSLOVICH, E.W. & NORRISH, K.,1962. The cell-dimensions and symmetry of the layer-lattice silicates. 1. Some structural considerations. Am.Mineral. 47, 599-616.

RAMBERG, H.,1955. Natural and experimental boudinage and pinch-and-swell structures. J.Geol. 63, 512-527.

RAMBERG, H.,1967. Gravity, Deformation and the Earths' Crust. Academic Press, London and New York.

RAMBERG, H., 1972. Theoretical models of density

stratification and diapirism in the earth. J. Geophys. Res. 77, 877-889.

RAMSAY, J.G.,1962. Interference patterns produced by the superposition of folds of 'similar' type. J.Geol. 60, 466-481.

RAMSAY, J.G.,1967. Folding and fracturing of rock. McGraw-Hill. New York. 568pp.

RAMSAY, J.G. & GRAHAM, R.H.,1970. Strain variation in shear belts. Can.J. Earth Sci. 7, 786-813.

RASTOGI, B.K.,1974. Earthquake mechanisms and plate tectonics in the Himalayan region. Tectonophysics, 21, 47-56.

REED, J.J.,1964. Mylonites, cataclasites and associated rocks along the Alpine Fault, South Island, New Zealand. N.Z.J.Geol.Geophys. 7, 645-684.

REINHARDT, B.,1966. Geologie und Petrographie der Monte Rosa-Zone, der Sesia-Zone und des Canavese im Gebiet zwischen Valle d'Ossola und Valle Loana (Prov. di Novara, Italien). Schweiz.Mineral.Petrogr.Mitt.46, 553-678.

RICHARDSON, S.W.,1968. Staurolite stability in a part of the system Fe-Al-Si-O-H. J.Petrol.9, 467-488.

RICHARDSON, S.W., GILBERT, M.C. & BELL, P.M. 1969. Experimental determination of the Kyanite-Andalusite and Andalusite-Sillimanite equilibria: the Aluminosilicate triple point. Am.J.Sci. 267, 259-272.

RIEKELS, L.M.,1973. Preferred orientation in a quartz mylonite from the Moine Thrust. M.Sc.Thesis, Univ. Illinois, Chicago.

ROBERTS, J.L.,1970. The intrusion of magma into brittle rocks. In: Mechanism of Igneous Intrusion. G.Newall and N.Rast (Eds.) Gallery, Liverpool. 287-338.

ROEDER, D.H.,1973. Subduction and orogeny. J.Geophys. Res. 78, 5005 - 5024.

ROEDDER, E.,1962. Ancient fluids in crystals. Sci.Am.207, 38-47.

ROEDDER, E. & COOMBS, D.S.,1967. Immiscibility in Granitic

melts, indicated by fluid inclusions in ejected granitic blocks from Ascension Island. J.Petrol. 8, 417-451.

RUTHERFORD, M.J.,1973. The phase relations of Aluminous Iron Biotites in the System $KAlSi_3O_8$ - $KAlSiO_4$-Al_2O_3-Fe-O -H. J.Petrol. 14, 159-180.

RUTTEN, M.G.,1969. The geology of Western Europe. Elsevier, Amsterdam. 520pp.

RUTTER, E.H.,1972. The Influence of interstitial water on the Theological behaviour of calcite rocks. Tectonophysics, 14, 13-33.

RUTTER, E.H.,1974. The influence of temperature, strain rate and interstitial water in the experimental deformation of calcite rocks. Tectonophysics, 22, 311-334.

SANDER, B.,1970. An introduction to the study of Fabrics of Geological Bodies. Pergamon Press. Braunschweig.

SANDERSON, D.J.,1973. The Development of fold axes oblique to the regional trend. Tectonophysics, 16, 55-70.

SAPOUNTZIS, E.,1973. About the occurrence of wollastonite in the area of Xanthi (N.Greece). Neues.Jahrb.Mineral. Abh. 120, 98-107.

SASSI, F.P.,1971. Isochemical post-kinematic feldspathisation : a genetic model. Schweiz.Mineral.Petrogr.Mitt.51, 451-461.

SASSI, F.P. & ZANFERRARI, A.,1972. Il significato geologico del complesso del Turntaler (Pusteria), con particolare riguardo alla successione di eventi metamorfici prealpini nel basemento austridico delle Alpi Orientali. Soc. Geol. Ital., Boll.91, 533-557.

SASSI, F.P. & SCOLARI, A.1974. The b_o value of Potassic white micas as a barometric indicator in low-grade metamorphism. Contrib.Mineral.Petrol. 45, 143-152.

SASSI, F.P., ZANFERRARI, A., ZIRPOLI, G., BORSI, S. & DEL MORO, A.,1974. The Austrides to the south of the Tauern Window and the Periadriatic Lineament between Mules and Mauthen. Neues.Jahrb.Geol. Palaeontol. Monatsh.7, 421-434.

SCHEURING, B., AHRENDT, H., HUNZIKER, J.C. & ZINGG, A., 1974. Palaeobotanical and geochronological evidence for the Alpine Age of the metamorphism of the Sesia Zone. Geol.Rundsch, 63, 305-325.

SCHIAVINATO, G.,1946. Il giacimento a wollastonite ed altri minerali di contatto presso Alpe Bazena (Adamello meridionale). Padua Univ., Int.Geol.Mineral.Mem.

SCHMID, S.,1973. Geologie des Umbrailgebiets. Eclogae. Geol. Helv. 66, 101-210.

SCHMIDEGG, D.,1936. Steilachsige Tektonik und Schlingenbau auf der Südseite der Tiroler Zentralalpen. Geol.Bundesant. Wien. Jahrb. 86, 115-149.

SCHMIDT, K., JÄGER, E., GRÜNENFELDER, M. & GRÖGLER, N., 1967. Rb-Sr and U-Pb Altersbestimmungen an Proben der Ötztal-Kristallins und des Schneeberger Zuges. Eclogae Geol.Helv. 60, 529-536.

SCLATER, J.G. & FRANCHETEAU, J.,1970. The implications of terrestial heat flow observations on current tectonic and geochemical models of the crust and upper mantle of the earth. Roy.Astron.Soc., Geophys. J.20, 509-542.

SCHREYER, W. & SEIFERT, F.,1969. Compatibility relations of aluminium silicates in the systems $MgO-Al_2O_3-SiO_2-H_2O$ and $K_2O-MgO-Al_2O_3-SiO_2-H_2O$ at high pressures. Am.J.Sci. 267, 373-388.

SCHWANDER, H., HUNZIKER, J.C. & STERN, W.,1968. Mineralchemie von Hellglimmern. Schweiz.Mineral.Petrol.Mitt.48, 357-390.

SCHWERDTNER, W.M. 1970. Hornblende lineations in Trout Lake area, Lsc la Rouge map sheet, Saskatchewan. Can.J.Earth Sci. 7, 884-899.

SCOTFORD, D.M.,1969. Metasomatic augen gneiss in Greenschist facies, Western Turkey. Geol.Soc.Am.Bull. 80, 1079-1094.

SEIFERT, F.,1970. Low temperature compatibility relations of cordierite in haplopelites of the system $K_2O-MgO-Al_2O_3-SiO_2-H_2O$. J.Petrol. 11, 73-99.

SEIFERT, F. & SCHREYER, W.,1970. Low temperature stability limit of Mg-cordierite in the range 1-7 kilobars water pressure. A redetermination. Contrib.Mineral.Petrol. 27, 225-238.

SAKI, Y.,1972. Lower grade stability limit of epidote in the light of natural occurrences. J.Geol.Soc.Japan, 78, 405-413.

SHERWIN, J. & CHAPPLE, W.H.,1968. Wavelength of single layer folds - a comparison between theory and observation. Am.J.Sci. 266, 167-179.

SHIEH, Y.N.& TAYLOR, H.P.Jr., 1969. Oxygen and hydrogen isotope studies of contact metamorphism in the Santa Rosa Range, Nevada, and other areas. Contrib.Mineral.Petrol. 20, 306-356.

SIBSON, R.H.,1973. Interactions between temperature and pore-fluid pressure during earthquake faulting and a mechanism for partial or total stress relief. Nature: Phys. Sci. 243, 66-68.

SMITH R.L.,1960. Ash flows. Geol.Soc. Am.,Bull.71, 795-842.

SMITH, A.G.,1971. Alpine deformation and the oceanic areas of the Tethys, Mediterranean and Atlantic. Geol.Soc.Am., Bull. 82, 2039.

SOPER, N.J.,1971. The earliest Caledonian structures in the Moine Thrust belt. Scot. J.Geol. 7, 241-247.

SPRY, A., 1963. The origin and significance of snowball structure in garnet. J.Petrol. 4, 211-222.

SPRY, A.,1969. Metamorphic Textures. Pergamon Press, Oxford. 350 pp.

STEIGER, R.,1964. Dating of orogenic phases in the central Alps by K-Ar ages of hornblende. J.Geophys.Res.69, 5407-5421.

STEPHANSSON, O.,1974. Stress-induced diffusion during folding. Tectonophysics, 22, 233-251.

STESKY, R.M., BRACE, W.F., RILEY, D.K. & ROBIN, P.Y.F.1974. Friction in faulted rock at high temperature and pressure. Tectonophysics, 23, 177-203.

STORRE, B. & NITSCH, K-H., 1972. Die Reaktion 2 Zoisit + 1 CO_2 ⇌ 3 Anorthit + 1 Calcit + 1 H_2O. Contrib.Mineral. Petrol. 35, 1-10.

SUZUKI, T.,1970. Röntgenographische gefügeanalyse (mit dem Zählrohr - Texturgoniometer) von Quarzschiefen aus Zentral-Shikoku, Japan. In: Experimental and Natural Rock Deformation. P.Paulitsch (Ed.) Springer-Verlag. Berlin/ Heidelberg. 1-18.

SYLVESTER, A.G. & CHRISTIE, J.M.,1968. The origin of crossed-girdle orientations of optic axes in deformed quartzites. J.Geol. 76, 571-580.

TABOR, R.W. & CROWDER, D.F.,1969. On batholiths and volcanoes; intrusion and eruption of Late Cenozoic magmas in the Glacier Peak area, North Cascades, Washington, U.S. Geol. Surv., Prof. Paper 604, 1-67.

TALBOT, C.J.,1970. The minimum strain ellipsoid using deformed quartz veins. Tectonophysics, 9, 47-76.

TELL, I.,1974. Hydrothermal studies on fluorine metamorphic reactions in siliceous dolomite. Contrib. Mineral. Petrol. 43, 99-110.

TERMIER, P.,1903. Les Nappes des Alpes orientales et la synthese des Alpes. Geol.Soc. Fr., Bull.4, 711-766.

THAKUR, V.C.,1974. Analysis of type of tectonic strain in polyphased deformed Molare area, Tessin, Switzerland, using deformed pebbles. Geol.Rundschau, 63, 326-334.

THAYER, T.P.,1966. Serpentinisation considered as a constant-volume metasomatic process. Am.Mineral. 51, 685-710.

THAYER, T.P., 1967. Chemical and structural relations of Ultramafic and Feldspathic rocks in Alpine intrusive complexes. In: Ultramafic and Related Rocks, P.J.Wyllie (Ed). Wiley, N.Y., 222-239.

THOMAS, L.A. & WOOSTER, W.A.,1951. Piezocrescence - the growth of Dauphiné twinning in quartz under stress. R.Soc. Lond., Proc. 208A. 43-62.

THOMPSON, A.B.,1974. Calculation of muscovite-paragonite-alkali feldspar phase relations. Contrib.Mineral.Petrol. 44, 173-194.

TILLEY, C.E.,1947. The dunite-mylonites of St.Paul's Rocks (Atlantic). Am.J.Sci. 245, 483-491.

TOBSCHALL, H.J.,1974. Untersuchungen zur "Short Distance" variabilitat der Zusammensetzung von Hellglimmern niedrig-metamorpher Pelite des Beaume - Tales (Mittlere Cevennen) Neues Jahrb. Mineral. Abh. 121, 1-42.

TREAGUS, S.H.,1973. Buckling stability of a viscous single-layer system, oblique to the principal compression. Tectonophysics 19, 271-289.

TRENER, G.B.,1906. Geologische Aufnahme im nördlichen abhang der Presanella Gruppe. Geol.Bundesanst. Wien Jahrb. 56.

TRIBOULET, C.,1974. Les Glaucophanites et roches associees de l'Ile de Groix (Morbihan, France): étude mineralogique et petrogenetique. Contrib.Mineral.Petrol. 45, 65-90.

TRUMPY, R.,1971 Stratigraphy in mountain belts. Geol. Soc. Lond., Q.J. 126, 293-318.

TRUMPY, R.,1973. The timing of orogenic events in the Central Alps. In: Gravity and Tectonics. K.A. De Jong & R. Scholten (Eds). J.Wiley & Sons, N.Y. Toronto. 229-251.

TULLIS, J.,1968. Preferred orientation in experimental quartz mylonites. EOS (Am.Geophys.Union, Trans.) 49, 755.

TULLIS, J., CHRISTIE, J.M. & GRIGGS, D.T.,1973. Microstructives and preferred orientations of experimentally deformed quartzites. Geol.Soc.Am., Bull.84, 297-314.

TURCOTTE, D.L. & SCHUBERT, G.,1973. Frictional heating of the descending lithosphere. J.Geophys.Res. 78, 5876-5886.

TURNER, F.J.,1968. Metamorphic Petrology. McGraw Hill. N.Y., 403 pp.

TURNER, F.J. & VERHOOGEN, J.,1960. Igneous and Metamorphic Petrology. McGraw Hill, New York, 2nd edition. 694 pp.

TURNER, F.J. & WEISS, L.E.,1963. Structural analysis of metamorphic tectonites. McGraw Hill, N.Y. 545 pp.

TUTTLE, O.F.,1949. Structural petrology of planes of liquid inclusions. J.Geol. 57, 331-356.

TUTTLE, O.F. & BOWEN, N.L.,1958. Origin of granite in the light of experimental studies in the system $NaAlSi_3O_8$-$KalSi_3O_8$-SiO_2-H_2O. Geol.Soc.Am., Mem. 74, 1-153.

VANCE, J.A.,1962. Zoning in igneous plagioclase: normal and oscillatory zoning. Am.J.Sci. 260, 746-760.

VANCE, J.A.,1965. Zoning in igneous plagioclase: patchy zoning. J.Geol. 73, 636-651.

VECCHIA, O.,1957. Significato del fascio tettonico Giudicario-Atesino (Dal Benaco a Merano: un problema geologico). Soc.Geol.Ital., Boll. 76.

VELDE, B.,1965. Phengite micas: synthesis, stability and natural occurrence. Am.J.Sci. 263, 886-913.

VELDE, B.,1967. Si^{4+} content of natural phengites. Contrib. Mineral.Petrol. 14, 250-258.

VERHOOGEN, J.,1948. Thermodynamics of a magmatic gas phase. California Univ. Dept. Geol.Sci. Bull.28, 91-136.

VERNON, R.H.,1970. Comparative grain-boundary studies of some basic and ultrabasic granulites, nodules and cumulates. Scott.J.Geol. 6, 337-351.

VERNON, R.H.,1974. Controls of mylonitic compositional layering during non-cataclastic ductile deformation. Geol.Mag. 111, 121-123.

WENK, E. & KELLER, F.,1969. Isograde in Amphibolitserien der Zentralalpen. Schweiz.Mineral.Petrogr. Mitt.49, 157-198.

WENK, H.R.,1973. The structure of the Bergell Alps. Eclogae Geol. Helv. 66, 255-291.

WILKINSON, P., 1956. The structural history of the region east of Loch Eriboll, Sutherland. In: Structural Petrology and problems of the Caledonides. F.C.Phillips (Ed). Advancement Sci., Lond. 12, 573-574.

WILSON, C.J.L.,1973. The prograde microfabric in a deformed quartzite sequence. Mt. Isa, Australia. Tectonophysics, 19, 39-81.

WINKLER, H.G.F.,1967. Petrogenesis of metamorphic rocks: Springer-Verlag, New York, 237 pp.

WOLETZ, G., 1967. Schwermineralvergesellschaftungen aus ostalpinen sedimentatsionsbecken der kreidezeit. Geol. Rundsch. 56, 308-319.

WONES, D.R.,1963. Physical properties of synthetic biotites on the join phlogopite-annite. Am.Mineral. 48, 1300-1321.

WOOD, B.L.,1972. Metamorphosed ultramafites and associated formations near Milford Sound, New Zealand. N.Z.J. Geol. Geophys. 15, 88-128.

WRIGHT, T.L.,1967. The microclase-orthoclase transformation in the contact aureole of the Eldora Stock, Colorado. Am.Mineral. 52, 117-136.

WYLLIE, P.J.,1973. Experimental petrology and global tectonics - a preview. Tectonophysics, 17, 189-209.

YODER, H.S.,1969. Calc-alkaline Andesites: experimental data bearing on the origin of their assumed characteristics. In: Proceedings of the Andesite conference, A.R.McBirney (Ed). Oregon, Dept.Geol. Mineral.Ind., Bull.65, 77-89.

YODER, H.S., STEWART, D.B. & SMITH, J.R.,1956. Ternary feldspars. Carnegie Inst. Washington, Yr.Book, 55, 190-194.

ZIJDERVELD, J.D.A., HAZEU, G.J.A., NARDIN, M. & VAN DER VOO, R., 1970. Shear in the Tethys and the Permian palaeomagnetism in the Southern Alps, including new results. Tectonophysics, 10, 639-661.

ZWART, H.J., 1969. Metamorphic facies series in the European Orogenic Belts and their bearing on the causes of orogeny. Geol.Assoc. Can., Spec. Pap. 5, 7-16.

Appendix 1

Review of oscillatory and patchy zoning

Many interpretations of oscillatory normal zoning have been made. (Phemister, 1934; Harloff, 1927; Hills, 1936; Verhoogen, 1948). Vance (1962) amplified the diffusion - supersaturation theory (Hills, 1936) and showed that a high volatile content late in the magma crystallization history results in a normally zoned rim. Oscillatory normal zoning was explained by the gradual rise of a moderately dry magma and related pressure and temperature reductions. Bottinga et al (1966) have measured concentration gradients in a volcanic glass adjacent to a bytownite phenocryst, showing that crystallization rate is, in part, diffusion controlled. Plagioclase discriminates against Mg, Fe and Si but preferentially absorbs Al, which is hence the controlling element for its growth. Although no variations in Ca and Na were found, subsequent work by Lofgren (1974) on experimental growth of plagioclase showed that gradients in Ca, Na, Al and Si are present in the 5 to 10 m adjacent to the crystal. Bottinga et al assume that crystal growth rate is initially greater than the diffusional flux of Al in the boundary layer, resulting in decreasing An content. The rate of decrease becomes less pronounced as crystallization proceeds, and finally a transient steady state is reached. After a sufficient temperature or temperature-pressure drop, supersaturation occurs and kinetic factors then control the growth rate with recurrent initial An rich growth on a flat crystal surface followed by rapid growth on a step-like lattice.

Vance (1965) has considered the growth of patchy zoning and shown that it is generally restricted to granodiorites, quartz-diorites and tonalites. The liquidus and solidus curves for the Ab - An system move upwards and decrease in slope at higher pressures (Bowen, 1913; Carr, 1954; Vance, 1965) provided that P H_2O is less than P total. If calcic plagioclase is crystallizing at depth, then a "rapid" uprise of the magma will cause a <u>pressure</u> and temperature decrease, with an accompanying slight increase

in P H_2O (Yoder et al, 1956) amplifying the downward shift of the plagioclase solidus - liquidus curves. This would result in partial resorption of the already existing calcic plagioclase as the melt attempted to establish equilibrium (by becoming more calcic), followed by the rapid growth of more sodic plagioclase. Vance (1965) attributes the poikilitic inclusions in this more sodic plagioclase to melt trapped in the crystal cores after partial resorption and sodic plagioclase crystallization. These inclusions can always be related to the melt composition. Patchy zoning is believed to be a diagnostic igneous texture indicating that a crystal phase was present in the magma, which itself was neither superheated nor saturated in volatile components, when upward displacement initiated resorption.

APPENDIX 2

Measurements of deformed and undeformed xenoliths in the Adamello Massif.

2(a)

The measurements of undeformed xenoliths were taken in the Upper Val Presena where only a weak flow foliation is present in medium to coarse-grained tonalite.

Deformed xenoliths were measured close to the margin of the tonalite on the spur of Croz di Stavel, east of the Val di Stavel. The road, constructed by the Austrians to the fort of Pozzi Alti provides convenient access, and good artificial exposures of the marginal parts of the tonalite.

Graphs of the two sets of measurements are given in Figure 52. Ratios are calculated by the best fit compatible lines for each locality. Generally strain ratios agree well.

2(b)

M193 Coarse-grained biotite-quartz-diorite with several large deformed xenoliths.

(Y)	(Z)	Ratio	(X)	(Z)	Ratio
30.0cm.	7.5cm.	4.0	2.5cm.	0.5cm.	5.0

$$k = \frac{X/Y - 1}{Y/Z - 1} = 0.083$$

M454 Coarse-grained biotite-quartz-diorite with xenoliths showing near perfect ellipsoidal shape. Moderately strong foliation. Measurements in planes orthogonally related to the foliation.

(Y)	(Z)	Ratio	(X)	(Z)	Ratio
17.6cm.	4.5cm.	3.91	17.4cm.	4.5cm.	3.82
13.1cm.	3.0cm.	4.37	6.8cm.	1.3cm.	5.23
15.0cm.	4.6cm.	3.26	23.5cm.	6.7cm.	3.51
13.5cm.	5.3cm.	2.55	12.8cm.	2.1cm.	6.10
54.8cm.	12.2cm.	4.50	12.5cm.	2.5cm.	5.0
		18.59			23.66
	Av. Ratio	3.72		Av. Ratio	4.73

$$k = \frac{X/Y - 1}{Y/Z - 1} = 0.099$$

Figure 52.

1. Measurements of undeformed xenoliths in the Val Presena. The xenoliths are fine-grained and biotite rich and lie in a matrix of coarse-grained tonalite.

The X,Y and Z axes shown are related to the weak flow foliation at M 112, such that XY is coincident with the foliation plane. The foliation trends approximately parallel to the intrusion margins. Long axes of small hornblende crystals vary up to 40° either side of the X direction in the XZ plane. At M 113 X/Y, Y/Z and X/Y ratios are not significantly different, and rare elongate xenoliths show no relationship to the flow foliation here. Graphical mean values for each data set are given.

2. Measurements of deformed xenoliths on the northern flank of the Croz di Stavel.

In all outcrops the XY plane is coincident with the strong biotite foliation. The maximum elongation of the xenoliths is generally coincident with the dip direction of the foliation plane. In the XZ plane 90% of xenolith long axes lay within 2° of the foliation trace.

M 113

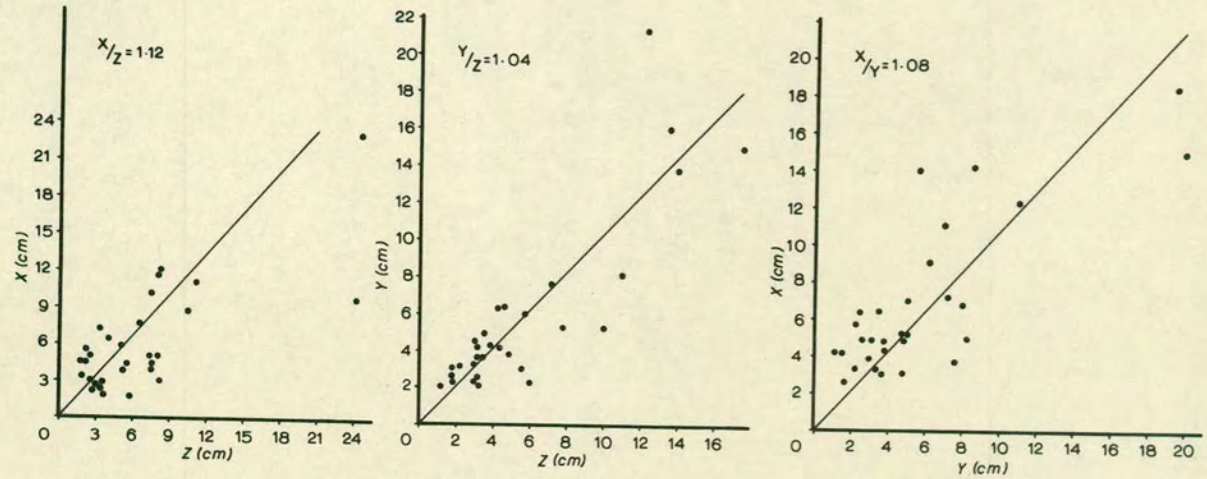

M 112

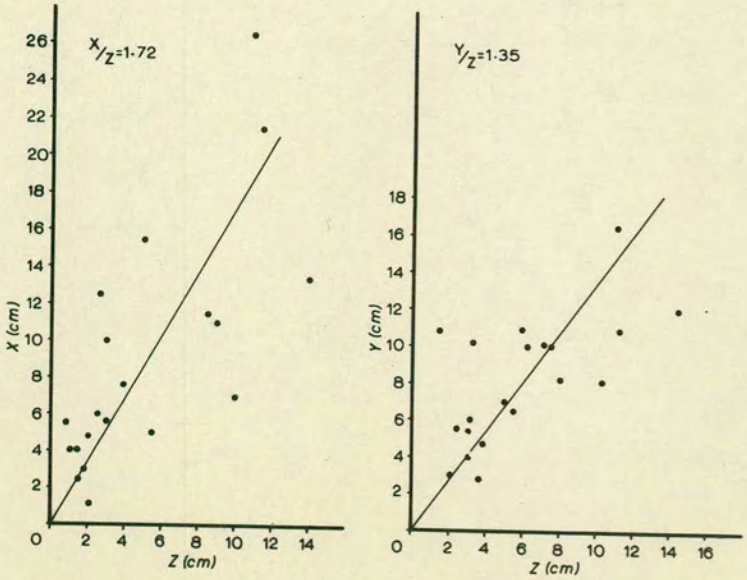

X/Y = 1·27

M 44

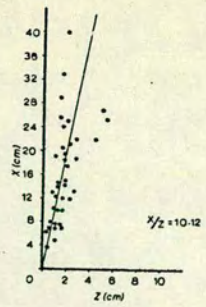

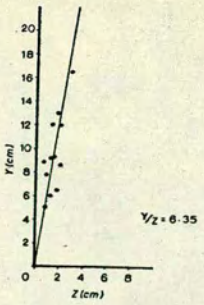

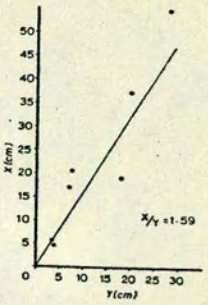

M 45B

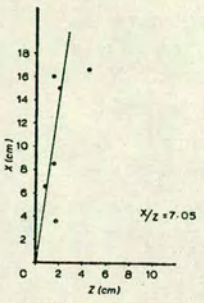

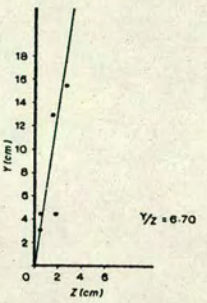

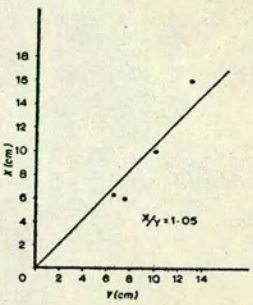

M 462

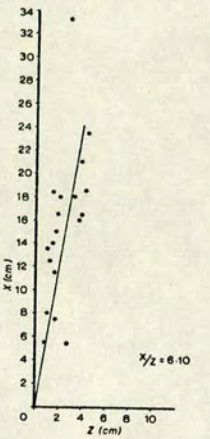

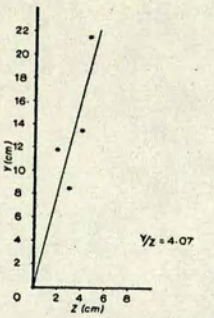

X/Y = 1·50

M 45C

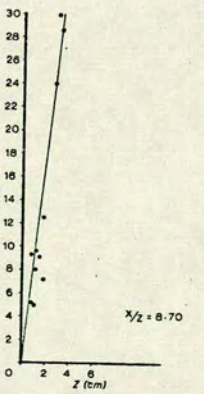

Y/Z = 5·40

X/Y = 1·60

M 45A

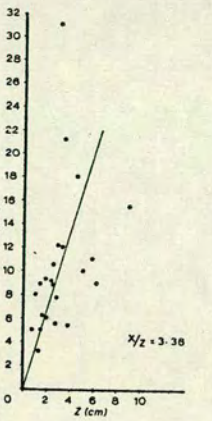

Y/Z = 2·47

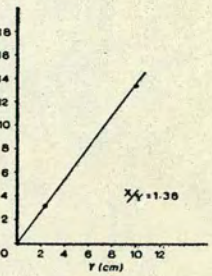

Smaller xenoliths show higher $^{X}/_{Z}$ ratios.

e.g. 9 cm. by 0.8 cm. Ratio 11.25

9.3cm. by 0.9 cm. Ratio 10.03

It is possible that these xenoliths were elongate initially.

M457 Medium-grained biotite-quartz-diorite with ellipsoidal xenoliths. Moderate foliation.

Measurements in planes orthogonally related to the foliation.

(Y)	(Z)	Ratio	(X)	(Z)	Ratio
9.2cm.	3.7cm.	2.49	20.7cm.	7.0cm.	2.96
37.4cm.	22.1cm.	1.69	8.5cm.	3.0cm.	2.83
5.0cm.	1.1cm.	4.54	19.0cm.	5.5cm.	3.45
9.1cm.	3.5cm.	2.60	5.3cm.	1.5cm.	3.53
		11.32			12.77
	Av. ratio	2.83		Av.ratio	3.19

$$k = \frac{^{X}/_{Y} - 1}{^{Y}/_{Z} - 1} = 0.0875$$

M458. Medium-grained biotite-quartz-diorite with slightly flattened ellipsoidal xenoliths. Weak foliation.

(Y)	(Z)	Ratio
9.8cm.	6.2cm.	1.58
35cm.	20cm.	1.75
	Av. ratio	1.66

Taking k = 0.09

$^{X}/_{Z}$ = 1.76

M458A

Very weak foliation.

(X)	(Z)	Ratio
32cm.	20cm.	1.6

M458B

Xenoliths lie at random angles in non-foliated biotite-quartz-diorite. Ratios range 1.0 to 1.1 in near spherical xenoliths.

APPENDIX 3.

Feldspar Augen Measurements in Stavel Gneiss.

These measurements were taken at T8 where a band of markedly augen gneiss occurs within the Stavel Gneiss. Although some feldspars have indistinct margins, measurements were only taken of those with well-defined shapes. The measurements are plotted on graphs as shown in Figure 53 and geometrical ratios in the XZ, XY and YZ planes found to be compatible.

Figure 53. - Measurements of K feldspar augen in the Stavel Gneiss. The XY measuring plane is approximately coincident with the phengite foliation. The relative orientations of the X, Y and Z axes and the local structural features are given in Figure 17(b). The feldspars are more elongate in the less K feldspar rich parts of the gneiss. Minor f_5 folds are not present in the augen -rich parts of the gneiss.

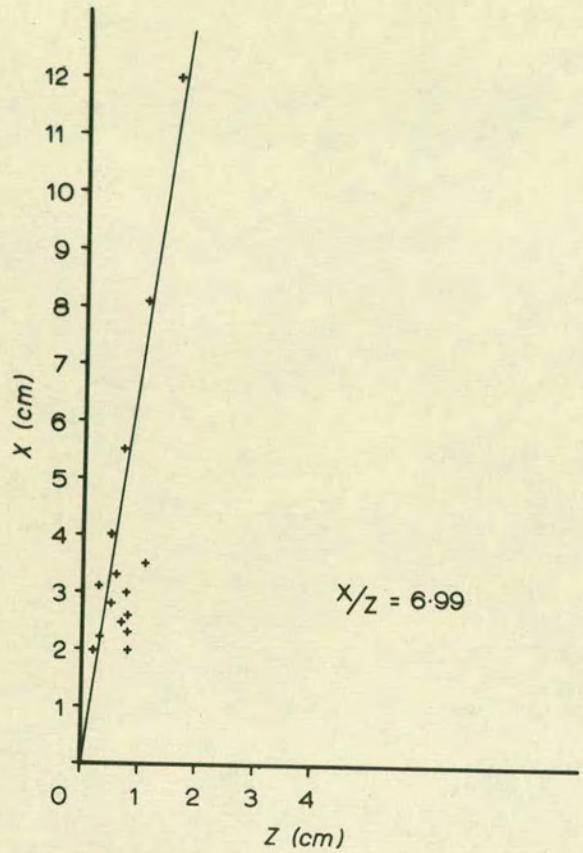

$$k = \frac{X/Y - 1}{Y/Z - 1}$$

$$= \frac{2{\cdot}73 - 1}{2{\cdot}56 - 1}$$

$$= 1{\cdot}11$$

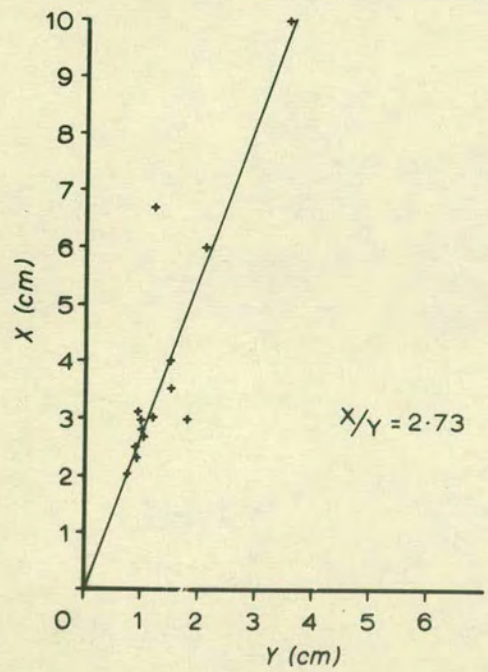

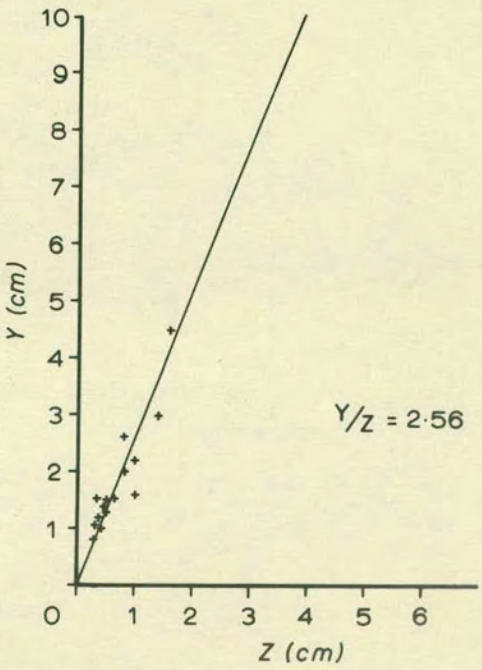

APPENDIX 4.

Strain estimates in mylonite and mylonitic gneiss.

4(a). Average values for groups of 5 sillimanite porphyroblasts in quartz-feldspar-biotite-muscovite-sillimanite gneiss (M150).

Taking X and Y to lie in the mylonitic foliation with X coincident with the maximum dip direction.

X	Z	Ratio	Y	Z	Ratio
5.5cm.	0.3cm.	18.33	6 cm.	0.6cm.	10.0
3.5cm.	0.3cm.	11.66	6.8cm.	0.55cm.	12.26
4.5cm.	0.3cm.	15.0	6.4cm.	0.575 cm.	11.13

(Average for 10 measurements.)

In the gneiss 3 m to the north similar measurements:-

X	Z	Ratio	Y	Z	Ratio
1cm.	0.4cm.	2.5	2cm.	0.5cm.	4.0

(Average for 5 measurements.)

Minimum tectonic strain

$$X:Y:Z = 11.13/2.5 : 15/4 : 1$$
$$= 4.45 : 3.75 : 1$$

$$k = \frac{X/Y - 1}{Y/Z - 1} = 0.068$$

4(b) Measurements of K feldspar in 55 cm. wide deformed pegmatite in quartz-feldspar-chlorite (biotite) gneiss, (M366).

Lineation plunges 8° to090°.

In vertical plane containing lineation.			In vertical plane perpendicular to lineation.		
(X)	(Z)	Ratio	(Y)	(Z)	Ratio
4.3cm.	2.1cm.	2.05	3.0cm.	2.2cm.	1.36
3.3cm.	1.8cm.	1.83	4.0cm.	2.6cm.	1.54
1.6cm.	1.0cm.	1.6	4.5cm.	2.8cm.	1.61
2.3cm.	1.2cm.	1.92	2.0cm.	1.3cm.	1.54
2.1cm.	1.2cm.	1.75	2.0cm.	1.1cm.	1.82
2.1cm.	1.1cm.	1.91	2.0cm.	1.0cm.	2.0
		11.06			9.87
	Av. ratio	1.84		Av. ratio	1.64

X : Y : Z = 1.84 : 1.64 : 1

$$k = \frac{X/Y - 1}{Y/Z - 1} = 0.187$$

4(c)

T362 Phyllonitic mylonite with deformed quartz aggregates. Measurements taken using 6x eyepiece and 2.5x objective. 100 divisions = approx. $2/3$ of field of view. Sections cut orthogonally related to mylonitic foliation and down dip lineation.

(X)	(Z)	Ratio	(X)	(Y)	Ratio	(Y)	(Z)	Ratio
251	2	125.5	117	15	7.8	112	5.0	22.4
218	2.25	96.9	175	21	8.3	53	2.5	26.5
107	0.7	152.9	82	12	6.8	39	1.7	22.9
157	1.2	130.8	340	46	7.4	78	3.0	26.0
51	0.75	68.0	150	20	7.5	41	1.2	34.2
62	1.2	51.7			37.8			132.0
190	1.8	105.6	Av.ratio		7.6	Av.ratio		26.4
122	1.8	67.8	Geometrical ratio		7.49	Geometrical ratio		22.4
68	0.9	75.6						
		874.8						
Av. ratio		97.3						
Geometrical ratio		122.5						

The geometrical ratios are derived from best fit lines to the sets of measurements as shown in Figure 45(a). X/Z and Y/Z are taken as the more accurate values since they give more compatible values after the initial aspect ratios have been taken in account. X/Y is taken as 8.03/1.

4(d)

T124A pelitic gneiss containing quartz, andesine, K feldspar, biotite, muscovite and sillimanite.

Aspect ratios.

In plane perpendicular to the foliation.

		Ratio
5.5 mm.	4.3mm.	1.28
5.0 mm.	4.5mm.	1.11
4.0 mm.	2.5mm.	1.13
3.0 mm.	3.0mm.	1.00
		5.28
	Av. ratio	1.13

(equivalent to XZ plane when deformed).

In plane perpendicular to foliation and to previous plane.

		Ratio
4.05 mm.	3.0 mm.	1.35
4.0 mm.	2.0 mm.	2.00
6.0 mm.	4.0 mm.	1.50
5.0 mm.	2.8 mm.	1.79
		6.64
	Av. ratio	1.66

(equivalent to YZ plane when deformed).

Appendix 5

In constructing the fold profiles resulting from buckling of a planar quartz vein, a combination of simple shear and pure flattening (k = 0; Flinn, 1962) strain was applied. The finite strains measured in mylonite zones and mylonite structures are broadly compatible with this type of deformation. Since veins lying initially at less than 90° to the shear direction will lie in the extension field throughout such deformation, these cases are not considered.

Deformation was applied in two steps, each consisting of a simple shear (γ) of 3.5 and 15% shortening normal to the shear zone. Since the mylonite forms a zone of preferential deformation, any stress across the zone can be resolved into normal and shear stresses and a total strain of γ = 7 and 30% shortening was chosen for the model.

If we designate the shear strain as process A, and flattening as process B, then, as shown on Figure 54 the order of application of these processes is very important. Since the processes are non commutative (i.e. A.B. $\neq$ B.A.) with regard to the degree of rotation then we must model it in very small steps. Alternatively a semi-quantitative result may be obtained by applying the processes A and B in the orders A.B. and B.A. and averaging the result. Figure 49 illustrates this approach for initial orientations of 120°, 160° and 170°. The difference is most marked for initial vein orientations lying at greater than 160° to the shear direction. The flattening deformation reduces the degree of rotation by simple shear until the vein passes the 90° line, whereupon the two processes promote more rapid rotation. The field of contraction resulting from simple shear deformation of a unit volume sphere is enlarged by flattening and most veins lie in the contraction field for a large part of their deformation.

Once buckling has occurred the subsequent strain and rotation of fold limbs will be partly controlled by further compression and partly by rotation effects. The fold axial planes will always correspond to the XY plane of the

Figure 54. - Graph showing the rotational and qualitative strain changes during deformation of a discordant planar vein by successive simple and pure shear increments. At each stage a simple shear strain of 3.5 and a shortening of 15% normal to the shear plane is applied. If applied in different orders the two processes do not result in the same rotational and strain effects. The difference is most marked when the initial angle between the vein and simple shear plane is between 165° and 175°. At high shear strains and initial angles of $<165°$ differences are small. The field of extension for simple shear and flattening is shaded and the rotation of the X direction with such deformation is also shown.

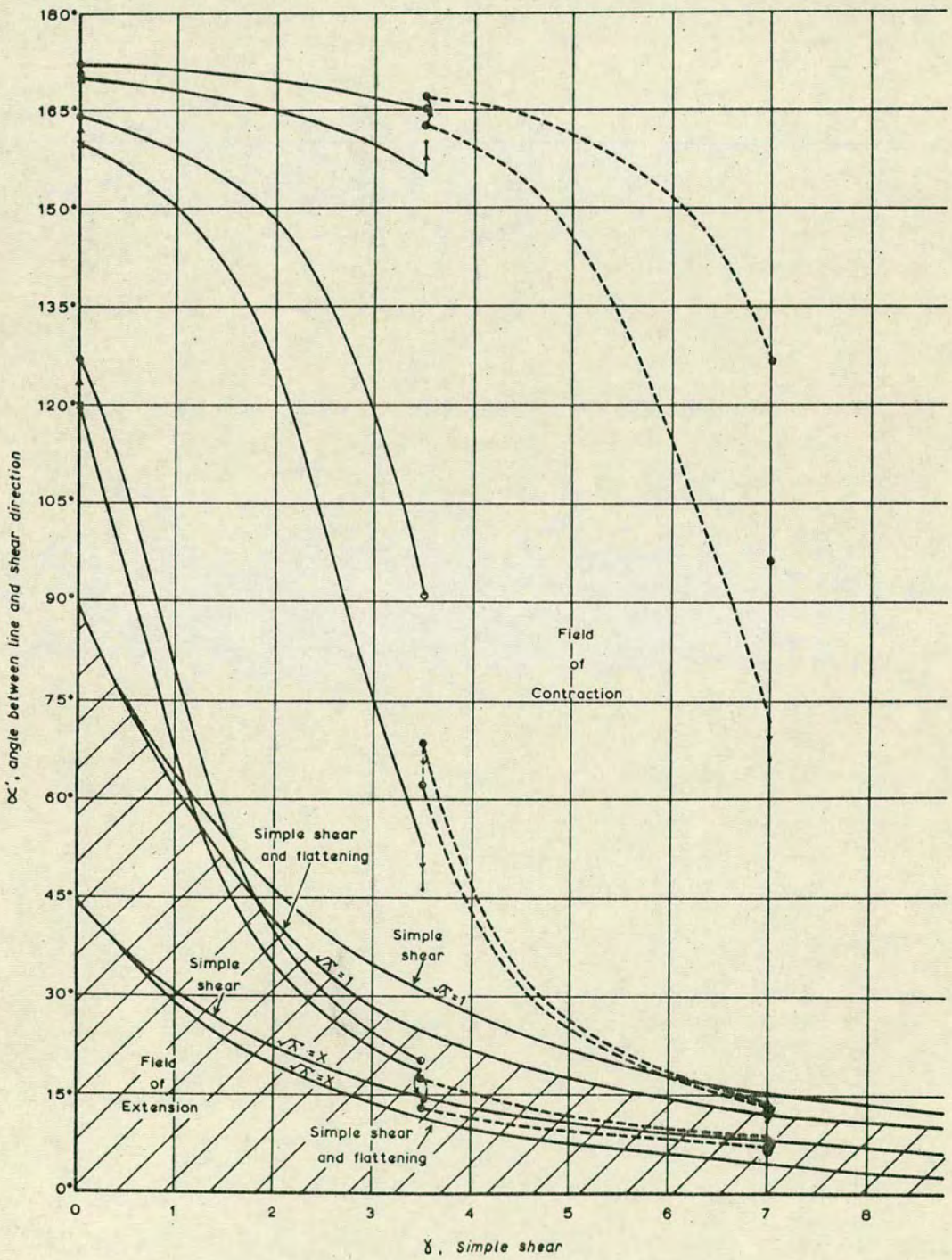
180°
165°
150°
135°
120°
105°
90°
75°
60°
45°
30°
15°
0°
0
1
2
3
4
5
6
7
8
α', angle between line and shear direction
γ, Simple shear
Field of Contraction
Simple shear and flattening
Simple shear
Simple shear
Field of Extension
Simple shear and flattening

finite strain ellipse. One set of limbs will generally lie close to the shear direction (line of no finite elongation, $\sqrt{\lambda} = 1$) and the adjoined fold limbs will be preferentially thinned and rotated. Intrafolial folds (Higgins, 1971 p.64) with a sense of rotation opposite to the simple shear are formed by this process.

The calculations for the initial orientation of 160° are set out below :-

$\gamma = 3.5$, 15% shortening

$\cot \alpha' = \cot \alpha + \gamma$ (Ramsay,1967,p.88)

$\cot \alpha' = \cot 160^\circ + 3.5$

$\therefore \alpha' = 53^\circ 01'$

$\tan \theta' = \frac{Z}{X} \tan \theta$ (Ramsay 1967, p.67)

$\therefore \theta' = \tan^{-1}(0.785.1.328)$

$= 46^\circ 12'$

15% shortening, $\gamma = 3.5$

$\tan \theta' = \frac{Z}{X} \tan \theta$

$\theta' = \tan^{-1}(0.785.0.364)$

$\theta' = 64^\circ 03'$

$\cot \alpha' = \cot \alpha + \gamma$

$\cot \alpha' = \cot 164^\circ 03' + 3.5$

$\therefore \alpha' = 90^\circ 55'$

average = $68^\circ 33'$

$\gamma = 7$, 30% shortening

$\cot \alpha' = \cot \alpha + \gamma$

$\cot \alpha' = \cot 68^\circ 33' + 3.5$

$\alpha' = 14^\circ 57'$

$\tan \theta' = \frac{Z}{X} \tan \theta$

$\therefore \theta' = \tan^{-1}(0.747.0.267)$

$\theta' = 11^\circ 17'$

30% shortening, $\gamma = 7$

$\tan \theta' = \frac{Z}{X}$, $\tan \theta$

$\therefore \theta' = \tan^{-1}(0.747.215451)$

$\therefore \theta' = 62^\circ 15'$

$\cot \alpha' = \cot \alpha + \gamma$

$\therefore \cot \alpha' = \cot 62^\circ 15' + 3.5$

$\alpha' = 13^\circ 57'$

average = $12^\circ 37'$

For flattening strain $X = Y > Z$ ($k = 0$)

Assuming no volume loss, a unit sphere deforms to an oblate ellipsoid such that

$$\frac{4}{3}\pi r^3 = \frac{4}{3}\pi a.\ b.\ c$$

where a, b, c are the semi axes of the ellipsoid

Since $X = Y$ then $a = b$

then $r^3 = 1 = a^2.c$

$$a^2 = \frac{1}{c}$$

where c is the shortening.

For 15% shortening $c = 1 - 0.15 = 0.85$

$$\therefore a = \frac{1}{0.85} = 1.085$$

Hence $\frac{Z}{X} = \frac{0.85}{1.085} = 0.785$

Similarly for 30% shortening $\frac{Z}{X} = 0.747$ (note that a decrease in area occurs in the XZ plane).

The strain along a fold train is simply calculated by

$$\sqrt{\lambda} = \frac{c/\sin \alpha'}{\text{initial length}}$$

Values for the line $\sqrt{\lambda} = 1$ were calculated using

$$\cos^2 \theta' = \frac{\lambda_2' - 1}{\lambda_2' - \lambda_1'} \quad \text{(Ramsay 1967, p.66)}$$

using the $X(\sqrt{\lambda_1})$ and $Z(\sqrt{\lambda_2})$ values for the total finite strain ellipse (flattening and shear strain). It is interesting that the effect of flattening on the fields of extension and contraction is most marked around $\gamma = 3$ for the above model; buckling will occur for a greater period if some flattening occurs.

The effects of rotation by flattening and pure shear will be equal and opposite when

$\cot \alpha + \gamma = \frac{Z}{X} \cdot \cot \alpha$ where α is the initial angle to the shear direction.

$$\therefore \frac{Z}{X} = 1 + \gamma . \tan \alpha$$

for $\gamma = 3.5$ and flattening of 15%, $\alpha = 176^\circ 34'$
for $\gamma = 7$ and flattening of 30%, $\alpha = 176^\circ 37'$